Food Flavor

ACS SYMPOSIUM SERIES **988**

Food Flavor

Chemistry, Sensory Evaluation, and Biological Activity

Hirotoshi Tamura, Editor
Kagawa University

Susan E. Ebeler, Editor
University of California

Kikue Kubota, Editor
Ochanomizu University

Gary R. Takeoka, Editor
Agricultural Research Service, U.S. Department of Agriculture

Sponsored by the
ACS Division of Agricultural and Food Chemistry, Inc.

American Chemical Society, Washington, DC

The paper used in this publication meets the minimum requirements of American National Standard for Information Sciences—Permanence of Paper for Printed Library Materials, ANSI Z39.48–1984.

PRINTED IN THE UNITED STATES OF AMERICA

Foreword

The ACS Symposium Series was first published in 1974 to provide a mechanism for publishing symposia quickly in book form. The purpose of the series is to publish timely, comprehensive books developed from ACS sponsored symposia based on current scientific research. Occasionally, books are developed from symposia sponsored by other organizations when the topic is of keen interest to the chemistry audience.

Before agreeing to publish a book, the proposed table of contents is reviewed for appropriate and comprehensive coverage and for interest to the audience. Some papers may be excluded to better focus the book; others may be added to provide comprehensiveness. When appropriate, overview or introductory chapters are added. Drafts of chapters are peer-reviewed prior to final acceptance or rejection, and manuscripts are prepared in camera-ready format.

As a rule, only original research papers and original review papers are included in the volumes. Verbatim reproductions of previously published papers are not accepted.

ACS Books Department

Preface

The investigation of nature is an infinite pasture-ground where all may graze, and where the more bite, the longer the grass grows, the sweeter is its flavor, and the more it nourishes.

Aldous Huxley

As we near the end of the first decade of the 21st century, where will the investigations of food and beverage flavor lead? Certainly, the exponential growth in identification of new flavor compounds, experienced during the 1970s and 1980s, has slowed. And the advances in separation science that made identification of these new compounds possible have led to the relatively mature fields of gas chromatography and high-performance liquid chromatography. However, the pasture-ground for new discoveries is still growing and nourishing new flavor chemists and new developments in flavor chemistry. These proceedings, based on a symposium held at the Pacific Region of the American Chemical Society in December 2005, in Honolulu, Hawaii provide excellent evidence for the future growth and the needs for new understandings of flavor chemistry.

In the first section of this book (Chapters 1–4) the focus is on new and improved approaches for identifying and quantifying flavor compounds. At the time of the symposium and publication of this proceedings, we are well into the "–omics" (including metabolomics) era of science; the need to rapidly measure large numbers of compounds simultaneously while still providing the selectivity and sensitivity needed to measure flavor compounds present in low ppb and ppt levels is pushing analytical chemists to the limits of the currently available technology. As shown in these chapters, developments in multi-dimensional separations, new chromatographic stationary phases, diverse sensors for rapidly detecting multiple compounds, and the ability to

quantitatively measure interactions between flavors and matrix components are among the areas of current and future development.

Flavor chemistry and formation are the focus of the next two sections (Chapters 5–16). Understanding how agricultural practices and food processing conditions affect the synthesis and degradation of flavors is of growing interest as scientists and consumers continue to recognize that conditions which provide the most stable products for storage or transportation are not always the same as those conditions that provide the maximum desirable flavor qualities. New food sources for modern consumers, often based on foods of indigenous diets, also continue to contribute to increasing diversity of flavors and unique chemistries. Finally, identification of genes and enzymes involved in flavor formation in foods, such as strawberries, will lead to improved varieties of fruits and vegetables as well as coming full circle to improving our understanding of how agricultural and food processing conditions can be optimized to maximize expression and activity of genes and enzymes for improved flavor attributes.

Although flavor chemists have often previously focused on sensory properties of individual compounds, the challenges that scientists are currently trying to address are understanding how sensory perception of flavor compounds changes as a function of interactions with other flavor compounds and with other nonvolatile matrix components. The fourth section of these proceedings (Chapters 17–21) focuses on these complex interactions as well as on the sensory factors that influence consumer choice in selecting foods with maximal nutritional value.

Finally, in the last section (Chapters 22–23), there is increasing recognition that the biological activity of essential oils and flavors extends to not only activation of sensory receptors for taste, aroma, color, and mouthfeel, but also that many flavor compounds can also provide beneficial health effects in preventing degenerative diseases such as heart disease and cancer.

We hope that readers of these proceedings will come to agree with Aldous Huxley that the investigation of flavor chemistry is an infinite pasture-ground that continues to thrive and provide new insights and challenges for analytical chemists, food scientists, biochemists, and geneticists working toward the common goal of understanding and improving food and beverage flavor. We also hope that these chapters may provide inspiration to a new generation of scientists who will grow and expand the field even further.

Acknowledgments

Hirotoshi Tamura
Department of Biochemistry and Food Science
Kagawa University
2393 Miki-Cho
Kita-Gun
Kagawa 761–0795
Japan

Susan E. Ebeler
Department of Viticulture and Enology
University of California
One Shields Avenue
Davis, CA 95616

Kikue Kubota
Laboratory of Food Chemistry
Department of Nutrition and Food Science
Ochanomizu University
2–1–1 Otsuka
Bunkyo-ku
Tokyo 112–8610
Japan

Gary R. Takeoka
Western Regional Research Center
Agricultural Research Service
U.S. Department of Agriculture
800 Buchanan Street
Albany, CA 94710

Chapter 1

Comprehensive Two-Dimensional Gas Chromatography: Application to Aroma and Essential Oil Analysis

M. D. R. Gomes da Silva[1], Z. Cardeal[2], and P. J. Marriott[3,*]

[1]REQUIMTE, Departamento de Química, Faculdade de Ciências e Tecnologia, Universidade Nova de Lisboa, 2829–516 Caparica, Portugal
[2]Chemistry Department, ICEx, Federal University of Minas Gerais, Avenida Antonio Carlos 6627, 31270–901 Belo Horizonte, MG, Brazil
[3]Australian Centre for Research on Separation Science, School of Applied Sciences, RMIT University, GPO Box 2476V Melbourne 3001 Australia
Corresponding author: Philip.Marriott@rmit.edu.a

Comprehensive two-dimensional gas chromatography (GC×GC) is a powerful analytical tool that can be applied to food and essential oil samples to enhance separation capacity and spectral resolution capabilities. This analytical technique also allows better peak identification assignments when used in tandem with spectrometric detection systems by means of fewer interferences and thus true mass spectra of the individually isolated compounds in the 2D space. The development of more accurate and sensitive quantification methodologies permit improved characterization of complex samples, or target compounds in complex matrices. New approaches to isolation of aroma compounds from the matrix, for olfactory assessment based on targeted multidimensional GC are possible.

3

Aroma Analysis:
Sampling, hyphenated separations and the multidimensional approach

Flavor results from compounds that are divided into two broad classes of compounds: those that are responsible for taste and those that are responsible for odors, the latter designated as aroma compounds. The matrix can affect perception of the odor and taste (*1*). The compounds that are considered as aroma substances are primarily those that are present in the matrix or sample headspace in concentrations higher than the odor and/or taste threshold.

Essential oils are mainly obtained by steam distillation or simultaneous distillation extraction where temperature and pressure are carefully selected in order to avoid, as far as possible, loss of volatile compounds by thermal decomposition, oxidation or hydrolysis (*2, 3*). Microextraction procedures have been developed in order to analyze trace levels of certain important taste- and odor-causing compounds in water (*4*). The novel analytical scale headspace technique of solid phase micro-extraction (SPME) (*5*), has become a popular, simple, solvent free method for headspace analysis with the variety of coated fibers offering some degree of sampling selectivity. Whilst quantification in equilibrium and non-equilibrium situations is possible (*6*), careful experimental procedure and prudent data handling is required. An analogous method named stir bar sorptive extraction (SBSE) was developed (*7*), increasing the volume of the sorptive phase. This technique has also been applied to flavor analysis, after thermal desorption of the coated bar prior to GC or multi-dimensional GC analysis (*8-10*).

Essential oils are very complex samples that constitute volatile compounds (less than 100 u) to semi-volatile compounds (around 300 u). Those samples are mostly comprised of terpenoid compounds, which present many isomeric cyclic or linear structures, various degrees of unsaturation, substitutions, and oxygenated moieties, that produce similar or identical mass spectra, normally chromatographically associated within complex groups in a narrow retention time window (*11*) and thus appropriate column phase selection, injection and detection system choice are usual analytical criteria (*12*). Hyphenation of the GC separation step with spectroscopic techniques is often required for absolute component identification. Thus high resolution GC (HRGC) in tandem with Fourier transform infrared (HRGC-FTIR) is a very powerful identification tool. Nevertheless it demands very high solute concentrations and quantitative component separations for collection of sufficiently clean spectra (*13*). HRGC-MS is nowadays the most popular hyphenated technique aimed towards the characterization and identification of complex volatile sample constituents. Nevertheless, notwithstanding the continuous development of instrumentation, techniques and analytical methods in the field of GC and MS, total separation of all the compounds of a mixture and their unique identification is still either impractical or physically unachievable because of the high sample complexities

(large number of compounds, structural similarities, isomeric forms and wide concentration range). As a result of this, similarities in the retention times of many compounds are expected causing clustering of many compounds within a small region, independent of the stationary phase used, and consequently co-elutions occur. Clearly a different strategy to using a single column separation approach is required if increased resolution is demanded.

New analytical technique development to maximize compound separation is an evolutionary process. From packed to capillary GC, then multiple separation phases using sequential column coupling, to multidimensional GC (MD-GC) and finally comprehensive two-dimensional GC (GC×GC). This evolution is aimed towards achieving more 'chromatographic space' in order to obtain a suitable (or increased) separation of all, or a selection of, compounds present in the sample (14,15) considering that a single GC column is physically and statistically limited by the maximum number of theoretical plates and peak capacity (16, 17). Whilst the maximum capacity of a capillary GC column can be calculated (17-19), the statistical theory of overlap – STO (17, 20, 21) provides a more realistic measure of a sample with randomly distributed peaks. Since essential oils may contain hundreds of compounds over a wide concentration range, co-elutions are inevitable. A complex chromatogram may be simplified by means of a MD-GC system, where a heart-cut device, e,g., a live T-piece, allows the isolation of a particular retention time window, quantitatively transferring those compounds from the first column (pre-column), to the second column (analytical column), where only the transferred compounds are analyzed. In most of the cases, the second column will be able to separate the transferred analytes, providing that the stationary phase is chosen accordingly. In spite of the elegance of the separation approach, MD-GC may be a very time consuming method to implement, with long analysis times. This may make the method unsuitable for routine analysis. Additionally, a multitude of consecutive narrow transfers is not advisable with most systems described to date, since as more compounds are delivered to the second column, there is an increased likelihood of co-elution and so this defeats the purpose of the analysis.

Mass spectral similarity of terpenoid compounds having retention times that do not differ significantly (or perhaps not at all on some column phases), makes the identification task very difficult and sometimes even impossible. Commercial spectral libraries are increasingly complete and specific, providing better algorithmic calculations. This results in GC/MS being one of the most used techniques for routine identification, however for essential oil separations it still a necessary to attain aroma full separation of peaks for reliable peak identity confirmation. Associating mass spectral data with compound retention indices for columns with different polarity, represents an improved tool in compound identification by using 1D-GC/MS (22, 23).

Whilst the hyphenated analytical system of GC/MS has become the workhorse separation/identification tool in the essential oil laboratory, fast separation may exceed the capability of quadrupole analyzers to give reliable

unbiased spectra The introduction of time of flight MS (TOFMS) now gives the possibility to collect mass spectra, which are independent of the part of the GC peak which is sampled, and so should maintain the same mass spectral m/z profile for the whole of a given chromatographic peak. The high ion extraction ratio of TOFMS, which is able to generate up to 500 summed spectra per s, with all m/z ions simultaneously detected, avoids such spectral deformation or bias. The TOFMS analyzer should allow effective spectral deconvolution, even in grossly co-eluting situations. This represents a true spectral resolution capability (*24*). The TOFMS permits the use of very fast GC (which may be defined as a method which produces peaks of base widths < 0.3 s) as an analytical methodology for routine fast GC analysis, with appropriate MS identification of complex mixtures. This has become the analyzer of choice for comprehensive 2D GC.

Comprehensive Two-Dimensional Gas-Chromatography (GC×GC)

Introduction

In the early to mid 1990s, a new multidimensional chromatographic mode which as been termed comprehensive two-dimensional gas chromatography (GC×GC) was introduced. The GC×GC method employed a coupled column ensemble which comprised a first and second dimension column (termed ^{1}D and ^{2}D respectively), with the latter providing a very fast elution of components sampled from the first column. A chromatographic method is considered comprehensive if a) the transfer from the first to the second column is qualitatively and quantitatively complete; and b) the orthogonality principle is respected, *i.e.*, both separations systems are independent, and the separation on the first column is preserved on the second one (*25-27*). However, in order to provide significant additional separation capacity, simple joining of the columns will not produce the required effect.

In GC×GC the two columns must be connected in series, through a suitable interface (*28-30*). The sample is then transferred from the first to the second column (usually without mass losses). The interface comprises a modulator, which either performs heating (to accelerate solute into a narrow band in the second column) or cooling (to retard analyte and cause on-column trapping or cryofocusing of the bands) or both, depending on the design. The modulation is thus the sequential liberation of the solute from the first column onto the second column, preserving and further fractionating the separation obtained on the first column. Since the different sampled zones of an eluate are thermally focused before the separation on the second column, the resulting segments (peaks) of the modulation are now more intense in the second column since each peak becomes much narrower. The modulated chromatogram is then transformed to a contour plot of two dimensions by means of a suitable computer software, or to a

3D plot, which is the presentation of the linear chromatograms projected on the 2nd dimension for each modulation. The independent 2nd dimension chromatograms are aligned in a bidimensional plane where the X axis represents the separation on the first column, the Y axis the separation achieved on the second column and the Z axis the intensity of detector response (resulting here in a 3D plot). The practical implementation of GC×GC analysis is to sample each ^{1}D peak a number of times (usually at about the same time duration as the peak's standard deviation) and deliver each separate zone to the ^{2}D column. The individual ^{2}D analyses are generally to be completed before the next sampling event occurs.

The separation mechanisms in both columns should be based on different and independent physico-chemical interactions. For example, the following coupling of column phases may be considered appropriate: boiling point vs. polarity; boiling point/chirality vs. polarity; or even high polarity vs. low polarity configurations. Such combinations will be selected in order to maximize the individual column peak capacities and separation power towards sample component (26,28,29). Normally fast GC is performed in the second dimension column, which is achieved through reduced dimensions of diameter, length and film thickness, allowing the total time of the ^{2}D chromatographic run to never exceed more than a few s; the actual total run time of the 1D-GC run will be approximately the same as for the GC×GC analysis of the same sample.

This review will not describe the essential features of GC×GC, for which reviews are available and may be consulted, and neither the specifics nor requirements of the technique. Rather, in this review, an overview of the application of the GC×GC technique is given for food and essential oil sample analysis in order to illustrate the power of this methodology in the separation, identification, spectral resolution and information content of the technique. In spite of the crucial importance of the sample preparation step for aroma analysis, sampling techniques combined with GC×GC will not be further discussed here beyond the earlier introductory comments (see above).

Prospects and capabilities

GC×GC and Chiral Analysis

Enantioselective GC analysis is commonly performed using capillary columns coated with cyclodextrin derivatives (CDD) diluted in a suitable polymeric stationary phase (31). When CCD coated columns are used to perform a separation of standard mixtures of different enantiomeric compounds, normally one achieves relatively easily an adequate resolution of the individual enantiomers of chiral compounds. However, when complex matrix analysis is performed, as for example for essential oils, the separation of the individual compounds can be more problematic or even impossible, if a 1D-GC analysis is

performed. In fact, in such kinds of matrixes, most of the compounds will present at least one enantiomer, which may double the number of compounds to be separated in a single 1D-GC run. According to the statistical theory of overlap (STO) explained above, this can introduce separative limitations. Moreover, the matrix interferences will even pose more limitations to the resolving power of the column for the target chiral compounds. The enantio-MDGC approach referred to elsewhere (32,33), can provide an elegant way of separating, with good resolution, those target compounds. For complex matrices, or for enantioselective characterization of many compounds in a mixture, completing such an analysis according to principles of heart-cutting methods may be very time consuming, and potentially not suitable for routine analysis, depending upon the MDGC setup, and ease of column flow balancing.

Consequently, GC×GC finds a fertile application field here, not only because of the enhanced column capacity provided, and its ability to maintain the resolving power already achieved through use of a first enantio-selective dimension, but ideally the total run time should be more suitable for routine analysis if a single GC×GC analysis can resolve all enantiomers of interest.

Two different column configurations are possible when running GC×GC for chiral separation. In one case, the ^{1}D column is an achiral coated column, and the ^{2}D column will be a chiral coated column. This column configuration one can refer as GC×enantio-GC (GC×eGC); the opposite or reverse configuration will be enantio-GC×GC (eGC×GC). In both cases the goal is to achieve good resolution between all the target enantiomeric compounds present. It should be noted that in conventional MDGC methods (i.e., heart-cutting) the only logical implementation is to use an enantioselective column as the second column. In this instance enantiomers of a chiral compound will be unresolved on the first, achiral column, and then both can be quantitatively heart-cut to the enantioselective column. In GC×GC, because of the separation on each column is preserved, eGC×GC is now a possibility. Figure 1 shows the latter column configuration (eGC×GC) applied to *Melaleuca alternifolia* essential oil analysis (34).

The primary column was an EtTBS-β-CD coated column of dimensions 25 m x 250 μm i.d. x 0.25 μm d$_f$, and contained 30% β-cyclodextrin derivative (in stationary phase PS086) as the chiral selector. The second (polar) column was a BP20 coated column, of dimensions 0.8 m x 100 μm i. d. x 0.10 μm d$_f$. In Figure 1, one can observe that the target enantiomeric compounds are very well resolved, both between themselves and from the matrix interferences. Note that any peaks that are vertically aligned will have coeluted on the first (enantioselective) column, and hence unlike in the 1D case where FID cannot be used for such overlapping peaks, for eGC×GC FID can be used for quantification since the peaks are adequately resolved on the ^{2}D column. The time to perform this separation did not exceed 50 min, which would most likely require more time if performed in an enantio-1D-GC system which employed multiple heart-cuts or injections. Moreover, quantification of the individual compounds is possible as well, using available software which is relatively 'user friendly'.
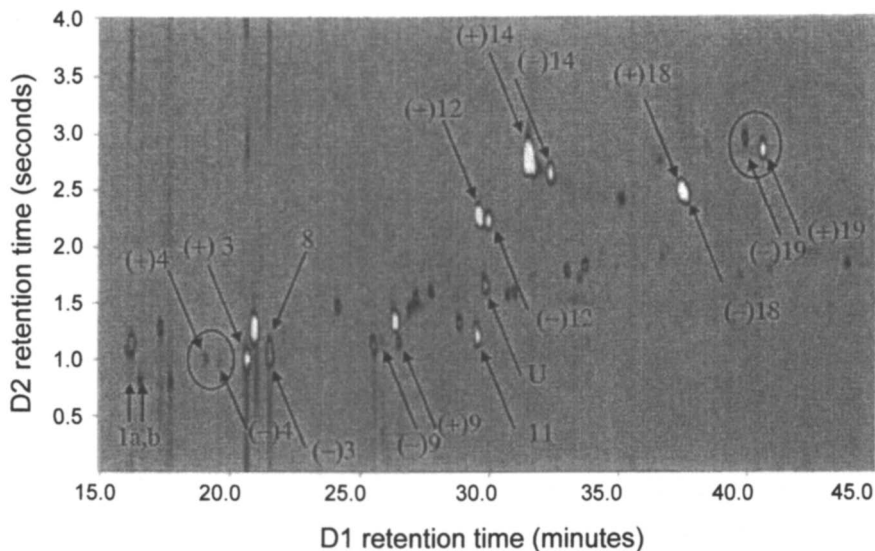
Figure 1. Comprehensive 2-dimensional separation space for the enantio-GC×GC analysis of Melaleuca alternifolia essential oil. Individual isomers are differentiated by a (+) or (-) sign, or a,b where the correct assignment of isomers was not confirmed. 1a) α-thujene (enantiomer); 1b) α-thujene (enantiomer); 3 sabinene; 4 β-pinene; 8 p-cymene; 9. limonene; 11. γ-terpinene; 12. trans-sabinene hydrate; 14 cis-sabinene hydrate; 18. terpinen-4-ol: 19. α-terpineol. U. unidentified component. Used with permission of the copyright holder (Reference (34)). See text for column details.

Another example of an eGC×GC separation is shown in Figure 2. Here, a standard mixture of suspected contact allergens was submitted to comprehensive analysis, and all the enantiomeric constituents were well resolved. Using the opposite approach (*i.e.*, reverse to that above) of GC×eGC (*35*), a comparatively good result is achieved, keeping the overall run time below 10 min, achieving resolved separations and suitable quantitation. Figure 3 shows the GC×eGC analysis of bergamot essential oil, combining a 10 m x 100 μm ^{1}D column and a 1 m x 250 μm ^{2}D column. Reduced pressure ^{2}D condition provided by a mass spectrometer detector (the 10 m narrow bore first column acts as a restrictor to the wider bore second column, and leads to vacuum conditions in the ^{2}D column) were used in order to achieve fast run analysis and good separation power with relatively low elution temperature, providing improved resolution.

Note that enantioselectivity on a 1 m column is a difficult task, with best results for compounds that have very good k value difference for the two enantiomers. The short ^{2}D chiral column simply will have insufficient resolving power to adequately separate enantiomers of most components. GC×GC does,
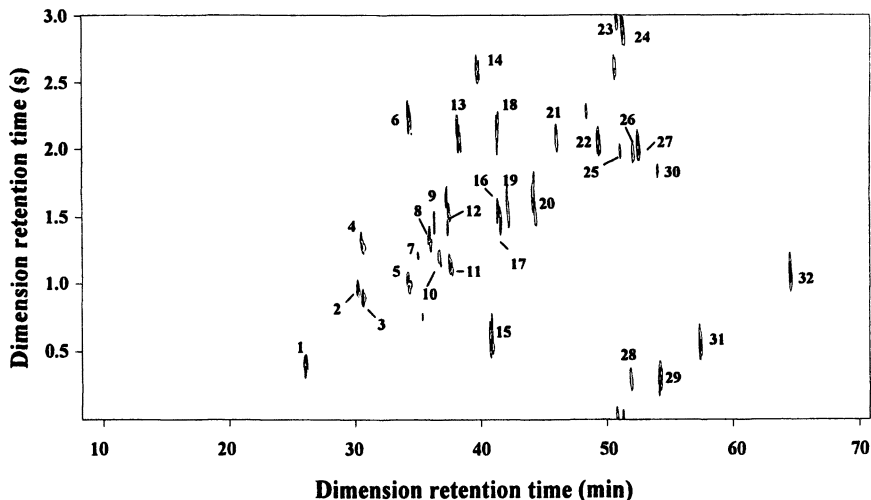
Figure 2. Enantio-GC×GC-FID contour plot of a standard mixture containing suspected allergens. Peak identification: 1. (+)-limonene; 2. (-)-linalool; 3. (+)-linalool, 4. phenylacetaldehyde; 5. methyl oct-2-ynoate; 6. benzyl alcohol; 7. citral; 8. (+)-citronellol; 9. (-)-citronellol; 10. citral; 11. methyl non-2-ynoate; 12. geraniol; 13. hydroxycitronellal; 14. cinnamaldehyde; 15. eugenol; 16. α-isomethyl ionone (enantiomer); 17. α-isomethyl ionone (enantiomer); 18. anisyl alcohol; 19. cinnamyl alcohol; 20. isoeugenol; 21. coumarin; 22. amyl cinnamaldehyde; 23. lyral (enantiomer); 24. lyral (enantiomer); 25. farnesol (isomer); 26. farnesol (isomer); 27. hexyl cinnamaldehyde ; 28. amyl cinnamic alcohol; 29. phenylmethyl propional; 30. benzyl benzoate; 31. benzyl salicylate; 32. benzyl cinnamate. ^{1}D column: 2,3-diEt-6-TBDMS-β-cyclodextrin (MEGA; 20 m x 0.25 mm i.d., 0.25 μm d$_f$); ^{2}D column: BP20 (SGE International; 1.0 m x 0.1 mm i.d., 0.10 μm d$_f$). Carrier gas H$_2$ at 1.5 mL.min^{-1}. Oven temperature programming: 35 °C (5 min), 3 °C.min^{-1} to 225 °C (10 min); injector T: 220 °C; detector T (FID): 250 °C. Split injection (30:1) of 1 μL standard mixture in hexane.

however, remain an attractive goal, since enantiomeric excess (ratio of the two enantiomers) can be measured directly by peak area ratio in a single ^{2}D chromatogram. This would be akin to drawing a vertical line in Figure 3, passing through the two enantiomers and measuring their area ratios. Still, special conditions, such as vacuum outlet are required to achieve this result. It is likely that a method such as this will be difficult to apply routinely. Stereochemical analysis of the monoterpene region of essential oils frequently provides sufficient information to determine the authenticity of essential oils (*36, 37*) hence these GC×GC methodologies above highlight opportunities for increasing the throughput of these important analyses for quality assurance purposes.
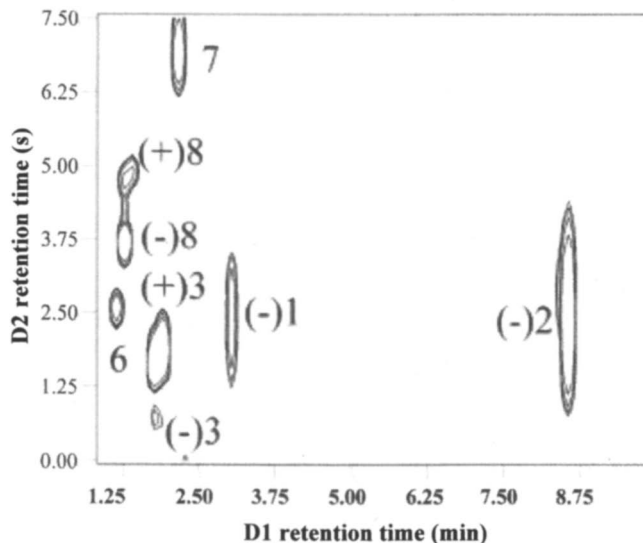
*Figure 3. 2D separation space for the GC×eGC/MS analysis (SIM m/z 93 ion)
of bergamot essential oil (monoterpene region shown). Identity of components:
linalool (1), linalyl acetate (2), limonene (3), (±)-pinene (6), γ-terpinene (7)
and sabinene (8). Used with permission of the copyright holder (Reference
(35)). See text for column details.*

GC×GC/MS and Retention Indexes (*I*)

The hyphenated GC×GC chromatographic method, whether in chiral or
achiral applications, represents a major step towards achieving full matrix
characterization. Although mass spectrometry of itself, without any other
physico-chemical information, does not provide unequivocal positive
identification of a particular compound, it constitutes a powerful tool towards that
goal and hence justifies its popularity as a routine analytical tool. In fact, if one
considers as an example, monoterpenes or sesquiterpenes, one can easily verify
that many mass spectra, representing different compounds, have almost the same
mass spectral pattern. Moreover, since the existing spectral libraries are mostly
quadrupole generated spectral libraries, any comparison with ion trap (ITD) or
TOFMS generated spectra must be accompanied by a careful final assignment,
since mass spectral differences can be observed for the same compound using the
three mentioned mass detectors which may be either more, or less, important in
library structure assignment. So, any identification sustained only on matching
the mass spectra obtained with the library reference spectra, can lead to
potentially wrong identifications. The linear retention index (LRI) concept,
proposed by van den Dool and Kratz (*38*) can support MS data, through

providing two independent informational tools on which compound identity can be based (*39, 40*)

Retention indices are reproducible, especially in apolar phases, and can be reliably applied as an auxiliary tool for positive identification when the mass spectrum fragmentations are interpreted. Dedicated in-house retention libraries are even more reliable, and owing to the need to have positive identification, fragrance houses rely heavily upon both *I* and MS data, and *I* data on two different columns operated in 1D mode are also often used to support or confirm identification.

In GC×GC the opportunity exists now for using two sets of column retention index data in the single analysis, since the two columns are used simultaneously; one can obtain not only retention index data from the ^{1}D column, but consideration of the ^{2}D column retention data can assist in correct peak assignment, and consequently be used for identification. Normally the ^{2}D column, for orthogonality purposes and to generate as much chromatographic space as possible on the second dimension, will be a column of different polarity than the first dimension. So if an apolar coated column is used in the first dimension, a polar phase such as polyethylene glycol is normally used on the second dimension column. New polar cyano phases are now being introduced to GC×GC applications as well. With the complementary polarity information now provided through this ^{2}D column, one has three different sets of data capable of aiding in characterizing a particular compound (retention data on the first column associated with boiling point when an apolar column is used, retention data on the second column associated to polarity, and finally MS data), that together can be exploited in order to have more confidence in identification assignment for compounds. A successful approximation to this methodology was described (*41*) allowing pyrazine identification through the alignment generated on the second dimension, explained on the basis of different substitution patterns around the pyrazine ring; this study considered only retention times on both dimensions. When applying this concept to lavender essential oil characterization, but using 1D-GC calculated retention data and extrapolating them to a GC×GC run (*42*), easier identification of compounds resulted.

Recently more than 300 compounds were identified in pepper samples, by means of GC×GC/MS considering, for the first time, the LRI actually obtained when compounds elute on the first dimension (the chromatographic course is constituted by two columns of different polarity, in an apolar/polar configuration), and MS data. ^{2}D peak position (retention) data were considered as well, as an auxiliary tool for positive identification, considering the information concerning the polarity of the identified compounds correlated with the mass identification performed by spectral matching with MS libraries. Figure 4 is a GC×GC contour plot obtained for one of the pepper species studied (*43*).

Whilst a compound's position in 2D space must be a powerful indicator of its physico-chemical properties – where indices can be considered a parameter embodying physico-chemical properties – applying such data to predict a

compound's GC×GC position has been little investigated. Whilst it is possible to invoke trends such as a later eluting compound on a polar ^{2}D column should be a more polar compound, this has not been reduced to reliable simulation of or a useful metric for predicting 2D data. Retention index data would be attractive reference database information to use for this purpose, but one problem arises. With a non-polar – polar column set it will not be possible to easily extract ^{2}D column retention index data, since alkanes are required to be sufficiently retained to bracket the retained compounds. This is because the alkanes will be little retained on the polar ^{2}D column.
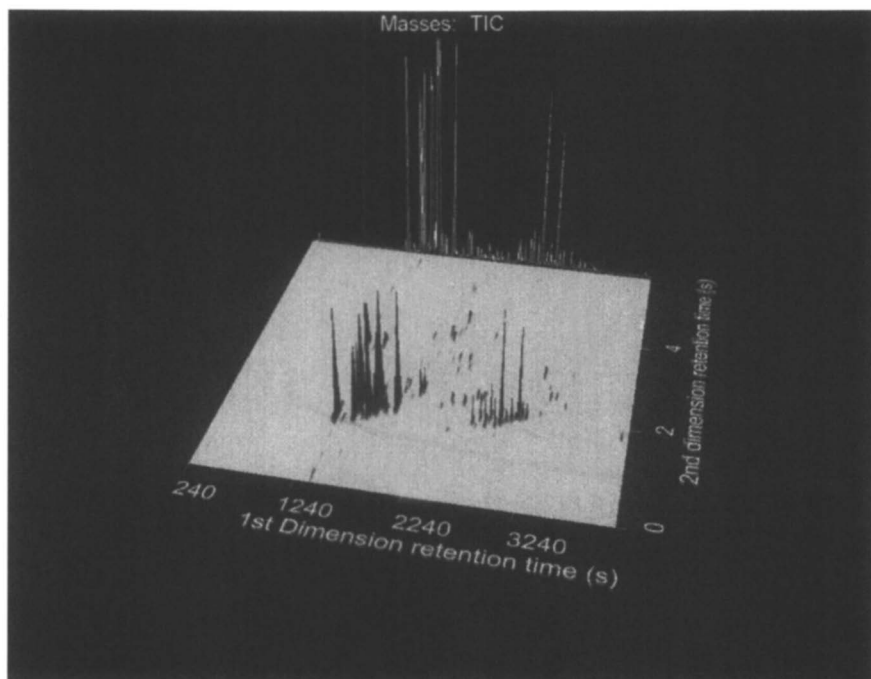
Figure 4: HS-SPME-GC×GC/TOFMS contour plot for the analysis of a Brazilian pepper sample. Analytical conditions in reference (43).

It was shown by Western and Marriott (*44, 45*) that in this case, on the more polar column a polar reference compound set (*e.g.*, alcohols) would be required. This means reference databases would have to be converted to *e.g.*, alcohol reference data, on the appropriate phase. Temperature dependency of reference index data will also be required. Nevertheless, opportunities to develop such an approach exist, and if valuable, will undoubtedly be investigated by researchers in the future.

GC×GC as a Fingerprint Technique for Facile Data Comparison, and Biosynthesis Processes Monitoring

The GC×GC result comprises a two-dimensional (2D) plot where the axes represent total first dimension (^{1}D) and second dimension (^{2}D) time, respectively. The latter corresponds to, or should define, the maximum modulation period (P_M), which is a critical parameter in establishing GC×GC operation. Generally P_M should be selected to approximate the ^{1}D peak standard deviation time (σ); excessive retention should be avoided since this demands a longer ^{2}D time - and hence longer P_M – which may lead to under-sampling of the peak (46). Alternatively, if P_M is too small, some peaks may not elute within one modulation cycle, resulting in peak wrap-around, and the peaks appearing in the two dimensional plot out of the correct modulation cycle and at a position which does not correctly represent its absolute ^{2}t$_R$ value (nor its physico-chemical properties). Orthogonality, or a high degree of orthogonality, can be achieved by combining column configurations with different retention mechanisms or varying/tuning the operation conditions (carrier flow, oven temperature program) (47) of the second dimension as a function of the progress of the first dimension (48). Orthogonality is thus independent of the modulation process, and it is an important criterion since it determines the magnitude of two-dimensional separation space that will be used in relation to the potential maximum separation power. When retention correlations across both dimensions occur, the goal of attaining maximum peak capacity is reduced compared to what is theoretically possible. In an extreme situation, when high correlation is achieved, peaks can be aligned diagonally across both dimensional axes, meaning that the 2D separation effectively represents, or is reduced to, a one single dimension separation in a ^{2}D system (47). This would mean that only one dimension (or correlated property) of the sample is exploited in effecting the 2D analysis.

In general practice GC×GC is performed under proper selection of column relative phase ratios (β), column dimensions, carrier gas flow, and temperature of two different polarity columns in order to use the maximum separation space offered by the two dimensions. However, the degree of separation orthogonality achieved will depend upon how well or poorly correlated are the stationary phases of the two dimensions and even in an optimum orthogonality situation sample resolution might not be achievable. It has been observed that the most favourable 2D result should arise when the *method* dimensionality matches the *sample* dimensionality. Perhaps this is more clearly stated as saying that the method dimensionality should be able to fully exploit the sample dimensionality. This recognises that the mechanisms by which the method will achieve separation are accessible to the sample components, and so offer differentiation of the sample components in the *n*-dimensional space (49).

When orthogonality principles are achieved, the GC×GC system can be explored in all its intrinsic potential, with enhanced system peak capacity, and good-to-optimum peak resolution. Moreover, it has been demonstrated, that the reproducibility of the contour plots obtained by GC×GC systems are quite reliable, for both qualitative and quantitative measurements, regardless of the modulator used (*50-52*). So, the graphical advantage offered by the 2D plot can be used to simply compare contour plots between each other in order to find comparative relationships. In fact, even for an untrained operator, the lone identification of the appearance or disappearance of a certain compound or group of compounds, enabling sample comparison, can now be done. This cannot be done so easily in 1D analytical data presentation. For quick screening (from 5 to 20 min analysis time), GC×GC can be used to monitor, in a reliable way, sample-to-sample changes. Hyphenation is possible with selective chemical detectors, and can be performed not only at the research level, but also in industrial situations for rapid sample comparison. An obvious application is analysis of out-of-specification samples where presence of new compounds, or of compounds above trigger levels, should be readily monitored. This was the case with the distillation process of Brazilian *cachaça* beverage, where comparative fingerprints of samples were used to determine the turning point of the distillation product (Figure 5).

Comparison has been also made between different *cachaça* types, aged in three different wood materials (Figure 6), allowing easier visual differentiation between very similar products. Potentially, the use of fingerprinting of GC×GC data for product authenticity purposes or product falsification control can be extended to the possibility of enantiomeric separation on one of the two dimensions, and hyphenation with mass spectrometry or even with isotope ratio mass spectrometry (provided that fast data acquisition is possible). The application of statistical data processing, such as multivariate analysis, can become easier and less time consuming, since more information is now available from the contour plot, and there exists more scope in choosing the data to be computed. This selectivity is important because not all of the data contained within a chromatogram will be important for a given classification (*53*).

In a study of Chinese medicinal products, a volatile headspace analysis of ginseng by SPME with GC×GC was used to compare with that of angelica. Major peaks in ginseng were found to be not unique to ginseng, however some minor components appeared to be associated with only ginseng, and so ginseng in a tonic product could be suspected based on these minor components. Finding unique, minor components in a poorly resolved 1D analysis will be considerably more difficult (*54*). This sample-to-sample comparison should become a widely used – and increasingly recognised – valuable attribute of GC×GC in the future.
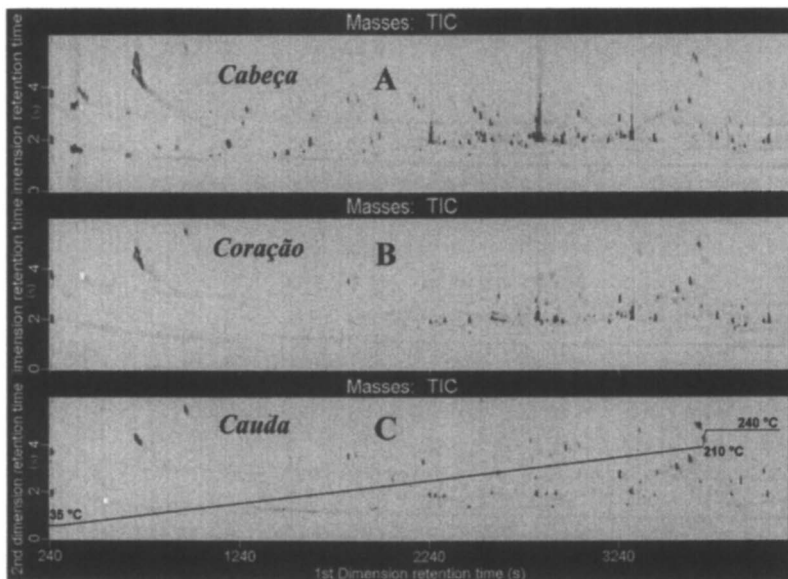
*Figure 5. Monitoring of the distillation process during cachaça production.
A represents the contour plot obtained for the first fraction (cabeça "head")
with high content of ethanol (not shown since mass scanning was started after
ethanol elution) and the more volatile and semi-volatile compounds.
B represents the coração "core" fraction richer in the semi-volatile compounds
and C, the cauda "tail" fraction that corresponds to the end of the distillation
and enhanced water content, where the less volatile compounds dominate. The
oven temperature programming profile is presented on the bottom contour plot.*

GC×GC-FID, GC×GC-NPD, GC×GC/qMS and GC×GC/TOFMS: Method Comparison

Another important feature of GC×GC is the possibility to compare contour plots when different detection methods are applied. Experience shows that, regardless of the detector used, if the chromatographic condition and operational procedures are held constant the contour plots obtained in each situation are comparable; they may just need a small degree of alignment. This was the case for the quantitation of methoxypyrazine in wine by GC×GC-NPD and GC×GC/TOFMS after isotope dilution (55). A similar comparison is shown in Figure 7 for the case of Brazilian pepper when GC×GC-FID and GC×GC/qMS were performed in order to identify VOC after HS-SPME sampling.

As one can observe, the contour plots are quite similar, although some wrap around effect is evident in the GC×GC/qMS contour plot. This can be explained by the fact that in addition to the ^{2}D column, 0.5 m of interface silica column is
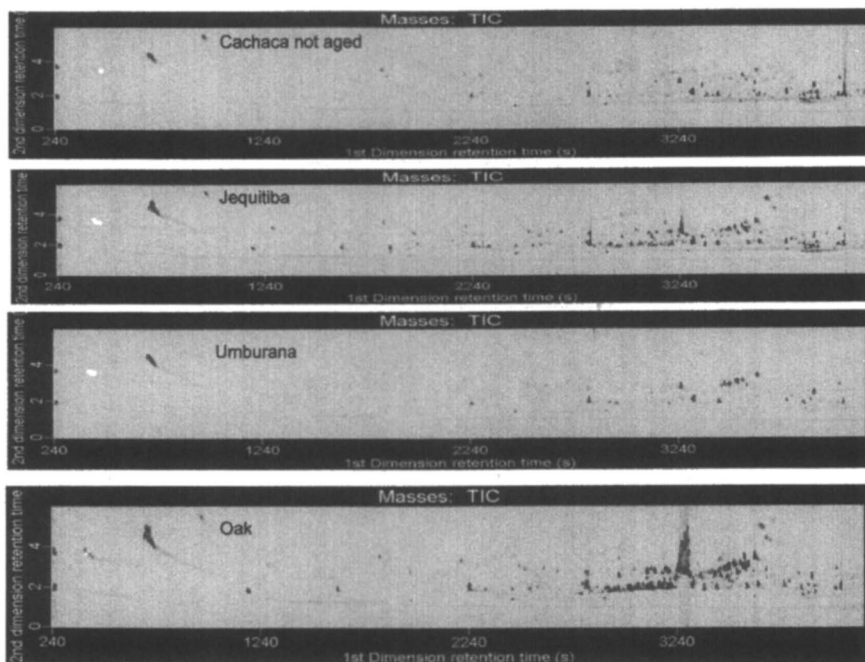
Figure 6. Contour plots showing different cachaça types, aged in three different wood materials. The top contour plot shows the original cachaça (not aged) and the three contour plots below are the GC×GC analyses after the same aging period in three different wood materials. Oven programming conditions are as shown in Figure 5.

present in the qMS case leading to reduced flow rate in the ^{2}D column. Consequently, some peaks now elute from the ^{2}D column in the next cycle of modulation (wrap-around). Nevertheless the similarities are obvious and peak assignments easy. This has the advantage of allowing use of FID for quantitative measurements, whereas qMS can be used for identification purposes.

Although the acquisition rate for qMS is less than optimum for GC×GC analysis, the 20+ Hz reached by qMS when a mass range of about 40-400 u are scanned has proven to be quite sufficient (*43,56*). On the other hand FID has a maximum acquisition rate of 100-200 Hz, which is much more suitable for quantitative analysis. So, using these two techniques in tandem confers a great analytical advantage. Small shifts in retention time, in the first and second dimension, occur when GC×GC-FID, GC×GC/qMS and GC×GC/TOFMS are performed. This can result from the vacuum and interface column effects when detection by FID is compared with both mass detectors (atmospheric *vs* vacuum detection), and between the latter two as a consequence of the different interface column length. These differences should be readily accountable during data comparison.
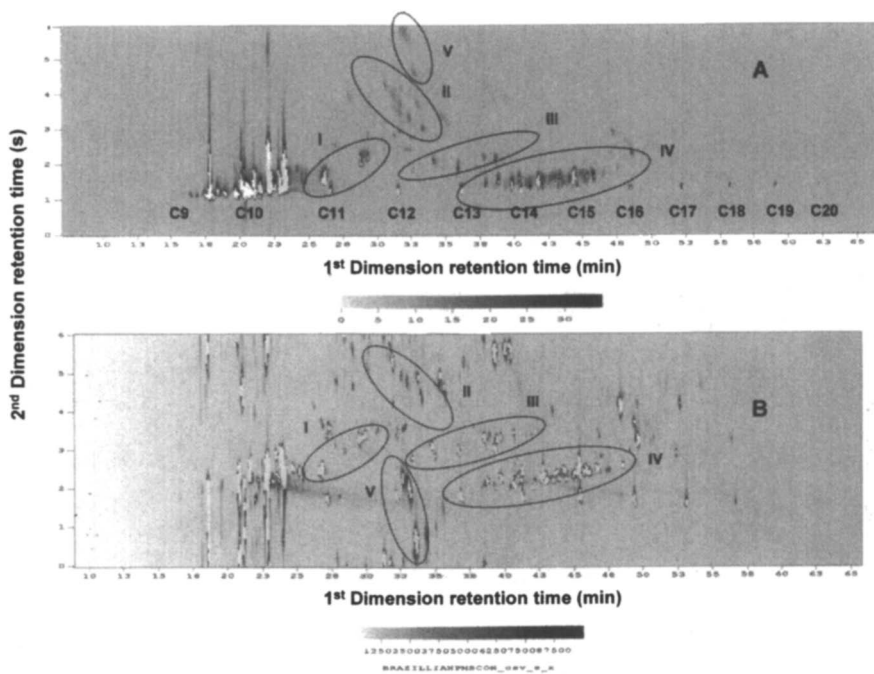
Figure 7. (A) HS-SPME-GC×GC-FID contour plot, and (B) HS-SPME-GC×GC/qMS for the analysis of Brazilian pepper sample. Hydrocarbons from C9 to C20 have been added from a stock solution to the pepper samples, as indicated. The contour settings are presented at the bottom of each contour plot. Used with permission of the copyright holder (Reference (43)). The Roman numerals highlight zones of comparable or fingerprint regions. Zone V exemplifies wrap-around peaks, easily identifiable in this example.

In more likelihood, retention deviation between the systems can be tolerated, depending on the reliability of the spectra and the matching obtained, especially if standards are co-injected. It can be anticipated that more work will be performed in that direction in order to determine the magnitude of the deviations and the degree of acceptance of those values. For the pepper study, TOFMS provided identification of more than three times the number of peaks found by using qMS due to its higher sensitivity and acquisition rate, which constitutes an important condition for hyphenation with GC×GC. At present the fewer placements of GC/TOFMS instruments (and cost) may be of concern to some users for routine laboratory adoption. Attention should also be paid to developing TOFMS dedicated mass spectral libraries, to complement the libraries now generated by using quadrupole MS. This may explain why spectral matching may be better when qMS data are compared in some instances (*41*).

GC×GC-Olfactometry

The mass spectrometric data obtained after a GC run for a particular sample allows the possibility of identification assignments even in some cases where (overlapping) impurities are still present in the analysis. Nevertheless, the real sensory contribution, in terms of olfactometric perception, is absent from the GC/MS result. In order to establish a relationship between a sample's overall odor and the individual sensorial impact to that odor arising from compounds present in the sample, the GC effluents need to be monitored by means of human subjects. As sensorial detectors, they should be able to describe the individual sensorial perception of each compound eluted from the chromatographic column. This method is known as gas chromatography-olfactometry (GC-O).

Among the various methods proposed in the literature to give information on the organoleptic characteristics of different products, three techniques are considered to give satisfactory answers to evaluate the odor profile, identifying the key odorants and the intensity of each. Aroma extract dilution analysis (AEDA) uses successive dilutions of the extract, giving a flavor dilution factor (FD), which corresponds to the highest dilution at which an odorous compound is detectable (57, 58). Another dilution method determines a value called "CHARM", calculated from the stage of the dilution series and the duration of odor perception at the dilution level in which it was perceived, resulting in production of an "aromagram" (59). The second method called "OSME" measures the perceived intensity of aroma at the column effluent. This takes into account the quantitative aspect of olfactometric detection for a single GC injection (60). The third method consists of calculating a frequency of odor detection by a trained panel of more than eight different panelists (61). The individual resulting aromagrams allow odor profile comparisons, as peak intensities are related to the frequencies of odor detection: "NIF" and "SNIF" (respectively "Nasal Impact Frequency" and "Surface of Nasal Impact Frequency). This method is a citation index method, which is faster to set up since it does not require the particular training that the "OSME" method does.

GC-O is a powerful technique to determine the individual contribution of a particular compound to the overall odor perception of the sample. Nevertheless, since the odor compositions generate, in general, very complex chromatograms, co-elutions are frequent. Analyzing the same sample in two different columns with different polarities, is then almost compulsory in order to generate accurate results. Moreover, a GC-O sniff run should not exceed 20 to 30 min in order to not exhaust the subjects performing the sniffing (62). Due to this fact, the GC-O analysis is usually performed with rapid oven-temperature programming (e.g. 6-10 °C.min^{-1}) which consequently increases the probability of co-elutions, increasing the difficulty in identification of the compound or compounds responsible for a given odor. Thus, a trace odor-active compound may be masked by a larger odor-inactive compound. On the other hand, as described by Eyers and co-workers (62) in a study of coriander volatile compounds by means

of GC-O, co-eluting odor-active compounds results in the perception of "odor-clusters". An elegant solution to identify character-impact odorants where co-elution occurs, is to use multidimensional GC techniques. In that work, GC×GC was able to reveal the complexity of the clusters.

Figure 8 shows a schematic model which may be proposed for GC×GC screening after odor cluster detection, heart-cutting to a long ^{2}D column, and olfactometry detection. Run 1 employs a short 1.5 m ^{2}D column without modulation (GC-O), then with modulation (GCxGC-FID or MS) to identify the odor window(s); the 2D GC×GC plot reveals the full composition of the odor region in contour format. The second run (t-MDGC) allows the full odor region to be cryotrapped as 1 event and delivered to the long 10 m column, where simultaneous enhanced (complete) separation and olfactory detection of each component is achieved. Enantio-GC (on ^{2}D) can also be performed at this stage.

Multidimensional GC techniques can thus play an important role here in order to simplify the laborious use of different types of columns, since after the heart-cut event there is an improved probability that a particular odor impact compound can now be isolated from the surrounding impurities. This will allow full sensorial characterization of components on the one hand, and if GC×GC is used, one can simultaneously also address detection limitations for analyzing minor or trace components by means of signal enhancement obtained after peak modulation. This may be very important, since it is not unlikely that trace amounts of a particular compound, have a significant contribution to the odor of a particular matrix.

Likewise, there are many examples where odors are recorded olfactorially, where GC-FID fails in giving a response, such as when the odor threshold of some compounds are particularly low and consequently easily detectable by the human nose although not by FID. Thus the sensitivity increase of GC×GC may assist in locating an odor-active peak. After a first screening process, the odor impact regions of a chromatogram can be chosen, and after successive target heart-cuts GC×GC-FID and GC×GC-O can be performed after splitting the GC effluent towards two different columns of same phase composition and dimensions. Clearly, the new opportunities for advanced analysis in the essential oils area, based upon the now very active research area of comprehensive two-dimensional gas chromatography, will make major contributions to our understanding of oil composition and sample characterization in the future.

Acknowledgements

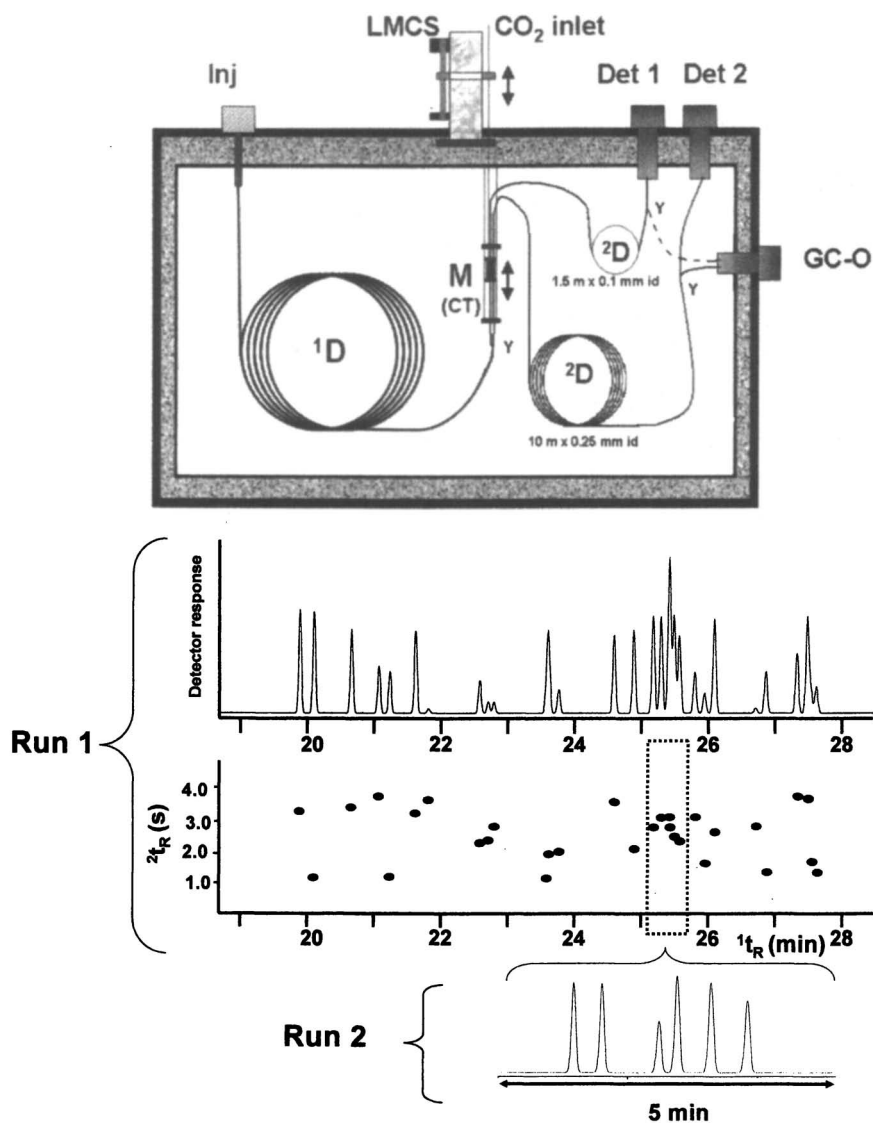*Figure 8. Schematic model of olfactometry detection with GC×GC and target MDGC (t-MDGC). See text for operational description. The LMCS device is the cryotrapping modulation method proposed to be used in this procedure.*

References

1. Belitz, H.-D.; Grosch, W.; Schieberle, P.; *Food Chemistry*, 3rd revised Edition; Springer-Verlag Berlin-Heidelberg, Germany, 2004.
2. Buldini, P. L.; Ricci, L.; Sharma J. L. *J. Chromatogr. A* **2002**, *975* 47-70.
3. Nickerson, G. B.; Likens, S. T. *J. Chromatogr.* **1966**, *21*, 1-5.
4. Bao, M.L.; Barbieri, K.; Burrini, D.; Griffini, O.; Pantani, F. *Wat. Res.* **1997**, *31*, 1719-1727.
5. Arthur, C.L.; Pawliszyn, J. *Anal. Chem.* **1990**, *62*, 2145-2148.
6. Ai, J. In *Applications of Solid Phase Microextraction*; Pawliszyn, J., Ed.; Royal Society of Chemistry, Cambridge, UK, 1999; p 22.
7. Baltussen, E.; Sandra, P.; David F.; Cramers, C. *J. Microcol. Sep.* **1999**, *11*, 737-747.
8. Bicchi, C.; Iori, C.; Rubiolo, P; Sandra, P. *J. Agric. Food Chem.* **2002**, *50*, 449-459.
9. Hayasaka, Y.; MacNamara, K.; Baldock, G. A.; Taylor, R. L.; Pollnitz, A. P. *Anal. Bioanal. Chem.* **2003**, *375*, 948-955.
10. Kreck, M.; Scharrer, A.; Bilke, S.; Mosandl, A. *Flavour Fragr. J.* **2002**, *17*, 32-40.
11. Adams, R. P. In *Identification of Essential Oil Components by GC/MS*; Allured Publishing Corporation, Carol Stream, IL, USA, 1995.
12. Sandra, P.; Proot, P. M.; Diricks, G.; David F. In *Capillary Gas Chromatography in Essential Oil Analysis*; Sandra P.; Bicchi, C., Eds.; Huethig Verlag, Heidelberg, Germany, 1987; p 29.
13. Smith, S. L. In *Capillary Gas Chromatography in Essential Oil Analysis*; Sandra, P.; Bicchi, C., Eds.; Huethig Verlag, Heidelberg, Germany, 1987; p 367.
14. David, F.; Sandra, P. In *Capillary Gas Chromatography in Essential Oil Analysis*; Sandra, P.; Bicchi, C., Eds.; Huethig Verlag, Heidelberg, Germany, 1987; p 387.
15. Bertsch, W. *J. High Resol. Chromatogr.* **1999**, *22*, 647-665.
16. Grushka, E. *Anal. Chem.* **1970**, *42*, 1142-1147.
17. Bartle K. D. In *Multidimensional Chromatography*; Mondello, L.; Lewis, A. C.; Bartle, K. D., Eds.; John Wiley & Sons Ltd, Chichester, West Sussex, UK, 2002; p 3.
18. Grob, G.; Grob, K.; Grob. K. Jr. *J. Chromatogr.* **1978**, *156*, 1-20.
19. Grob, G.; Grob, K.; Grob. K. Jr. *J. Chromatogr.* **1981**, *219*, 13-20.
20. Davis, J. M.; Giddings, J. C. *Anal. Chem.* **1983**, *55*, 418-424.
21. Martin, M.; Herman, D. P.; Guiochon, G. *Anal. Chem.* **1986**, *58*, 2200-2207.
22. Shibamoto, T. In *Capillary Gas Chromatography in Essential Oil Analysis*; Sandra, P.; Bicchi, C., Eds.; Huethig Verlag, Heidelberg, Germany, 1987; p 259.

23. Vernin, G.; Petitjean, M.; Metzger, J.; Fraisse, D.; Suon, K. N.; Scharff, C. In *Capillary Gas Chromatography in Essential Oil Analysis*; Sandra, P.; Bicchi, C., Eds.; Huethig Verlag, Heidelberg, Germany, 1987; p 287.

24. Holland, J. F.; Gardner, B. D. In *Flavor, Fragrance and Odour Analysis*; Marsili, R., Ed.; Marcel Dekker, New York, NJ, USA, 2002; p 107.

25. Bertsch, W. J. *J. High Resol. Chromatogr.* **2000**, *23*, 167-181.

26. Dallüge, J.; Beens, J.; Brinkman, U. A. Th. *J. Chromatogr. A* **2003**, *1000*, 69-108.

27. Schoenmakers, P.; Marriott, P. J.; Beens, J. *LC•GC Europe* **2003**, *June*, 1-4.

28. Phillips, J. B.; Beens, J. *J. Chromatogr. A.* **1999**, *856*, 331-347.

29. Marriott, P. J.; Shellie, R. *Trends Anal. Chem.* **2002**, *21*, 573-583.

30. Dimandja, J. M. D. *American Laboratory* **2003**, *35*, 42-53.

31. Bicchi, C.; D'Amato, A.; Rubiolo, P. J. *J. Chromatogr. A.* **1999**, *843*, 99-121.

32. Schomburg, G.; Husmann, H.; Hübinger, E.; König, W. *J. High Resolut. Chromatogr.* **1984**, *7*, 404-410.

33. Mondello, L.; Casilli, A.; Tranchida P. Q.; Furukawa, M.; Komori, K.; Miseki, K.; Dugo, P.; Dugo, G. *J. Chromatogr. A* **2006**, *1105*, 11-16.

34. Shellie, R.; Marriott, P.; Cornwell, C. *J. Sep. Sci.* **2001**, *24*, 823-830.

35. Shellie, R.; Marriott, P. *Anal. Chem.* **2002**, *74*, 5426-5430.

36. Bicchi, C.; D'Amato, A.; Manzin, V.; Rubiolo, P. *Flavour Fragrance J.* **1997**, *12*, 55-61.

37. Mosandl, A. *J. Chromatogr. A.* **1992**, *624*, 267-292.

38. van den Dool, H.; Kratz, P. D. *J. Chromatogr.* **1963**, *11*, 463-471.

39. Shao, Y.; Marriott, P.; Shellie, R.; Hügel, H. *Flavour Fragr. J.* **2003**, *18*, 5-12.

40. Shellie, R. A.; Marriott, P. J. *Analyst* **2003**, *128*, 879-883.

41 Ryan, D.; Shellie, R.; Tranchida, P.; Casilli, A.; Mondello, L.; Marriott, P. *J. Chromatogr. A.* **2004**, *1054*, 57-65.

42. Shellie, R.; Mondello, L.; Marriott, P. J; Dugo G. *J. Chromatogr. A* **2002**, *970*, 225-234.

43. Cardeal, Z. L.; Gomes da Silva, M. D. R.; Marriott, P. J. *Rap. Comm. Mass Spec.* (submitted).

44. Western, R. J.; Marriott, P. J. *J. Sep. Sci.* **2002**, *25*, 832-838.

45. Western, R. J.; Marriott, P. J. *J. Chromatogr. A* **2003**, *1019*, 3-14.

46. Murphy, R. E.; Schure, M. R.; Foley, J. P. *Anal. Chem.* **1998**, *70*, 1585-1594.

47. Ryan, D.; Morrison, P.; Marriott, P. J. *J. Chromatogr. A.* **2005**, *1071*, 47-53.

48. Venkatramani, C. J.; Xu, J.; Phillips, J. B. *Anal. Chem.* **1996**, *68*, 1486-1492.

49. Mayadunne, R.; Nguyen, T.-T.; Marriott, P. J. *Anal. Bioanal. Chem.* **2005**, *382*, 836-847.

50. Shellie, R.; Marriott, P.; Leus, M.; Dufour, J.-P.; Mondello, L.; Dugo, G.; Sund, K.; Winniford, B.; Griffith, J.; Luonge, J. *J. Chromatogr. A.* **2003**, *1019*, 273-278.

51. Ong, R.; Lundstedt, S.; Haglund, P.; Marriott, P. *J. Chromatogr. A.* **2003**, *1019*, 221-232,

52. Adahchour, M.; Wiewel, J.; Verdel, R.; Vreuls, R. J. J.; Brinkman, U. A. Th. *J. Chromatogr. A.* **2005**, *1086*, 99-106.

53. Johnson, K. J.; Synovec, R. E. *Chemometrics and Intelligent Laboratory Systems* **2000**, *60*, 225-237.

54. Di, X.; Shellie, R. A.; Marriott, P. J.; Huie, C. W. *J. Sep. Sci.* **2004**, *27*, 451-458.

55. Ryan, D.; Watkins, P.; Smith, J.; Allen, M.; Marriott, P. *J. Sep. Sci.* **2005**, *28*, 1075-1082.

56. Ryan, D.; Shellie, R.; Tranchida, P.; Casilli, A.; Mondello, L.; Marriott, P. *J. Chromatogr. A.* **2004**, *1054*, 57-65.

57. Grosch, W. *Trends Food Sci. Technol.* **1993**, *4*, 68-73.

58. Guichard, H.; Lemesle, L; Ledauphin, J.; Barillier, D.; Picoche, B. *J. Agric. Food Chem.* **2003**, *51*, 424-432.

59. Acree, T. A.; Barnard, J.; Cunningham, D. G. *Food Chem.* **1984**, *14*, 273-286.

60. Klesk, K; Qian, M. *J. Food Sci.* **2003**, *68*, 697-700.

61. Ott, A.; Fay, L. B.; Chaintreau, A. *J. Agric. Food Chem.* **1997**, *45*, 850-858.

62. Eyres, G.; Dufour, J.-P.; Hallifax, G.; Sotheeswaran, S.; Marriott, P. J. *J. Sep. Sci.* **2005**, *28*, 1061-1074.

<center>

Chapter 2

Analytical and Sensory Characterization of Chiral Flavor Compounds via Capillary Gas Chromatography on Cyclodextrins Modified by Acetal-Containing Side Chains

</center>

<center>

K.-H. Engel, M. Dregus, Ch. Becker, H. Reder, and E. Takahisa

Chair of General Food Technology, Center of Food and Life Science, Technical University of Munich, D–85350 Freising-Weihenstephan, Germany

</center>

Cyclodextrins (CD) are the most popular chiral stationary phases presently used in gas chromatographic analysis of chiral flavor compounds. To improve their gas chromatographic performance, the free hydroxy groups have been subjected to various types of derivatizations. This contribution describes a new class of CD-derivatives obtained by introducing acetal functions at positions 2 and 3 of the glucose units. Octakis(2,3-di-*O*-methoxymethyl-6-*O-tert*-butyldimethylsilyl)-γ-cyclodextrin has been synthesized as first representative. To investigate the influence of the size of the cyclodextrin torus, acetal moieties were also attached to the corresponding α- and β-analogs. In addition, chain length and type of the acetal groups were modified. The introduction of acetal moieties as side chains proved to be a useful strategy to improve the properties of cyclodextrins as chiral stationary phases in GC. Outstandingly high α-values were observed for important classes of flavor compounds. The high separation factors obtained made it possible to assess the odor properties of enantiomers via capillary gas chromatography/olfactometry without the difficulties arising from peak overlapping.

25

<center>

In Food Flavor; Tamura, H., el al.;
ACS Symposium Series; American Chemical Society: Washington, DC, 2008.

</center>

Introduction

State-of-the-art approaches to separate enantiomers by capillary gas chromatography are based on the use of modified cylodextrins (CD) as chiral stationary phases (*1,2*). To make these oligosaccharides suitable as stationary phases, the free hydroxy groups have been subjected to various types of derivatizations mainly involving alkylations and acylations (*3,4*). Recently, a new class of modified cyclodextrins bearing acetal functions at positions 2 and 3 of the glucose units has been introduced. Octakis(2;3-di-*O*-methoxymethyl-6-*O*-*tert*-butyldimethylsilyl)-γ-cyclodextrin (2,3-MOM-6-TBDMS-γ-CD) and heptakis(2,3-di-*O*-methoxymethyl-6-*O*-*tert*-butyldimethylsilyl)-β-cyclodextrin (2,3-MOM-6-TBDMS-β-CD) have been shown to be suitable for the separation of enantiomers of a broad spectrum of volatiles from various chemical classes (*5,6*).

This chapter presents examples demonstrating the versatility of this novel type of modified cyclodextrins. In particular, the influence of the size of the CD torus and of the length of the alkoxymethyl side-chains on the enantioseparations will be shown.

Pronounced enantioseparations have been achieved for some methyl branched ketones, cyclic pentenolones and furanone derivatives. The high α-values allow a sufficient separation of enantiomers and thus an unequivocal determination of their qualitative and quantitative odor properties by gas chromatography/olfactometry (GC/O). Examples of this approach will be given.

Experimental

Synthesis of Octakis(2,3-di-*O*-methoxymethyl-6-*O*-*tert*-butyldimethylsilyl)-γ-cyclodextrin (2,3-MOM-6-TBDMS-γ-CD).

Octakis(6-*O*-TBDMS)-γ-cyclodextrin was synthesized by derivatization of γ-cyclodextrin (Wako Pure Chemical Industries; Osaka, Japan) with *tert*-butyldimethylchlorosilane (Merck-Schuchardt; Hohenbrunn, Germany) according to a previously described procedure (*7*). This intermediate was heated at 100 °C under high vacuum overnight using a bulb-to-bulb distillation apparatus. The obtained dry octakis(6-*O*-TBDMS)-γ-cyclodextrin (214 mg, 0.097 mmol) was dissolved in dried dichloromethane (10 mL). Diisopropylethylamine (3.6 g, 28 mmol) was added at room temperature under stirring. The clear solution was cooled to 0 °C in an ice-water bath and methoxymethyl chloride (1.62 g, 20.1 mmol) (Aldrich; Steinheim, Germany) was added drop-wise. After stirring at 0 °C for 15 min, the solution was allowed to warm up to room temperature and then stirred at 40 °C overnight. After TLC analysis showed completion of the reaction, the mixture was poured into a

water/MTBE mixture and extracted with MTBE. The organic phase was washed with 1N HCl aq., water, sodium bicarbonate solution and saturated sodium chloride solution, and was dried over anhydrous magnesium sulfate. After concentration and purification by column chromatography (silica gel 60; toluene:ethanol = 9:1, v/v), 186 mg of the titled compound was obtained as a fine white powder.

Octakis(2,3-di-*O*-ethoxymethyl-6-*O*-*tert*-butyldimethylsilyl)-γ-cyclodextrin (2,3-EOM-6-TBDMS-γ-CD) and octakis(2,3-di-*O*-(2-methoxyethoxy)methyl-6-*O*-*tert*-butyldimethyl-silyl)-γ-cyclodextrin (2,3-MEM-6-TBDMS-γ-CD) (Figure 1) were synthesized according to the same procedure using ethoxymethyl chloride (Aldrich; Steinheim, Germany) and (2-methoxyethoxy)methylchloride (from Fluka; Buchs, Switzerland) as derivatization reagents (*8*).

Hexakis(2,3-di-*O*-methoxymethyl-6-*O*-*tert*-butyldimethylsilyl)-α-cyclodext-rin (2,3-MOM-6-TBDMS-α-CD) and heptakis(2,3-di-*O*-methoxymethyl-6-*O*-*tert*-butyldimethyl-silyl)-β-cyclodextrin (2,3-MOM-6-TBDMS-β-CD) were obtained by reaction of the corresponding 6-TBDMS-CD with methoxymethyl chloride, in analogy to the synthesis of the 2,3-MOM-6-TBDMS-γ-CD.

Preparation of the Capillary Columns

The cyclodextrin derivative was diluted (0.11 mol/kg) in polysiloxane OV-1701vi (Supelco; Bellefonte, USA). Untreated fused-silica capillary column (30 m, 0.25 mm *i.d.*) (Microquartz; Munich, Germany) was deactivated using phenyl-dimethylsilane and coated with the stationary phase by means of the static coating method (*9*). The concentration of the OV-1701vi-diluted phase in the coating solution was 0.4% (w/v), which resulted in a stationary phase film thickness of 0.25 μm. After conditioning, the overall performance of the column was tested using the Grob-I test mixture (*9*).

Characterization of Enantioseparation

The enantiodifferentiations on the chiral stationary phases were characterized by the parameters k (retention factor), α (separation factor) and R (resolution). These parameters were determined under isothermal chromatographic conditions.

Determination of Sensory Qualities and Odor Thresholds

Sensory qualities and odor thresholds of selected chiral compounds were determined by means of gas chromatography-olfactometry (GC/O) and aroma extract dilution analysis (AEDA) (*10*) using stock solutions in diethyl ether of

the reference compound (*E*)-2-decenal (1 mg/mL) and the test compounds (3-methyl-2-pentanone and 5-methyl-3-heptanone: 90 mg/mL; dihydroisophorone: 60 mg/mL; furaneol and emoxyfurone: 30 mg/mL; filbertone and coronol: 3 mg/mL). The sensory properties of the compounds were determined by three experienced assessors. Each panelist evaluated each set of dilutions obtained by AEDA at least three times. The odor of a dilution was considered as "perceived" if the assessor detected the odor at the sniffing port three times. The odor threshold is given as concentration range: the lower value corresponds to the concentration, at which no odor was detected. The higher value corresponds to the concentration at which a substance could be detected for the last time in the course of the dilution process. Each value is the mean of the data from three panelists. GC/O analysis was performed on 50% 2,3-MOM-6-TBDMS-γ-CD in OV-1701vi (enantiomers) and on DB-WAX (racemic compounds).

Results and Discussion

Structures of the Synthesized CD Derivatives

The structures of the synthesized cyclodextrin derivatives are shown in Figure 1. After blocking the 6-hydroxy position of the glucose unit with the bulky *t*-butyldimethylsilyl (TBDMS) group, acetal functions were introduced in positions 2 and 3 by reaction with the corresponding alkoxymethyl chlorides. To investigate the influence of the size of the CD torus on enantioseparations, methoxymethyl groups were introduced in α, β and γ-cyclodextrins (6, 7 and 8 glucose units, respectively). Modifications of the acetal-containing side chains were achieved by introducing the elongated ethoxymethyl moiety (2,3-EOM-6-TBDMS-γ-CD) and the polar (2-methoxyethoxy)methyl group (2,3-MEM-6-TBDMS-γ-CD).
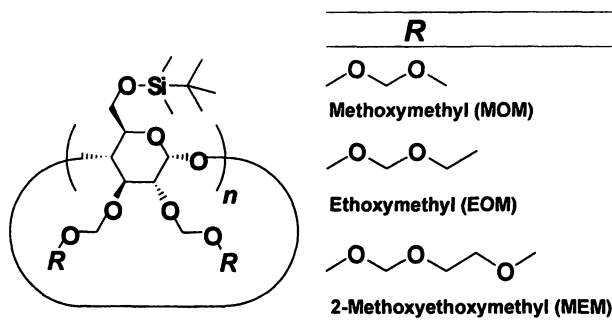

Figure 1. Incorporation of acetal moieties into cyclodextrins.

Enantioseparations on 2,3-MOM-6-TBDMS-γ-CD

2,3-MOM-6-TBDMS-γ-CD is suitable for the separation of enantiomers of a broad spectrum of volatiles from various chemical classes. A total of 125 pairs of enantiomers could be separated (5). As examples, Figure 2 presents enantioseparations for a methyl branched ester, a methyl branched ketone, monoterpenes and norisoprenoids.
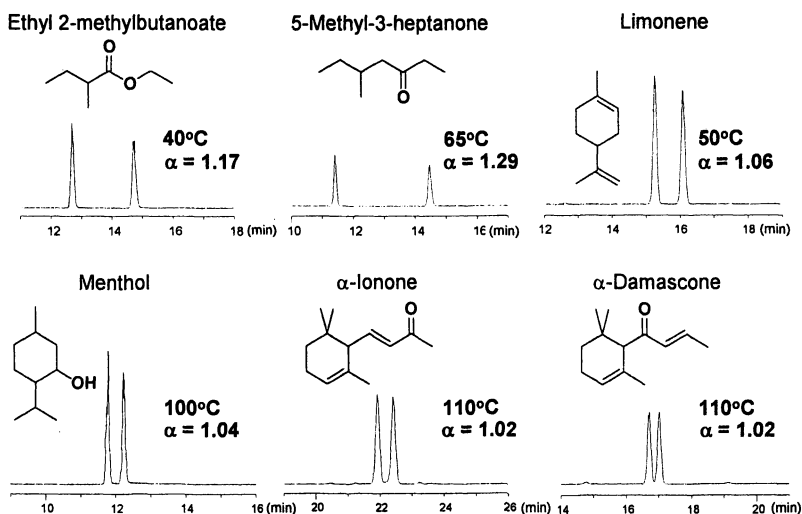

Figure 2. Enantioseparations on 2,3-MOM-TBDMS-γ-CD.

Figure 3 shows the separation of the enantiomers of a homologous series of γ- and δ-lactones, an important class of naturally occurring aroma compounds.

Effect of Torus Size

The spectrum of compounds for which enantiomers could be separated on 2,3-MOM-6-TBDMS-β-CD was more limited compared to the γ-CD derivative and the enantioseparations achieved were generally less pronounced (6). Unusually high separation factors were observed for 2-alkyl esters of short chain acids (C_2-C_6). For 2-pentyl acetate (α: 3.80; 40°C) it could be shown that only one enantiomer is retained significantly on the chiral stationary phase whereas the other one behaves like the hydrocarbons used as references (6). As shown in Figure 4, chain elongation of the acid moieties results in drastic reduction of the resolutions of the enantiomers of 2-pentyl alkanoates on 2,3-MOM-6-TBDMS-β-CD. In contrast, on 2,3-MOM-6-TBDMS-γ-CD the separation of the enantiomers of 2-pentyl acetate was not as pronounced. However, baseline separation of the enantiomers could be achieved for the homologous series of 2-pentyl alkanoates.
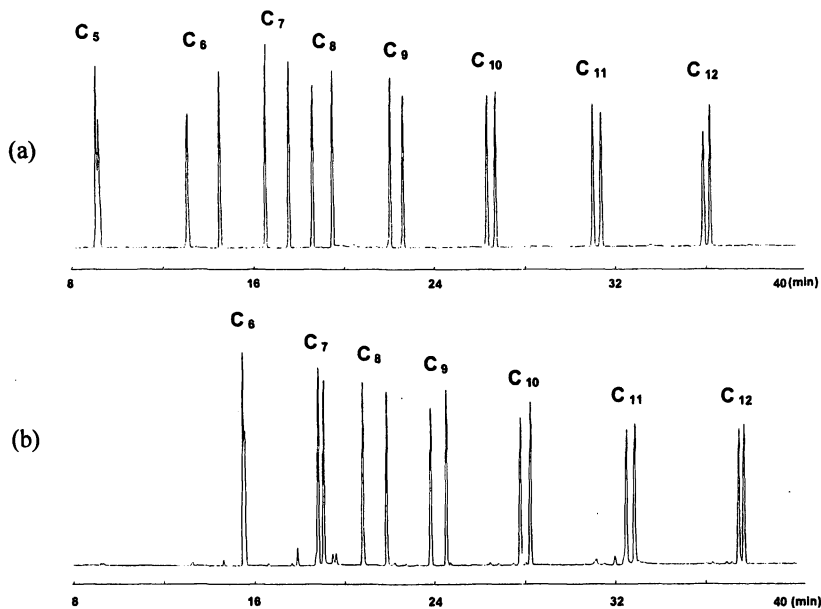
Figure 3. Separation of lactones enantiomers using 2,3-MOM-TBDMS-γ-CD
(a) γ-lactones (C_5-C_{12}), (b) δ-lactones (C_6-C_{12})
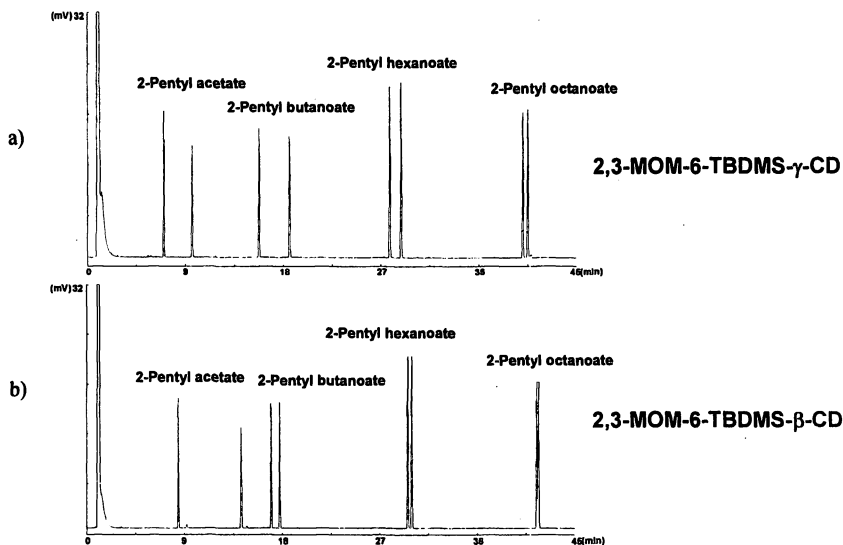*Temperature: 100 °C/ 2 min hold// 2.0 °C/min rate.*

Figure 4. Enantioseparation of 2-pentyl alkanoates
Temperature: 40 °C/ 2 min hold // 2.0 °C/min rate.

As shown in Table I, elongation of the chain length of the alcohol esterified in 2-alkyl esters resulted in steady decreases of the α-values on both stationary phases.

Table I. Enantioseparation of 2-Alkyl Acetates

	2,3-MOM-6-TBDMS-β-CD		2,3-MOM-6-TBDMS-γ-CD	
	α	T (°C)	α	T (°C)
2-Pentyl acetate	3.80	40	2.44	35
2-Heptyl acetate	1.72	70	1.30	60
2-Nonyl acetate	1.25	95	1.10	90

Using 2,3-MOM-6-TBDMS-γ-CD as stationary phase, high α-values have been observed for hydroxyketones, methyl branched ketones, cyclic pentenolones and furanones (5). Representatives from these classes were chosen to demonstrate the effect of the size of the CD-torus on enantioseparations. As shown in Figure 5, the resolutions generally decreased with decreasing size of the CD torus.

Effect of Alkoxymethyl Side Chains

As shown in Figure 6 for coronol, furaneol and acetylfuraneol, elongation and increase of the polarity of the alkoxymethyl side-chain drastically reduced the resolutions of enantiomers. Similar effects have been demonstrated for 3-methyl-2-pentanone, filbertone and acetoin (6).

Sensory Evaluation of Enantiomers by GC/O

It has been demonstrated for a broad spectrum of chiral compounds that enantiomers may have different sensory properties (11). Capillary gas chromatography-olfactometry using chiral stationary phases offers the possibility to assess odor qualities as well as odor thresholds of enantiomers. One of the essential prerequisites for a successful application of this approach is the sufficient resolution of the enantiomers. Considering the high separation factors achieved for the enantiomers of many important aroma compounds on 2,3-MOM-6-TBDMS-γ-CD, this chiral stationary phase seemed an ideal tool for sensory assessments via GC/O. Methyl branched ketones and some cyclic compounds were selected as candidates. Table II shows odor properties for the
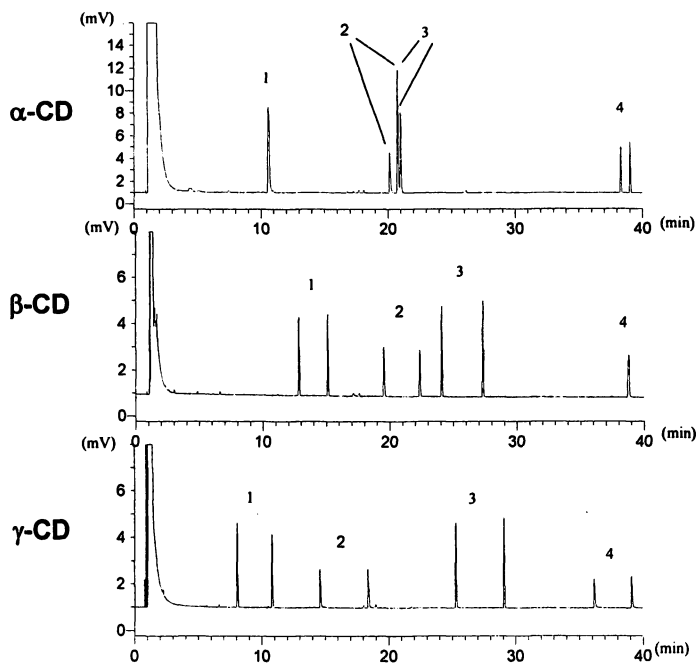
*Figure 5. Effect of torus size on enantioseparation (2,3-MOM-TBDMS-CDs)
(1): 3-methyl-2-pentanone, (2): acetoin, (3): filbertone; (4): coronol
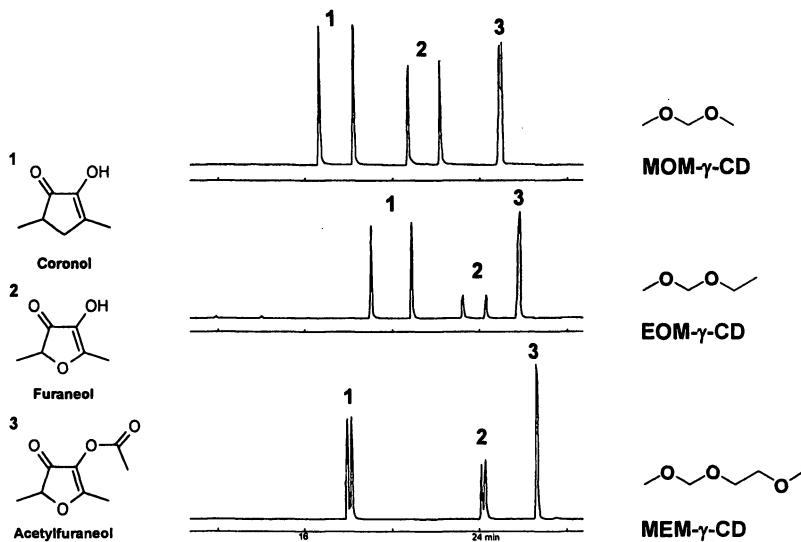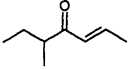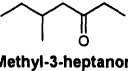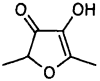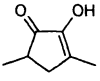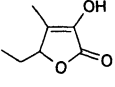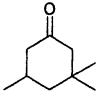Temperature: 100 °C/ 2 min hold// 2.0 °C/min rate*

*Figure 6. Effect of alkoxymethyl side chains on enantioseparations
Temperature: 70 °C/ 2 min hold// 2.0 °C/min rate.*

33

enantiomers obtained by GC/O on 2,3-MOM-6-TBDMS-γ-CD and for the racemic mixtures determined by GC/O on DB-WAX column.

The enantiomers of 3-methyl-2-pentanone differed significantly both in odor quality and potency. The enantiomer exhibiting a fruity, sweet note was approximately seven times more potent than its antipode. A comparison with the data obtained for filbertone showed that a structural modification of the methyl branched ketone by chain elongation and insertion of a double bond in α-

Table II. Sensory Properties of Enantiomers of Some Aroma Compounds

compound	odor quality [a]	odor threshold [e] (ng/L in air)	
methyl branched ketones			
3-Methyl-2-pentanone	(I) [b] solvent, adhesive (II) [c] fruity, sweet	(I) (II) (rac.) [d]	11000 - 22000 1500 - 3000 500 - 1000
Filbertone	(I) roasty, hazelnut, sweet (II) roasty, hazelnut, sweet	(I) (II) (rac.)	0.55 - 1.1 0.3 - 0.6 0.4 - 0.8
5-Methyl-3-heptanone	(I) spicy, dill, salad herbs (II) spearmint, menthol, salad herbs	(I) (II) (rac.)	180 - 360 120 - 240 140 - 280
cyclic compounds			
Furaneol	(I) sweet, fruity, strawberries, caramel (II) sweet, fruity, strawberries, caramel	(I) (II) (rac.)	5 - 10 1.5 - 3 0.4 - 0.8
Coronol	(I) musty, moldy (II) caramel, sweet	(I) (II) (rac.)	150 - 300 30 - 60 16.5 - 33
Emoxyfurone	(I) spicy, bouillon cube (II) spicy, bouillon cube, sweet, coffee	(I) (II) (rac.)	10 - 20 10 - 20 12 - 24
Dihydroisophorone	(I) mate tea, floral, spicy (II) mate tea, floral, spicy	(I) (II) (rac.)	325 - 650 190 - 380 135 - 270

[a] Determined after injection of 0.5 μl of stock solutions as described under Experimental. [b] First eluted enantiomer. [c] Second eluted enantiomer. [d] Racemic mixture. [e] Thresholds of the enantiomers determined on 2,3-MOM-6-TBDMS-γ-CD; thresholds of racemic mixtures determined on DB-WAX.

position to the carbonyl group results in a drastic reduction of the odor threshold of the racemic mixture. However, both enantiomers of filbertone exhibited the same odor qualities and in contrast to previously reported GC/O data (12,13), there were no significant differences between the thresholds of the enantiomers.

For 5-methyl-3-heptanone the odor thresholds of the enantiomers also did not differ significantly. However, the enantiomers show distinct differences in odor qualities.

The cyclic pentenolone coronol (2-hydroxy-3,5-dimethyl-2-cyclopenten-1-one) has been identified as a volatile constituent of roasted sesame seeds (14). Only one of the enantiomers exhibited a caramel, sweet note whereas the less potent antipode possessed a musty, moldy character.

The odor threshold determined for racemic furaneol is in agreement with the formerly reported value of 1.0 ng/L in air (15). Both enantiomers exhibited the typical fruity and caramel-like notes; one of them was slightly more potent.

Emoxyfurone (5-ethyl-3-hydroxy-4-methyl-2(5H)-furanone) is known as key aroma compound of various foods, such as coffee, barley malt, chardonnay wine, blackberries and raspberries (16-20). The odor descriptions reported in these studies vary considerably. GC/O assessment on 2,3-MOM-6-TBDMS-γ-CD revealed spicy and bouillon cube-like notes for both enantiomers and additional sweet and coffee-like character for one of the enantiomers. Both enantiomers possessed the same odor threshold.

Both enantiomers of dihydroisophorone had mate tea-like, floral and spicy odor qualities and exhibited only slight differences in odor potency.

The few examples investigated in this study reflect the spectrum of "odor scenarios" to be expected for chiral volatiles: (i) the sensory properties of the enantiomers differ both in quality and intensity (3-methyl-2-pentanone, coronol); (ii) the enantiomers possess similar odor qualities but differ in odor thresholds (furaneol); (iii) the enantiomers possess similar odor thresholds but differ in odor qualities (5-methyl-3-heptanone, emoxyfurone); (iiii) there are no differences between the enantiomers in terms of odor quality and potency (filbertone, dihydroisophorone).

Acknowledgement

References

1.   Juwancz, Z.; Szejtli, J. Trends Anal. Chem.. 2002, 21, 379-388.
2.   König, W. A.; Hochmuth, D. H. J. Chromatogr. Sci. 2004, 42, 423-439.

3. Bicchi, C. In *Flavour and Fragrance Chemistry*; Lanzotti, V.; Taglialatela-Scafati, O., Eds.; Kluwer Acaademic Publisher: Dordrecht, 2000; pp 177-186.

4. Schurig, V. *Trends Anal. Chem.*. **2002**, *21*, 647-660.

5. Takahisa, E.; Engel, K.-H. *J. Chromatogr. A.* **2005**, *1063*, 181-192.

6. Takahisa, E.; Engel, K.-H. *J. Chromatogr. A.* **2005**, *1076*, 148-154.

7. Fuegedi, P. *Carbohydr. Res.* **1989**, *192*, 366-3698.

8. Takahisa, E. Modified cyclodextrins as chiral stationary phases for capillary gas chromatographic separation of enantiomers. Dissertation, Technical University Munich, 2005.

9. Grob, K. *Making and Manipulating Capillary Columns for Gas Chromatography*; Huethig: Heidelberg, 1986.

10. Ullrich, F.; Grosch, W. *Z. Lebensm Unters. Forsch.* **1987**, *184*, 277-282.

11. Brenna, W.E. ; Fuganti, C.; Serra, S. *Tetrahedron- Asymmetr.* **2003**, *14*, 1-42.

12. Güntert, M.; Emberger, R.; Hopp, R.; Köpsel, M.; Silberzahn, W.; Werkhoff, P. *Z. Lebensm. Unters. Forsch.* **1990**, *192*, 108-110.

13. Güntert, M.; Emberger, R.; Hopp, R.; Köpsel, M.; Silberzahn, W.; Werkhoff, P. In *Flavor Science and Technology*; Bessiére, Y.; Thomas A. F., Eds.; John Wiley & Sons: Chichester, 1990; p. 29.

14. Nakamura S.; Nishimura O.; Masuda H.; Mihara S. *Agric. Biol. Chem.* **1989**, *53*, 1891-1899.

15. Blank, I.; Schieberle, P. *Flavour and Fragrance Journal* **1993**, *8*, 191-195.

16. Sanz, Ch.; Czerny, M.; Cid, C.; Schieberle, P. *Eur. Food Res. Technol.* **2002**, *214*, 299-302.

17. Fickert, B.; Schieberle, P. *Nahrung* **1998**, *42*, 371-375.

18. Büttner, A. *J. Agric. Food Chem.* **2004**, *52*, 2339-2346.

19. Klesk, K.; Qian, M. *J. Agric Food Chem.* **2003**, *51*, 3436-3441.

20. Klesk, K.; Qian, M.; Martin, R. R. *J. Agric Food Chem.* **2004**, *52*, 5155-5161.

Chapter 3

Improved Application of Semiconducting Metal Oxides as a Detector for High-Resolution Gas Chromatography

Hajime Komura[1], Mariko Sugimura[2], Kazuo Onaga[2], and Hiroshi Koda[2]

[1]Suntory Institute for Bioorganic Research, Wakayamadai 1–1–1, Shimamoto, Mishimagun, Osaka 618–8503, Japan
[2]FiS Inc., Kitazono 3–36–3, Itami, Hyogo 664–0891, Japan

Platinum impregnated metal oxide semiconductor gas sensing elements, one with tungsten oxide and the other with tin oxide, were successfully applied as the detection element for high-resolution gas chromatography when moisturized oxygen was used as reagent gas. Among the semiconductors, the tin oxide semiconductor had greater selectivity, more sensitivity to fatty acids and less sensitivity to hydrocarbons. In contrast, the tungsten oxide semiconductor had more universal sensitivity to the compounds tested.

In general, when we perform non-routine GC analyses the choice of detector(s) can influence the results we obtain. In the case of flavor analysis, particularly identifying impact aroma compound(s), GC-Sniffing or GC-O (GC-Olfactometry), becomes one of the key and unavoidable experiments. However, GC-Sniffing is stressful to researchers since the analysis must be performed continuously and a high level of concentration is required. Therefore, it would be convenient to have a detector which has similar selectivity to our nose since it could be used to run the samples prior to GC-Sniffing to determine which retention time regions upon GC-Sniffing to concentrate.

© 2008 American Chemical Society

Among gas sensing elements, metal oxide semiconductors (MOS) might be suitable candidates for detecting organic volatiles because MOS elements use some type of "active oxygen" species present on the surface of the element to oxidize the organic components when the sensor element encounters them. The change in the amount of "active oxygen" on MOS can be monitored as the change of the conductivity of the MOS (*1*). In addition to the chemical nature of the element, MOS sensor elements have high element stability and durability, high data reproducibility, and high uniformity between production lots though they are inexpensive. Because of these benefits, they are used in different types of household equipment such as gas leak detectors and breath analyzers, as well as in scientific apparatus such as "e-noses". However, the MOS element is slow to recover after sensing because of the slow regeneration of the "active oxygen" level on the element. This phenomenon has to be overcome when we incorporate the MOS element in the detector for high resolution gas chromatography which produces peak widths as narrow as a couple of seconds or less. Application of metal oxide semiconductors to a detector for high resolution GC has been studied mainly by two independent groups (*2, 3*). Kohl et al. (*4*) achieved a dramatic improvement in appearance of peak sharpness, almost comparable to the FID responses by plotting the first derivative of the conductance change of the element against retention time. However, the problem of slow regeneration of "active oxygen" has not been overcome.

Experimental

Chemicals

Solvents used in this experiment were the highest grade available from Nacalai Tesque, Japan, and were used without re-distillation. All of the authentic chemicals used for chromatography were purchased from Nacalai Tesque or from Tokyo Kasei Kogyo Co., Ltd. (TCI), Japan.

GC Samples

An artificial mixture for the test chromatograms was prepared by dissolving authentic chemicals, hexanal **1**, 3-methylbutyl acetate **2**, *d*-limonene **3**, 2-octanone **5**, 2,3,5-trimethylpyrazine **6**, 1-octanol **9**, and benzyl alcohol **11**, in ethanol at the final concentration *ca.* 100 ppm.

A lemon flavor mixture was obtained from a flavor house, and diluted with ethanol prior to GC analysis.

The red wine extract was prepared in the following way: a red wine (200 mL), purchased in Osaka, was distilled under reduced pressure at *ca.* 2.0 kPa

(*ca.* 15 mmHg), on a water-bath heated to 40 °C. A finger-type cold trap (cooled with dry-ice/ethanol mixture) was placed between the distillate receiver and vacuum pump while the condenser and receiver were chilled with coolant maintained at –5 °C. Distillation was finished after the residue level reached *ca.* 50 mL. The distillates in the receiver and cold trap were combined for extraction. Combined distillate (*ca.* 150 mL) was diluted with *ca.* 150 mL of water, and extracted 3 times with 150 mL aliquots. of methylene chloride. The extracts were combined, dried over anhydrous sodium sulfate, concentrated under atmospheric pressure to 1 mL, and stored in a refrigerator until GC analysis.

GC Equipment

Agilent Technologies' 5890 Series II gas chromatograph with an FID was controlled by ChemStation software (Rev. A.09.03). A DB-WAX (30 m × 0.25 mm id, d_f - 0.25 μm; J&W Scientific) was used. Helium was used as carrier gas at appropriate flow rates. The column effluent was split to the FID and the sensor detector with a Chromfit Y Splitter (GL Science, Tokyo). The split ratio between the FID and the sensor detector was set to 7:1 by adjusting the internal diameters and the lengths of the empty capillary columns after the Y-splitter.

For GC analysis the oven temperature was programmed from 50 °C (10 min isothermal) to 200 °C at 4 °C/min (final hold was 30 min). The injector and detector temperatures were 230 °C.

Sensor Detector

Bead type metal oxide sensor elements, a K-type with tungsten oxide and an EN1-type with tin oxide both impregnated with a small amount of platinum, were prepared according to a published method (*5*). The sensor element (Figure 1C) was placed in a sensor holder (Figure 1B) so that reagent gas and column effluent could reach the element efficiently. For operation, the sensor bead was heated by applying direct current to the heater coil imbedded in the sensor element. The temperature was controlled by adjusting the input voltage of the heater current. The conductivity changes of the sensor element were detected as voltage changes by a circuit operating at DC 5 V. The signal outputs from the sensor and the FID were transferred to ChemStation *via* an Agilent AD converter, Interface 35900E, and stored as data files.

The reagent gas, moisturized oxygen gas, was obtained by bubbling flow-controlled oxygen gas through purified water (supplied by an Elix plus Milli-Q water purification system, Millipore) in a moisturizing flask. In this experiment, 10 mL/min oxygen from a cylinder was introduced to a moisturizing flask. The moisturized oxygen was then introduced to the T-connector interface (Figure 1A) assembly on which a sensor holder (Figure 1B) was sitting. The interface

assembly, built on an extra injection port and heated to 250 °C using auxiliary temperature control in ChemStation, was covered with glass wool to maintain the temperature. An empty capillary column was connected to the end of the separation column. It was inserted at the bottom of the modified injection port and passed through the T-connector interface to reach as close as possible to the sensor bead without touching it.
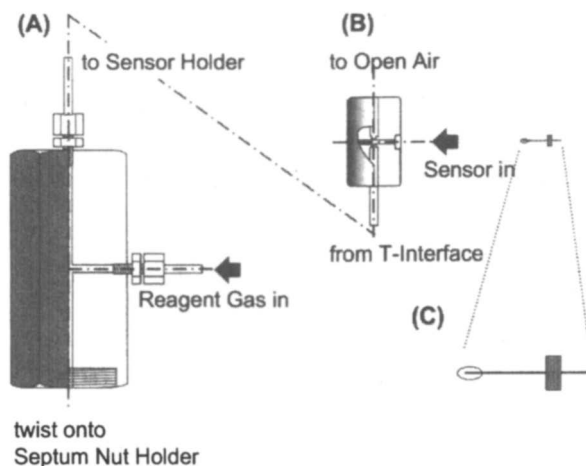

Figure 1. Schematic diagrams of the T-connector interface (A), sensor holder (B) and sensor element (C). Diagrams are not to scale.
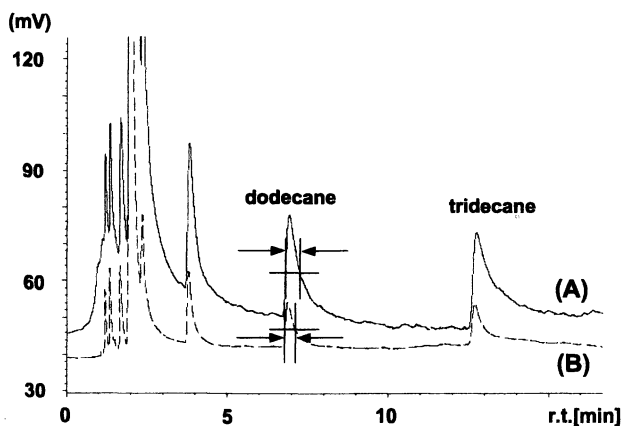

Figure 2. Effect of moisture in oxygen on hydrocarbon responses obtained on the EN1-type sensor. (A) Without and (B) with moisture in reagent gas. The gaps between arrows represent the peak widths at half height.

Results and Discussion

For this study, we selected two types of MOS elements, a K-type with tungsten oxide and an EN1-type with tin oxide, both impregnated with a small amount of platinum. To improve the recovery after sensing, high temperatures, *ca.* 440-450 °C for EN1 and 450-460 °C for K-type, were applied to the element using a heating coil imbedded in the element. Application of oxygen as a reagent gas was successful in improving peak shape though it did cause a loss of sensitivity. However, oxygen alone was not sufficient for improving peak shape. Addition of moisture to oxygen gave a slight improvement (Figure 2). The peak widths at half height of *n*-dodecane and n-tridecane decreased from 25.4 s to 15.9 s and from 37.0 s to 20.0 s, respectively, with the EN1-type sensor. Therefore, moisturized oxygen was used as the reagent gas throughout the experiments. The effect of oxygen can be rationalized by the direct effect of oxygen on the generation of "active oxygen" species on the ceramics. However, no rationalization of the effect of moisture could be postulated. For capillary GC a flow rate of 10 mL/min of reagent gas was sufficient. When higher flow rates of reagent gas were applied, cooling of the element and dilution of the effluent were observed.

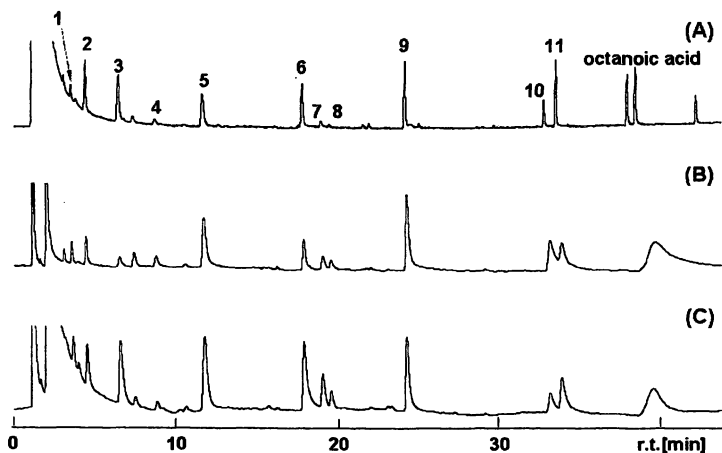*Figure 3. Comparison of the signal responses on (A) FID, (B) EN1-type, and (C) K-type elements*

For test runs, eight compounds with different functional groups were chosen to see if any differences in detector response could be observed. The compounds were hexanal **1**, 3-methylbutyl acetate **2**, *d*-limonene **3**, 2-octanone **5**, 2,3,5-trimethylpyrazine **6**, 1-octanol **9**, benzyl alcohol **11**, and dibutyl sulfide.

However, dibutyl sulfide was later omitted because the sulfide was easily oxidized and its original concentration was difficult to maintain. Drastic peak broadening was observed at retention times about 35 min and longer (Figure 3). At this retention time the oven temperature was about 150 °C. After several examinations it became clear that this was because of the "cold spot effect" caused by cold reagent gas flow introduced without preheating. Though the T-connector interface block (Figure 1A) itself was heated as high as 250 °C, cooling of the capillary column running through the interface occurred. Further improvement is needed to eliminate this problem such as to heat the reagent gas before it contacts the capillary column in the T-connector. Except for the cold spot problem, application of moisturized oxygen improved the peak shape with peak widths at half height being about three times wider than those obtained by FID (Figure 4).
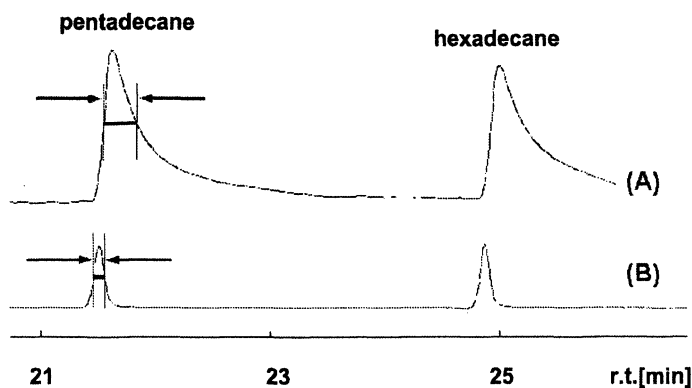

Figure 4. Comparison of peak widths at half height (the gaps between the arrows) on (A) K-type element and (B) FID. Sample: Hydrocarbon mixture.

Comparing the chromatograms obtained with K-type and EN1-type elements (Figure 3), the K-type with tungsten oxide based element gave a closer response to the FID showing that it had a low selectivity for the test compounds. On the other hand, the EN1-type with tin oxide based element had more selectivity to the test mixture. Among the test compounds, 3-methylbutyl acetate **2**, limonene **3**, and 2,3,5-trimethylpyrazine **6** had lower responses with the EN1-type element. The chromatographic data obtained on the K-type and the EN1-type elements are summarized in Table I. In general, the amount of the component is better correlated to peak area than to peak height. However, in the case of MOS elements, peak areas are drastically affected by the slow recovery rate towards the baseline level caused by slow regeneration of the "active oxygen" on the element. Therefore, peak heights were employed for comparing

the response from each element. The relative peak heights to 1-octanol are listed in Table I, together with the peak height ratio between EN1 and K-types. It is obvious that the EN-1-type element is the least sensitive to limonene **3** and the most sensitive to hexanoic acid **10**. Among others, hexanal **1** and the monoterpene cyclic ethers, *cis-* and *trans-*limonene oxides **7** and **8** had a slightly higher response, while alcohols including benzyl alcohol were in a medium group.

A lemon flavor mixture and red wine extract were analyzed as examples of practical analysis. In the case of lemon flavor most of the monoterpenes except citrals were poorly detected with the EN1-type (Figure 5). It should be noted that cineoles, terpineols, and linalool were not detected with the EN1-type though alcohols and ethers were expected to display medium or slightly higher sensitivity based on the results presented in Figure 3. This might be related with the fact that on electron impact ionization mass spectrometric detection these compounds tend to lose their oxygen functional group by a decomposition to the corresponding dehydrated hydrocarbons. The hydrocarbons have little or no response on the EN1-type sensor as shown with limonene **3**. In the red wine samples several components were observed as intense peaks at retention times of *ca.* 12.0 min, 15.5 min, 19.5 min, 23.5 min, 24.5 min, and 28.0 min, on the EN1-type sensor (Figure 6). These peaks might be some short chain fatty acids which are abundant in wines.

Table I. Comparison of the selectivity of two sensing elements

RT* (min)	Compound	Relative Height**		Ratio***
		EN1	K	EN1/K
3.6	hexanal **1**	28	23	125
4.4	3-methylbutyl acetate **2**	36	60	60
6.5	limonene **3**	13	84	15
8.8	3-methylbutanol **4**	15	18	86
11.7	2-octanone **5**	66	90	74
17.9	2,3,5-trimethylpyrazine **6**	40	59	68
19.0	*cis-*limonene oxide **7**	19	16	115
19.6	*trans-*limonene oxide **8**	12	9	134
24.2	1-octanol **9**	100	100	100
33.2	hexanoic acid **10**	40	12	339
33.8	benzyl alcohol **11**	37	31	119

*Compounds and retention times as shown in Figure 3.

Peak height normalized to 1-octanol **9 peak as 100.
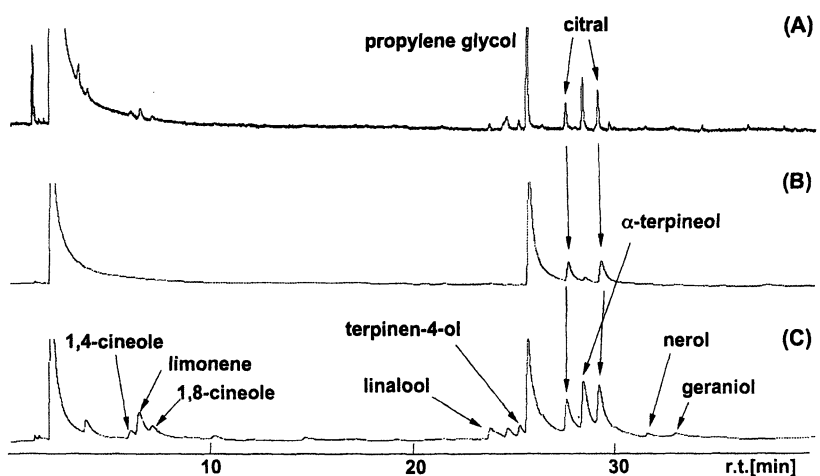
***Ratio expressed as a percentage.

Figure 5. Comparison of the signal responses on (A) FID, (B) EN1-type, and (C) K-type elements. Sample: Lemon flavor mixture.
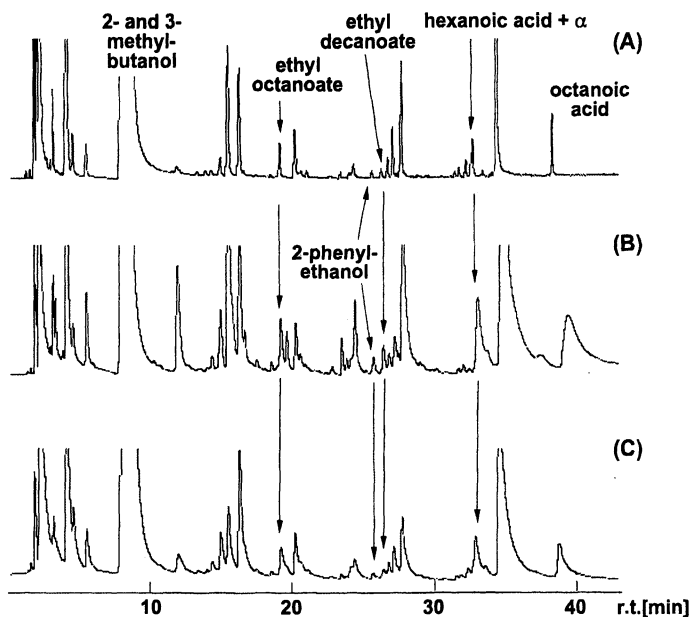

Figure 6. Comparison of the signal responses on (A) FID, (B) EN1-type, and (C) K-type elements. Sample: Red wine extract.

Conclusion

Metal oxide gas sensing elements, K-type with tungsten oxide and EN1-type with tin oxide, were successfully applied as the detectors in high resolution GC by the application of moisturized oxygen as a reagent gas. However, further improvement is required, particularly the cold spot problem and peak broadening caused by slow regeneration of the "active oxygen" species on the semiconductor element. This could be achieved by mathematical treatment of the data and/or by improving the regeneration itself. More variation in the sensor elements with wider functional group selectivity should be considered in order to develop the metal oxide semiconducting element into a facile GC detector. Though at this stage, two types of MOS elements studied in this paper did not respond in a similar way to the human nose to replace GC-Sniffing. Developing new elements with unique selectivity and their combinations would open a way to "e-nose" detectors for high-resolution GC. In addition, when the multi-sensor element detector becomes practical it can be combined with chemometrics to allow wider varieties of information to be mined. Thus its refinement should facilitate new application tools which could be used in fields such as metabolomic analysis.

References

1. Bardeen, J.; Morrison, S. R. *Physica* **1954**, *20*, 873-884.
2. Hivert, B.; Hoummady, M.; Mielle, P.; Mauvais, G.; Henrioud, J. M.; Hauden, D. A. *Sensors & Acutuators B* **1995**, *26-27*, 242-245.
3. Hofmann, T.; Schieberle, P.; Krummel, C.; Freiling, A.; Bock, J.; Heinert, L.; Kohl, D. *Sensors and Actuators B* **1997**, *41*, 81-87.
4. Kohl, D.; Eberheim, A.; Schieberle, P. *Thin Solid Films* **2005**, *490*, 1-6.
5. Ihokura, K. *New Materials & New Process* **1981**, *1*, 43-50.

Chapter 4

Measurement of Flavor–Soy Protein Interactions in Low-Moisture Solid Food Systems by Inverse Gas Chromatography

Qiaoxuan Zhou and Keith R. Cadwallader*

Department of Food Science and Human Nutrition, University of Illinois at Urbana-Champaign, 1302 West Pennsylvania Avenue, Urbana, IL 61801

Selective binding of flavor compounds by soy proteins can lead to persistence of off-flavors and/or flavor fade in formulated soy products. Currently, there is limited information concerning binding of volatile flavor compounds by soy proteins in low-moisture foods. An inverse gas chromatographic (IGC) method was developed and applied to study the influence of flavor compound chemical structure and environmental relative humidity (RH) on flavor-soy protein interactions in solid food systems. Binding of selected buttery flavor compounds to wheat versus soy-containing crackers was measured to evaluate the potential of using this technique to measure flavor binding in real foods. Sensory evaluation also was conducted to further evaluate the possibility of using IGC data to predict the sensory impact of flavor binding.

45

Flavor is an important factor in determining food product acceptance. Flavor-food matrix interactions directly impact flavor quality by influencing flavor retention during processing and storage as well as affecting the rate and extent of flavor release during food consumption. Strong binding of certain flavor compounds not only can cause flavor fade but also may result in unbalanced flavor profiles or even development of objectionable flavors.

Soy is an ideal food in terms of its nutritional value, and studies have linked the consumption of soy with numerous health benefits (*1,2*). However, soy consumption in the U.S. has been somewhat limited because American consumers find soy-associated flavors unacceptable. These off-flavors include beany, green, and grassy aromas and bitter and astringent tastes (*3-5*). In addition to the presence of off-flavors, soy protein can selectively bind with flavor compounds. This binding can result in retention of off-flavors and/or flavor fade, both of which will negatively impact consumer acceptance of soy products (*5-7*).

Attempts have been made to better understand soy protein-flavor interactions (*8-15*). Most studies were conducted with aqueous model systems and made use of static headspace or equilibrium dialysis techniques (*8-13*). In general, the equilibrium-based methods are not sensitive enough for the study flavor binding under conditions that simulate real food systems. Furthermore, these methods do not allow for the study of protein-flavor binding in dry and semi-dry food systems. Few studies have been concerned with flavor binding by soy proteins in the dry state (*14,15*). In addition, the influence of moisture, a key variable affecting binding, has not been adequately evaluated. Therefore, there is need for a rapid and sensitive method for evaluation of flavor-matrix interactions in low-moisture systems. Especially desired is a method that can evaluate the impact of humidity on flavor binding and which gives results relevant to sensory studies.

Due to its extreme sensitivity, inverse gas chromatography (IGC) has great potential for the measurement of adsorption of flavor compounds at very low concentrations to closely simulate conditions encountered in real foods (*16-20*). In addition, IGC is suitable for the study of flavor binding in dry and semi-dry materials under controlled relative humidity.

The present report summarizes our studies on the development and validation of an IGC system for the study of the binding of selected volatile compounds by soy protein isolate under controlled relative humidity (*21,22*). In addition, the ability of IGC to predict sensory impact of flavor binding in a real food system is also discussed (*23*).

Materials and Methods

Materials

Analytical grade (> 99% purity) hexane, 1-hexene, limonene, ethyl butyrate, 2-hexanone, hexanal, *trans*-2-hexenal, 1-hexanol, *cis*-3-hexen-1-ol, *trans*-2-

hexen-1-ol, diacetyl (butane-2,3-dione), butyric acid, γ-butyrolactone, hexanal, 2-ethylbutyric acid and pentane-2,3-dione were obtained commercially (Aldrich Chemical Co.; St Louis, MO). Food grade (> 99% purity) diacetyl and butyric acid used in crackers prepared for sensory study were obtained from Aldrich Flavor and Fragrance (St Louis, MO). Representative soy protein isolates (protein content > 90%; fat content < 4%) were provided by Archer Daniels Midland Co. (ADM; Decatur, IL). Other ingredients (flour, shortening, baking powder, and salt) used to prepare the crackers were purchased at a local supermarket.

IGC Column Preparation

Sieved soy protein isolate or ground cracker was packed into a deactivated glass tube (17.8 cm x 4 mm I. D.; Supelco; Bellefonte, PA) (*21*). Each column was connected to the IGC system and conditioned to the desired temperature and RH level under carrier gas for at least 48 h prior to experiments, and was re-conditioned whenever temperature was changed.

Preparation of Soda Crackers

Plain soda crackers used in IGC measurements were prepared using the formulations given in Table I (*23*). Diacetyl or butyric acid flavored crackers used in sensory study were prepared by adding 10 μL of an aqueous flavor solution (containing 1.311 mg of butyric acid or 2.877 mg of diacetyl) to 30 g of freshly prepared and ground plain crackers, which was kept in a 250 mL Teflon®-lined screw cap glass bottle and allowed to reach equilibrium.

Table I. Cracker Formulations

ingredient	wheat cracker	soy-containing cracker
flour (g)	100.0	75.0
SPI (g)	0.0	25.0
salt (g)	2.0	2.0
baking powder (g)	2.4	2.4
shortening (g)	11.2	11.2
water (g)	59.2	64.0

SOURCE: Reproduced from reference 23. Copyright 2006 American Chemical Society.

IGC Measurements

The IGC instrument used in the present study was modified from a conventional GC (6890 Series; Agilent Technologies, Inc., Palo Alto, CA) equipped with a flame ionization detector (FID). Desired RH conditions were readily created and precisely controlled by mixing a dry and a wet (saturated with water vapor) helium gas flows at proper ratio. The configuration of the instrumentation and the methodology for conducting IGC experiments have been described in detail (*21, 22*). Measurements were performed on two different columns for each RH-SPI set studied, with the mean values reported. Statistical analysis (*t*-test or ANOVA; $p < 0.05$) was conducted to determine statistical differences between means.

Sensory Analysis

Prior to sensory evaluation, 2.0 g of the flavored cracker were transferred to a sniffing bottle (125 mL Nalgene Teflon® FEP wash bottle with siphon tube removed from the cap; Fisher Scientific, Pittsburgh, PA). Each bottle was covered with aluminum foil and labeled with a 3-digit random number. Perceived cracker headspace aroma intensity was evaluated using the 2-AFC with warm-up method developed by Thieme and O'Mahony (*24*). A total of 30 panelists (21 female, 9 male; 19 to 55 y old) participated in this study. Data of the 2-AFC tests were analyzed by beta-binomial statistics using the IFPrograms™ software (v. 7.3; The Institute for Perception, Richmond, VA).

Results and Discussion

System Performance

Results showed excellent repeatability between replicate injections and very good reproducibility across columns (variation < 3% and 6%, respectively). Thermodynamic data determined for hexane, hexanal and 1-hexanol under dry conditions were comparable to available literature values (*21*). Typically, an isotherm can be generated in hours (*21*), which demonstrates the rapid and high throughput nature of this method for sorption isotherm measurement.

Effect of Flavor Molecule Functional Group on Binding

Heat of adsorption data determined at 0% RH suggested that apparently binding strengths of the selected volatile probes to soy proteins were related to

the functional groups these compounds carry (Figure 1; *22*). For hydrocarbons, mainly weak nonspecific interactions (van der Waals dispersion forces) were likely involved, thus only weak binding forces were observed. For the ester, ketone, aldehyde and alcohol compounds probably both specific (hydrogen bonding, dipole forces) and nonspecific interactions were involved as suggested by their higher binding strengths. The strongest interaction forces observed for the three alcohols indicate that high-energy hydrogen bonding and/or more than one hydrogen bond was involved. The importance of functional group on the binding of volatile flavor compounds to soy protein in dry state (*14*) or in solution (*10-13*) had been previously suggested. Other thermodynamic and sorption data determined (data not shown) were in good agreement with the heat of adsorption data.

Effect of Flavor Molecule Stereochemistry on Binding

Both thermodynamic and sorption data determined at 0% RH show that binding of 1-hexene to soy proteins was similar to that of hexane (Figure 1, *22*), suggesting that the presence of a double bond did not have a significant influence on the binding of weak interacting compounds (such as alkanes). However, the presence of double bond together with a strongly interacting functional group could have a significant influence on flavor-soy protein interaction probably through altering molecule stereochemistry. For example, *trans*-2-hexenal interacted more strongly and adsorbed more to soy proteins than hexanal (Figure 2), which could be attributed to the fact that the carbonyl group of *trans*-2-hexenal is more exposed allowing for greater interaction. In addition, the existence of a conjugated double bond in the *trans*-2-hexenal molecule further enhances molecule rigidity as well as electron density of the carbonyl end, facilitating its binding to soy proteins as was supported by the experimental data. The observed higher retention by soy proteins of both *trans*-2-hexen-1-ol and *cis*-3-hexen-1-ol over 1-hexanol could be attributed to differences in the stereochemistry of these compounds (*22*).

Under each humidified condition evaluated (30%, 40% and 50% RH), the relative binding strengths and sorption of these volatiles to soy proteins still follow the same trend as observed at 0% RH (Figure 1, *22*), indicating that functional group still makes a substantial contribution to the interactions with soy proteins under humidified conditions. However, differences caused by functional group were less profound compared with those observed under dry conditions. In addition, the contribution of molecule stereochemistry to the binding of polar flavor compounds to soy proteins was overshadowed in the presence of moisture (Figure 1). All these indicate the great impact water may have on flavor-soy protein interactions.
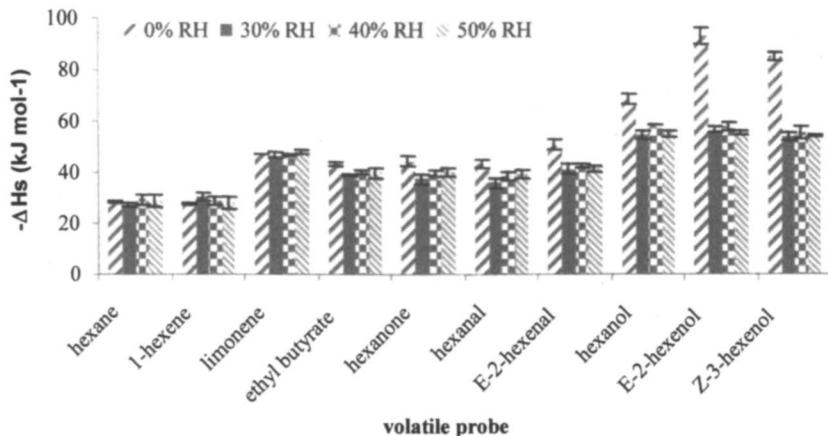
Figure 1. Heats of adsorption for individual volatile probes at different relative humidities (RHs). Error bars represent standard deviations (n=2) (Data from reference 22. Copyright 2006 American Chemical Society.)
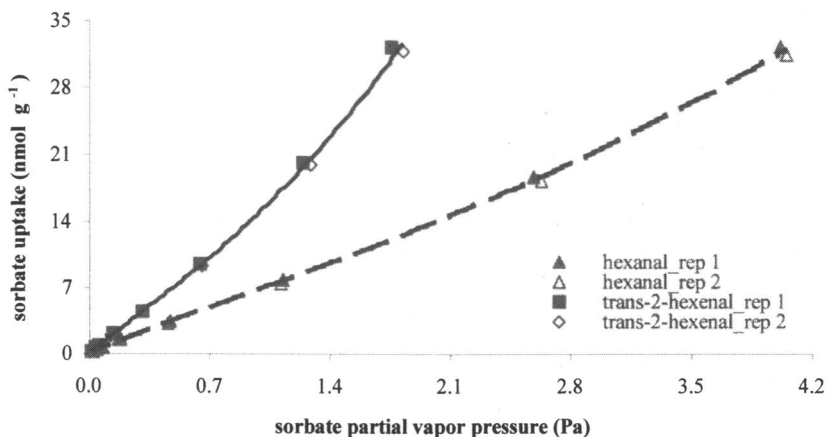

Figure 2. Sorption isotherms determined on SPI for hexanal and trans-2-hexanal at 35° C and 0% RH.

Effect of Relative Humidity on Binding

For the relatively polar volatile probes, their interaction strengths with soy proteins decreased when the RH level was increased from 0% to 30%, suggesting that competition for high-energy binding sites between flavor compound and water exists (Figure 1; 22). When the RH level was further increased from 30% to 40% and 50%, no significant difference was observed in

their binding potentials to soy proteins (Figure 1), suggesting that their interactions with soy proteins were relatively weak and limited. On the other hand, both thermodynamic and sorption data suggest that the binding of hexane, 1-hexene and limonene to soy proteins is not affected by the presence of water (Figure 1), which further supports their weak interactions with soy proteins. It should be made clear though that it may not be appropriate to directly compare adsorption on surfaces containing adsorbed water (ternary system) to adsorption on dry surface (binary system). However, the comparisons we made here can help to show the impact of environmental RH on the flavor binding properties of soy proteins.

Flavor-Cracker Interactions Measured by IGC

A humidity level of 15% RH was selected for IGC experiments to closely simulate the water activity (a_w) conditions of the crackers we prepared. Again, both thermodynamic and sorption data (Table II, *23*) suggested that binding of these selective buttery flavor compounds with the individual cracker system was related to the chemical class they belong, which further demonstrates the importance of flavor compound chemical nature in flavor-matrix interactions in real foods.

Table II. Heats of Adsorption (-△H ± Standard Deviation) and Sorption Constants (S ± Standard Deviation) Determined for Individual Flavor Compounds on Wheat and Soy-Containing Crackers at 15% RH

parameter	Cracker	diacetyl	hexanal	γ-butyrolactone	butyric acid
-△H (kJmol^{-1})[a]	wheat	29.6 ± 0.2	35.7 ± 0.4	45.4 ± 0.2	57.3 ± 2.5
	Soy	29.1 ± 0.4	35.6 ± 0.1	49.3 ± 0.2	69.3 ± 0.9
S (nmol g^{-1} Pa^{-1}) [b]	wheat	9.07 ± 0.10	65.8 ± 1.5	438 ± 11	1160 ± 94
	Soy	9.46 ± 0.03	67.7 ± 0.0	477 ± 7	2182 ± 6

[a] Based on data determined at 30, 35 and 40 °C. [b] Data determined at 35 °C.
SOURCE: Reproduced from reference 23. Copyright 2006 American Chemical Society.

When comparison was made across the two cracker systems for each volatile flavor compound studied, it was found that both diacetyl and hexanal interacted to about the same extent with the two cracker systems, suggesting that they cannot compete with water for polar binding sites under the humidity level studied (15% RH) (*23*). Gamma-butyrolactone and especially butyric acid showed higher binding with the soy-containing cracker than with the wheat cracker (Table II), indicating their capability to compete with water to some

extent for polar binding sites. The much greater influence of soy protein on the binding strength of butyric acid to the cracker suggests that the inclusion of soy significantly increased system polarity, and hence, facilitated greater binding of polar flavor compounds. The determined sorption isotherms (Figure 3, *23*) further showed that a significantly higher amount of butyric acid was bound to the soy-containing cracker than to the wheat cracker. Furthermore, the Langmuir isotherm determined with the soy-containing cracker system (Figure 3) indicates that binding sites of different energy levels exist. Meanwhile, the linear isotherm observed with the wheat cracker reflects the relatively homogeneous surface nature of the wheat cracker.

The soy protein content is not the only difference between the two cracker systems. In particular, the starch content of the soy-containing cracker would be lower than for the wheat cracker since SPI was substituted for 25% of the wheat flour in the soy cracker. This difference in starch content could have some influence on the difference observed between the the binding potentials of the two cracker systems.

Flavor-Cracker Interactions Evaluated by Sensory Analysis

In this part of the study, sensory analysis by means of orthonasal evaluation was conducted to examine whether there is an actual difference in sensory impact due to differential binding. Diacetyl and butyric acid were selected and their binding with the two crackers were evaluated using a 2-AFC with warm-up method (*24*) to determine whether a difference exists between the headspace aroma intensities of flavored wheat versus soy-containing crackers.
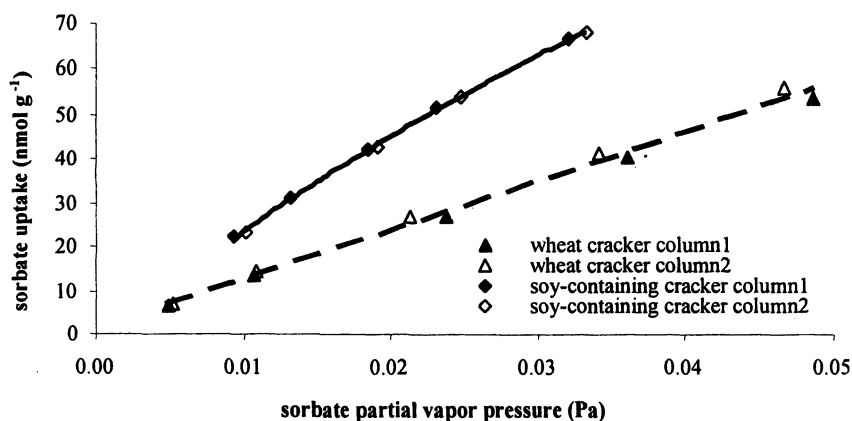

Figure 3. Sorption isotherms determined for butyric acid on wheat versus soy-containing crackers at 35° C and 15% RH. (Reproduced from reference 23. Copyright 2006 American Chemical Society.)

Results showed that the perceived headspace aroma intensities were not significantly different between the two diacetyl flavored crackers ($p < 0.2232$; estimated probability of the data: 0.5333) (*23*). Meanwhile, significant differences were observed between the butyric acid flavored crackers ($p < 0.0015$; estimated probability of the data: 0.6333).

The perceived aroma intensity of a food upon sniffing is determined by not only the type but also the amount of volatile flavor compounds present in the gas phase (headspace) above the food, and the later is affected by flavor-matrix interactions and hence the distribution of a specific flavor compound between the food matrix and the headspace (*25-27*). Therefore, measurement of the perceived specific headspace aroma intensity is an indirect way to evaluate binding of the added flavorant by the food matrix. In the present study, since the same amount of a flavor compound (diacetyl or butyric acid) was added to the two crackers and equilibrated, the similar headspace aroma intensities of the two crackers suggested similar binding of diacetyl to the crackers, while the significantly different perceived odor intensities between the crackers indicated that binding of butyric acid to the two crackers differed. As such, general agreement was found between sensory evaluation and IGC data.

Conclusions

Results from this study demonstrate that the chemical structure of a volatile flavor compound determines its binding to dehydrated soy proteins. Furthermore, relative humidity greatly influences the interaction potential of polar flavor compounds. Using real food model systems, both IGC and sensory analysis data determined from the present study reveal that addition of soy protein to a wheat cracker system may affect its flavor binding properties. Results from this study shows that IGC could be a useful technique for characterizing flavor-matrix interactions and may provide useful information aiding in prediction of sensory impact in real foods.

Acknowledgements

References

1. Messina, M.J. In *Soybeans: Chemistry, Technology, and Utilization;* Liu, K., Ed.; Aspen Publishers Inc.: Gaithersburg, MD, 1999; pp 442-477.

2. Friedman, M.; Brandon, D. *J. Agric. Food Chem.* **2001**, *49*, 1069-1086.
3. Liu, K. In *World Soybean Research Conference. VI*; (Compiled and arranged by) Kauffman, H.E.; Superior Printing: Champaign, IL., 1999; pp 409-418.
4. Rah, J.; Hasler, C.; Painter, J.; Chapman-Novakofski, K. *J. Nutr. Educ. Behav.* **2004**, *36(5)*, 238-244.
5. MacLeod, G.; Ames, J. *Crit. Rev. Food Sci. Nutr.* **1988**, *27*, 219-400.
6. Wilson, L.A. In *World Soybean Research Conference. VI;* (Compiled and arranged by) Kauffman, H.E.; Superior Printing: Champaign, IL., 1999; pp 394-402.
7. Schutte, L.; Van den Ouweland, G. *J. Am. Oil Chem. Soc.* **1979**, *56*, 289-290.
8. Beyeler, M.; Solms, J. *Lebensm-Wiss. Technol.* **1974**, *7*, 217-219.
9. Gremli, H. *J. Am. Oil Chem. Soc.* **1974**, *51*, 95A-97A.
10. Damodaran, S.; Kinsella, J. *J. Agric. Food Chem.* **1981a**, *29*, 1249-1253.
11. Damodaran, S.; Kinsella, J. *J. Agric. Food Chem.* **1981b**, *29*, 1253-1257.
12. O'Keefe, S.; Wilson, L.; Resurreccion, A.; Murphy, P. *J. Agric. Food Chem.* **1991a**, *39*, 1022-1028.
13. O'Keefe, S.; Resurreccion, A.; Wilson, L.; Murphy, P. *J. Food Sci.* **1991b**, *56*, 802-806.
14. Aspelund, T.; Wilson, L. *J. Agric. Food Chem.* **1983**, *31*, 539-545.
15. Crowther, A.; Wilson, L.; Glatz, C. *J. Food Process Eng.* **1981**, *4*, 99-115.
16. Greene, S.; Pust, H. *J. Phys. Chem.* **1958**, *62*, 55-58.
17. Kiselev, A.; Yashin, Y. In *Gas Adsorption Chromatography*; Kiselev, A.; Yashin, Y., Eds.; Plenum Press: New York, 1969; pp 104-145.
18. Gray, D.; Guillet, J. *Macromolecules* **1972**, *5*, 316-211.
19. Gauthier, H.; Coupas, A.; Villemagne, P.; Gauthier, R. *J. Appl. Polym. Sci.* **1998**, *69*, 2195-2203.
20. Cantergiani, E.; Benczedi, D. *J. Chromatogr. A* **2002**, *969*, 103-110.
21. Zhou, Q.; Cadwallader, K.R. *J. Agric. Food Chem.* **2004**, *52*, 6271-6277.
22. Zhou, Q.; Cadwallader, K.R. *J. Agric. Food Chem.* **2006**, *54*, 1838-1843.
23. Zhou, Q.; Lee, S.-Y., Cadwallader, K.R. *J. Agric. Food Chem.* **2006**, *54*, 5516-1843.
24. Thieme, U.; O'Mahony, M. *J. Sensory Studies* **1990**, *5*, 159-176.
25. Marin, M.; Baek, I.; Taylor, A.J. *J. Agric. Food Chem.* **1999**, *47*, 4750-4755.
26. Taylor, A.J. *Intern. J. Food Sci. Technol.* **1998**, *33*, 53-62.
27. van Osnabrugge, W. *Food Technol.* **1989**, *43*, 74-82.

Chapter 5

Volatile Components and Characteristic Odorants in Headspace Aroma Obtained by Vacuum Extraction of Philippine Pineapple (*Ananas comosus* [L.] Merr.)

Takashi Akioka and Katsumi Umano

Division of Tokyo Fundamental Research, Takata Koryo Company, Ltd., 1–5–23, Suidou, Bunkyo-ku, Tokyo 112–0005, Japan

Volatile components and characteristic odorants in headspace aroma of Philippine pineapple (*Ananas comosus* [L.] Merr.) were studied by use of vacuum extraction with a passivated stainless steel canister. Among 56 chemicals identified, 26 were aliphatic methyl esters accounting for approximately 93% of the total volatiles, including methyl 2-methylbutanoate and methyl hexanoate as the major components. GC-Olfactometry of the components obtained by the vacuum extraction led to the detection of methyl 2-methylbutanoate, ethyl 2-methylbutanoate, acetaldehyde, (3*E*,5*Z*)-1,3,5-undecatriene, methyl butanoate, and methyl (*E*)-3-hexenoate as potent odorants.

Pineapple has been cultivated in South America since the 15th century and has spread to tropical and subtropical areas. The Philippines and Thailand have become representative producer countries subsequently. Pineapple is one of the most popular tropical fruits in the world due to its unique sweet and sour flavor and taste as juice and canned fruit as well as fresh fruit.

Studies of the constituents and potent odorants in pineapple aroma have been reported by many researchers (Berger *et al.* (*1*), Takeoka *et al.* (*2*), Umano *et al.* (*3*), Engel *et al.* (*4*), Tokitomo *et al.* (*5*), Wu *et al.* (*6*), and Brat *et al.* (*7*)). More than 300 compounds have been reported as constituents of pineapple

57

aroma (*8–10*) including aliphatic esters, alcohols, aldehydes, sulfur-containing compounds, furanones, and hydrocarbons. Steam distillation under reduced pressure, static and dynamic headspace sampling, and solvent extraction were employed to preconcentrate analytes in the above studies.

Recently, the rapid and automated enrichment technique by the combination of a passivated stainless steel canister and proprietary preconcentrator has been used for the analysis of volatile organic compounds (VOCs) in environmental research (*11–14*). The above special canister is commercially available in several sizes (0.2 L – 15 L) from Entech Instrument Inc. (Simi Valley, CA). Every canister is totable to collect volatiles for research purposes. The stainless steel canister that has a thin fused silica layer chemically bonded to the metal interior surface is also reported to be able to conserve volatile compounds stably for more than 28 days (*15*).

The enrichment technique with a canister for headspace volatiles accompanies the process of the direct absorption of volatiles to canister from solid or liquid sample and successive concentration of absorbed volatiles. As the characteristic feature of this headspace sampling, some amount of volatiles in sample matrix as well as those in the headspace of a sample can be transferred simultaneously and rapidly into the canister by drawing the headspace gas of a sample and simultaneously reducing the pressure of headspace in sample vessel. Because the technique includes the absorbing process of headspace volatiles into a canister with reduced pressure in sampling, it is called "vacuum extraction". The above technique is a certain type of headspace sampling but is different from the established procedures of dynamic and static headspace sampling that include the process of sweeping headspace volatiles onto adsorbents by an inert gas or the static headspace sampling with gas-tight syringe and solid-phase microextraction. This unique technique seems to be excellent for the collection of highly-volatile compounds such as VOCs in environmental research and can be expected to present interesting information on headspace aroma of fruit. In the present study, vacuum extraction was applied to the headspace analysis of pineapple aroma and the odor dilution analysis of headspace volatiles obtained by vacuum extraction was developed to assess potent odorants of pineapple aroma.

Materials and Methods

Materials and Reagents

Pineapples (*Ananas comosus* [L.] Merr.) imported from the Philippines were purchased from a local market. Reference compounds listed in Table II were obtained from commercial sources: nos. 1–17, 19–24, 26, 27, 29, 30, 32, 34, 38, 40, 44–46, 51, 52, 54, 55, 58 (Sigma-Aldrich Japan, Tokyo), nos. 31, 50,

53 (Tokyo Chemical Industry, Tokyo), nos. 47 and 48 (Bedoukian Research, Inc., Danbury, CT). The following compounds were prepared from the corresponding acid and alcohol: nos. 18, 28, 33, 35–37, 39, 41, 42, 56. (3*E*,5*Z*)-1,3,5-undecatriene was synthesized according to the literature (*16*). Methyl *S*-methyl thiocarbonate was prepared by the reaction of methyl chloroformate and sodium thiomethoxide in our laboratory.

Vacuum Extraction of Headspace Volatiles from Pineapple

After removal of the core and skin, pineapple flesh was cut approximately into 3 cm cubes (total weight, 1.2 kg) and was placed in a 2 L separable flask. The flask was allowed to stand for 20 minutes to allow distribution of pineapple volatiles into the headspace. Meanwhile, the inside pressure of the 6 L canister (Silonite® coated canister, Entech Instruments Inc.) was reduced to 13 Pa with a proprietary canister cleaner (Entech 3100A, Entech Instruments Inc.). The evacuated canister was fixed to the flask containing the pineapple flesh as shown in Figure 1. Subsequently, the canister's valve was opened to absorb the headspace gas in the flask. This operation lowered the inside pressure of the flask. After the canister's valve was closed, the stopcock of purge gas tube was opened to recharge the headspace of the flask to atmospheric pressure with nitrogen gas. The canister's valve was opened again to absorb the headspace gas in the flask. The above operations of vacuum extraction were repeated until the inside pressure of canister reached 75 kPa. The inside pressure of canister was finally increased to 180 kPa by the pressurization with nitrogen gas from a steel cylinder for the instrumental analysis of headspace volatiles.
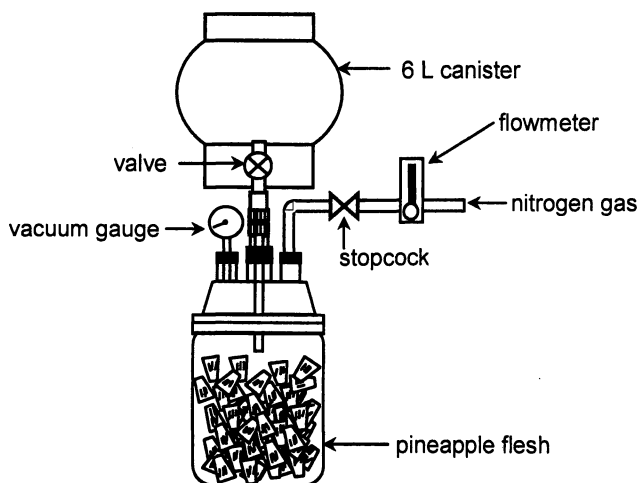

Figure 1. Apparatus of vacuum extraction with a canister for headspace sampling of pineapple aroma.

Instrumental Analyses of Volatiles

The canister containing headspace volatiles was connected to a proprietary preconcentrator (Entech 7100A, Entech Instruments Inc.). The volatiles enriched in the preconcentrator were analyzed by gas chromatography (GC) (Agilent 6890N, Agilent Technologies, Palo Alto, CA) and gas chromatography/mass spectrometry (GC/MS) (Agilent 6890N GC interfaced to Agilent 5973 inert mass selective detector). A DB-Wax column, 60 m × 0.25 mm i.d., 0.25 μm film thickness (J&W Scientific, Folsom, CA) was used for GC and GC/MS. The oven temperature was held at 40 °C for 5 min and then programmed to 200 °C at 5 °C/min. The detector and injector temperatures were 250 °C and 200 °C, respectively. MS was operated in the electron impact mode at 70 eV. In the GC analysis, the column effluent was split into three detectors, flame ionization detector (FID), pulsed flame photometric detector (PFPD) (O.I. Analytical, College Station, TX), and olfactory detector port (ODP) (Gerstel GmbH & Co. KG, Mülheim an der Ruhr, Germany) in the following ratio: 1+1+3, v/v/v. The headspace gas volume introduced from a canister into GC and GC/MS for aroma analysis was 1400 mL and 300 mL, respectively. The headspace gas was necessary for GC analysis much more than that for GC/MS analysis due to the split of the column effluent to three detectors in the former analysis as described previously. The reproducibility of quantitative data obtained in the GC analysis was examined by nine measurements with 1400 mL of standard gas of 3-nonanone each time (RSD = 3.4%).

The retention index and mass spectrum of each component were used for the identification by the comparison with those of the reference compound. Three compounds were tentatively identified by comparing their mass spectrum with that in the Wiley Registry (Agilent Technologies).

Odor Dilution Analysis of Headspace Volatiles Obtained by Vacuum Extraction

The odor dilution analysis of headspace volatiles obtained by vacuum extraction was designed to investigate the potent odorants among them. The flavor dilution (FD) factor of the odorants in pineapple aroma was expected to be determined by a stepwise reduction of the volume of the gas introduced into the GC from the canister as shown in Table I. The validity of this procedure was verified and will be described later. GC-Olfactometry (GC-O) was performed by three trained panelists. The odorants detected by the panelists through ODP were recorded with their retention time and odor description. The components detected by three panelists were determined to be a declared odorant.

Table I. FD-factor in Odor Dilution Analysis using Canister

FD-factor	1	2	4	8	16	32	64	128
Volume-canister (mL) [a]	1400	700	350	175	88	44	22	11

[a] The volume of the gas introduced into the GC from the canister.

Results and Discussion

The compounds identified were listed with their GC peak area percent and retention indices on a DB-Wax column in Table II. Among 56 components identified in the instrumental analysis, 26 compounds were aliphatic methyl esters accounting for 93.2% of the total GC peak area percent. The major volatile components were methyl 2-methylbutanoate (44.2%), methyl hexanoate (25.1%), methyl butanoate (7.1%), methyl propanoate (7.0%), and methyl acetate (4.8%).

Takeoka *et al.* (*2*) also reported those esters as the major components in the headspace aroma of pineapple. A small amount of unsaturated aliphatic methyl esters were also identified for the first time from pineapple such as methyl 2-methyl-3-butenoate, methyl 2-methyl-(*E*)-2-butenoate, methyl (*Z*)-2-hexenoate, methyl (*Z*)-4-heptenoate, and methyl (*Z*)-5-octenoate. GC analysis using the PFPD, which is one of the selective and sensitive detectors for sulfur-containing compounds, led to the identification of methyl 2-(methylthio)acetate and methyl 3-(methylthio)propanoate that are well-known constituents of pineapple aroma. In addition to them, a trace quantity of methyl S-methyl thiocarbonate was found for the first time in pineapple aroma. The mass spectrum of methyl S-methyl thiocarbonate was as follows: m/z (relative intensity); 108(5), 107(6), 106(100), 75(52), 61(18), 60(18), 59(59), 47(83), 46(26), 45(40).

The headspace analysis involving vacuum extraction revealed highly-volatile compounds such as acetaldehyde, methyl acetate, ethyl acetate, and methyl propanoate in relatively large quantity. This is the feature of vacuum extraction using canister that has been valued for the environmental analyses of VOCs. In the analysis of aroma, this procedure seems to be suitable for the headspace analysis focused on top note constituents. To the contrary, this extraction technique may not be suitable for the flavor analysis of the compounds in bottom note that have relatively high boiling points and polarity. Chida *et al.* (*17*) reported that compounds such as aliphatic alcohols and aldehydes (>C16) were not extracted by high vacuum distillation with canister due to their low vapor pressure. Because of this feature of vacuum extraction, furaneol which is one of the well-known characteristic odorants in pineapple aroma (*5, 18*) may not have been detected in this research. Considering the sample matrix of pineapple with its high water content, the desorption of furaneol directly from pineapple flesh using vacuum extraction seems to be difficult due to its high hydrophilicity. Takeoka *et al.* (*2*) also reported that furaneol was not detected in the dynamic headspace sampling of intact pineapple and blended pineapple pulp.

The odor dilution method is one of the practical techniques for the detection of the potent odorants in aroma components. Higashi *et al.* (*19*) reported the aroma direct dilution analysis of sidestream smoke VOCs in tobacco by using a gas-sampling bag and preconcentrator for characterization of their odor profiles. In this research, the new method of odor dilution analysis for headspace volatiles obtained by vacuum extraction was applied to detect the potent odorants which are mainly responsible for the top note of pineapple.

Table II. Volatile Components in Headspace Aroma of Pineapple

Peak No.	Compound	$I^{\,a}$	$ID^{\,b}$	GC peak area %
1	acetaldehyde	701	A	0.6
2	methyl acetate	827	A	4.8
3	ethyl acetate	884	A	3.5
4	methyl propanoate	908	A	7.0
5	methanol	915	A	0.5
6	methyl 2-methylpropanoate	922	A	2.9
7	ethanol	941	A	0.3
8	2,5-dimethylfuran [c]	949	A	tr
9	ethyl propanoate	953	A	tr
10	ethyl 2-methylpropanoate	965	A	tr
11	propyl acetate	972	A	tr
12	methyl butanoate	984	A	7.1
13	methyl 2-methylbutanoate	1011	A	44.2
14	methyl 3-methylbutanoate	1018	A	0.3
15	ethyl butanoate	1035	A	tr
16	2-methyl-3-buten-2-ol	1040	A	tr
17	ethyl 2-methylbutanoate	1061	A	0.1
18	methyl 2-methyl-3-butenoate [c]	1066	A	tr
19	ethyl 3-methylbutanoate	1068	A	tr
20	methyl pentanoate	1096	A	0.6
21	diethyl carbonate	1108	A	tr
22	2-methylbutyl acetate	1121	A	0.1
23	3-methylbutyl acetate	1123	A	tr
24	myrcene	1161	A	tr
25	methyl S-methyl thiocarbonate [c]	1174	A	tr
26	methyl hexanoate	1188	A	25.1
27	methyl 2-methyl-(E)-2-butenoate [c]	1191	A	tr
28	methyl (Z)-2-hexenoate [c]	1210	A	tr
29	(Z)-β-ocimene	1231	A	tr
30	ethyl hexanoate	1236	A	tr
31	methyl 5-hexenoate	1236	A	tr

Table II. *Continued.*

Peak No.	Compound	I [a]	ID [b]	GC peak area %
32	γ-terpinene [c]	1240	A	tr
33	methyl (E)-4-hexenoate	1242	A	tr
34	(E)-β-ocimene	1247	A	0.3
35	(E)-2-methyl-2-butenyl acetate [c]	1248	A	tr
36	methyl (Z)-3-hexenoate	1259	A	tr
37	methyl (E)-3-hexenoate	1263	A	0.1
38	terpinolene [c]	1277	A	tr
39	methyl 2-hydroxy-2-methylbutanoate	1284	A	tr
40	methyl heptanoate	1289	A	0.1
41	methyl (E)-2-hexenoate	1290	A	tr
42	methyl (Z)-4-heptenoate [c]	1333	A	tr
43	(3E,5Z)-1,3,5-undecatriene	1389	A	tr
44	methyl octanoate	1391	A	0.8
45	nonanal	1395	A	tr
46	methyl 2-(methylthio)acetate	1410	A	tr
47	methyl (Z)-5-octenoate [c]	1429	A	0.1
48	dehydro-p-cymene [c]	1433	A	tr
49	1,3,5,8-undecatetraene	1440	B, C	tr
50	methyl (E)-3-octenoate	1453	A	tr
51	α-copaene	1497	A	tr
52	decanal	1500	A	tr
53	dimethyl malonate	1512	A	tr
54	benzaldehyde	1519	A	tr
55	methyl 3-(methylthio)propanoate	1525	A	0.1
56	methyl (Z)-4-decenoate	1625	A	tr
57	α-amorphene	1681	B	tr
58	α-terpineol	1702	A	tr
59	α-muurolene	1717	B	tr

[a] Retention index on DB-Wax column.

[b] A, Identified by comparison of the compound's mass spectrum and retention index with that of a reference compound;

B, Tentatively identified;

C, The geometries of the double bonds were not determined.

[c] Newly identified in pineapple.

[tr] GC peak area % < 0.1.

The linearity of the correlation between the volume of the gas introduced into the GC from the canister and GC peak area of the components was verified first to confirm that the odor dilution analysis is applicable to the components obtained by vacuum extraction. The representative compounds identified in the present study such as acetaldehyde, methyl 2-methylbutanoate, methyl hexanoate, and (E)-β-ocimene were used in this verification. The GC peak area of those compounds was measured according to a stepwise reduction of the volume of the gas from canister introduced into GC as shown in Table I. The correlation of GC peak area to a stepwise reduction of the volume of the gas from canister was derived from the mean of duplicate measurements on the above four representative compounds. The linear correlation coefficients (R^2) for the four compounds were all greater than 0.99 as shown in Figure 2. This indicates that the volume of the gas transferred into the GC from the canister correlates highly with the GC peak area of each component. Consequently, the amount of component introduced onto the GC column is proportional to the volume of the gas taken from the canister and the odor dilution analysis can be implemented by reducing the gas volume in a stepwise manner.

Table III shows the potent odorants in pineapple aroma at the conclusion of odor dilution analysis applied in the present study. The FD-factor of each component was provided according to the volume of the gas taken from the canister as described in Table I. Fifteen components were perceived as characteristic odorants and 12 were identified among them. The odorants with the highest FD-factor were methyl 2-methylbutanoate and ethyl 2-methylbutanoate (FD = 128) followed by acetaldehyde (FD = 32), methyl butanoate (FD = 32), methyl (E)-3-hexenoate (FD = 32), and (3E,5Z)-1,3,5-undecatriene (FD = 32). The high FD-factor of methyl 2-methylbutanoate and methyl butanoate may be attributable to their large quantity. However, the high FD-factor of (3E,5Z)-1,3,5-undecatriene was probably caused by its significantly low odor threshold in air (0.01–0.02 ng/L) (4) with pineapple-like and green notes. Acetaldehyde was also shown to be a potent odorant because of its low odor threshold in air (1.5 μg/L) (20). Methyl and ethyl 2-methylbutanoate and (3E,5Z)-1,3,5-undecatriene were also reported as characteristic odorants in the headspace analysis (2, 5). Methyl 3-(methylthio)propanoate, which is known to have a characteristic pineapple flavor, was not detected as a potent odorant due to its trace quantity. Methyl S-methyl thiocarbonate, which is newly identified as a sulfur-containing component of pineapple aroma, possesses a low odor threshold in water (approximately 50 ppb) with sulfurous and litchi-like notes but was not perceived in GC-O due to its trace quantity in the headspace. Two components were weakly perceived as odorants with green and fruity notes but their structures have not yet been elucidated.
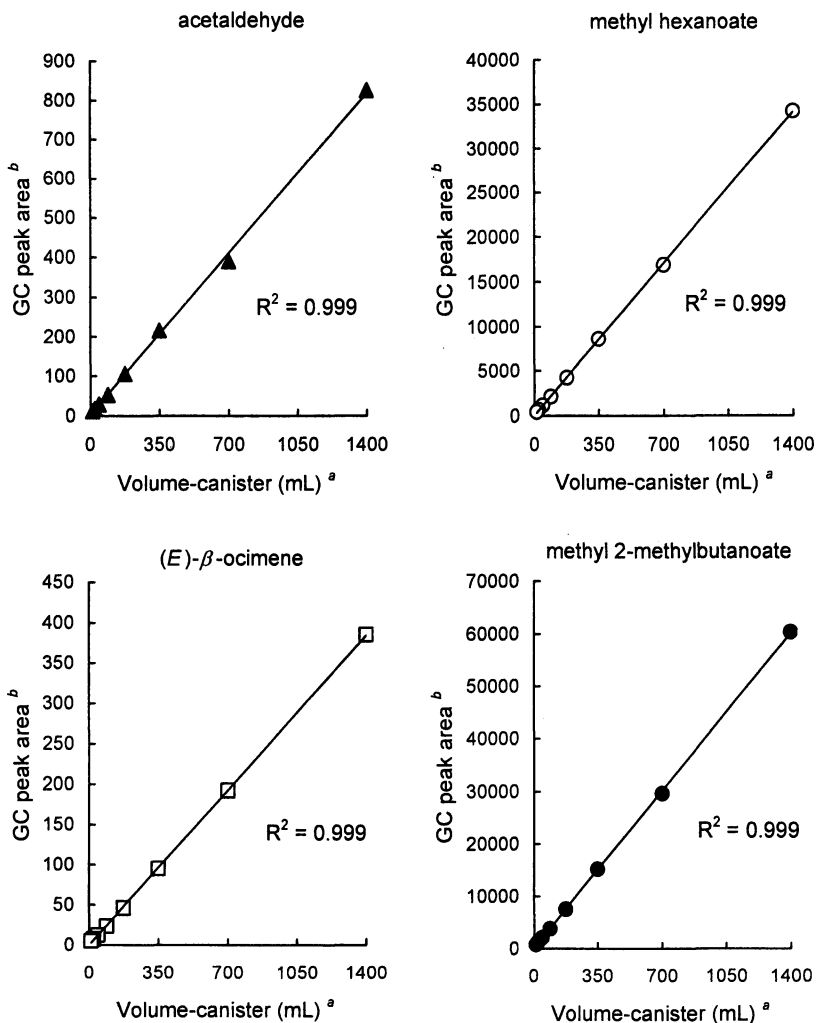
Figure 2. Correlation between the volume of the gas taken from the canister and GC peak area (FID detection) of representative compounds of pineapple volatiles. [a] The volume of the gas introduced into the GC from the canister. [b] GC peak area was the mean value of duplicate measurements.

Table III. Potent Odorants of Headspace Aroma from Pineapple

Compound [a]	Odor Description [b]	FD-factor	Volume-canister (mL)
methyl 2-methylbutanoate	fruity	128	11
ethyl 2-methylbutanoate	fruity, pineapple-like	128	11
acetaldehyde	solventy, pungent	32	44
(3E,5Z)-1,3,5-undecatriene	pineapple-like, green	32	44
methyl butanoate	sweaty, apple-like	32	44
methyl (E)-3-hexenoate	sweaty	32	44
methyl 2-methylpropanoate	fruity	8	175
methyl hexanoate	green, fruity	8	175
ethyl 2-methylpropanoate	fruity	2	700
1,3,5,8-undecatetraene [c, d]	fruity, green	1	1400
methyl acetate	fruity	1	1400
methyl pentanoate	fruity	1	1400
2-methylbutyl acetate	fruity, solventy	1	1400
unknown (1047 [e])	green	1	1400
unknown (1228 [e])	fruity	1	1400

[a] The compound was identified by comparison with reference compound based on odor description, retention index on DB-Wax column and mass spectrum.

[b] Odor description at ODP.

[c] Tentatively identified.

[d] The geometries of the double bonds were not determined.

[e] Retention index on DB-Wax column.

References

1. Berger, R.G.; Drawert, F.; Kollmannsberger, H.; Nitz, S.; Schraufstetter, B. *J. Agric. Food Chem.* **1985**, *33*, 232-235.

2. Takeoka, G.; Buttery, R.G.; Flath, R.A.; Teranishi, R.; Wheeler, E.L.; Wieczorek, R.L.; Guentert, M. In *Flavor Chemistry: Trends and Developments*; Teranishi, R.; Buttery, R.G.; Shahidi, F., Eds.; ACS Symposium Series 388; American Chemical Society: Washington, DC, 1989; pp 223-237.

3. Umano, K.; Hagi, Y.; Nakahara, K.; Shoji, A.; Shibamoto, T. *J. Agric. Food Chem.* **1992**, *40*, 599-603.

4. Engel, K.-H.; Heidlas, J.; Tressl, R. In *Food Flavours: The Flavour of Fruits*; Morton, I.D.; Macleod, A.J., Eds.; Developments in Food Science 3C; Elsevier: Amsterdam, 1990; pp 195-219.

5. Tokitomo, Y.; Steinhaus, M.; Büttner, A.; Schieberle, P. *Biosci. Biotecnol. Biochem.* **2005**, *69*, 1323-1330.

6. Wu, P.; Kuo, M.-C.; Hartman, T.G.; Rosen, R.T.; Ho, C.-T. *J. Agric. Food Chem.* **1991**, *39*, 170-172.

7. Brat, P.; Hoang, L.N.T.; Soler, A.; Reynes, M.; Brillouet, J.-M. *J. Agric. Food Chem.* **2004**, *52*, 6170-6177.

8. *Volatile Compounds in Food. Qualitative and Quantitative Data* 7th ed.; Maarse, H.; Visscher, C.A., Eds.; TNO Biotechnology and Chemistry Institute: Zeist, The Netherlands, 1996.

9. Teai, T.; Claude-Lafontaine, A.; Schippa, C.; Cozzolino, F. *J. Essent. Oil Res.* **2001**, *13*, 314-318.

10. Elss, S.; Preston, C.; Hertzig, C.; Heckel, F.; Richling, E.; Schreier, P. *Lebensm.-Wiss. Technol.* **2005**, *38*, 263-274.

11. *Compendium Method TO-14A* 2nd ed.; Center for Environmental Research Information, Office of Research and Development, U.S. Environmental Protection Agency, Cincinnati, Ohio, 1999.

12. *Compendium Method TO-15* 2nd ed.; Center for Environmental Research Information, Office of Research and Development, U.S. Environmental Protection Agency, Cincinnati, Ohio, 1999.

13. Moezzi, B.; Winward, M.R.; Cardin, D.B., *TO-14 Application Note*; Entech Instruments, Inc., California, 1999.

14. Cardin, D.B.; Langford, K.; Shetty, V., *Application Note:902*; Entech Instruments, Inc., California, 1999.

15. Ochiai, N.; Tsuji, A.; Nakamura, N.; Daishima, S.; Cardin, D.B. *J. Environ. Monit.* **2002**, *4*, 879-889.

16. Näf, F.; Decorzant, R.; Thommen, W.; Wilhalm, B.; Ohloff, G. *Helv. Chim. Acta* **1975**, *58*, 1016-1037.

17. Chida, M.; Sone, Y.; Tamura, H. *J. Agric. Food Chem.* **2004**, *52*, 7918-7924.

18. Pickenhagen, W.; Velluz, A.; Passerat, J.-P.; Ohloff, G. *J. Sci. Food Agric.* **1981**, *32*, 1132-1134.

19. Higashi, N.; Shikata, H.; Shimoda, M.; Hayakawa, I. *Beitr. Tabakforsch Int.* **2004**, *21*, 32-39.

20. Nagata, Y.; Takeuchi, N. *Bulletin of Japan Environmental Sanitation Center* **1990**, *17*, 77-89.

Chapter 6

C$_{13}$-Norisoprenoid Concentrations in Grapes as Affected by Sunlight and Shading

Silke M. G. Stevens[1,2] and Susan E. Ebeler[1]

[1]Department of Viticulture and Enology, University of California,
One Shields Avenue, Davis, CA 95616
[2]Current Affiliation: General Mills, Inc., 5603 Becton venue,
Minneapolis, MN 55436

Volatile C$_{13}$-norisoprenoids contribute important flavor properties to many grape and wine varieties, however factors influencing their formation are not well understood. We evaluated the effects of different levels of sunlight exposures on norisoprenoid concentrations in White Riesling and Cabernet Sauvignon grapes at variable maturity levels. In addition to allowing the grapes specific amounts of sunlight using shade cloth to control levels between 4 - 97% of full sun exposure, UV-A/B light (300 - 400 nm) was also controlled in some trials. The norisoprenoid content of grapes from these trials were compared to those of grapes grown under natural shade conditions, i.e., grapes that were shaded by their own leaves. In Cabernet, the concentration of the norisoprenoid, vitispirane, increased linearly ($r^2 = 0.969$, p< 0.001) as sunlight exposure increased. Removing UV-A/B light had little effect on norisoprenoid concentrations in White Riesling grapes. Surprisingly, norisoprenoid concentrations in both Cabernet and Riesling were approximately three times higher in berries from naturally shaded vines compared to grapes from vines which had the applied shade cloth with a similar level of light exposure (~ 4%).

C_{13}-Norisoprenoids are volatile secondary metabolites that are important aroma constituents of both red and white grape varieties, including Cabernet Sauvignon, Syrah, Chardonnay, Semillon, Riesling, and Sauvignon blanc (*1 - 9*). The norisoprenoids contribute complex aromas to these wines ranging from kerosene-like (TDN; 1,1,6-trimethyl-1,2-dihydronaphthalene), to eucalyptus or camphor-like (vitispirane; 6,9-epoxy-3,5(13)-megastigmadiene and Riesling acetal; 2,2,6,8-tetramethyl-7,11-dioxatricycloundec-4-ene), to floral-like (β-damascenone; megastigma-3,5,8-triene-7-one and β-ionone; 4-(2,6,6-trimethyl cyclohex-1-ene-1-yl) but-3-ene-2-one). In addition, many of the norisoprenoids have very low aroma thresholds. For example, the aroma threshold of β-damascenone is 9 ng/L, making it one of the most potent flavorants known (*10*). The norisoprenoids are thought to arise from carotenoid breakdown (*11*) and some of them occur in the grape as glycosidically bound precursors (*12*). Enzymatic and acidic reactions during crushing, fermentation, and bottle-aging result in cleavage of the bound sugar, releasing the free norisoprenoid aglycone.

A number of variables influence norisoprenoid levels in grapes. Chief among these factors is maturity, with norisoprenoid levels increasing significantly only during the last few weeks of ripening prior to harvest (*10*). The increase in norisoprenoid levels is accompanied by a steady decrease in total carotenoid concentrations (*13, 14*). Specific clonal and varietal differences in norisoprenoids are also observed (reviewed by *15*).

External factors such as sunlight, temperature, and vine canopy manipulations have also been shown to influence norisoprenoid levels (*4 – 6, 16*). Photochemical degradation of the carotenoids is thought to be largely responsible for the effects of these external variables on norisoprenoid levels. However, in these earlier studies differences in photosynthetically active radiation (PAR) among the various treatments were not always determined. Recently, Gerdes et al. (*15*) showed that in White Riesling grapes, sunlight exposures greater than 20% of full sun exposure (beginning at veraison) increased bound TDN and Riesling acetal levels. Interestingly, they also observed that at low levels of sunlight exposure, leaf removal with addition of shade cloth resulted in significantly lower levels of TDN compared to control samples (no leaf removal, natural shading), even though levels of PAR were similar between the two treatments (3-4% of full sun exposure). Reasons for these effects are not clear, however, Schultz et al. (*17*) and Steel and Keller (*18*) have shown that carotenoid concentrations in grapes may be influenced by exposure to UV-B irradiation. The applied shade cloth used by Gerdes et al. filtered wavelengths of light from 400 – 800 nm while leaves will filter and reflect light of specific wavelengths which may influence carotenoid synthesis and degradation.

In our previous studies, shading treatments were applied to the vines at veraison and only one variety of white grape was studied. However, Razungles et al. (*16*) have also observed that in the red grape variety, Syrah, the timing of

sunlight exposure can influence levels of both the carotenoid precursors and the norisoprenoid degradation products. Therefore, the objectives of the current study were to monitor the effects of sunlight exposure in a red grape variety, Cabernet Sauvignon. In addition, the shade treatments were applied early in the growing season and were maintained throughout the season until harvest; norisoprenoid levels were monitored periodically throughout the entire growing season. Finally, shade cloths that specifically filtered UV-A/B light (300-400 nm) were also evaluated for their effects on norisoprenoid formation in White Riesling grapes.

Materials and Methods

Grapes

The study took place during the 2000 and 2001 growing seasons. The Cabernet Sauvignon (Clone 8) grapes were located at the UC Davis Tyree Vineyard, Davis, CA. The vines were own-rooted, 9 years old (planted in 1992), planted in an east-west row orientation with 8' x 12' vine spacing, and they were cane-pruned. The vines were drip irrigated as needed throughout the growing season to maintain an approximately 50% evapotranspiration rate.

The White Riesling vines (unknown clone) were located in a commercial vineyard in Placer County, California (~ 900 m elevation). The vines were planted on AXR-1 rootstock, were 18 years old (planted in 1982), planted in a north-south row orientation with 9' x 12' vine spacing on a single bilateral cordon trellising system. Irrigation was applied as needed throughout the summer at the first sign of water stress (~ 2 times throughout the season).

Shade Treatments

Cabernet Sauvignon

Shade cloth of differing densities (John Mahaney Co., Sacramento, CA) was used to provide variable levels of sunlight exposure to the grape clusters. A 60 cm x 60 cm piece of cloth was stretched across a wire frame that was placed in the ground so that the cloth was approximately 15 cm from the clusters. Spacing between adjacent screens was ~25 cm and air was allowed to move freely between the frame/shade cloth and the grape vine/clusters. Leaves were removed and shade cloth applied to give the following levels of sunlight (400-800 nm) to the cluster (expressed as percent of ambient, full sun exposure): 4%,

18%, 31%, 37%, 50%, 71%, and 97%. In addition, a natural shade treatment (which corresponded to ~4% of full sun exposure) was obtained by maintaining the original leaf shading of the clusters. Treatments were established 19 June 2001 (3 months before harvest) and each treatment was duplicated on a separate vine. Actual photosynthetically active radiation (PAR) at each cluster was measured on several days and at several times throughout the experiment (9:00, 12:00, and 15:00 Pacific Daylight Time) to ensure that shade levels remained consistent throughout the experiment. Leaves were removed as necessary in order to maintain the treatments throughout the growing season. PAR was measured using a handheld Li-Cor LI-189 quantum sensor (Li-Cor Inc., Lincoln, NE).

White Riesling

Leaves were removed and shade cloth applied as described in above for Cabernet Sauvignon to give a high (71% of ambient) and a low (4% of ambient) level of sunlight exposure (400 - 800 nm) to White Riesling vines. To separate vines, a UV-A/B filter (TAP Plastics, Sacramento, CA) was applied in combination with the shade cloth so that light with wavelengths of 300 - 400 nm was also screened. UV-B (280 - 315 nm) filters were also tested, but results were highly variable due to difficulties with maintaining the filter and no data are reported. UV filters were cleaned weekly to remove dust build up. A natural shade treatment (which corresponded to ~4% of ambient light), was obtained by maintaining the original leaf shading of the clusters. In addition to this natural shade treatment, separate vines were maintained with natural shading plus the addition of the UV-A/B filter in front of the clusters to filter out light of 300-400 nm. The treatments were established in mid-July 2000, each treatment was duplicated on a separate vine, and PAR at each cluster was measured and maintained throughout the growing season.

Harvesting

Clusters from the duplicate vines from each treatment were sampled every 4 weeks after initiation of the treatments and until veraison. After veraison, clusters were sampled every 2 weeks until the grapes reached 23 °Brix. All clusters were harvested at 23 °Brix, as determined in the vineyard with a handheld refractometer. Clusters were picked, cooled to ~10°C, transported to the laboratory, and stored frozen at –20°C prior to extraction and analysis.

Isolation and Analysis of C_{13}-Norisoprenoids

Grapes from each of the treatments were crushed and gently pressed through a cheese cloth to obtain the juice (grapes from duplicate vines were combined together prior to crushing). Free volatiles were isolated from ~150 mL juice by liquid/liquid extraction using pentane/diethyl ether (1:1 v:v) as the extracting solvent. Internal standard (2-octanol) was added to the juice prior to the extraction. After the extraction was complete (18 hours) the organic phase was dried over anhydrous sodium sulfate and concentrated to 1.5 mL on a Vigreux column. The concentrated extract was stored at < 10°C until GC-MS analysis. Immediately prior to GC-MS analysis, the extract was further concentrated to 100 µL under a gentle nitrogen stream. All samples were extracted in duplicate.

Using the juice remaining from the liquid/liquid extraction, bound volatiles in White Riesling were isolated using simultaneous distillation and extraction (SDE) for 1 hour with pentane/diethyl ether as described by Gerdes et al. (15). In 2001, bound volatiles from Cabernet were hydrolyzed enzymatically. The bound volatiles from the juice were isolated using an Amberlite XAD-2 column followed by incubation with a commercial pectinase/β-glucosidase enzyme mixture (SIHA-Panzyme-AromeG, Bergerow, Germany). Hydrolyzed norisoprenoids were isolated by extraction into pentane and reduction to 50 µL volume for analysis by GC-MS. Internal standard (1-heptanol) was added to the juice prior to extraction. All samples were extracted in duplicate.

All extracts were analyzed by gas chromatography with mass spectrometric detection (GC-MS) using a Hewlett Packard 6890 GC with a 5972 MSD and ChemStation software. Helium was the carrier gas at a flow rate of 0.8 mL/min and the MSD interface temperature was 260°C. A 30 m x 0.25 mm i.d. x 0.25 µm film thickness DB-Wax (polyethylene glycol) column (J&W Scientific, Folsom, CA) was used for all analyses. The oven temperature was programmed from an initial temperature of 50°C to a final temperature of 240°C at a rate of 4°C/min. The oven was held at the final temperature (240°C) for 25 min. The injector temperature was 230°C and 1 µL of concentrated extract was injected in the splitless mode.

Peak identity of individual peaks was confirmed by comparison of retention times and mass spectra (obtained in full scan mode) with those of authentic standards injected under identical conditions.

For quantitation, the GC-MSD was operated in Selected Ion Monitoring (SIM) mode. Peak areas of m/z 172, 207, and 192 were used for quantitation of TDN, Riesling acetal, and vitispirane, respectively. These masses correspond to the molecular ion for TDN and vitispirane and M-1 for Riesling acetal. Concentration of each peak was calculated relative to the peak area of the internal standard, 2-octanol or 1-heptanol. Norisoprenoid levels were calculated on a per berry basis as well as on a concentration basis. No significant difference in results was observed between these two methods and so all results are reported on a concentration basis.

Results and Discussion

Effects of Variable Sunlight Exposure on Norisoprenoids in Cabernet Sauvignon

No measurable amounts of norisoprenoids were found until one month after veraison for all treatments (data not shown). Only bound vitispirane was positively identified and quantified in the Cabernet Sauvignon samples, therefore no data on free vitispirane or other norisoprenoids is presented. During sample preparation, the grapes were crushed and immediately filtered resulting in limited skin contact time and limited extraction of norisoprenoids from the skin. During actual winemaking, extraction conditions may vary and skin contact may be longer than was typical for our extractions. The effects of skin contact and extraction time on norisoprenoid extraction and concentration were not evaluated in this study.

Levels of bound vitispirane increased approximately 3 fold as sunlight exposures increased from 4% to 97% of full sun exposure (Figure 1). These results are consistent with results previously observed in several grape varieties. For example, Gerdes et al. (15) observed that levels of the norisoprenoids, TDN and Riesling acetal, increased in Chardonnay and White Riesling grapes as sunlight exposure increased from 4% to 97% of full sun exposure. In the study of Gerdes et al., the norisoprenoids increased more than 6 fold as sunlight exposures increased, an effect which was greater than that observed here. It is not clear if this is due to differences in the actual norisoprenoids measured,
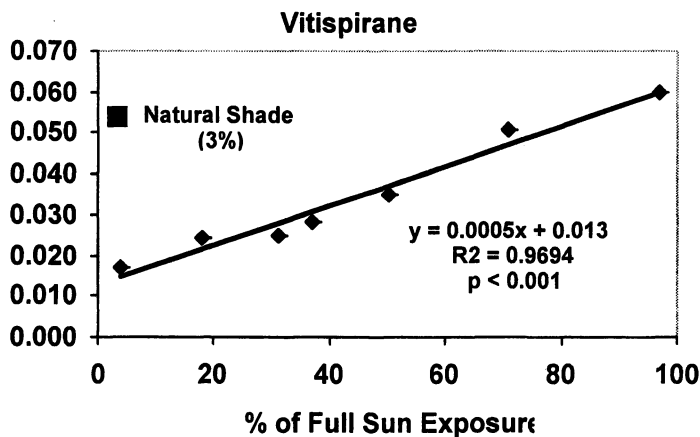
Figure 1. Levels of bound vitispirane in Cabernet Sauvignon grapes with different levels of sunlight exposure. (n = 2)

differences between years, or differences between red and white grape varieties. Marais et al. (*4*) also observed increases in several norisoprenoid levels in shaded Riesling grapes (and corresponding wines) compared to sunlight exposed grapes, although no actual sunlight levels were reported in this study. Razungles et al. (*16*) observed that increased sunlight exposure for Syrah grapes resulted in increased levels of norisoprenoids, although again, actual sunlight exposure levels were not measured.

Whether the observed results in our study are due to differences in sunlight exposure or to differences in temperature for the various treatments cannot be positively determined. We have observed differences in average temperature of ~3°C for naturally shaded compared to sun-exposed treatments, however, differences in temperature among the various sun exposure levels were less than 3°C. Further studies designed to better distinguish temperature effects from sunlight exposure effects are needed.

Interestingly, our results indicted that vitispirane levels were approximately three times higher in berries from the naturally shaded vines compared to grapes from the vines which had the applied shade cloth treatment with a similar PAR level (3-4% of full sun exposure for both treatments); norisoprenoid concentrations were 5.4 x 10^{-2} μg/mL vs 1.7 x 10^{-2} μg/mL for naturally shaded vs leaf removal + shade cloth treatments (Figure 1). In fact, the vitispirane concentration in the naturally shaded vine was as high as the concentration in the highest sun exposure treatment (97% of full sun exposure; Figure 1). This result is consistent with previous observations by Gerdes et al. (*15*) where TDN levels were measured in White Riesling wines. Lee et al. (*19*) also observed that the method by which sunlight exposure is altered has significant effects on norisoprenoids in Cabernet. In the study of Lee et al., similar to the results observed here, when no leaves or shoots were removed from the vine, high levels of norisoprenoids were observed, even though light intensity at the exposed clusters was low. The reasons for this effect are unknown. As discussed by Lee et al. (*19*) differences in sunlight exposure to the vine foliage may result in either direct or indirect effects on norisoprenoid levels in the fruit.

Effects of UV Exposure on Norisoprenoids in White Riesling

As with the Cabernet Sauvignon, no measurable amounts of norisoprenoids were found in the White Riesling grapes until 1 month after veraison for all treatments (data not shown). Only bound TDN and Riesling acetal were positively identified and quantified, therefore no data on free compounds or other norisoprenoids will be presented.

We observed no significant effects of UV-A/B exposure on TDN and Riesling acetal concentrations in White Riesling (Figure 2). Schultz et al. (*17*) observed that carotenoid levels in Riesling grapes skins at harvest were reduced
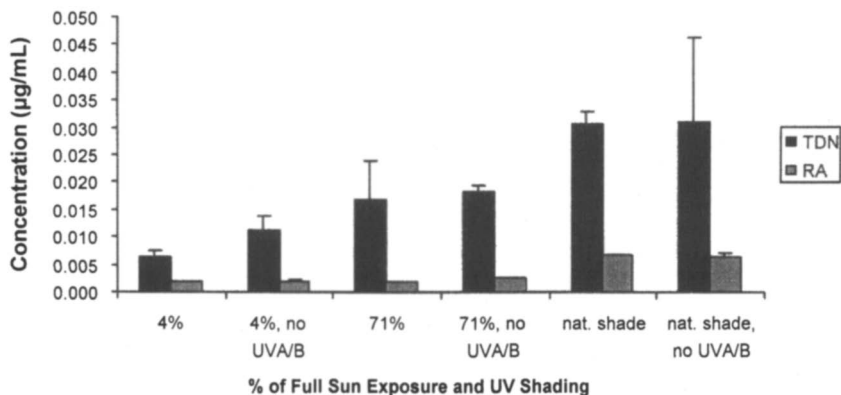
Figure 2. Effect of UV light on TDN and Riesling acetal (RA) in White Riesling grapes. (n = 2)

at higher UV-B light exposures (these authors compared ambient UV-B exposure to that where UV-B light was removed with a UV-B absorbing film). They proposed that although carotenoids were higher at veraison in grapes receiving the higher exposures to UV-B light, the higher levels of UV-B light enhanced degradation of the carotenoids so that levels of carotenoids at harvest were actually reduced or not different from samples with UV light removed. Steel and Keller (*18*) observed similar effects in Cabernet Sauvignon grapes. These effects of UV-B light on carotenoid degradation might be expected to result in increased norisoprenoid levels during ripening, however neither Schultz et al. nor Steel and Keller measured norisoprenoid concentrations. In our study, carotenoid precursors were not measured. Further work evaluating a range of UV-A/B light levels, and monitoring both carotenoid precursors and norisoprenoid levels is needed. In addition, further work is needed to see if decreasing or increasing other wavelengths of light may have different effects on norisoprenoids in grapes.

Conclusions

In this study, the norisoprenoid, vitispirane, increased in Cabernet Sauvignon grapes as sunlight exposure increased when exposure was controlled by trimming leaves and applying screens to filter light from 400 - 800 nm. Naturally shaded grapes, which received ~3-4% of full sun exposure had vitispirane levels as high as the highest level of sun exposure (97%) when leaves were removed. In White Riesling grapes, filtering of UV light in the range of 300 - 400 nm did not affect concentrations of TDN and Riesling acetal. Further

work relating norisoprenoid concentrations in grapes to the concentrations in the corresponding wines is needed. In addition, further work to relate the observed analytical results to sensory measurement of grape and wine flavor are needed.

Acknowledgements

References Cited

1. Sefton, M. A.; Skouroumounis, G. K.; Massy-Westropp, R. A.; Williams, P. J. *Aust. J. Chem.* **1989**, *42*, 2071-2084.
2. Abbott, N. A.; Coombe, B. G.; Sefton, M. A.; Williams, P. J. In *Actualités Oenologiques 89*; Ribéreau-Gayon, P.; Lonvaud, A., Eds.; Dunod: Paris, 1990; pp 94-99.
3. Francis, I. L; Sefton, M. A.; Williams, P. J. *J. Sci Food Agric.* **1992**, *59*, 511-520.
4. Marais, J.; van Wyk, C. J.; Rapp, A. *S. Afr. J. Enol. Vitic.,* **1992**, *13*, 23-32.
5. Marais, J.; van Wyk, C. J.; Rapp, A. *S. Afr. J. Enol. Vitic.* **1992**, *13*, 33-44.
6. Marais, J.; Versini, G.; van Wyk, C. J.; Rapp, A. *S. Afr. J. Enol. Vitic.* **1992**, *13*, 71-77.
7. Razungles, A.; Günata, Z.; Pinatel, S.; Baumes, R.; Bayonove, C. *Sci Aliments* **1993**, *13*, 59-72.
8. Sefton, M. A.; Francis, I. L.; Williams, P. J. *Am. J. Enol. Vitic.* **1993**, *44*, 359-370.
9. Sefton, M. A.; Francis, I. L.; Williams, P. J. *J. Food Sci.* **1994**, *59*, 142-147.
10. Strauss, C. R.; Wilson, B.; Anderson, R., Williams, P. J. *Am. J. Enol. Vitic.* **1987**, *38*, 23-27.
11. Enzell, C. *Pure & Appl. Chem.* **1985**, *57*, 693-700.
12. Winterhalter P.; Sefton, M. A.; Williams, P. J. *J. Agric. Food Chem.* **1990**, *38*, 1041-1048.
13. Razungles, A. J.; Bayonove, C. L.; Cordonnier, R. E.; Sapis, J. C. *Am. J. Enol. Vitic.* **1988**, *39*, 44-48.
14. Razungles, A.; Bayonove, C. In *La Viticulture à L'aube du IIIe Millénaire, Numéro hors Série, J. Internat. Sci. Vigne et Vin;* Bourd, J.; Guimberteau, G., Eds; Vigne et Vin Publications Internationales: Martillac, 1996, 33; pp. 85-88.

15. Gerdes, S. M.; Winterhalter, P.; Ebeler, S. E. In *Carotenoid-Derived Aroma Compounds*; Winterhalter, P.; Rouseff, R. L., Eds.; ACS Symp. Ser. 802; American Chemical Society: Washington, DC, 2002; pp 262-272.
16. Razungles, A. J.; Baumes, R. L.; Dufour, C.; Sznaper, C. N.; Bayonove, C. L. *Sci. Aliments* **1998**, *18*, 361-373.
17. Schultz, H. R.; Löhnertz, O.; Bettner, W.; Bálo, B.; Linsenmeier, A.; Jähnisch, A.; Müller, M.; Gaubatz, B.; Váradi, G. *Vitis* **1998**, *37*, 191-192.
18. Steel, C. C.; Keller, M. *Biochem. Soc. Trans.* **2000**, *28*, 883-885.
19. Lee, S.-H.; Seo, M.-J.; Riu, M.; Cotta, J. P.; Block, D. E.; Dokoozlian, N. K.; Ebeler, S. E. *Am. J. Enol. Vitic.*, **2006**, Submitted.

Chapter 7

Effects of Characteristic Volatiles of Boiled Celery on Chicken Broth Flavor

Yoshiko Kurobayashi[1,2], Akira Fujita[2], and Kikue Kubota[1]

[1]Laboratory of Food Chemistry, Department of Nutrition and Food Science, Ochanomizu University, 2–1–1, Otsuka, Bunkyo-ku, Tokyo, Japan
[2]Technical Research Center, T. Hasegawa Company, Ltd., 335, Kariyado, Nakahara-ku, Kawasaki, Japan

The organoleptic properties of characteristic odorants of boiled celery, a food ingredient often used to enhance the flavors of soups and simmered food preparations, were investigated. 3-*n*-Butylphthalide, sedanenolide, and sedanolide in their optically active forms, were found to be the most potent odorants in both raw and boiled celery. These phthalides were also found to possess richer and more natural celery-like notes than the phthalides in optically unnatural forms. Sensory evaluations using chicken broth revealed that volatile constituents contributed to the flavor-enhancing effects of celery, and these phthalides were the major components for the effects.

Celery (*Apium graveolens* L. var. *dulce*) is one of the most popular and uniquely aromatic vegetables in the world. In Western cuisine celery is used as a staple for preparations of soups and simmered foods, because it is known to have the remarkable abilities to enhance complex flavors, reduce the unpleasant flavors of other materials, and improve overall palatability.

Assuming that these effects are conferred by odor constituents of celery, we examined the organoleptic properties of celery odor through chemical and sensory analyses.

78 © 2008 American Chemical Society

Analysis of Volatile Components of Boiled Celery

The odor impressions of boiled celery are quite different from those of raw celery. Though both have a spicy note, the former tends to be mild and sweet while the latter tends to be sharp and green. Many researchers have investigated the odor components of celery and found alkylphthalides as potent contributors to celery odor (*1-3*). No studies, however, have elucidated the roles of these three alkylphthalides in thermally induced change or identified the organoleptic properties of these alkylphthalides as flavor enhancers or reducers in practical cooking. The major phthalides are shown in Figure 1.

Odor Active Components in Raw and Boiled Celery

A bunch of celery stalk was divided into two portions and cut into 1 cm squares. One portion, weighing 1,200 g, was soaked in 2,400 g of distilled water for 1 hour; the other was boiled in 2,400 g of distilled water in a stainless steel pot for 1 hour (mimicking culinary preparation). After the preparations were filtered, each filtrate was extracted with 300 mL of diethyl ether three times, and the oil layer was concentrated to approximately 50 mL under atmospheric pressure and distilled using solvent-assisted flavor evaporation (SAFE) apparatus (*4*). The distillates were dried over Na_2SO_4 and then concentrated to approximately 20 μL and subsequently analyzed by gas chromatography (GC) with a non-polar capillary column, GC-mass spectrometry (GC/MS), and GC-olfactometry (GC/O) using the technique of aroma extract dilution analysis (AEDA) (*5*).

Figure 2 shows aromagrams of raw and boiled celery. Seven compounds, i.e., 3-*n*-butylphthalide, sedanenolide, *trans*- and *cis*-sedanolide, (3*E*,5*Z*)-1,3,5-undecatriene, myrcene and (*E*)-2-nonenal, were identified in both raw and boiled materials. Two compounds, i.e., (*Z*)-3-hexenal and (*Z*)-3-hexenol, were dominant in the raw materials and four compounds, i.e., 2-methylbutanoic acid, sotolon, *β*-damascenone and *β*-ionone, were dominant in the boiled materials. Among these compounds, 3-*n*-butylphthalide (**1**), sedanenolide (**2**), and *trans*- and *cis*-sedanolides (**3, 4**) had the highest FD-factors in both concentrates. The odor characteristics of these compounds, sweet spicy and green spicy, were strongly reminiscent of celery note and appeared to contribute most to the odors of raw and boiled celery.

Quantification of Phthalides

The phthalides were quantified to elucidate differences between raw and boiled states. In devising the quantification, we took steps to prevent losses in the phthalide recovery. In brief, the celery stalks were homogenized in distilled water and divided into two portions. One portion was filtered immediately and the other was filtered after refluxing for 1 hr at atmospheric pressure. The
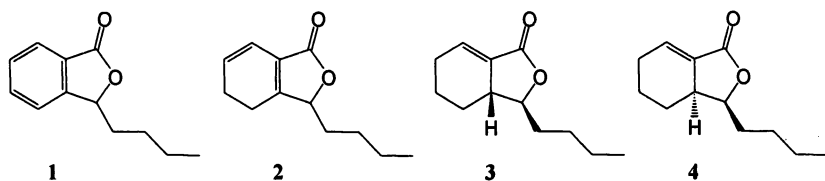
Figure 1. Phthalides identified as most odor active components in celery odor.
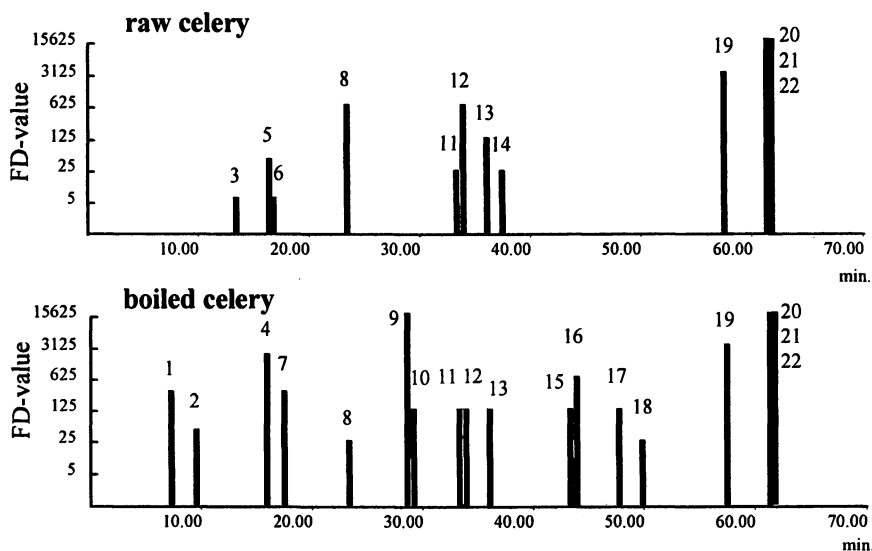
Figure 2. Aromagrams of raw and boiled celery stalks. 3; (Z)-3-hexenal (green) , 6;
(Z)-3-hexenol (green), 7; 2-methylbutanoic acid (valeric) , 8; myrcene (metallic), 9;
sotolon (sweet spicy), 11; (E)-2-nonenal (cardboard-like), 13; (3E,5Z)-1,3,5-undecatriene
(fragrant fruity), 16; β-damascenone (sweet fruity), 18; β-ionone (floral fruity), 19; 3-*n*-
butylphthalide (green spicy), 20; sedanenolide (sweet spicy), 21; *trans*-sedanolide (sweet
spicy), 22; *cis*-sedanolide (sweet spicy).

residues were extracted with methanol and filtered again. Both filtrates of each sample were centrifuged together, then the upper layers were applied on Porapak Q® columns (2.5 cm i.d. x 13 cm, Waters Co., Ltd., Milford, MA, USA). After desorption with diethyl ether and pentane (3:2), 3-propylidenephthalide was added as an internal standard (IS). The amounts of phthalides were determined by gas chromatography using the calibration curves of IS and each compound.
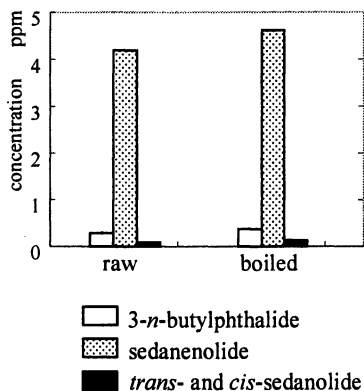
Figure 3. Concentrations of phthalides in raw and boiled celery stalks.

Figure 3 shows the concentrations of phthalides in raw and boiled celery stalks. Sedanenolide and 3-*n*-butylphthalide were the first and second most abundant of the three compounds in both materials. There were no significant differences in the amounts of phthalides between the raw and boiled materials.

These results indicate the importance of the phthalides does not change after boiling. We also suppose that the sweet and mild notes of boiled celery are characterized by other thermally-generated compounds, i.e., 2-methylbutanoic acid, sotolon, β-damascenone and β-ionone, and thermally-reduced compounds, i.e., (Z)-3-hexenal and (Z)-3-hexenol.

Distribution and Sensory Properties of Optically Pure Phthalides in Celery

Optically pure 3-*n*-butylphthalide and sedanenolide were isolated from racemic 3-*n*-butylphthalide (Givaudan, Schweiz AG, Duebendorf, Switzerland) and natural celery essential oil (Ikeda Bussan, Tokyo, Japan), respectively, by a high performance liquid chromatography (HPLC) equipped with a chiral separative column, CHIRALCEL OB-H, 0.46 cm x 25 cm (Dicel Chemical Industries, Ltd., Tokyo, Japan). The (3*S*,3a*R*)-sedanolide was obtained

commercially (Wako Pure Chemical Industries, Ltd. Osaka, Japan). The enantio separation of the phthalides in natural celery odors was performed by a GC/MS equipped with a chiral separative column, CHIRAMIX® (60 m x 0.25 mm i.d.) (6).

Gas chromatograms of phthalides in raw and boiled celery volatiles are shown in Figure 4. (-)-3-*n*-Butylphthalide and (-)-sedanenolide were dominant in raw and boiled celery, at the ratios of 94 and 96% ee, 94 and 90% ee, respectively. (-)-(3*S*,3a*R*)-sedanolide was optically pure in both samples.

The odor qualities of (-)-3-*n*-butylphthalide, (-)-sedanenolide and (-)-(3*S*,3a*R*)-sedanolide were green spicy, sweet spicy, and extremely sweet spicy, respectively. The first two compounds were reminiscent of natural celery more strongly than their (+)-isomers.
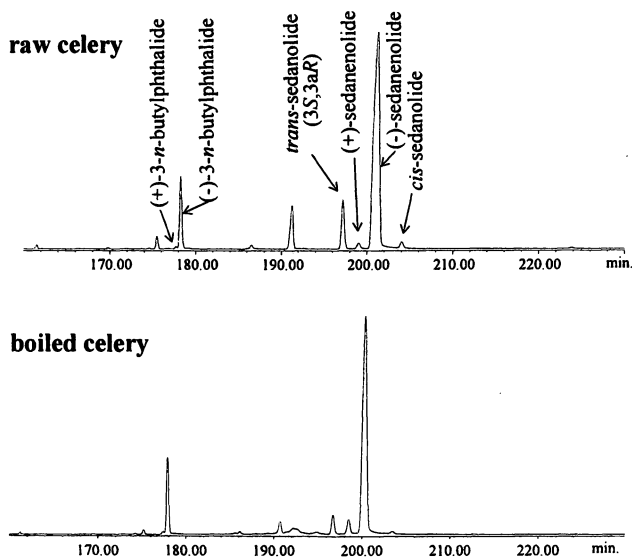
Figure 4. Gas chromatograms of phthalides in raw and boiled celery stalks.
Column : CHIRAMIX® (0.25 mm i.d. x 60 m)

Flavor-Enhancing Effect of Volatile Constituents of Celery on Chicken Broth

One purpose of using celery in a soup preparation is to add celery flavor. Another more important purpose is to enhance the overall flavor of the soup itself. Empirical observations have confirmed that even when used at levels too low to give a distinct celery odor, celery is effective to produce a favor-able flavor including complex senses such as "thickness," "mellowness,"

"robustness," "clear," "duration in the mouth," and "less unpleasantness." In a review of the complex flavors and palatability of food preparations related with umami substances, Yamaguchi found that the addition of monosodium glutamate (MSG) to beef broth improved the overall palatability while enhancing flavor characteristics such as "continuity," "full-bodied," "impact," "mildness," and "thickness" (7). According to Yamaguchi, these flavor characteristics expressed the Japanese concept of "koku," an important factor of palatability. We considered the favorable flavor brought by celery to be same as "koku." Besides MSG, many taste substances, i.e., sugars, salts, amino acids, some special peptides and alliin, were reported to influence flavor-enhancing effects in food preparation (8-11), though not in ways that have yet been fully discussed or studied. To investigate further, our group examined the effects of celery odor as a flavor enhancer in a chicken broth prepared from animal materials only. We carefully evaluated the changes in the flavor when celery constituents were added to the broth.

Evaluation of Flavor-Enhancing Effect of Celery Constituents

One thousand grams of chicken bone and meat was boiled in 6,000 g of deionized water for 3 hours down to 3,000 g with skimming off the scum and fat. The broth was filtered through gauze and stored at -20°C. Before evaluation, 0.3% NaCl was added. Five hundred grams of celery stalks were cut into 1 cm square pieces and boiled in 2,000 mL of distilled water for 20 min, and then distilled under atmospheric pressure for 40 min. The distillate was used as the "celery odor constituents", and the water residue was used as the "taste constituents."

A panel of 12 females (age range: 22 to 26 years old) well trained in sensory analysis conducted two evaluation sessions.

The samples were prepared by adding extracts of natural celery or odor compounds to chicken broth. The concentration of each extract or odor compound was preliminarily set below a detectable level. In the session, a simple chicken broth alone (control) and two or three samples of chicken broth prepared with celery extract or odor compound kept at 60°C were presented. The panel was asked to taste each sample in the mouth, rate the overall palatability of each flavor of sample in comparison with the control on a line scale ranging -1 to 1 (weak on the left, neutral at zero, strong on the right), and describe their flavor impressions in their own language. The mean scores were analyzed by ANOVA.

In the first evaluation session, the panel evaluated how the odor and taste constituents of the celery affected the chicken broth flavor. The samples were prepared by adding of 0.7% of celery odor constituents and 7% of taste constituents to chicken broth. Distinct flavor of celery was not perceived in both samples in those low concentrations.
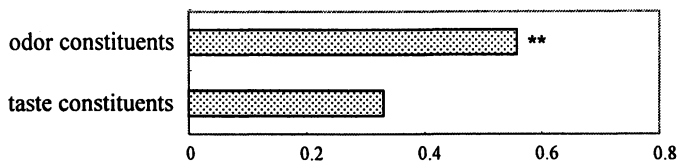
Figure 5. Overall palatability of the chicken broth prepared with the odor and taste constituents of celery. **: significant difference P<0.01

Figure 5 shows the average scores of the samples, and Table I presents the free descriptions of the flavor impressions. Both scores of samples containing the odor and taste constituents for overall palatability were higher than that of the control (both scores were positive in the bar graph), but the difference was significant only in the sample containing odor constituents. Most of the panel failed to discern the celery-like flavor in either sample. Instead, they tended to perceive the changes produced by the addition of celery constituents as reductions in unpleasant flavors (e.g., "greasiness" and "unpleasant meatiness") and increases in pleasant flavors (e.g., "sweetness, " "umami, " "mellowness, " and "pleasant meatiness") in both samples. We considered these changes to be enhanced flavor.

These results suggested that the odor constituents of the celery contributed to the flavor-enhancing effect more than the taste components.

In the second session, the panel evaluated the effects of the three phthalides previously identified as the most potent odorants in celery. Samples containing 3-*n*-butylphthalide, sedanenolide, and sedanolide at levels of 0.2 ppm, 0.7 ppm, and 0.2 ppm, respectively, were evaluated by the same method used in the first session.

Table I. Odor Impressions of Chicken Broth Prepared with the Odor and the Taste Constituents of Celery [a]

Odor Constituents	Taste Constituents
refined	greasy, fatty
juicy meaty	fatty
less greasiness	unpleasant meaty flavor
less unpleasant meatiness	less unpleasant flavor
clear	clear
mellow	umami
favorable meaty	sweet
sweet	
umami	

[a] The odor impressions are relative to the control with no added celery constituents.

As shown in Figure 6 and Table II, the mean scores of all samples on overall palatability were significantly higher than the control score. The celery-like flavor was only discerned in the sample containing sedanolide, and only by three of the panel. Most panelists perceived the changes of flavors as a reduction in unpleasant meatiness and an increase in pleasant flavors ("refinedness, " "mildness, " "sweetness, " "richness" and "umami "). These effects were almost the same as those of the celery odor constituents in the first session. On this basis, we concluded that these phthalides are the strongest contributors to the effects of celery in soup.
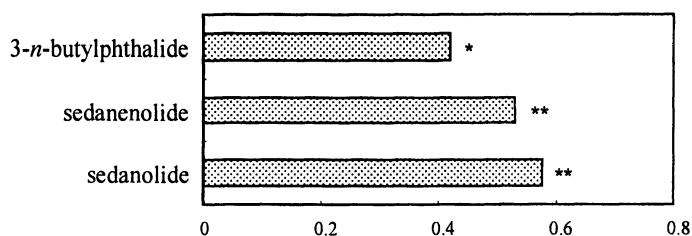
Figure 6. *Overall palatability of the chicken broth prepared with phthalides.*
*: significant difference P<0.05, **: significant difference P<0.01

Table II. Odor Impressions of Chicken Broth Prepared with Phthalides[a]

3-n-Butylphthalide	Sedanenolide	Sedanolide
less unpleasant meatiness	less unpleasant meatiness	less unpleasant meatiness
less greasiness	less greasiness	less greasiness
rich	rich	refined
refined	complex	.mellow
mellow	refined	sweet
sweet	sweet	umami
vegetable-like	pleasant meaty vegetable-like	celery-like

[a] The odor impressions are relative to the control with no added phthalides.

Conclusion

Our results have shown that the phthalides, i.e., 3-*n*-butylphthalide, sedanenolide and sedanolide, contribute to both the characteristic odor of raw and boiled celery and the flavor-enhancing effects of celery in soup preparation.

The addition of odor constituents and the addition of the phthalides individually enhanced the flavor of chicken broth as if celery was boiled together with chicken meat. Most of the panel indicated that the effects of celery odor constituents and the phthalides improved the palatability (by decreasing unpleasant flavor and enhancing sweetness, umami, pleasant meatiness, richness, refinement, mellowness, etc.). The distinctive perception of celery flavor did not influence these effects.

References

1. *Volatile compounds in foods 8.2th;* Nijssen, B.; van Ingen-Vissher, K.; Donders, J. Eds.; TNO Nutrition and Food Research Institute: Zeist, The Netherlands, 2002.
2. Uhlig, J.; Chang, A.; Jen, J. J. *J. Food Sci.* **1987**, *52*, 658-660.
3. MacLeod, G.; Ames, J. *Phytochemistry* **1989**, *28*, 1817-1824.
4. Engel, W.; Bahr, W.; Schieberle, P. *Eur. Food Res. Technol.* **1999**, *209*, 237-241.
5. Ullrich, F.; Grosch, W. *Z. Lebensm. Unters. Forsch.* **1987**, *184*, 277-282.
6. Tamogami, S.; Awano, K.; Amaike, M.; Takagi, Y.; Kitahara, T. *Flavour Fragr. J.* **2001**, *16*, 349-352.
7. Yamaguchi, S. *Jpn. J. Taste and Smell Res.* **1997**, *4*, 515-518.
8. Yamaguchi, S. *Jpn. J. Taste and Smell Res.* **2002**, *9*, 393-396.
9. Ogasawara, M. *Koryo*, **2003**, *217*, 113-118.
10. Watanabe, K.; Lan, H.-L.; Yamaguchi, K.; Konosu, S. *Nippon Shokuhin Kogyo Gakkaishi*, **1990**, *37*, 439-445.
11. Ueda, Y.; Sakaguchi, M.; Hirayama, K.; Miyajima, R.; Kimizuka, A. *Agric. Biol. Chem.* **1990**, *54*, 163-169.

<div align="center">Chapter 8</div>

Identification of Aroma Components during Processing of the Famous Formosa Oolong Tea "Oriental Beauty"

Miharu Ogura[1], Tomomi Kinoshita[3], Bun-ichi Shimizu[3],
Fumiharu Shirai[1], Kazuhiko Tokoro[1], Mu-Lien Lin[2],
and Kanzo Sakata[3]

[1]Central Research Laboratory, TAKASAGO International Corporation,
1–4–11 Nishi-yawata, Hiratsuka city, Kanagawa 254–0073, Japan
[2]Tea Research and Extension Station, 324 Chunghsin Road, Yangmei,
Taoyuan, 326, Taiwan
[3]Institute for Chemical Research, Kyoto University, Uji, Kyoto
611–0011, Japan

Oriental Beauty (Pom-Fong tea) is a high-grade tea that has a pronounced honey aroma and a rich flavor of ripe fruit. It is produced *via* a higher degree of fermentation from tea leaves infested by tea green leafhoppers (*Jacobiasca formosana*) in Taiwan. We have carried out aroma analyses of tea samples obtained during processing to know the molecular basis of production of the characteristic aroma. Two series of tea samples were prepared by the same method from healthy leaves and those infested by the insect. As a result of aroma analysis, the amount of the aroma components produced from the infested tea leaves was higher than the non-infested tea leaves as the fermentation progressed. 2,6-Dimethylocta-3,7-diene-2,6-diol (DOD) in the infested tea leaves was found to have been generated even in the leaves and at early stages of the manufacturing processes. Chiral analysis of DOD showed high enantiopurity and its absolute configuration was the same as linalool and 3,7-dimethylocta-1,5,7-trien-3-ol (hotrienol), suggesting that DOD and hotrienol are biosynthesized from linalool.

87

There are various aroma types of oolong tea. Oriental Beauty, in particular, has a very unique flavor compared with other teas, and is also called Formosa oolong tea, Pom-Fong tea, Champagne oolong tea, White Tip oolong tea, etc. This is one of the tea products representing Taiwan.

Aroma analyses of oolong tea has been reported by several researchers (*1, 2*). The major components of Chan Pin oolong tea were reported by Kawakami *et al.* (*3*). In our study, the key odorous compounds of Oriental Beauty and the change of aroma profile at each step of the manufacturing process were investigated by GC/MS and aroma extract dilution analysis using a sniffing–GC (*4, 5*). As hotrienol and DOD are characteristic aroma components in this oolong tea, aroma formation should be focused on the tea manufacturing procedures or the leaves.

In comparison with other oolong tea, a unique manufacturing process enables a preparation of this oolong tea. The characteristic points are in the tea leaves and the process *via* the higher degree of fermentation. The leaves infested by the tea green leafhopper, *J. formosana*, are used as raw materials for tea manufacturing. The leafhoppers suck the juvenile leaves using their needle-like mouthparts that cause the leaves to become curved with tiny yellow wounding spots. By the continuous infestation, especially under the dry conditions in the season, the leaves become stunted. The infested leaves with severe symptoms are used for manufacturing Oriental Beauty. This is a very unique and important point.

Another unique point is the manufacturing process. The steps of solar withering are longer, more times of turning over are applied, and the additional steps, wetting and softening, are carried out before rolling. Thus, the degree of fermentation becomes higher. The infusion of Oriental Beauty has a unique and rich aroma like a ripened fruit and honey after these manufacturing processes.

We think that these unique features induce synthesis of many volatile compounds in the leaves in response to different stresses such as insect infestation, light stress, drought stress, and wounding. To understand the biochemical process of flavor formation during manufacturing, we have investigated the changes of tea aroma formation throughout the manufacturing process as well as the differences of volatile components between the tea samples prepared in the same manner from healthy tea leaves and infested ones.

Materials and Methods

Tea Sample Preparation

Two types of leaves (with/without insect infestation) were used for tea sample production: leaves of cv. Chinshin Dahpan cultivated under the best quality control and those of the same variety plucked from tea plants to be intentionally infested by leafhoppers were harvested in June 2004. The non-

infested tea samples were prepared from leaves of the same cultivar plucked in September 2004 because the healthy leaf samples obtained in June 2004 were found to be slightly infested. Each tea sample was prepared *via* general manufacturing process of Oriental Beauty using these tea leaves after panning process. Run 7 shows the ordinary manufacturing process for the tea. To examine the change of aroma profile at each step of earlier processing where enzyme reactions possibly occur, two series of seven kinds of tea samples were prepared as shown in Table 1: *e.g.*, AF and BF samples were prepared by subjecting freshly plucked leaves to panning and the following processes without solar and indoor witherings as well as turning over from infested and healthy leaves, respectively.

Preparation of Aroma Extract

Each tea sample (5.0 g) was brewed with 75 g of deionized boiling water for 10 min. After filtration, the filtrate volume was adjusted to 50 mL, and 50 μL of an ethanol solution containing 0.01% 3-octanone as an internal standard was added. The solution was saturated with sodium chloride and was extracted with 20 mL of dichloromethane. The extract was dried over anhydrous sodium sulfate for 12 h. The solvent was carefully removed with a Kuderna-Danish evaporative concentrator. The aroma extracts were analyzed by GC and GC/MS.

Instrumental Methods

Gas Chromatography (GC). GC analysis was performed on a HP 6890 gas chromatograph (Agilent Technologies, Inc., Palo Alto, CA), equipped with an FID and a HP-20M fused silica capillary column (25 m × 0.2 mm i.d., film thickness 0.1 μm, Agilent Technologies). The oven temperature was programmed from 55 °C to 215 °C at 4 °C/min. Helium was used as the carrier gas and the linear velocity was 18 cm/s. The split ratio was 1:50. The injector and detector temperatures were 250 °C.

Gas Chromatography/Mass Spectrometry (GC/MS). GC/MS analysis was performed on a GCMS-QP-2010 (Shimadzu), equipped with a BC-WAX fused silica capillary column (50 m × 0.2 mm i.d., film thickness 0.15 μm, GL Sciences, Inc., Tokyo, Japan). The oven temperature was programmed from 70 °C to 220 °C at 4 °C /min. Helium was used as the carrier gas and the linear velocity was 28 cm/s. The split ratio was 1:50. Mass spectra were obtained at 70 eV (EI) with an ion source temperature of 200 °C. The identification of the components was made by comparison of their GC retention times and mass spectra to those of authentic compounds.

Enantio-MDGC/MS System. Enantio-MDGC/MS analysis was performed with a multidimensional gas chromatograph, MDGC-2010 (Shimadzu Corporation, Kyoto, Japan). The two capillary columns of the MDGC were

Table I. Preparation of Tea Samples

Run	Solar Withering	Indoor Withering	Turning Over	Panning	Wetting and Softening	Rolling	Drying	Tea leaves[a] Infested	Tea leaves[a] Healthy (not infested)
1	⇑			⇑	⇑	⇑	⇑	AF	BF
2	⇑			⇑	⇑	⇑	⇑	ASW	BSW
3	⇑	⇑	1 time	⇑	⇑	⇑	⇑	AT1	BT1
4	⇑	⇑	2 times	⇑	⇑	⇑	⇑	AT2	BT2
5	⇑	⇑	3 times	⇑	⇑	⇑	⇑	AT3	BT3
6	⇑	⇑	4 times	⇑	⇑	⇑	⇑	AT4	BT4
7	⇑	⇑	5 times	⇑	⇑	⇑	⇑	AT5	BT5

[a]. F, fresh leaves; SW, solar withering; T1~T5, 1~5 times of indoor-withering and turning-over.

coupled with a switching device. The precolumn was identical with the column of the GC/MS system described above. The oven temperature was programmed from 70 °C to 220 °C at 9 °C /min. Helium was used as the carrier gas and the linear velocity was 45 cm/s. Split (1:20) and splitless injections were used. The injector temperature was 250 °C. The detector was an FID and the temperature was 250 °C. The main column used was a Beta-DEX^{TM} 225 (25 m × 0.25 mm i.d., film thickness 0.25μm, Supelco, Bellefonte, PA). The oven temperature was programmed from 70 °C to 100 °C at 1 °C /min. Mass spectra were obtained at 70 eV (EI) with an ion source temperature of 200 °C. Constituents were identified by comparison of their mass spectra and retention times with those of authentic compounds.

Results and Discussion

Volatile Components

To identify aroma components induced by the stresses in tea leaves and during the manufacturing process, the infusion of each tea leaf sample was extracted and analyzed by GC and GC/MS. Gas chromatograms of these aroma extracts are shown in Figure 1. Most of the aroma components gradually increased as the fermentation progressed. The rate of increase of the volatile components in the tea produced from infested leaves was much higher than that of the tea sample from healthy leaves. Twenty-four main aroma compounds were selected from aroma components shown in Fig. 1 and the relative ratio of each GC area to internal standard was examined. To compare these components between tea samples with and without insect infestation at different steps of the tea manufacturing process, four samples (AF, BF, AT5, BT5) were summarized in Table II. Alcoholic aroma compounds, especially benzyl alcohol, 2-phenylethanol and hexanol, were increased as the fermentation progressed as well as the linalool oxides and hexenoic acids. The increasing ratio of these compounds in the infested tea leaves was almost the same as those in the non-infested tea leaves.

When the aroma components between the infested (AF) and healthy leaves (BF) were compared to elucidate the effect of insect infestation on volatiles, the prominent difference was observed in compound number nineteen, namely, 2,6-dimethylocta-3,7-diene-2,6-diol (DOD). The amount of DOD in AF is about 15 times higher than that in BF. The level of hotrienol in AF is also about 70 times higher than that in BF. These compounds were confirmed to be diagnostic for the insect infestation as previously reported (6). Moreover, the complicated manufacturing procedures, which are considered to cause the stress-responsive biochemical reactions in tea leaves for their self-defense against many kinds of stresses such as draught stress during withering, injuring stress during turning over and so forth, was demonstrated to be necessary for the rich aroma of Oriental Beauty.

Enantioselective Analysis

We found large differences in the amounts of hotrienol and DOD between the healthy and infested tea leaves. DOD was a characteristic compound in infested tea leaves. Simultaneous enantioselective analysis of DOD and related compounds, linalool and hotrienol, was achieved by using an enantio-MDGC/MS system equipped with an achiral precolumn and a chiral main column.

The optically active hotrienol and DOD as authentic references were synthesized to identify the absolute configuration of these compounds. The *R*-form of hotrienol was synthesized from commercial available (*R*)-linalool (*7*). The *R*-form of DOD was synthesized by epoxidation and reduction of the optically active hotrienol.

DOD and hotrienol had high enantiopurity in both the infested and the non-infested tea samples, while linalool showed lower optical purity as shown in Table III. The predominant absolute configurations of these three compounds were the *S*-forms. No significant racemization was observed during the tea processing. The biosynthesis of DOD has not yet been elucidated though DOD is considered to be derived from the oxidation of linalool.

Conclusion

The profiles of aroma components of Oriental Beauty were investigated during the manufacturing process. As the fermentation progressed, the amounts of the aroma components produced in infested tea leaves became much higher than those in non-infested tea leaves. We confirmed that insect infestation and higher fermentation were necessary to produce Oriental Beauty rich in the characteristic aroma. DOD was even contained in fresh tea leaves, indicating that DOD was a key volatile compound produced by insect infestation. DOD was present in high optical purity in the tea leaves and its absolute configuration was the same as those of hotrienol and linalool. This clearly indicates that DOD is produced *via* enzyme reactions. The identification of the enzymes and cDNAs involved in the biosynthesis of DOD is now in progress.

Acknowledgments
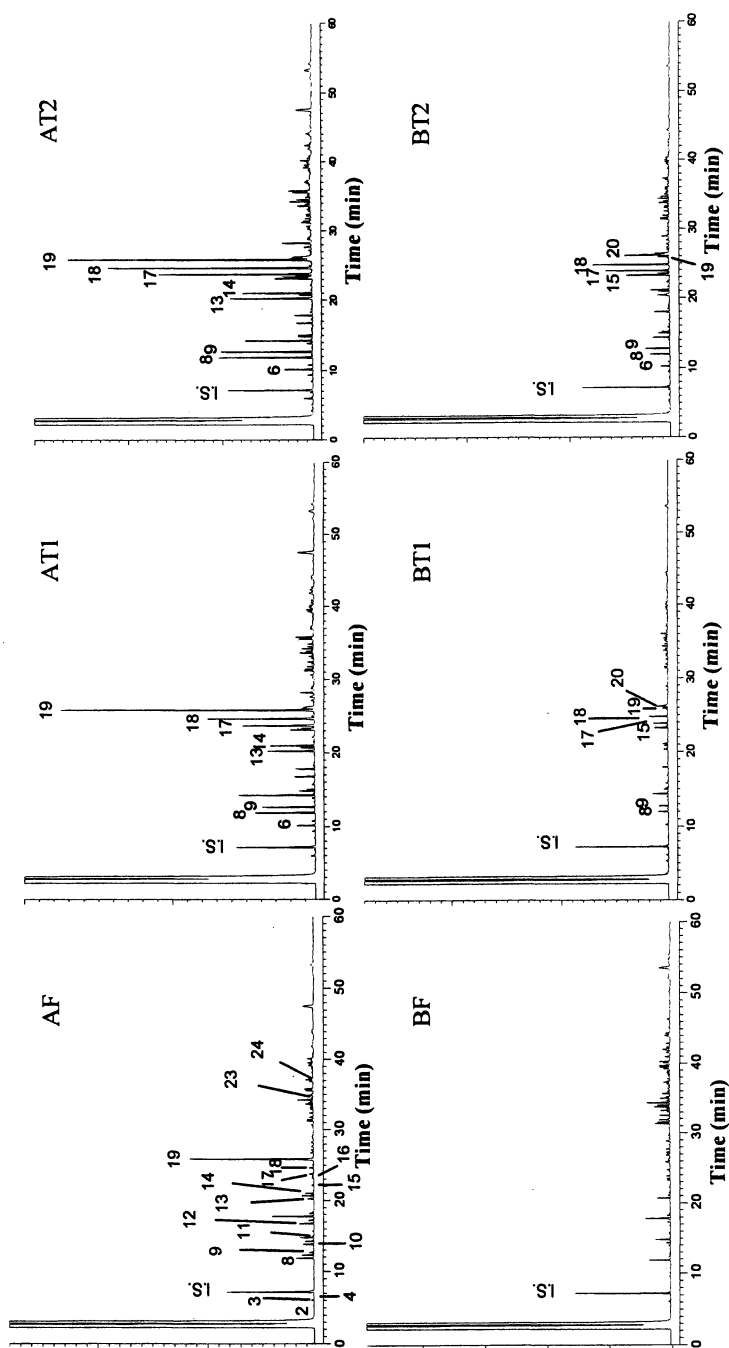
Figure 1-1. Gas chromatograms of tea aroma extracts. Upper chromatograms are Infested samples, and lower are healthy (not infested) samples. I.S. is internal standard (3-octanone).
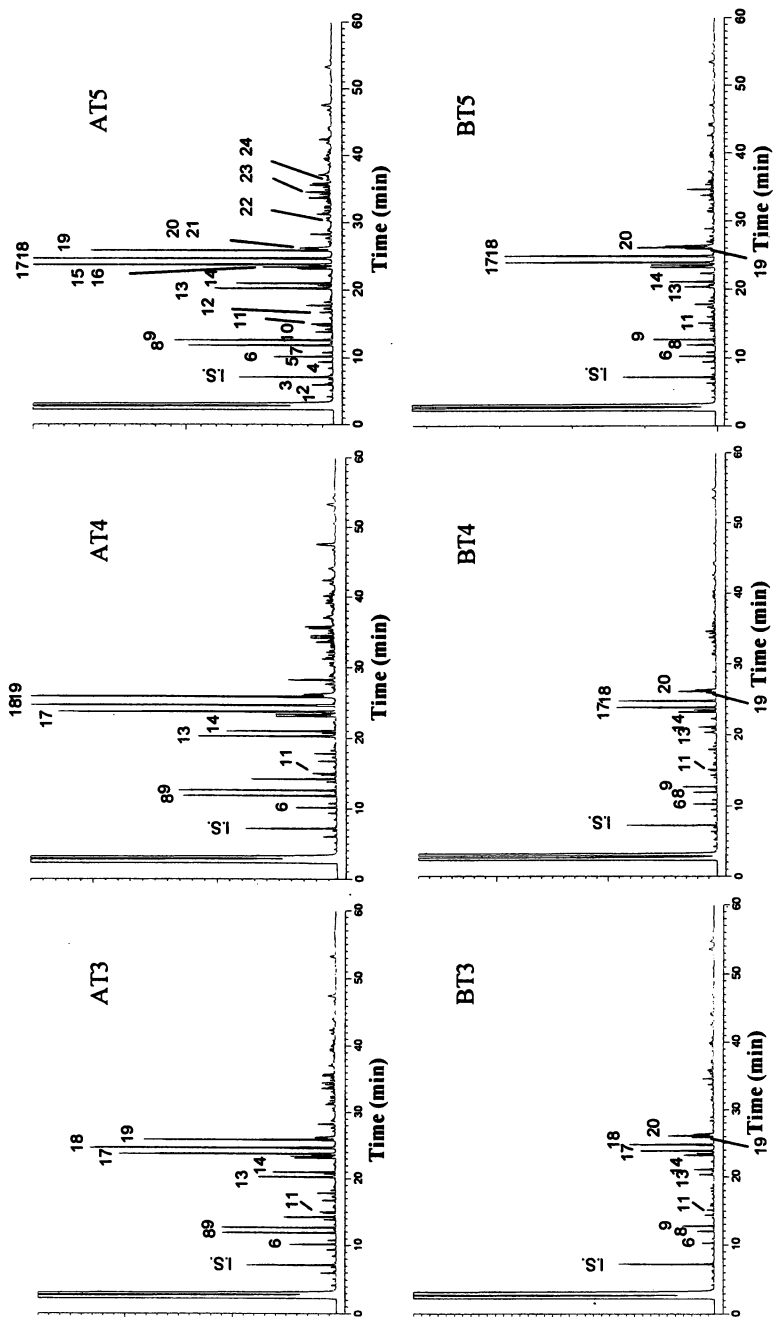
Figure 1-2. Gas chromatograms of tea aroma extracts. Upper chromatograms are Infested samples, and lower are healthy (not infested) samples. I.S. is internal standard (3-octanone).

Table II. Comparison of Tea Aroma Components

No.	Compound	Area/I.S. Area			
		BF	BT5	AF	AT5
1	Hexanal	0.0046	0.052	nd	0.040
2	1-Penten-3-ol	0.0057	0.057	0.0027	0.047
3	Isoamyl alcohol	nd	0.034	0.0024	0.20
4	Amyl alcohol	0.0047	0.074	0.010	0.064
5	Hexanol	nd	0.17	nd	0.18
6	(Z)-3-Hexenol	nd	0.46	nd	0.71
7	(E)-2-Hexenol	nd	0.11	0.0016	0.13
8	trans-Linalool 3,6-oxide (Linalool oxide I)	trace	0.36	0.040	1.8
9	cis-Linalool 3,6-oxide (Linalool oxide II)	0.016	0.72	0.067	1.7
10	Benzaldehyde	nd	0.075	0.0014	0.24
11	Linalool	0.014	0.20	0.022	0.24
12	3,7-Dimethylocta-1,5,7-trien-3-ol (hotrienol)	0.0029	0.060	0.20	0.16
13	trans-Linalool 3,7-oxide (Linalool oxide III)	trace	0.43	0.11	1.6
14	cis-Linalool 3,7-oxide (Linalool oxide VI)	0.052	0.61	0.14	1.2
15	Caproic acid	0.063	1.3	0.043	0.60
16	Geraniol	nd	0.87	0.036	0.87
17	Benzyl alcohol	0.038	3.5	0.11	4.3
18	2-Phenylethanol	0.065	3.6	0.11	4.4
19	2,6-Dimethylocta-3,7-diene-2,6-diol (DOD)	0.12	0.43	1.8	3.1
20	(Z)-3-Hexenoic acid	nd	1.6	nd	0.47
21	(E)-2-Hexenoic acid	nd	1.1	nd	0.68
22	3,7-Dimethylocta-1,7-diene-3,6-diol	nd	0.049	nd	0.22
23	2,6-Dimethylocta-2,7-diene-1,6-diol	nd	0.46	0.073	0.44
24	Methyl jasmonate	0.12	0.080	0.038	trace

nd: not detected

Table III. Enantiomer Ratio of Hotrienol, DOD and Linalool

Tea samples		Hotrienol		DOD		Linalool	
		S	R	S	R	S	R
Infested leaves	AF	>99.9	nd	99.1	0.9	77.6	22.4
	AT5	95.5	4.5	98.7	1.3	82.5	17.5
Healthy leaves	BF	>99.9	nd	>99.9	nd	80.7	19.3
	BT5	94.1	5.9	98.0	2.0	94.3	5.7

nd: not detected

References

1. Sakata, K.; Mizutani, M. *Food & Food Ingred. J. Jpn.* **2003**, *208*, 991-1003.
2. Yamanishi, T. *Koryo* **2001**, *211*, 129-136.
3. Kawakami, M.; Ganguly, S. N.; Banerjee, J.; Kobayashi, A. *J. Agric. Food Chem.* **1995**, *43*, 200-207.
4. Ogura, M.; Otsuka, M.; Yamazaki, Y.; Shimizu, T.; Kawakami, Y.; Shirai, F. *The 47th Symposium on the Chemistry of Terpenes, Essential Oils, and Aromatics*, 2003, pp 13-15.
5. Kinoshita, T.; Sakata, K. *Koryo* **2006**, *229*, 113-120.
6. Chen, Z.; Xu, N.; Baoyu, H.; Zhao, D. *2004 International Conference on O-CHA (tea) Culture and Science*, Shizuoka, 2004, pp 90-93.
7. Yuasa, Y.; Kato, Y. *J. Agric. Food Chem.* **2003**, *51*, 4036-4039.

Chapter 9

Volatile Constituents of Mesquite (*Prosopis*) Pods

Gary Takeoka[1], Peter Felker[2], Dante Prokopiuk[3], and Lan Dao[1]

[1]Western Regional Research Center, Agricultural Research Service, U.S. Department of Agriculture, 800 Buchanan Street, Albany, CA 94710
[2]D'Arrigo Brothers Company, P.O. Box 850, Salinas, CA 93902
[3]Universidad Nacional del Nordeste, Facultad de Agroindustrias, Cdte. Fernández 755, Roque Sáenz Peña, Chaco, Argentina

Mesquite is the common name in North America for leguminous desert plants of the genus *Prosopis* that has about 44 species native to North America, South America, Africa and south Asia. Mesquite pods were a major food source of indigenous people in the semi deserts of North and South America before the arrival of Europeans. The pods, which contain about 10% protein and 10-40% sucrose, have a cinnamon, café mocha and coconut aroma. Volatiles were isolated from mesquite pods by closed loop dynamic headspace sampling. A total of 121 volatiles were identified (14 of which were tentatively identified) using GC and GC/MS.

Mesquite (*Prosopis spp.*) are woody leguminous plants that belong to the family Leguminosae and grow in arid and semiarid regions of America, Africa and Asia. The 44 *Prosopis* species range in size from multi-stemmed, 2-inch trunk diameter, 8 ft. tall shrubs in the deserts of southern New Mexico to 60 ft. tall trees with 6 ft. diameter trunks in the river bottoms of northwestern

98

Argentina. Most people in the U.S. know mesquite for the flavor the smoke imparts to grilled steaks and seafood. However, the plant has attracted attention due to its ability to tolerate high temperatures and low rainfall, its capacity to grow in saline soil and its ability to fix nitrogen (*1-3*). *Prosopis spp.* produce indehiscent fruit (pods) that contain 13 to 50% sugar, 27 to 32% dietary fiber and 11 to 17% protein (*2, 4*). The sugars in the pod exo mesocarp flour consist of about 92% sucrose, 3% glucose and 5% fructose (*5*).

The majority of the scientific papers reporting on nutritional value and composition of *Prosopis* pods are modifications of (*5*) in which the pods are fractionated by a dry milling process into (a) a high fiber/low protein fraction corresponding to the pod endocarp, (b) a high protein fraction corresponding to the endosperm of the seed, (c) a high galactomannan gum fraction resulting from the seed and (d) a high sucrose fraction resulting from the pod mesocarp. However, several commercial firms (http://www.cocinadevega.com) grind the entire pod to produce a flour. For mesquites of the Sonoran desert, one would expect the proximate compostion of the entire pod to be similar to that of *P. velutina* reported by Meyer et al. (*5*) of 22% sugar, 12% protein, 2.5% fat, 22% crude fiber and 3.5 % ash. The reported proximate composition of the *P. alba* flour was 7.2% protein, 2.2% fat, 3.1% ash, 26.5% total dietary fiber and 59% total sugars and that of the *P. pallida* flour was 8.1% protein, 0.8% fat, 3.6% ash, 32.2% total dietary fibre and 48.5% total sugars (*6*). Thus the mesocarp flours are lower in protein, lower in fiber, lower in fat but higher in sugar.

Meyer et al. (*5*) found that the high protein fraction, mainly resulting from the seeds had 61% protein and 8% fat. Thus the fat content of the seeds was several times greater than that of the flour alone. As mentioned in detail later, hexanal, which is an aldehyde resulting from lipid oxidation, is often used as an assay for rancidity of flour products. Thus the high lipid content of the seeds could result in rancidity due to the oxidation of the several fold higher lipid content than that of the pod mesocarp.

The pods can be milled to produce flour which is sold commercially and is used in pastries and baked goods. The pods and flour have a cinnamon, café mocha and coconut aroma. Our goal was to elucidate what volatiles are responsible for these pleasant sensory attributes.

Experimental

Materials

Classic Sonoran and Sweet Peruvian mesquite meal was purchased from Cocina deVega, Inc. (Golden Valley, MN). *Prosopis alba* pod mesocarp flour (harvested in 2003) was obtained from Roque Sáenz Peña, Chaco, Argentina.

Sample Preparation

Dynamic Headspace Sampling. The powdered mesquite pods (30 g) were placed in a 1 L round-bottomed flask along with 54 g NaCl (previously heated to 150 °C to remove volatiles) and 150 mL purified water (Milli-Q Plus, Millipore Corporation, Bedford, MA). The flask was fitted with a Pyrex head to allow the sweep gas to enter the top of the flask (via a Teflon tube) and exit out of a side arm through a Tenax trap (ca. 10 g of Tenax [Alltech Associates, Deerfield, IL], fitted with ball and socket joints). The system was purged with purified nitrogen (200-400 mL/min) for 2 min and immediately connected to an all Teflon diaphragm pump that recirculated nitrogen around the loop (closed loop sampling) at 6 L/min for 3 h. The sample was continuously stirred during the sampling period with a magnetic stirrer. After sampling, the Tenax trap was removed and the volatiles eluted with 70 mL of freshly distilled diethyl ether containing ca 0.001% Ethyl antioxidant 330 (1,3,5-trimethyl-2,4,6-tris(3,5-di-tert-butyl-4-hydroxybenzyl)benzene). The ether was carefully concentrated to ca. 50 µL using a warm water bath (50-60 °C) and a Vigreux column.

Capillary Gas Chromatography

A Hewlett-Packard 6890 gas chromatograph equipped with a flame ionization detector (FID) was used. A 60 m × 0.32 mm i.d. DB-WAX fused silica capillary column (d_f = 0.25 µm; J&W Scientific, Inc. Folsom, CA) was employed. The injector and detector temperatures were 180 °C and 290 °C, respectively. The oven temperature was programmed from 30 °C (4 min isothermal) to 200 °C (held for 25 min at final temperature) at 2 °C/min. Helium carrier gas linear velocity was 36 cm/s (30 °C).

Capillary Gas Chromatography/Mass Spectrometry (GC/MS)

The system consisted of an HP 6890 gas chromatograph coupled to an HP 5973 quadrupole mass spectrometer (capillary direct interface). A 60 m × 0.25 mm i.d. DB-WAX fused silica capillary column (d_f = 0.25 µm) was used. Helium carrier gas was used at a headpressure of 22 psi. The oven temperature was programmed from 30 °C to 200 °C (held for 35 min at the final temperature) at 2 °C/min.

Odor Threshold Determinations

Odor thresholds were determined in water with reference standards (purified by preparative gas chromatography) with a panel of 16-22 members using procedures described previously (7).

Results and Discussion

Volatile constituents of ground mesquite pods were isolated by dynamic headspace sampling. Sample constituents were identified by comparison of the compound's Kovats index, I (8), and mass spectrum with that of a reference compound.

We investigated three mesquite pod samples. The first sample was *Prosopis alba*, pod mesocarp flour produced in Chaco, Argentina in 2003. The second and third flours were obtained commercially from Cocina deVega, a Classic Sonoran and Sweet Peruvian. The flours were raw though they were dried at between 38 and 54 °C. We identified a total of 121 compounds, 14 of which were tentatively identified. To our knowledge mesquite volatiles have not been previously studied with the exception of the identification of maltoxazine in *Prosopis tamarugo* pods by Schmeda-Hirschmann and Jakupovic (9). These researchers found that maltoxazine is a DNA binding constituent with almost the same activity as the standard inhibitor vinblastine. Maltoxazine was reported to occur at a concentration of 1 ppm and was said to contribute to the characteristic odor of *P. tamarugo* pods. This compound has been previously identified in beer and malt (10). We could not detect this constituent in any of the three samples we investigated.

Sample A represents the *Prosopis alba* sample while sample B and C represent the commercial Classic Sonoran and Sweet Peruvian samples. The *Prosopis alba* sample contained a much higher proportion of pyrazines than the commercial samples. Since our quantification studies have not yet been completed we can only speculate on the contribution of volatiles at this point. Methylpyrazine has a very high odor threshold of 60 ppm and probably doesn't contribute to the odor. 2,5-Dimethylpyrazine constitutes almost 12% of the sample A. Though it has a relatively high odor threshold of 1.7 ppm it may contribute to the odor with its chocolate, roasted nuts and earthy aroma. There is also a large proportion of 2,6-dimethylpyrazine at 3.22%. This compound has an odor of chocolate and roasted nuts. Ethylpyrazine has an odor threshold of 6.0 ppm and is present at relatively low levels in the samples. 2,3,5-Trimethylpyrazine has a nutty, roasted peanut, cocoa aroma. It constitutes about 1% of sample A and may contribute to the aroma due to its odor threshold of 91 ppb. 2,5-Dimethyl-3-ethylpyrazine has cocoa, chocolate, burnt almond and filbert-hazelnut aroma notes. This constituent is likely an important contributor to the aroma since it is a major constituent at 4.83% and has a low odor threshold of 0.4 ppb. Odor threshold values were not available for 2-methyl-6-vinylpyrazine and 2-propyl-3,6-dimethylpyrazine. γ-Hexalactone has a rather high odor threshold of 1600 ppb and probably doesn't contribute to the aroma. Though there are moderate levels of γ-pentalactone and γ-butyrolactone we suspect that these lactones have high odor thresholds like γ-hexalactone and don't contribute much to the aroma. γ-Octalactone and γ-nonalactone have lower odor thresholds (7 and 30 ppb, respectively) and might be expected to contribute

to the coconut aroma of mesquite flour. γ-Octalactone has a sweet, creamy, dairy, coconut aroma while γ-nonalactone has strong, sweet, soft coconut aroma. γ-Nonalactone is used in the formulation of synthetic coconut flavors (*11*). δ-Octalactone has an odor threshold of 0.5 ppm and has sweet, fatty, coconut, tropical, dairy notes. Massoia lactone has a coconut, creamy, fatty, sweet aroma (*11*). It has a similar structure to δ-decalactone except that it has a double bond in the 2 position of the ring. δ-Decalactone has an odor threshold of 100 ppb so we might expect that massoia lactone would have an odor threshold of a similar magnitude.

The Classic Sonoran sample had an abundance of aldehydes. Hexanal was the major volatile constituting almost 22% of the volatiles. Given its low odor threshold of 5 ppb it probably contributes to the aroma of sample B. While the lipid composition of the mesocarp flour and the whole pod are rather similar in both being about 2-2.5 %, evidently the type of fat in the seeds is more predisposed to oxidation to produce hexanal than is the fat in the mesocarp. The sample had 1.24% (*E*)-2-hexenal which probably contributed to the aroma with its low odor threshold of 17 ppb. Given the high sugar level in the samples it seems reasonable to have moderate levels of furfural ranging from 1.73% to 0.17%. The *Prosopis alba* sample also had moderate levels of 5-methylfurfural of almost 1%. Samples A and B had moderate levels of benzaldehyde, 1.7% and 4.13%, respectively. (*E,E*)-2,4-Decadienal probably contributes to the odor of sample B due to its very low odor threshold of 0.07 ppb.

There were relatively low levels of these four ketones, 2-pentanone, 2,3-butanedione, 2-methyl-3-pentanone, and 4-methyl-2-pentanone and their contribution is probably low. 3-Penten-2-one is a likely contributor to mesquite flavor with its low odor threshold of 1.5 ppb, particularly in sample B where it constituted 0.9%. There was a moderate level of 3-hydroxy-2-butanone in sample B but its odor threshold is relatively high at 800 ppb. Other possible contributors are 6-methyl-5-hepten-2-one and 3,5-octadien-2-one which have odor thresholds of 50 and 150 ppb, respectively. The highest levels were found in sample B with 0.96% and 0.89%. There were moderate levels of 6-methyl-3,5-heptadien-2-one but its odor threshold was 380 ppb.

The *Prosopis alba* sample had 0.39% and 0.97% of 2-acetylfuran and 5-methylfurfural, respectively. However, 2-acetylfuran and 5-methylfurfural have high odor thresholds, 10 ppm and 1.3 ppm and probably don't contribute to the odor. Acetophenone has a sweet, hawthorn, floral, almond aroma and could contribute to the odor with its odor threshold of 65 ppb. Furfuryl alcohol has an odor threshold of 2400 ppb. We don't know the odor threshold of 5-methyl-2-furfuryl alcohol but it is probably quite high too so these compounds probably have little if any contribution. Methyl salicylate has a minty, sweet, wintergreen aroma and an odor threshold of 40 ppb. A likely contributor is 2-methoxyphenol or guaiacol. This compound has a relatively low odor threshold of 3 ppb and has a sweet, smoky odor. Sample B contained 0.88%. Compounds such as benzyl alcohol, 2-phenylethanol, 2-acetylpyrrole, and methyl cinnamate have high odor

Table I. Volatile Constituents of Mesquite Pods

Constituent	I^{DB-WAX}		% area[a]		
	exp.	ref.	A	B	C
2-pentanone	979	973	-[b]	-	0.04
2,3-butanedione	981	966	-	-	0.05
pentanal	983	974	-	0.53	-
methyl butanoate	987	980	-	-	0.01
2-methyl-3-pentanone	998	998	-	0.04	-
4-methyl-2-pentanone	1005	1005	-	-	0.01
methyl 2-methylbutanoate	1011	1006	-	-	0.02
2-methylpropyl acetate	1016	1008	-	-	0.03
methyl 3-methylbutanoate	1021	1014	-	-	0.11
chloroform	1024	1012	-	-	0.01
toluene	1041	1034	-	0.01	0.01
2-methyl-3-buten-2-ol	1055	1032	-	0.17	-
2,3-pentanedione	1064	1050	-	-	0.06
dimethyl disulfide	1074	1078	0.06	0.02	0.14
hexanal	1081	1077	0.43	21.75	0.25
methyl pentanoate	1087	1080	-	-	0.01
(2-methyl-2-butenal)[c]	1088		-	-	0.03
2-methylpropanol	1098	1084			1.90
3-penten-2-one	1123	1121 (lit.)	0.28	0.90	0.15
methyl 4-methylpentanoate	1147	1137			0.01
butanol	1153	1138	0.06	0.30	0.08
1-penten-3-ol	1171	1152	0.10	2.75	0.11
2-heptanone	1181	1178	-	-	0.10
pyridine	1181	1181	1.03	0.05	-
heptanal	1184	1180	-	0.09	0.02
(1,3-dimethylbenzene)	1186		-	0.32	-
methyl hexanoate	1188	1181	-	-	0.09
limonene	1196	1197	-	-	0.02
2-methyl-1-butanol	1214	1203	-	comb.	0.34
3-methyl-1-butanol	1215	1205	0.71	4.79	0.55
(E)-2-hexenal	1218	1214	-	1.24	-
2-pentylfuran	1236	1224	-	0.04	-
thiazole	1253	1262	-	0.04	-
3-methyl-3-buten-1-ol	1255	1244	-	-	0.84
pentanol	1259	1246	0.35	2.91	0.13
(2-methyltetrahydrofuran-3-one)	1261		0.26	-	0.78
methylpyrazine	1265	1262	0.93	0.16	0.05
3-hydroxy-2-butanone	1281	1278	0.22	0.76	0.24
3-hepten-2-one	1299	1297	-	0.17	-

Table I. *Continued.*

Constituent	I^{DB-WAX} exp.	ref.	A	B	C
				% area[a]	
4-penten-1-ol	1306	1299	0.19	-	0.31
((Z)-2-penten-1-ol)	1331		-	1.61	-
2,5-dimethylpyrazine	1321	1320	11.92	-	0.11
2,6-dimethylpyrazine	1327	1326	3.22	0.04	-
ethylpyrazine	1332	1331	0.08	0.04	-
6-methyl-5-hepten-2-one	1337	1333	0.39	0.96	0.08
2,3-dimethylpyrazine	1345	1344	0.09	0.06	-
(methylcyclohexylketone)	1360		-	0.11	-
hexanol	1361	1350	0.60	5.06	-
(2-methyl-2-cyclopenten-1-one)	1374		-	0.06	-
dimethyl trisulfide	1375	1374	0.01	0.02	0.18
2-ethyl-6-methylpyrazine	1384	1383	0.20	-	0.03
(2-ethyl-3-methylpyrazine)	1388	-	-	0.02	-
2-ethyl-5-methylpyrazine	1389	1390	0.02	0.04	0.20
(Z)-3-hexen-1-ol	1392	1381	-	0.34	-
2,3,5-trimethylpyrazine	1402	1404	1.04	-	0.05
(E,E)-2,4-hexadienal	1402	1388	-	0.02	-
(E)-2-hexen-1-ol	1413	1404	-	0.09	-
(3-ethyl-2-methyl-1,3-hexadiene)	1416		-	0.04	-
5-hexen-1-ol	1418	1408	0.17	0.32	0.13
linalool oxide A (*trans*-THF)	1443	1442	0.05	0.40	-
2,5-dimethyl-3-ethylpyrazine	1447	1446	4.83	-	-
acetic acid	1452	1475	0.88	-	-
1-octen-3-ol	1458	1448	0.29	0.61	0.10
furfural	1461	1456	1.73	0.79	0.17
6-methyl-5-hepten-2-ol	1467	1462	0.15	0.11	-
linalool oxide B (*cis*-THF)	1477	1470	0.12	0.18	-
methyl 3-hydroxybutanoate	1483	1477	-	-	0.03
2-methyl-6-vinylpyrazine	1486	1485	0.11	-	-
(E,E)-2,4-heptadienal	1494	1489	-	0.07	-
2-acetylfuran	1499	1500	0.39	0.44	0.09
2-propyl-3,6-dimethylpyrazine	1509	1514	0.09	-	-
camphor	1510	1513	-	-	0.02
benzaldehyde	1514	1516	1.72	4.13	0.58
undecanal	1537	1601	-	0.20	-
propanoic acid	1540	1535	0.45	-	-
2,3-butanediol (threo)	1547	1539	0.59	0.42	0.43
linalool	1556	1546	-	0.02	0.04
5-methyl-2-furfural	1569	1567	0.97	-	-
2-methylpropanoic acid	1571	1568	-	-	1.00
3,5-octadien-2-one	1575	1566	-	0.89	-

Table I. *Continued.*

Constituent	exp.	Ref.	A	B	C
				% area[a]	
2,3-butanediol (meso)	1581	1576	0.23	0.29	0.05
6-methyl-3,5-heptadien-2-one	1590	1589	0.59	0.85	0.11
(2,6,6-trimethyl-2-hydroxycyclohexanone)	1600		-	0.38	-
γ-pentalactone	1605	1605	0.81	0.81	0.20
methyl benzoate	1614	1616	0.13	-	0.03
γ-butyrolactone	1618	1623	1.06	0.54	0.39
(2-acetyl-5-methylfuran)	1615		-	0.06	-
butanoic acid	1630	1650	0.65	0.24	0.10
acetophenone	1644	1645	0.62	0.28	0.15
(4-methylthiazole)	1662		-	0.27	-
furfuryl alcohol	1665	1656	1.30	-	0.24
(4-methyl-4-vinylbutyrolactone)	1669		-	0.15	-
3-methylbutanoic acid	1672	1680	6.80	4.50	4.35
(3,5,5-trimethyl-2-cyclohexene-1,4-dione)	1686		0.15	0.39	0.05
γ-hexalactone	1693	1699	0.25	0.46	0.09
(5-methyl-2-furfuryl alcohol)	1714		0.06	-	-
pentanoic acid	1745	1750	0.87	0.85	0.20
(5-ethyl-2(5H)-furanone)(2-hexen-4-olide)	1751		0.08	0.22	0.03
methyl phenylacetate	1755	1755	0.06	-	0.04
methyl salicylate	1768	1771	0.21	0.10	0.04
δ-hexalactone	1783	1801	0.10	-	0.05
γ-heptalactone	1795	1801	0.07	0.14	0.05
(E,E)-2,4-decadienal	1810	1808	-	0.18	-
(unknown)	1825		4.73	0.67	3.63
hexanoic acid	1849	1825	3.92	2.37	1.36
2-methoxyphenol	1859	1855	0.24	0.88	0.27
benzyl alcohol	1878	1874	0.89	0.87	0.22
2-phenylethanol	1912	1910	0.63	-	-
γ-octalactone	1917	1920	-	0.39	-
heptanoic acid	1957	1925	0.66	-	0.28
benzothiazole	1961	1954	-	0.35	-
δ-octalactone	1962	1970	0.31	-	0.27
2-acetylpyrrole	1976	1970	0.96	0.29	1.77
(unknown)	2003		17.61	2.21	19.19
(methyl ester diethylcarbamodithoic acid)	2010		-	0.19	-
2-pentadecanone	2012	2020	0.10	-	-
(unknown) (base peak 97; 68)	2025		-	-	0.64

Table I. *Continued.*

| Constituent | I^{DB-WAX} | | % area[a] | | |
	exp.	Ref.	A	B	C
γ-nonalactone	2028	2030	0.51	1.62	-
3-phenylpropanol	2033	2046	0.08	-	-
methyl cinnamate	2065	2076	0.44	-	0.28
4-methylphenol	2073	2078	0.10	-	-
3-methylphenol	2081	2085	0.06	-	-
4-phenyl-3-buten-2-one	2111	2117	0.02	-	-
γ-decalactone	2154	2147	-	-	0.05
octanoic acid	2172	2120	0.49	0.37	0.33
4-vinyl-2-methoxyphenol	2194	2180	0.10	0.03	0.13
massoia lactone	2228	2227	0.31	0.08	1.19
(2-heptadecanone)	2231		0.08	-	-

[A]*Prosopis alba,* pod mesocarp, Argentina, 2003; [B]Classic Sonoran (Cocina deVega, Inc.); [C]Sweet Pervian (Cocina deVega, Inc.). [a]Peak area percentage of total FID area excluding the solvent peaks (assuming all response factors of 1). [b]Not detected. [c]Tentative or partial identifications enclosed in parentheses.

thresholds, 10 ppm, 1.1 ppm, 170 ppm and 70 ppm, respectively, and probably don't contribute to the odor. 4-Vinylguaiacol has a low odor threshold of 3 ppb. This compound ranged from 0.03% to 1.3% in the samples and could contribute to the odor.

A variety of free fatty acids ranging from acetic acid to octanoic acid were identified. Acetic acid probably doesn't contribute to the odor with its high odor threshold of 22 ppm. Propanoic acid and 2-methylpropanoic acid also have high odor thresholds of 2.2 ppm and 3 ppm, respectively, and are unlikely odor contributors. Butanoic acid and 3-methylbutanoic acid have odor thresholds of 240 ppb and 250 ppb, respectively. The latter compound could contribute to the odor since it occurs at high levels ranging from 4.35% to 6.80%. Another possible contributor is hexanoic acid which despite its high odor threshold of 3 ppm occurs at levels ranging from 1.4% to 3.9%. The other acids such as pentanoic acid, heptanoic acid and octanoic acid probably don't contribute to the odor due to their high odor thresholds and low % areas.

Other compounds that may contribute to the odor include dimethyl disulfide, dimethyl trisulfide and 1-octen-3-ol. Dimethyl trisulfide has a very low odor threshold of 0.003 ppb or 3 ppt. 1-Octen-3-ol has an odor threshold about 433 times higher than dimethyl trisulfide but it still has a low odor threshold of 1.3 ppb and was present at 0.29% and 0.61% in samples A and B, respectively.

The unknown compound that was the major volatile in *P. alba* (17.61%) and *P. pallida* (19.19%) but only 2.21% of the *P. velutina* volatiles is apparently new to flavor chemistry. We are in the process of synthesizing this compound in order to definitively characterize its structure and this will be reported in a later communication.

In summary, we have studied the composition of three different samples of mesquite flours. The samples had surprisingly different compositions and we found the *Prospopis alba* sample had a more pleasant aroma than the two commercial samples. The supplier of the two commercial samples would not reveal their species and we suspect that these samples are mixtures of *Prosopis* species. We have received pods and flours of known species from southern California and South America. We will be analyzing these samples and completing our quantification studies.

References

1. Felker, P. *Econ. Bot.* **1981**, *35*, 174-186.
2. Becker, R.; Sayre, R. N.; Saunders, R. M. *J. Am. Oil Chem. Soc.* **1984**, *61*, 931-938.
3. Silva, S. *Prosopis juliflora* (Sw) DC in Brazil. In The Current State of Knowledge on *Prosopis juliflora*; Habit, M. A., Ed.; FAO-Plant Production and Protection Division: Roma, 1990.

4. Bravo, L.; Grados, N.; Saura-Calixto, F. *J. Sci. Food Agric.* **1994**, *65*, 303-306.
5. Meyer, D.; Becker, R.; Gumbmann, M. R.; Vohra, P.; Neukom, H.; Saunders, R. M. *J. Agric. Food Chem.* **1986**, *34*, 914-919.
6. Felker, P.; Grados, N.; Cruz, G; Prokopiuk, D. *J. Arid Environ.* **2003**, *53*, 517-528.
7. Guadagni, D. G.; Buttery, R. G. *J. Food Sci.* **1978**, *43*, 1346-1347.
8. Kováts, E. *Helv. Chim. Acta* **1958**, *41*, 1915-1932.
9. Schmeda-Hirschmann, G.; Jakupovic, J. *Bol. Soc. Chil. Quim.* **2000**, *45*, 645-647.
10. Tressl, R.; Helak, B.; Rewicki, D. *Helv. Chim. Acta* **1982**, *65*, 483-489.
11. Rodríguez-Burruezo, A.; Kollmannsberger, H.; Prohens, J.; Nitz, S.; Nuez, F. *J. Agric. Food Chem.* **2004**, *52*, 5663-5669.

Chapter 10

Painting and Memory in the Discovery of Aroma Chemicals: The Case of Sulfur Containing Odorants and Odorant Precursors in Axillary Sweat Odor

Antoine E. Gautier, Christian Starkenmann, Frédéric Begnaud, and Myriam Troccaz

Firmenich SA, Corporate R&D Division, P.O. Box 239, CH–1211 Geneva 8, Switzerland

The reminiscent human sweat-like odour of Sclarimol® (3-mercapto-1-methoxyhexane) and Aruscol® (3-mercapto-1-methoxyheptane), discovered in *Salvia sclarea* L. and *Ruta chalepensis* L., prompted us to look for sulfur compounds in human axillary sweat. This analytical work led us to the discovery of Transpirol™ ((*R/S*)-3-mercapto-3-methyl-1-hexanol), and to the development of a new technology: the MDGC-DCSI. This new invention allowed us to determine the enantiomer ratio of sulfur compounds in the natural extract. The same principle can be applied to GC-Olfaction (MDGC-DCSI-Ofactometry), in order to increase the difference in retention time between enantiomers eluted through the sniffing port. Finally this work addressed the question of which compound is the precursor of the Transpirol™ and after multiple liquid chromatography separations, [1-(2-hydroxyethyl)-1-methylbutyl]-*L*-cysteinylglycine (Cys-Gly-(*S*)-conjugate), was formally identified as the precursor excreted by axillary glands.

111

Introduction

Several years ago perfumers were interested to create artificial human sweat odours to improve perfume creations. Mr. Matthijs Van de Waal, who was involved in this project, was never satisfied with reconstitutions presented to him and he suggested that the missing top note was reminiscent of the odour of a Clary-sage (*Salvia sclarea* L.) field in full blossom. This led us to the discovery of Sclarimol® (3-mercapto-1-methoxyhexane) 1, a potent sulfur compound that was characteristic of the sweaty note. He experienced the same sensation when he was painting outdoors in Tuscany. After looking around, he realised that the human sweat-like malodour was emitted from a small bush, *Ruta chalepensis* L. This mismatch odour perception was produced by exceedingly potent sulfur compounds: a combination of Sclarimol® 1 and Aruscol® (3-mercapto-1-methoxyheptane) 2 (*1*) (Figure 1).
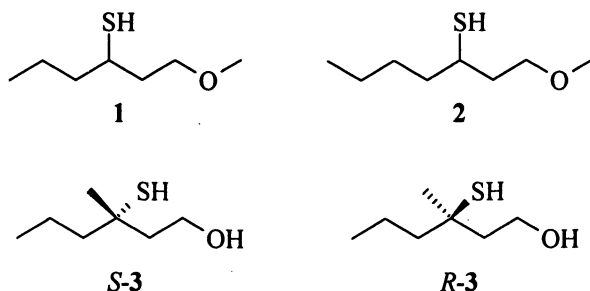
Figure 1. Chemical structures of Sclarimol® (3-mercapto-1-methoxyhexane) 1, Aruscol® (3-mercapto-1-methoxyheptane) 2, and Transpirol™ ((R/S)-3-mercapto-3-methyl-1-hexanol) 3.

This intriguing perception of human sweat odour prompted us to look for sulfur compounds in human axillary sweat. Since the pioneering work of W. B. Shelley in 1953 (*2*), it is known that the characteristic odour, which arises in the human axillae is liberated by skin bacterial strains from sterile, odourless, aqueous-soluble components of sweat secretions. A number of studies concerning the analysis of axillary sweat malodour have demonstrated significant impact of steroids (*3,4*) and volatile, short chain fatty acids such as (*E/Z*)-3-methylhex-2-enoic acid. This acid has been described as the predominant olfactory contributor to male sweat malodour (*5–7*). In addition, sulfur compounds may also be major olfactive descriptors for body odour, this was suggested in a patent application, although no structures and analytical data were shown (*8*).

Our first approach was to screen the human microflora for their ability to generate "sulphur notes". After extensive olfactive evaluation it was determined

that the strain of *Staphylococcus haemolyticus* produced the most "sulphury" sweat character.

Due to difficulties in analysis of sulfur compounds in complex mixtures, a new chromatography interface called DCSI (Double Cool Strand Interface) was developed to facilitate the work (described later in text). The non-volatile water-soluble precursor was finally identified and fully characterised using this technique. This manuscript is a review of our previously published papers on the subject.

Search for Volatile Sulfur Compounds in Sweat

The first challenge was to collect large amounts of clean and sterile sweat. This has been done in other groups by intradermal injection of adrenaline into the axilla area and trapping the apocrine excretions with a capillary tube (*9, 10*). As sulfur compounds have an excessively low odor threshold in air, in the range of pg/L (*11*), pre-concentrations steps are needed to identify minute amounts of sulfur compounds. The adrenaline injection on a large scale is thus not feasible in this context. For this reason, an exercise room and a sauna were built to collect underarm sweat from 42 Caucasian male volunteers. 500 mL of odourless sterile axilla sweat containing 2 mg/mL protein were collected over a period of 8 weeks. This odourless mixture was incubated with *St. haemolyticus* for 17 h at 37°C in semi-anaerobic conditions. The fermentation broth was then extracted with dichloromethane and thiol fractions were concentrated by affinity chromatography using an organomercury derivative covalently bound to an agarose gel (*13*). The retention indices were measured by GC-Olfactometry (GC-O) on both polar and apolar columns. A typical sweaty, sulfury odour was detected at I_{spb} 1157 (±5) and $I_{sp\text{-}wax}$ 1890 (±5). At these retention times a mass spectrum from GC-MS analyses gave the highest mass fragment m/z at 148, followed by a small [M + 2] ion accounting for 5% of the signal intensity. These first results gave a good indication of the presence of a molecule containing one *S*-atom. The two fragments at m/z 115 and 114 were consistent with a loss of 33 and 34 (SH and H_2S, resp.). The next fragment at m/z 97 was consistent with a loss of 17 (OH), which suggested the presence of an OH group in the parent molecule. From these indications and from previous analytical works relating the presence of (*E/Z*)-3-methyl-2-hexenoic acid, the structure of the unknown sweaty compound was postulated to be (*R/S*)-3-mercapto-3-methyl-1-hexanol, named Transpirol™ **3**. (*R/S*)-**3** was synthesized chemically and injected on both polar and apolar capillary columns coupled to GC-MS. Correlation of retention indices between the synthetic molecules at $I_{SP\text{-}wax}$ 1888 (±5) and $I_{SPB\text{-}1}$ 1153 (±5), and the sweat compound was demonstrated. The fragmentation pattern was also compared to the unknown sweat odorant molecule and was found to be identical. These results confirmed our first hypothesis that the most typical sweat malodor compound produced by *St. haemolyticus* is (*R/S*)-3-mercapto-3-methyl-1-

methyl-1-hexanol. This new sulfur compound was discovered simultaneously and independently by two other groups (14–16).

Development of a New Multidimensional GC Technique

Even when using comprehensive GC, currently the most powerful separation technique available, the compositional complexity of natural products leads to co-elution between compounds. Multidimensional GC (MDGC) is a well-known technique able to solve this problem by achieving an on-line "heartcut", i.e. targeted compounds eluting from the first column are transferred to the second one while others are vented. Up to now, the method of heartcutting consisted of either a valve or a pneumatic switch. However, both systems exhibit serious drawbacks with regard to the analyte adsorption and stability (17). Moreover, using these techniques implies using two GC ovens, in order to optimise the separation conditions on both the first and second columns. Therefore, a new design based on the cryocontrol of the analyte transfer through two strands of a capillary has been developed. This new interface, called the double cool strand interface (DCSI), is remarkably inert and is thus able to be used with labile compounds. It also allows the user to work under optimised separation conditions in both dimensions using only one oven. The DCSI principle is based on the controlled transfer of peaks between two strands of a capillary column passing through a longitudinally modulated cryogenic system (LMCS (18)). The target compounds and those following are respectively trapped in the first strand (trapping strand) and in the second strand (injection strand) until prior eluting peaks have been eluted from the second column (Figure 2). The target peak is then released into the second column, while the following peaks are trapped
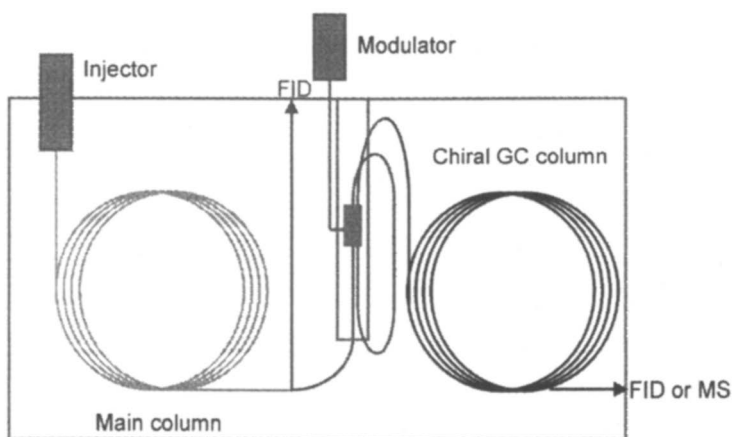
*Figure 2. Scheme of the MDGC with the double-cool-strand interface.
(Reproduced with permission from reference 21. Copyright 2005 Firmenich.)*

again in the injection strand. This operation allows the target peak to elute in a chromatographic zone free of interfering compounds (*17*). Conventional capillary columns and low acquisition rate detectors such as sniffing ports can be used with the DCSI interface. Moreover, when the target has been trapped, the oven temperature could be modified and new temperature rates could be applied to comply with the optimal separation condition required by the second column. The release of the target compounds from the trap corresponds to a new injection directly into the second column. This property is particularly useful for chiral separation, as chromatographic conditions have a drastic effect on the resolution of enantiomers in such devices.

First of all, MDGC-DCSI equipped with a chiral column as the second dimension has been applied to determine the enantiomer ratio of **3**. Before releasing the target compound into the chiral column, the oven temperature was cooled down according to Figure 3 to reach the optimal temperature for enantiomer resolution.
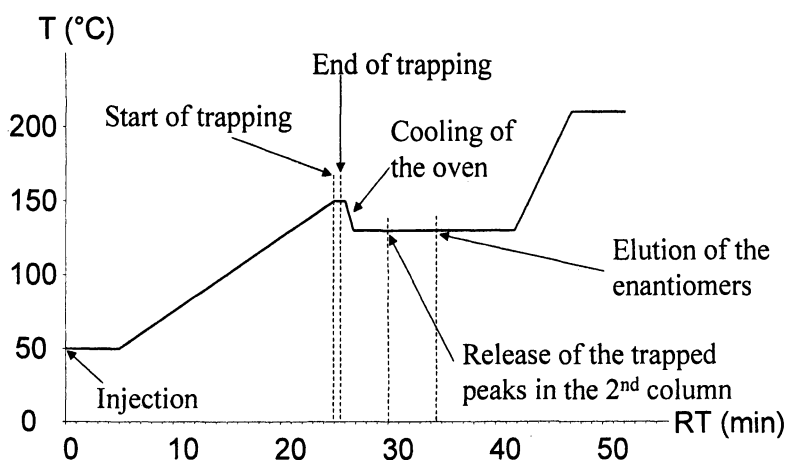
Figure 3. Oven temperature program with the main events occurring during the analysis of the axillary malodor extract.

With the above setup, **3** was well resolved. Injection of synthetic **3** leads to the assignment of peaks found in the extract (Figure 4). Due to the minute quantity of material in the sample, the enantiomer ratio could only be roughly estimated as *ca.* 3:1 (**3S:3R**) (*19*).

Secondly, the olfactive impact of both enantiomers was evaluated using a new Chiral-MDGC-DCSI-Ofactometry design (Figure 5). After the racemate has been resolved by the chiral column (1st dimension), the second enantiomer was trapped into the DCSI whereas the first one passed through the transfer line
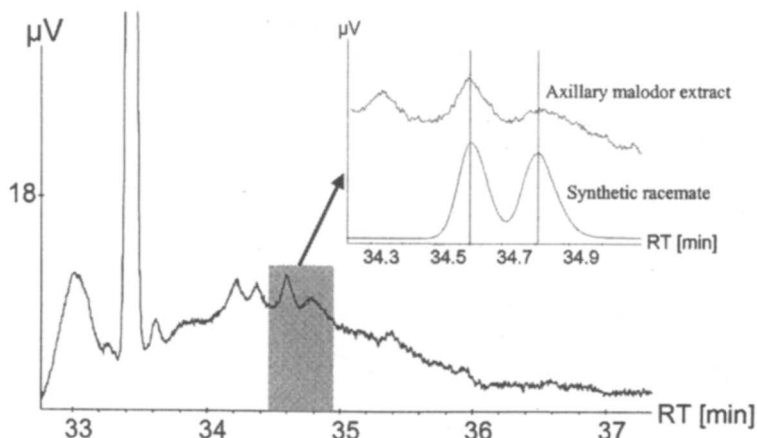
Figure 4. Chromatogram of the axillary malodor extract. Comparison with the injection of synthetic racemic 3-methyl-3-sulfanylhexan-1-ol 3. (Reproduced with permission from reference 19. Copyright 2006 Firmenich.)

placed after the interface and eluted through the sniffing port for olfactive evaluation. The delay before the remobilisation of the second enantiomer was determined to allow the panelist to fully recover from the first stimulus. Analyte **3** was so powerful and lingering that a time interval of 3 min between the two peaks was compulsory to reach an olfactive baseline. This method drastically improves the chiral resolution, which cannot be achieved with other techniques. With this system, a panelist can independently evaluate both enantiomers during a single run. This avoids the necessity to synthesise the pure enantiomers in order to olfactively characterize them, which may represent a difficult task. When their olfactive impact differs, access to pure enantiomers is necessary for peak assignments, which was the case for this work. Pure enantiomers were synthesized (*15*) and injected in the Chiral-MDGC-DCSI-Ofactometry system. Finally, the odor of 3*S* was described as "sweat, aggressive, onion and animal", whereas that of 3*R* was "more fruity, grapefruit and sulfury, less powerful". This confirmed that it is the *S* enantiomer, which predominantly contributes its character to the sweat odor (*19*).

Search for the Precursor of Volatile Sulfur Compounds in Sweat

We examined the mechanism of volatile sulfur compound release by identifying the immediate precursor of the key compound **3** in sterile sweat. It has been postulated that the action of a β-lyase on a Cys-(*S*)-conjugate generates Volatile Sulfur Compounds (VSCs) in sweat without clear specification of the
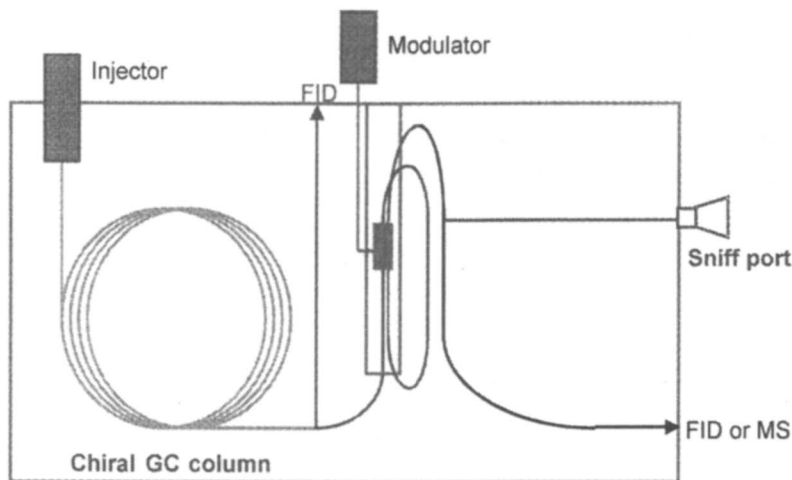
*Figure 5. Scheme of the Chiral-MDGC-DCSI-Olfactometry configuration.
(Reproduced with permission from reference 19. Copyright 2006 Firmenich.)*

exact nature of the non-volatile precursor (*8*). A cysteine conjugate has been postulated to be the direct precursor of **3** and this last compound may result from the cleavage of the C-(*S*) bond by a C-(*S*) *β*-lyase present in *Corynebacterium* (*15*). To prove the presence of Cys-(*S*)-conjugate, 287 mL of sterile axilla sweat was lyophilyzed, re-diluted in water, filtered and injected on an HPLC (Nucleodur C18 Pyramid®) coupled to a mass spectrometer. Unfortunately it was not possible to detect a mass spectrum corresponding to a Transpirol precursor. Only *N*-*α*-3-hydroxy-3-methylhexanoyl-(*L*)-glutamine ([M + 1]$^+$ = 275), and a minor peak of *N*-*α*-3-methyl-2-hexenoyl-(*L*)-glutamine ([M + 1]$^+$ = 257), known to be present in sweat (*20*), were detected. The sterile axillary sweat was then separated into five fractions by preparative HPLC using a Lobar® RP-18 SiO$_2$ column. Only the third fraction generated a typical sulfur sweaty malodour after incubation with the axillary strain of *Staphylococcus*. This sulfur note was confirmed by GC/MS to be due to Transpirol^{TM} **3**. It was then clear to us that the third fraction contained the precursors to **3**. The third fraction was further separated into sub-fractions using a preparative HPLC column (Nucleodur C18 Pyramid®). The only corresponding fraction which generated a typical sweat malodour when incubated with *St. haemolyticus* showed two peaks possessing [M + 1]$^+$ ions corresponding to 279 and 293. These last two peaks disappeared after treatment with *St. haemolyticus*. At the same time, new peaks were observed following GC-MS analysis of the bacterial treated fraction: a small broad peak with a molecular ion of *m/z* 134, at a retention index corresponding to I_{SPB1} 1080, was attributed to *syn* (and/or) *anti* 2-methyl-3-sulfanylpentan-1-ol; a larger peak with molecular ion of *m/z* 134 and a retention index I_{SPB-1} 1093 may correspond to 3-mercapto hexan-1-ol (*11, 12*) and a major

peak with a molecular ion of m/z 148 at I_{SPB-1} 1149 corresponds to (R/S)-3-mercapto-3-methyl-1-hexanol 3. After injection on a chiral column mounted on a GC equipped with an Atomic Emission Detector (GC-AED), it was also possible to evaluate enantiomeric ratios. The major enantiomer was found to be (S)-3-methyl-3-mercaptohexan-1-ol (S)-3, with an enantiomeric excess of 65% (Figure 6, trace A) (21). The determination of precursors was possible after careful examination of the data generated by HPLC-MS in positive mode. The major putative precursor present on the spectrum had a molecular ion, $[M + 1]^+$ of 293 and further fragmentation resulted in the formation of an ion having a MS^2 of m/z 276 (Figure 7), which then produced a fragment by MS^3 at m/z 179, which might be explained by the loss of 3-methylhexanol. In negative APCI-MS mode, the molecular ion, $[M - 1]^-$ of 291 forms a second generation ion at m/z 143, which might correspond to β-elimination of 3-methyl-3-sulfanylhexan-1-ol. The final structure of the precursor present in the active fraction was then postulated to be a Cys-Gly-(S)-conjugate 4 and not a Cys-conjugate as expected from previous studies (20). The structure identification was confirmed by chemical synthesis.

The activity was confirmed by the incubation of St. haemolyticus in a stationary phase with the synthetic precursor $(R-R/S)$-4 for 18 h at 37°C. The sweat odour associated with volatile sulfur compounds was clearly perceived, whereas no odour was present in controls consisting of $(R-R/S)$-4 incubated with buffer alone and St. haemolyticus incubated without any precursor. In our test conditions the percentage of conversion of the Cys-Gly-S-conjugate was shown to give better results compared to the synthetic Cys-S-conjugate without a clear identification of the enzyme responsible for this conversion (21). Moreover we could not identify the Cys-S-conjugate by HPLC analysis of our concentrated sterile sweat.

An ethyl acetate extract of the malodour sample generated by the incubation of St.haemolyticus with the synthetic precursor was injected on a chiral GC-AED (Figure 6, trace B). A racemic mixture of (R/S)-3-methyl-3-sulfanylhexan-1-ol (R/S)-3 was obtained with a chemical yield in excess of 75%, based on the amount of precursor incubated (21).

It has been clearly stated (15) that Staphylococci and specifically St. epidermidis do not have β-lyase activity and that only Corynebacterium spp. is able to release thiols from Cys-(S)-conjugates. Surprisingly, we demonstrated by these experiments that the incubation of synthetic 4 with the axillary strain St. haemolyticus can produce the sulfur compound 3.

The chemical composition of the sweat, bacterial metabolism, and odour effects of autolysis and chemical changes through ageing may determine the final body odour. The complexity of the interactions between skin secretions and skin flora add another dimension to this bio-environment. This study reveals that axillary cocci strains, St.haemolyticus, participate to give the final "bouquet" of axillary malodour through the generation of highly odorous thiols from a Cys-Gly-S-precursor. Further studies will try to elucidate the enzymes involved in this bio-conversion.
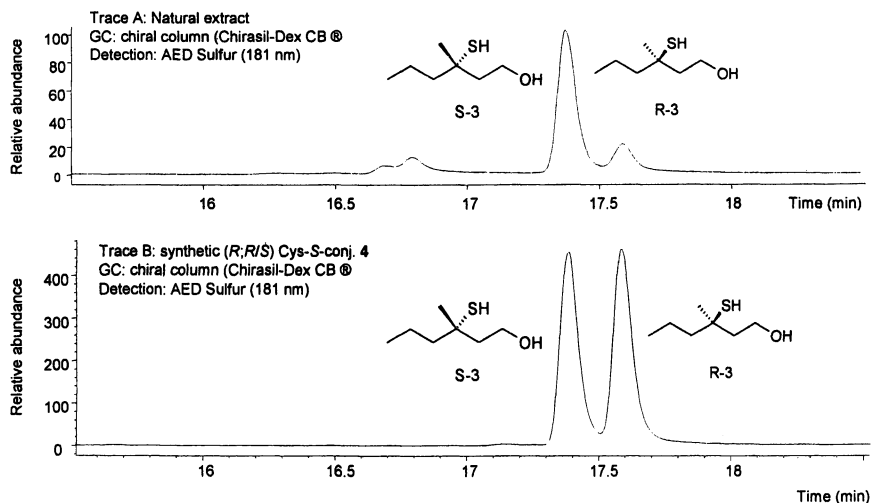
*Figure 6. Transformation of (R/;R/S) Cys-S-conj **4** by St. haemolyticus. trace A: incubation of concentrated natural extract containing **4** (21); trace B: incubation of synthetic (R/R/S)-**4**.*
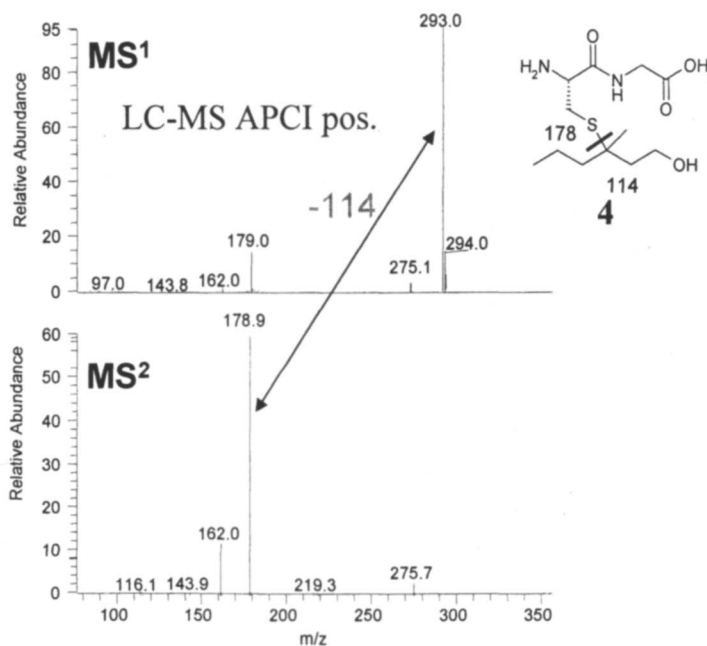
*Figure 7. LC-MS APCI full MS positive mass, and MS² of the natural [1-(2-hydroxyethyl)-1-methylbutyl]-L-cysteinylglycine (Cys-Gly-(S)-conjugate **4**.*

References

1. Van de Waal, M.; Niclass, Y.; Snowden, R.; Bernardinelli, G.; Escher, S. *Helvetica Chimica Acta* **2002**, *85*, 1246-1260.
2. Shelley, W. B.; Hurley, H. J.; Nichols, A. C. *Arch. Dermatol. Syphilol.* **1953**, *68*, 430-446.
3. Austin, C.; Ellis, J. *J. Steroid Biochem. Molec. Biol.* **2003**, *87*, 105-110.
4. Gower, D. B.; Mallet, A. I.; Watkins, W. J.; Wallace, L. M.; Calame, J.-P. *J. Steroid Biochem. Molec. Biol.* **1997**, *63*, 81-89.
5. Spielman, A. I.; Zeng, X. N.; Leyden, J. J.; Preti, G. *Experientia* **1995**, *51*, 40-47.
6. Zeng, X. N.; Leyden, J. J.; Brand, J.; Spielman, A. I.; McGinley, K.; Preti, G. *J. Chem. Ecol.* **1991**, *17*, 1469-1492.
7. Zeng, X. N.; Leyden, J. J.; Brand, J.; Spielman, A. I.; McGinley, K.; Preti, G. *J. Chem. Ecol.* **1992**, *18*, 1039-1055.
8. Lyon, S. B.; O'Neal, B. C. O.; van der Lee, H.; Rogers, B. International Patent No. 5,213,791, **1993**.
9. Aoki, T. *J. Invest. Dermatol.* **1962**, *38*, 41-44.
10. Leyden, J. J.; McGinley, K.; Heolzle, K.; Labows, J. N.; Kligman, A.M.*J. Invest. Dermatol.* **1981**, *77*, 413-416.
11. Engel K.H.: Tressl R. *J. Agric. Food Chemistry.* **1991**, *39*, 2249-2252.
12. Widder, S.; Sabater Luntzel, C.; Dittner, T.; Pickenhagen W. *J. Agric. Food. Chemistry.* **2000**, *48*, 418-423.
13. Full, G.; Schreier, P. *Lebensmittelchemie* **1994**, *48*, 1-4.
14. Hasegawa, Y.; Yabuki, M.; Matsukane, M. *Chemistry and Biodiversity* **2004**, *1*, 2042-2050.
15. Natsch, A.; Schmid, J.; Flachsmann, F. *Chemistry and Biodiversity* **2004**, *1*, 1058-1072.
16. Troccaz, M.; Starkenmann, C.; Niclass, Y.; Van de Waal, M.; Clark, A. J. *Chemistry and Biodiversity* **2004**, *1*, 1022-1035.
17. Begnaud, F.; Chaintreau, A. *Journal of Chromatography A* **2005**, *1071*, 13-20.
18. Kinghorn, R. M.; Marriott, P. J.; Dawes, P. A. *Journal of High Resolution Chromatography* **2006**, *23*, 245-252.
19. Begnaud, F.; Starkenmann, C.; Van de Waal, M.; Chaintreau, A. *Chemistry and Biodiversity* **2006**, *3*, 150-160.
20. Natsch, A.; Gfeller, H.; Gygax, P.; Schmid, J.; Acuna, G. *J. Biol. Chem.* **2003**, *278*, 5718-5727.
21. Starkenmann, C.; Niclass, Y.; Troccaz, M.; Clark, A. J. *Chemistry and Biodiversity* **2005**, *2*, 705-716.

Chapter 11

Effect of Irradiation and Other Processing Treatments on the Flavor Quality of Apple Cider

Terri D. Boylston[1], Loretta R. Crook[1,2], Cheryll A. Reitmeier[1], and Fransiska Yulianti[1]

[1]Department of Food Science and Human Nutrition, 2312 Food Sciences Building, Iowa State University, Ames, IA 50011–1061
[2]Glanbia Nutritionals Research and Development, 50 Falls Avenue, Suite 255, Twin Falls, ID 83301

Irradiation is an effective non-thermal processing treatment to inactivate foodborne pathogens and spoilage microorganisms in apple cider, although it can affect the flavor quality. The effects of irradiation, sorbate addition, and packaging treatment on the flavor quality of apple cider during storage were investigated. Free radicals generated during irradiation were quenched by sorbate to minimize the loss of esters and other volatile compounds that contribute to apple aroma. In the absence of sorbate, packaging materials and environments which minimize oxygen exposure were critical in preserving the desirable flavor quality of the irradiated apple cider during storage. Development of processing treatments to improve the safety of apple cider must consider their effect on the flavor compounds that impact consumer acceptability.

© 2008 American Chemical Society **121**

Introduction

Apple cider is a fresh-pressed, unfermented pulp-containing juice made from chopped and pressed apples. Esters, alcohols, and aldehydes are among over 200 volatile compounds that contribute to characteristic apple flavor (*1*). Researchers have identified specific compounds to be of particular importance to apple flavor, including butyl acetate, 2-methylbutyl acetate, hexyl acetate, ethyl 2-methylbutanoate, ethyl butanoate, butanol, hexanol, hexanal, and *trans*-2-hexenal (*1-5*). Synthesis of these flavor compounds occurs in the maturing and ripening fruit, with cultivar differences accounting for differences in the relative composition of volatile flavor compounds and overall flavor characteristics (*4*). During the processing of the apples into apple cider, oxidation of unsaturated fatty acids to C-6 aldehydes and reduction of these aldehydes to alcohols further contribute to the development of flavor (*6*). Differences in apple variety, maturity, and quality, cider processing parameters, and storage conditions contribute to variability in the flavor characteristics and quality of apple juice and cider (*7*).

Recent foodborne illness outbreaks associated with of *E. coli* O157:H7, *Cryptosporidium,* and other foodborne illnesses in apple cider (*8-11*) and other juices have contributed to major changes in the apple cider industry. The FDA has mandated that a warning label be placed on fruit and vegetable juice products that have not been processed to achieve a 5-log reduction in the most resistant pathogen present, currently recognized to be *C. parvum* (*12-13*). The recognized treatment for the apple cider to achieve the mandated 5-log reduction in microbial load is pasteurization at a minimum of 70° C for 6 seconds (*13*).

Although many producers currently pasteurize apple cider to comply with federal regulations, undesirable changes in flavor and appearance result from the heat treatment (*14, 15*). Pasteurization of apple juice results in a decreased fruit-aroma score accompanied by a decreased content of esters and an increased cooked aroma, attributed to the formation of furfural and hydroxymethylfurfural during heating (*2*). In addition, 5-methyl-2-furfural, benzaldehyde, and 2,4-decadienal, compounds that are formed during heating, have been identified in cooked apple slices (*16*).

Non-thermal processing treatments have been proposed as alternatives to pasteurization, causing inactivation of pathogenic and spoilage microorganisms with fewer changes in texture, color, and flavor. A 5-log microbial reduction in apple cider has been achieved with doses of 1.8 – 2.5 kGy (*17, 18*). Irradiation of apple cider at 2 and 4 kGy resulted in a decreased content of esters characteristic of apple flavor (*19*). Cardboard and musty flavors have also been detected by sensory panelists in irradiated apple cider containing potassium sorbate (*18, 19*).

Sorbates and benzoates, approved for use as chemical preservatives in apple cider, decrease spoilage and increase shelf-life, but contribute undesirable taste characteristics (*20*). Sorbates are most effective against the growth of yeasts and

molds with their activity against bacteria, including *E. coli* O157:H7, more limited (*21-23*). pH has a significant impact on the effectiveness of the preservative since the undissociated form of the acid has the greatest antimicrobial effect (*20, 21, 24*).

Processing treatments to improve safety, such as the irradiation of apple cider, must ultimately meet the consumers' demands for high flavor quality and acceptability. At Iowa State University, extensive research has been conducted to investigate the effects of irradiation, sorbate treatment, and packaging on the microbial safety and flavor quality of apple cider (*25-27*). In this chapter, we will highlight the results from these studies, focusing on the effects of these processing treatments on the flavor quality of apple cider, as assessed using instrumental and sensory evaluation techniques.

Overview of Methodology

For these studies, fresh apple cider consisting of dominant apple cultivars, with (0.1%) and without (0%) potassium sorbate, was obtained from a local Iowa cider producer. Pasteurized apple cider was pasteurized by the producer at 79° C for 2 s.

Raw apple cider was treated with electron beam irradiation at the Linear Accelerator Facility, Iowa State University, Ames, Iowa. For all experiments, the cider was irradiated at an expected dose of 2 kGy, based on previous research that demonstrated that a 2 kGy dose provides a 5-log reduction of *E. coli* O157:H7 in apple cider (*18*). Samples were at room temperature for 20 min during irradiation. Cider was held at 4° C following treatment.

Descriptive sensory evaluation, with a 10-member trained panel, evaluated the aroma and flavor characteristics of the apple cider. Selected attributes including sweetness, sourness, astringency, apple flavor, caramelized flavor, and musty flavor, were evaluated on a 15-cm line scale, with "0" corresponding to ratings of "none" and "15" corresponding to ratings of "intense". Protocols for sensory evaluation were approved by the Iowa State University Institutional Review Board (*25*).

Solid-phase microextraction (SPME) techniques, with absorption onto a SPME fiber (2cm-50/30μm divinylbenzene/carboxen/polydimethylsiloxane; Supelco, Inc., Bellefonte, PA) were applied for the isolation and concentration of volatile flavor compounds from the apple cider (*19*). Each sample was analyzed in duplicate. The volatile flavor compounds were thermally desorbed onto a fused-silica capillary column (SPB-5, 30m x 0.25mm x 0.25μm film thickness, Supelco, Inc.) via the splitless injection port of the gas chromatograph and detected using a flame ionization detector. Peak areas for the volatile compounds were determined. Volatile compounds were identified using authentic standards (Sigma-Aldrich, Milwaukee, WI; AccuStandard, Inc., New Haven, CT) and confirmed with GC-MS analyses (Micromass GCT, Waters

Corp., Milford, MA). Kovats retention indices, based on hydrocarbon standards, were calculated for all volatile compounds. Mass spectra of the volatile compounds were compared to a spectral library (Wiley Library) and a flavor and fragrance database (FlavorWORKS, Flavometrics, version 2.0, Anaheim Hills, CA) for identification.

Analysis of variance was conducted to determine the significance of main effects and interactions. Fisher's least square difference test was used for mean separation to determine significant treatment effects (SYSTAT, ver. 9.01, SPSS, Inc., Chicago, IL). A probability level of 0.05 was designated for significance.

Flavor Quality of Raw, Pasteurized, and Irradiated Apple Cider

In this study, the flavor characteristics of raw, pasteurized, and irradiated apple cider, with and without sorbate were evaluated using sensory and instrumental methods. Samples to be irradiated were packaged in transparent low-density polyethylene (LDPE; Nasco-Whirl Pak, Fort Atkinson, WI.) bags. All samples were analyzed within 24 hr of irradiation treatment to minimize any storage effects. The experiment was designed as a 2-way factorial with processing treatment and sorbate addition as the main effects. Three replications were conducted.

Processing treatment had a significant effect on apple flavor, as determined by the results of the descriptive sensory evaluation and the instrumental analysis of volatile flavor compounds. The intensity of the apple flavor sensory attribute (Figure 1) and the content of several volatile flavor compounds which are important contributors to apple flavor (Figure 2) were significantly lower in the irradiated cider than in the raw apple cider. These volatile flavor compounds included hexyl acetate, butyl 2-methylbutanoate, and hexyl 2-methylbutanoate. The apple flavor intensity and the contents of these volatile flavor compounds in the pasteurized apple cider were generally less than in the raw cider, but greater than in the irradiated apple cider. The contents of butyl acetate, 2-methylbutyl acetate, and hexanol, also important contributors to apple flavor, were not affected by processing treatment. The intensity of the sensory attributes, sourness, astringency, and caramelized flavor were not significantly affected by processing treatment.

The addition of sorbate resulted in a significantly higher intensity of sweetness in the apple cider, but did not significantly affect the pH or soluble solids contents of the apple cider (25). The content of many of the volatile flavor compounds present in apple cider were not affected by sorbate addition in this study.

The irradiation of apple cider containing sorbate resulted in the highest intensity of musty flavor of all the apple cider treatments (Figure 3). A model
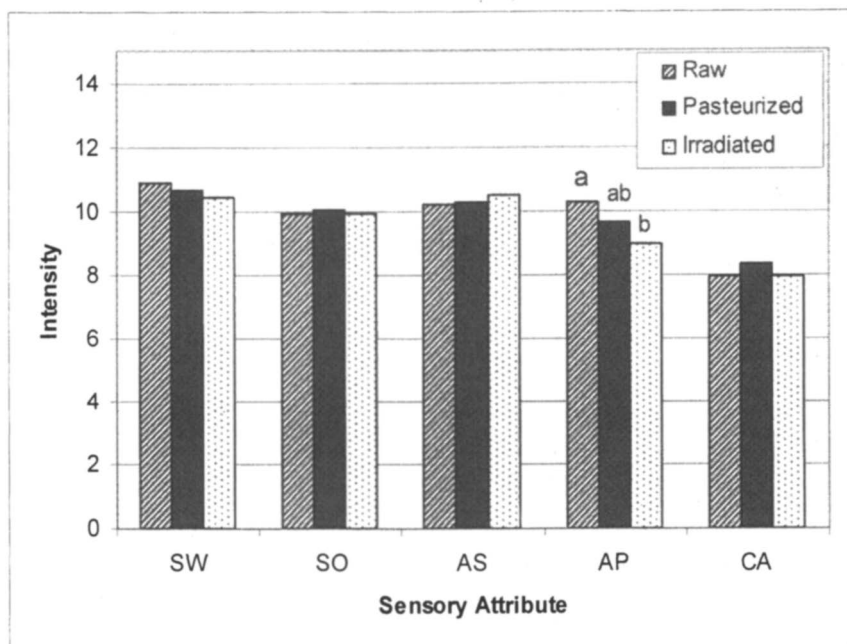
Figure 1. Intensity of flavor attributes in raw, pasteurized, and irradiated apple cider, as determined by the descriptive sensory evaluation panel. SW, sweetness; SO, sourness; AS, astringency; AP, apple flavor; CA, caramelized flavor. Means identified with different letters (a-b) are significantly different (P<0.05). (Data are from reference 25.)
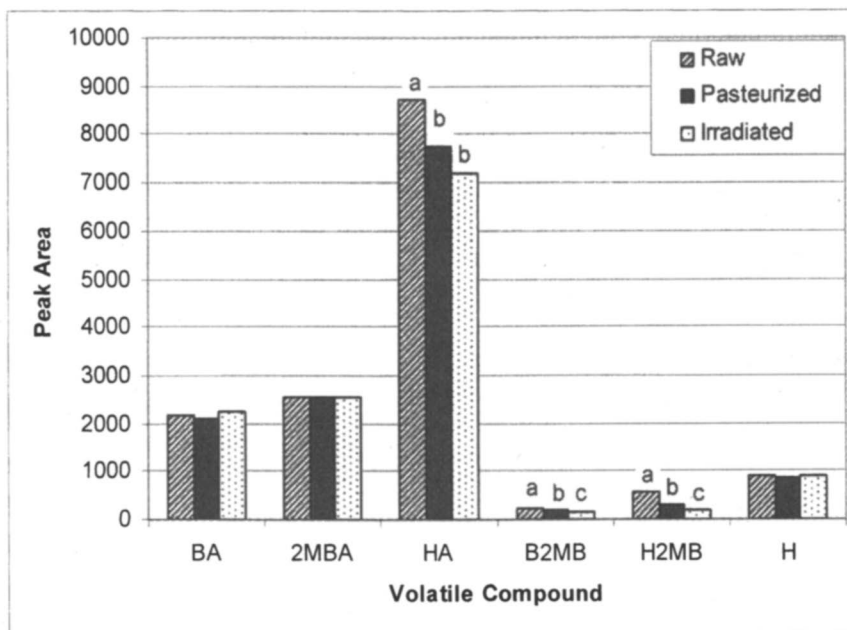
Figure 2. Contents of volatile flavor compounds in raw, pasteurized, and irradiated apple cider. BA, butyl acetate; 2MBA, 2-methylbutyl acetate; HA, hexyl acetate; B2MB, butyl 2-methylbutanoate; H2MB, hexyl 2-methylbutanoate; H, hexanol. Means identified with different letters (a-c) are significantly different (P<0.05). (Data are from reference 25.)

system demonstrated the development of the musty flavor is attributed to the degradation of the sorbate during the irradiation treatment (*25*). Off-flavors described as cardboard-like (*28*), moldy and musty (*29*), and pungent and irritating (30) have been previously detected in irradiated apple juice products containing sorbates.
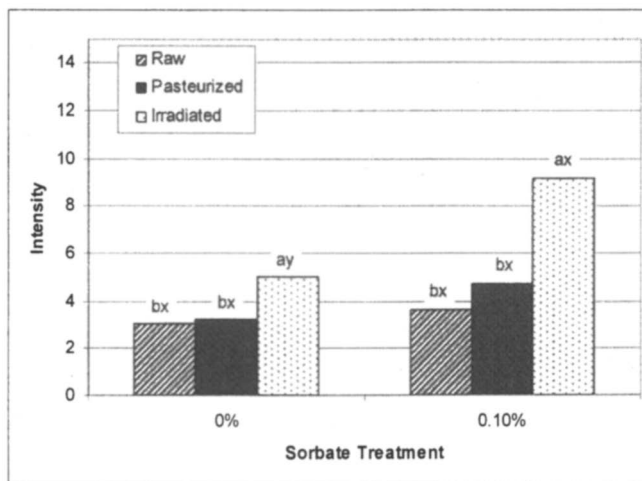
Figure 3. Effect of processing and sorbate treatments on the intensity of musty flavor in apple cider, as determined by descriptive sensory evaluation panel. Means identified with different letters are significantly different (P<0.05) with a-b indicating differences due to processing treatment and x-y indicating differences due to sorbate treatment. (Data are from reference 25).

The presence of sorbate during irradiation also had some interesting effects on the contents of several volatile flavor compounds (Figure 4).   Sorbate functions as a scavenger of hydrogen and hydroxyl radicals generated during irradiation (31), resulting in both beneficial and detrimental effects on the flavor quality of apple cider. The ability of the sorbate to scavenge these radicals has a protective effect on several of the esters which are key contributors to apple flavor (*19, 31*), as shown by higher contents of hexyl butanoate, ethyl 2-methylbutanoate, and other esters in the irradiated cider with sorbate, in comparison to the irradiated cider without sorbate. However, increased contents of hexanal, nonanal, and other volatile flavor compounds that contribute to the development of musty and other off-flavors is attributed to the degradation of the sorbate by the radicals and subsequent reactions with constituents in the apple cider during irradiation (*32*).
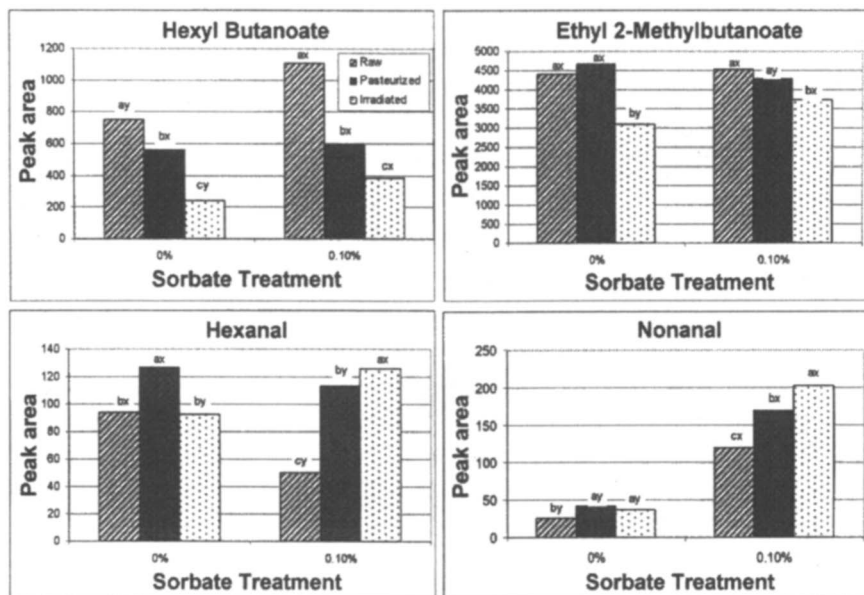
Figure 4. Volatile flavor compounds in apple cider, as influenced by processing and sorbate treatments. Means identified with different letters are significantly different (P<0.05)with a-c indicating differences due to processing treatment and x-y indicating differences due to sorbate treatment. (Data are from reference 25.)

Flavor Quality of Irradiated Apple Cider as Influenced by Packaging Materials and Sorbate Addition

In the previous study, irradiation of apple cider in low density polyethylene (LDPE) bags was shown to contribute to significant losses in the content of several esters and other volatile flavor compounds that contribute to the characteristic apple flavor. The characteristics of the packaging material may affect the flavor quality of the apple cider through the direct migration of volatile compounds from the packaging material into the food, the absorption of flavor compounds from the food by the packaging material, and the transmission of oxygen and light through the packaging material (*33*). Of the packaging materials available, LDPE demonstrates the greatest absorption of flavor compounds (*34, 35*). Thus, this study was designed to determine the role of packaging materials and sorbate addition on the flavor quality of apple cider treated with electron beam irradiation during a 3-week refrigerated storage period.

The penetration of the electron beams into a food is limited to 8 cm (*36*). Thus, packaging materials were selected that would have the appropriate dimensions for complete penetration. Raw apple cider, with and without sorbate (0.1%) was packaged in polystyrene flasks (PS; Costar, Cambridge, MA), LDPE film (Nasco-Whirl Pak), or nylon-6 film (N6; CleanFilm, Islandia, NY) prior to irradiation. Processing treatments were replicated two times. The experiment was designed as a 3-way factorial with packaging materials, sorbate addition, and storage time as the main factors.

The initial content of a majority of the volatile flavor compounds was not significantly affected by the irradiation, packaging and sorbate treatments. Storage time had a significant effect on the content of the volatile flavor compounds, as shown in Figure 5 for hexyl acetate, a major flavor compound in apples. Due to the complex interactions between the main factors, semi-log regression plots, as a function of storage time, were plotted to determine the effects of packaging material and sorbate addition on rates of change (slope of log GC peak area/week) of volatile flavor compounds during storage.

The addition of sorbate in the apple cider was effective in slowing the rate of loss of several esters and other key contributors to apple flavor (Figure 6). Sorbate effectively reduces fermentation reactions during storage through the inhibition of natural yeasts, contributing to higher soluble solids and lower titratable acidity contents (*26*). The inhibition of these fermentation reactions by the sorbate may also contribute to the preservation of the volatile flavor compounds during storage. In addition, the ability of the sorbate to quench free radicals generated during irradiation (*31, 32*) plays an important role in the preservation of the key volatile flavor compounds during storage (*19*).
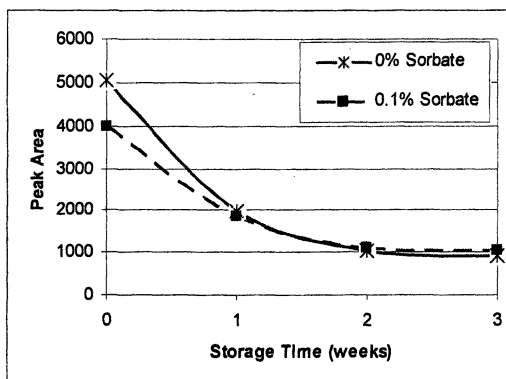
Figure 5. Effect of storage time on the hexyl acetate content of apple cider packaged and irradiated in LDPE. (Reproduced with permission from reference 26. Copyright 2004 Institute of Food Technologists)
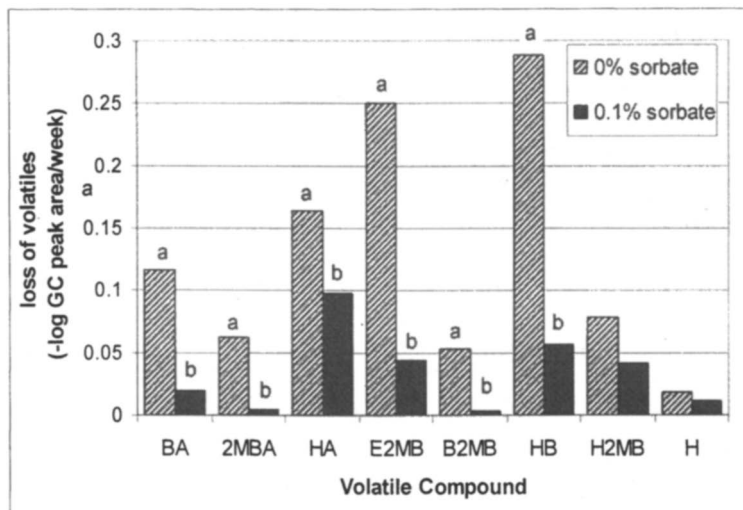
Figure 6. Effect of sorbate treatment on loss of volatile flavor compounds in apple cider during 3 weeks of refrigerated storage. BA, butyl acetate; 2MBA, 2-methylbutyl acetate; HA, hexyl acetate; E2MB, ethyl 2-methylbutanoate; B2MB, butyl 2-methylbutanoate; HB, hexyl butanoate; H2MB, hexyl 2-methylbutanoate; H, hexanol. Means identified with different letters (a-b) are significantly different (P<0.05). Data for packaging material are pooled. (Data are from reference 26.)

Packaging material also had a significant effect on the rate of loss of volatile flavor compounds during storage (Figure 7). The cider irradiated and stored in PS flasks had a significantly lower rate of loss than the cider irradiated and stored in LDPE film. The loss of esters and other volatile flavor compounds from the apple cider and irradiated in LDPE is attributed to the flavor sorption by the plastic polymers (35) and the inferior gas barrier properties of the LDPE films (37).

Flavor Quality of Irradiated Apple Cider as Influenced by Gas Environment and Sorbate Addition

Chemical degradation of flavor components contributes to losses of flavor quality in apple cider during storage. In the previous study, the greatest losses in volatile flavor compounds occurred in the cider packaged in LDPE. Both flavor sorption and diffusion of oxygen through the packaging material are believed to
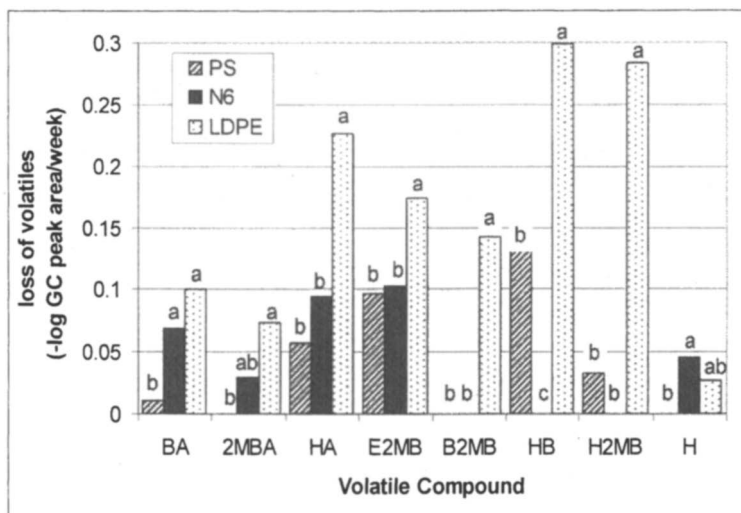
Figure 7. Effect of packaging material (PS, polystyrene; N6, nylon-6; LDPE, low-density polyethylene) on loss of volatile flavor compounds (-log GC peak area/week) in apple cider during 3 weeks of refrigerated storage. BA, butyl acetate; 2MBA, 2-methylbutyl acetate; HA, hexyl acetate; E2MB, ethyl 2-methylbutanoate; B2MB, butyl 2-methylbutanoate; HB, hexyl butanoate; H2MB, hexyl 2-methylbutanoate; H, hexanol. Means identified with different letters (a-c) are significantly different (P<0.05). Data for sorbate treatment are pooled. (Data are from reference 26.)

contribute to the losses in these flavor compounds. The presence of oxygen during irradiation and storage can result in detrimental effects on flavor and overall quality of apple cider. The objective of this study was to determine the effects of gas environment and sorbate addition on the flavor of irradiated apple cider during 7 weeks of refrigerated storage. The polystyrene (PS, Costar) flasks were selected for this study due to their low oxygen permeability and superiority as a packaging material in regards to the retention of volatile flavor compounds during irradiation and storage. Apple cider, with and without sorbate, was packaged in the PS flasks and exposed to atmospheric air, nitrogen flush, or oxygen flush prior to electron beam irradiation. Processing treatments were replicated two times. The experiment was designed as a 3-way factorial with storage time, sorbate addition, and gas environment as the main factors. As in the previous study, semi-log regression plots of contents of volatile flavor compounds versus storage time were plotted to determine rates of change of the volatile flavor compounds to focus on the effects of sorbate treatment and gas environment.

For many of the volatile flavor compounds that are key contributors to apple flavor, the interaction between sorbate addition and gas environment was significant. In the presence of sorbate (Figure 8A), differences in the rate of loss of the volatile flavor compounds were not significantly affected by the gas environment during irradiation. Thus, sorbate, in functioning as a radical scavenger, minimized the potential for degradation of the volatile flavor compounds in the presence of oxygen, in either the atmospheric air and oxygen flush treatments, in comparison to the nitrogen flush treatment. In the absence of sorbate (Figure 8B), losses in the esters and other volatile flavor compounds that contribute to apple flavor occurred at a faster rate than in the presence of sorbate. In addition, in the absence of sorbate, the gas environment had a greater impact on the stability of the volatile flavor compounds. An atmospheric air or nitrogen-flush environment during irradiation resulted in the greatest retention of key volatile compounds, including 2-methylbutyl acetate, ethyl 2-methylbutanoate, and butyl butanoate.

Conclusions

Processing, packaging, and sorbate treatments have a significant impact on the flavor quality of apple cider. Irradiation is an effective means to improve the safety of apple cider, however, packaging environments must be optimized to minimize oxygen exposure during irradiation to enhance the retention of esters and other important volatile flavor compounds. Sorbate was effective in slowing the loss of the volatile flavor compounds during irradiation and storage, but also contributed to the formation of a musty flavor, as detected by sensory panelists, when the apple cider was irradiated in the presence of oxygen. Because of the complex interactions that occur during processing, it is critical that processing treatments designed to improve the safety of food also consider the effects of those treatments the food's flavor quality and consumer acceptability.

Acknowledgments
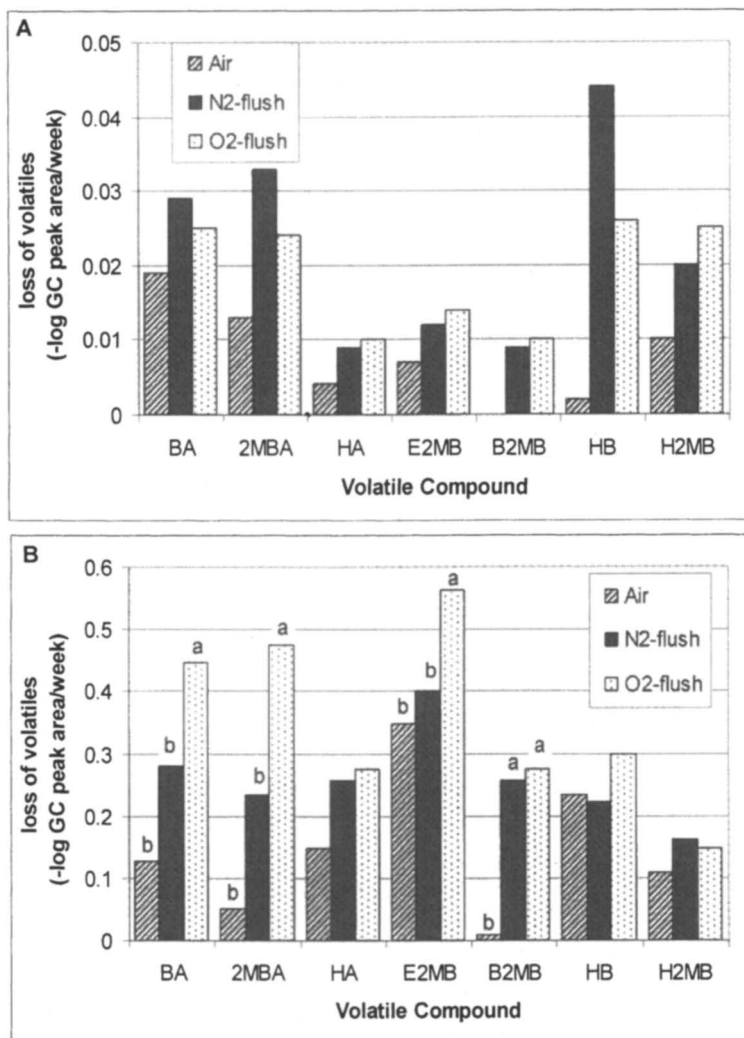
*Figure 8.   Effect of gas environment on loss of volatile compounds in apple
cider with (0.1% ; A) and without (0%; B) sorbate during 7 weeks of
refrigerated storage. BA, butyl acetate; 2MBA, 2-methylbutyl acetate; HA,
hexyl acetate; E2MB, ethyl 2-methylbutanoate; B2MB, butyl 2-methylbutanoate;
HB, hexyl butanoate; H2MB, hexyl 2-methylbutanoate. For cider with sorbate
(A), gas environment did not have a significant effect (P>0.05) on any of the
volatile compounds. For cider without sorbate (B), means identified with
different letters (a-b) are significantly different (P<0.05) (Data are from
reference 27).*

References

1. Young, H.; Gilbert, J.M.; Murray, S.H.; Ball, R.D. *J. Sci. Food Agric.* **1996**, *71*, 329-336.
2. Poll, L. *Lebensm.Wiss. Technol.* **1983**, *16*, 220-223.
3. Poll, L. *Lebensm.-Wiss. Technol.* **1985**, *18*, 205-211.
4. Cunningham, D.G.; Acree, T.E.; Barnard, J.; Butts, R.M.; Braell, P.A. *Food Chem.* **1986**, *19*, 137-147.
5. Lopez, M.L.; Lavilla, M.T.; Ribva, M.; Vendrell, M. *J. Food Qual.* **1998**, *21*, 155-166.
6. Poll, L. *Lebensm.-Wiss.Technol.* **1988**, *21*, 87-91.
7. Poll, L.; Flink, J.M. *Lebensm. Wiss. Technol.* **1983**, *16*, 215-219.
8. Besser, R.E.; Lett, S.M.; Weber, J.T.; Doyle, M.P.; Barrett, T.J.; Wells, J.G.; Griffin, P.M. *J. Amer. Med. Assoc.* **1993**, *269*, 2217-2220.
9. Goverd, K.A.; Beech, F.W.; Hobbs, R.P.; Shannon, R. *J. Appl. Bacteriol.* **1979**, *46*, 512-530.
10. Centers for Disease Control and Prevention. *Morbid. Mortal. Weekly Rep.* **1996**, *45*, 975-982.
11. Centers for Disease Control and Prevention. 1997. *Morbid. Mortal. Weekly Rep.* **1997**, *46*, 4-8.
12. Food and Drug Administration. *Code of Fed. Reg.* 21 CFR Part 101 ([Docket No. 97N-0524] RIN 0910-AA43) July 8, **1998**.
13. Food and Drug Administration. **2004**. Guidance for industry. Juice HACCP Hazards and Controls Guidance. First edition. [http://www.cfsan.fda.gov/~dms/juicgu10.html#v].
14. Splittstoesser, D.F.; McLellan, M.R.; Churey, J.J. *J. Food Protect.* **1996**, *59*, 226-229.
15. Fischer, T.L.; Golden, D.A. *J. Food Prot.* **1998**, *61*, 1372-1374.
16. Nursten, H.E.; Woolfe, M.L. *J. Sci. Food Agric.* **1972**, *23*, 803-822.
17. Buchanan, R.L.; Edelson, S.G.; Snipes, K.; Boyd, G. *Appl Environ. Microbiol.* **1998**, *64*, 4533-4535.
18. Wang, H.; Reitmeier, C.A.; Glatz, B.A. *J. Food Prot.* **2004**, *67*, 1574-1577.
19. Boylston, T.D.; Wang, H.; Reitmeier, C.A.; Glatz, B. *J. Agric. Food Chem.* **2003**, *51*, 1924-1931.
20. Ingham, S.C.; Schoeller, N.P. *Food Res. Int.* **2002**, *35*, 611-618.
21. Sofos, J.N.; Busta, F.F. In *Antimicrobials in Foods*; Branen, A.L.; Davidson, P.M., Eds.; Marcel Dekker, Inc.: New York, NY, 1983; pp. 141-175.
22. Baroody, T.; McLellan, M,R. *J. Food Qual.* **1986**, *9*, 415-423.
23. Zhao, T.; Doyle, M.P.; Besser, R.E. *Appl. Environ. Microbiol.* **1993**, *59*, 2526-2530.
24. Comes, J.E.; Beelman, R.B. *J. Food Protect.* **2002**, *65*, 476-483.

25. Yulianti, F.; Reitmeier, C.A.; Glatz, B.A.; Boylston, T.D. *J. Food Sci.* **2005**, *70*, S153-S158.
26. Crook, L.R.; Boylston, T.D. *J. Food Sci.* **2004**, *69*, C557-C563.
27. Crook, L.R.; Boylston, T.D.; Glatz, B.A. *J. Agric. Food Chem.* **2004**, *52*, 6997-7004.
28. Wang , H.; Reitmeier, C.A.; Glatz, B.A.; Carriquiry, A.L. *J. Food Sci.* **2003**, *68*, 1498-1503.
29. Zegota, H. *Z. Lebensm. Untersuch. Forsch.* **1991**, *192*, 7-10.
30. Fan, X.; Thayer, D.W. *J. Agric. Food Chem.* **2002**, *50*, 710-715.
31. Thakur, B.R.; Trehan, I.R.; Arya, S.S. *J. Food Sci.* **1990**, *55*, 1699-1710.
32. Thakur, B.R.; Arya, S.S. *Int. J. Food Sci. Technol.* **1993**, *28*, 371-376.
33. Askar, A. *Fruit Proc.* **1999**, 432-439.
34. Ayhan, Z.; Yeom, H.W.; Zhang, Q.H.; Min, D.B. *J. Agric. Food Chem.* **2001**, *49*, 669-674.
35. Van Willige, R.; Schoolmeester, D.; Van Ooij, A.; Linssen, J.; Voragen, A. *J. Food Sci.* **2001**, *67*, 2023-2031.
36. Kilcast, D. *Food Chem.* **1994**, *49*, 157-164.
37. Matsui, T.; Ono, A.; Shimoda, M.; Osajima, Y. *J. Agric. Food Chem.* **1992**, *40*, 479-483.

Chapter 12

Flavor Contribution and Formation of Epoxydecenal Isomers in Black Tea

Kenji Kumazawa, Yoshiyuki Wada, and Hideki Masuda

Ogawa and Company, Ltd., 15–7 Chidori Urayasushi, Chiba 279–0032, Japan

Two potent odorants responsible for the juicy and sweet note in black tea were identified as *cis*- and *trans*-4,5-epoxy-(*E*)-2-decenals. Of the two odorants, *cis*-4,5-epoxy-(*E*)-2-decenal has been identified for the first time in black tea, and it was assumed that both isomers in black tea were formed from linoleic acid in the tea leaves via 12,13-epoxy-9-hydroperoxy-10-octadecenoic acid. In addition, the following formation mechanism during black tea production was assumed. First, the withering and fermentation processes convert linoleic acid to its hydroperoxide in which the oxygen adds to the 13 carbon due to lipoxygenase activity. Subsequently, by heating during the drying process, the 13-hydroperoxide of linoleic acid produces epoxydecenal isomers via the *cis*- and *trans*-epoxyallylic radicals which are intermediates of 12,13-epoxy-9-hydroperoxy-10-octadecenoic acid. Furthermore, by application of aroma extract dilution analysis (AEDA) on the black tea infusion (Dimbula), it was found that these isomers were significantly important odorants for the flavor attribute of Dimbula, because they had high flavor dilution (FD) factors and a "sweet-juicy" odor quality.

136 © 2008 American Chemical Society

The steps involved in the processing of black tea include withering, leaf disruption (rolling and/or cutting), fermentation, drying and grading. For the characteristic process during black tea production, it utilizes an enzyme reaction. Namely, black tea leaves are processed by drying after making use of sufficient enzyme action during the withering and fermentation processes. On the other hand, the enzymes in green tea leaves are inactivated by steaming or parching during the first process, and there is only slight enzymatic action. Black tea flavor is quite different from that of green tea regardless of being made from the same kind of plant. For the flavor formation in black tea, in particular, it was pointed out that the enzyme action during the manufacturing process is very important (*1-4*). However, the influence of the enzyme action during the manufacturing process on the formation of the potent odorants is still mostly unresolved.

trans-4,5-Epoxy-(*E*)-2-decenal has been identified as a contributor to the aroma of black tea using AEDA (*5, 6*). On the basis of previous research on lipid degradation products, *trans*-4,5-epoxy-(*E*)-2-decenal has been proposed to originate from linoleic acid due to oxidation (*7, 8*). The formation pathway of this odorant formed from linoleic acid by oxidation has already been reported, and two routes have been proposed. On the other hand, it has been reported that tea leaves contain from 3 to 5 % fatty acids, and linoleic acid is one of the principal fatty acids (*9*). Therefore, *trans*-4,5-epoxy-(*E*)-2-decenal in black tea would be speculated to be generated from linoleic acid. However, the formation mechanism of this odorant in black tea is unclear.

The aim of this investigation was to elucidate the formation mechanism of the epoxydecenal isomers during the manufacturing of black tea leaves. The concentration of epoxydecenal isomers in black and green teas was compared and model experiments using linoleic acid and its hydroperoxides were performed. Furthermore, in order to clarify the contribution of these isomers to the flavor of Dimbula, which is one of the typical Ceylon black tea cultivars, an AEDA was completed.

Experimental

Materials

The black tea products are as follows: Dimbula (Sri Lanka), Uva (Sri Lanka), Nuwara eliya (Sri Lanka), Darjeeling (India), Assam (India), Java (Indonesia), Keemun (China). The Japanese green tea (Sen-cha) product was produced in Shizuoka prefecture (Japan). The tea infusions were prepared as follows: deionized hot water (3 L) at 85-90 °C (black tea) or 70-75 °C (green tea) was added to 150 g of tea, and the leaves were removed using coarse filter paper after standing for 5 min. The filtrate (3 L) was immediately cooled to about 20 °C in tap water. The *cis*- or *trans*-4,5-epoxy-(*E*)-2-decenal was

synthesized from *cis*- or *trans*-2-octenol as the starting materials by epoxidation with *m*-chloroperbenzoic acid, and the syntheses of the 4,5-epoxy-(*E*)-2-decenals followed by oxidation with Dess-Martin periodinane and the Wittig reaction (*10*). Structural characterization was performed using mass spectrometry and ^{1}H NMR measurements.

Isolation of the Volatiles from Tea Infusion

Each tea (black and green) infusion (1 L) was passed through a column packed with 10 g of Porapak Q (Waters). The adsorbed compounds were then eluted with 100 mL of methylene chloride. To remove the nonvolatile material, the eluate was distilled under reduced pressure (40 °C at 5×10^{-3} Pa) using the solvent assisted flavor evaporation (SAFE) method (*11*). The distillate was dried over anhydrous sodium sulfate, and the solvent was removed by rotary evaporation to leave about 5 mL. A further concentration was conducted in a nitrogen stream to about 150 μL. For the quantitative analysis, an internal standard (methyl undecanoate: 5.06 μg) was added to the eluate before the SAFE treatment, and then the acids in the tea distillate were removed using a saturated solution of $NaHCO_3$ (2 × 50 mL). For the identification experiments, the black tea volatiles were isolated from 450 g of the black tea (Dimbula) leaves by combining the adsorptive column method and the SAFE technique as described above, and the target compounds were enriched by silica gel column chromatography.

Model Experiment for Epoxydecenal Isomer Formation from Linoleic Acid

Linoleic acid hydroperoxides were obtained from oxidation of linoleic acid by soybean lipoxygense. The hydroperoxides were isolated by silica gel column chromatography, and used as soon as possible to avoid model reaction. The linoleic acid hydroperoxides (31.25 μmoles) or linoleic acid (31.25 μmoles) was dissolved in 5 g of glycerol trioctanoate containing $FeSO_4 \cdot 2H_2O$ (2 mg) and then heated for 60 min at 150 °C using a GC oven in a closed vessel. After cooling, methylene chloride (50 mL), containing methyl undecanoate (101 μg) as the internal standard, was added, and the flavor compounds and internal standard were isolated by the SAFE treatment.

Aroma Extract Dilution Analysis (AEDA) (*12*)

The original odor concentrate of the green tea infusion was stepwise diluted with methylene chloride to 4^n (n = 3-8), and aliquots (1 μL) of each fraction were

analyzed by gas chromatography-olfactometry (GC-O). The GC-O analysis conditions were the same as previously described (*13*).

Gas Chromatography-Mass Spectrometry (GC-MS)

The conditions of GC-MS analysis and identification of the components were the same as previously described (*13*). The quantities of the components in each volatile fraction of the tea infusions were determined from the extracted ion peak areas obtained by mass chromatography. The GC-MS was operated in the selected ion mode (SIM), and the extracted ions were monitored in the ranges listed in Table I. The calibration factors were determined in a mixture of equal amounts by weight of an odorant and internal standard compound.

Table I. Selected Ion and Calibration Factors for Mass Chromatography

Compound	Selected Ion (m/z)	Calibration Factor
cis-4,5-epoxy-(*E*)-2-decenal	68	0.10
trans-4,5-epoxy-(*E*)-2-decenal	68	0.08
methyl undecanoate[a]	200	1

[a] Internal standard.

Proton Magnetic Resonance Spectrometry (^{1}H NMR)

The ^{1}H NMR spectra were recorded in a $CDCl_3$ solution using a Bruker AVANCE 400 spectrometer operating at 400 MHz with tetramethylsilane as the internal standard.

Results and Discussion

Formation Mechanism of Epoxydecenal Isomers in Black Tea

The formation pathway of *trans*-4,5-epoxy-(*E*)-2-decenal formed from linoleic acid by oxidation has already been reported, and two routes have been proposed (Figure 1). Route A is the pathway in which 2,4-decadienal as the key intermediate reacts with peroxide (*8*), and route B is the pathway in which the 12,13-epoxy-9-hydroperoxy-10-octadecenoic acid decomposes by α-cleavage (*7*). Therefore, in the former route, if the other 2,4-alkadienals are included, the corresponding 4,5-epoxy-2-alkenals may also be produced, whereas in the latter route, 4,5-epoxy-2-decenal could mainly be expected.

R=(CH$_2$)$_5$COOH
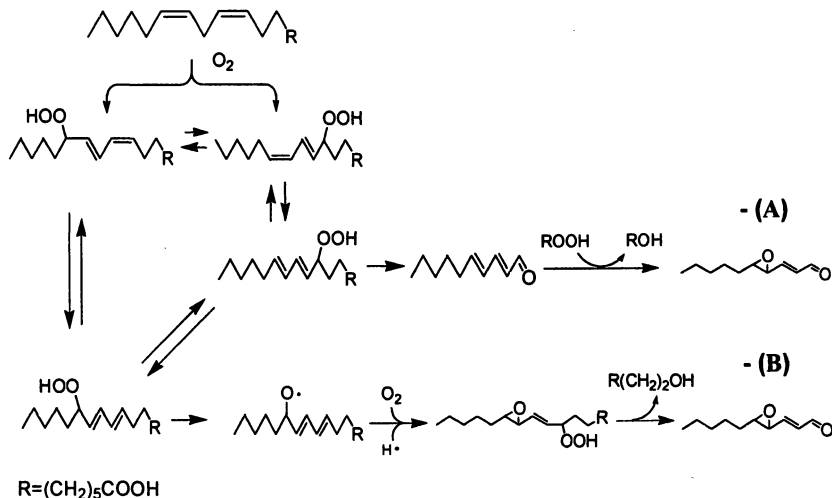
Figure 1. Proposed pathway for the formation of trans-4,5-epoxy-(E)-2-decenal from linoleic acid [according to Gardner and Selke (7) and Gassenmeier and Schieberle (8)]. (Reproduced from reference 14. Copyright 2006 American Chemical Society.)

In order to examine the formation pathway of the epoxydecenal isomers from the black tea, the homologous series of the 2,4-alkadienals and 4,5-epoxy-2-alkenals in the volatile fraction of the black tea infusion was then screened by GC-MS. In the black tea infusion, the variety of detected 2,4-alkadienals ranged from six to ten carbons. Based on the model experiments, all the 2,4-alkadienals from six to ten carbons reacted with the hydroperoxide, which were prepared from linoleic acid with soybean lipoxygenase, and produced all the corresponding 4,5-epoxy-2-alkenals. Therefore, if the 4,5-epoxy-(E)-2-decenal isomers are mainly formed from the 2,4-decadienals as intermediates, it is speculated that the homologous series of the 4,5-epoxy-2-alkenals would be detected in black tea.

In Figure 2, the chromatograms (polar and apolar GC columns) recorded with *m/z* 68, which are the typical fragment ion of the homologous series of 4,5-epoxy-2-alkenals, are shown. As a result, the homologues of four kinds of 4,5-epoxy-2-alkenals were detected in the black tea. The structure of *cis*-4,5-epoxy-(E)-2-decenal (**1**) and *trans*-4,5-epoxy-(E)-2-decenal (**2**) were confirmed by comparison of their retention indices and mass spectra to those of the actual synthetic compounds, and in addition, *trans*-4,5-epoxy-(E)-2-heptenal (**3**) and its isomer (**4**) were assumed from the corresponding literature data (*15*). However, the other 4,5-epoxy-2-alkenals could not be found in the black tea. Therefore, the formation of the 4,5-epoxy-(E)-2-decenals cannot be explained by route A
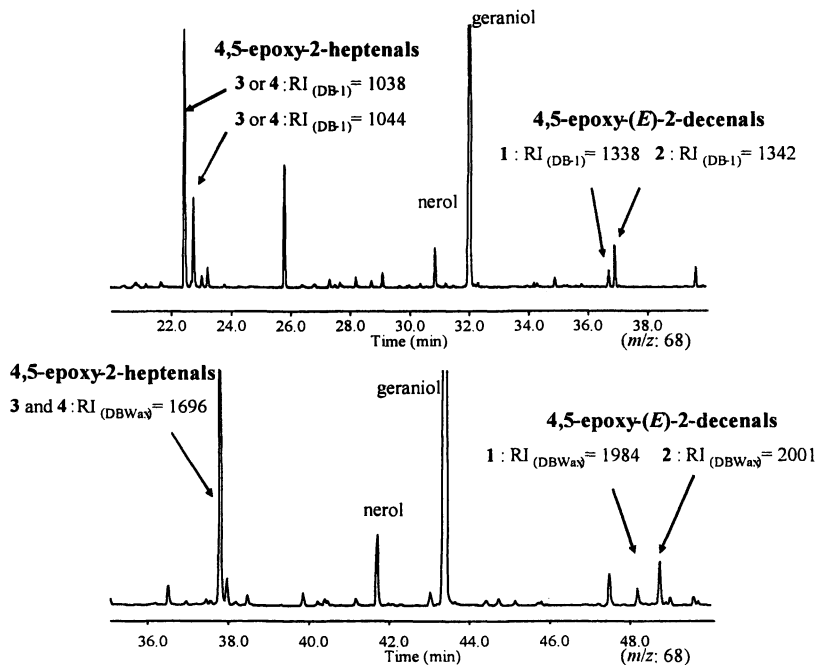
Figure 2. Mass chromatograms (top: DB-1, bottom: DB-Wax) of the volatile
concentrate of a black tea infusion showing the extracted ion which is the
typical fragment ion of the homologous series of 4,5-epoxy-2-alkenals. [cis-4,5-
epoxy-(E)-2-decenal (1), trans-4,5-epoxy-(E)-2-decenal (2), trans-4,5-epoxy-
(E)-2-heptenal (3), and isomer of 3 (4)].

via 2,4-decadienal as the intermediate, and it is presumed that both isomers (1, 2)
in the black tea were mainly formed from linoleic acid in the tea leaves via the
12,13-epoxy-9-hydroperoxy-10-octadecenoic acid (route B).

In addition, the difference in the content of both epoxydecenal isomers
could be recognized, and the content of 1 was less than that of 2. This chemical
behavior regarding the difference in contents 1 and 2 can be assumed to affect
the equilibration of the alkoxydiene radicals which are formed from the 13-
hydroperoxide of linoleic acid as the intermediate by heating. Namely, the
alkoxydiene radicals, which are capable of forming the extended and hindered
conformers of the carbon 12,13 bond (Figure 3), and the extended conformer is
more dominant than the hindered conformer. Therefore, it seems that the content
of the cis-epoxyallylic radical was less than that of the trans-epoxyallylic radical
formed from these alkoxydiene radicals (16, 17), and 1 and 2 in the black tea
were expected to be generated from the cis- or trans-epoxyallylic radical via the
hydroperoxide which oxidized carbon 9 with O_2.

extended conformer   **hindered conformer**

trans-epoxide   *cis*-epoxide

$R_1 = (CH_2)_6COOH$

$R_2 = (CH_2)_4CH_3$
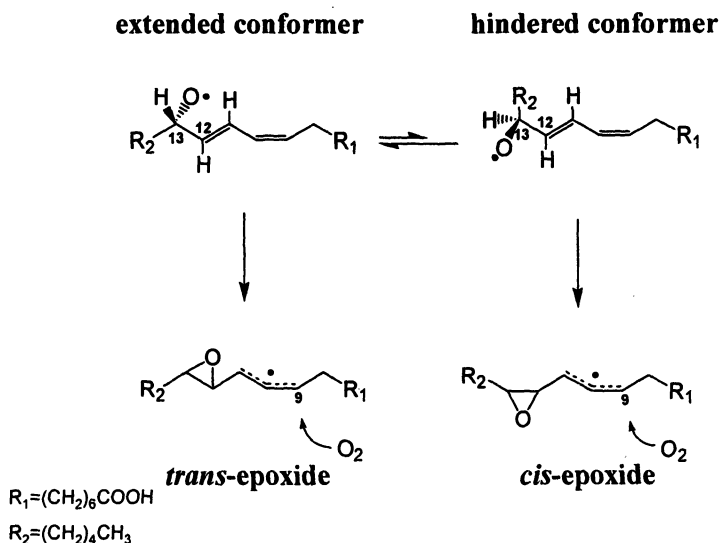
Figure 3. Hypothetical generation mechanism of cis- and trans-epoxides. (Reproduced from reference 14. Copyright 2006 American Chemical Society.)

Table II. Comparison of 4,5-Epoxy-(E)-2-decenal Isomers in Black Tea (Dimbula) and Japanese Green Tea (Sen-cha)

	Amount ($\mu g/L$)	
Odorant	*Black Tea (Dimbula)*	*Green Tea (Sen-cha)*
cis-4,5-epoxy-(E)-2-decenal	0.28	< 0.01
trans-4,5-epoxy-(E)-2-decenal	0.60	0.02

Source: Reproduced from reference 14. Copyright 2006 American Chemical Society.

Table III. Comparison of Generated Amount of 4,5-Epoxy-(E)-2-decenal Isomers from Linoleic Acid and Its Hydroperoxides

	Amount (μg)			
Odorant	*Non-heated*		*Heated*	
	Linoleic acid	*LH^a*	*Linoleic acid*	*LH^a*
cis-4,5-epoxy-(E)-2-decenal	< 0.01	< 0.01	0.13	2.56
trans-4,5-epoxy-(E)-2-decenal	< 0.01	< 0.01	0.43	6.53

[a] Linoleic acid hydroperoxydes

Source: Reproduced from reference 14. Copyright 2006 American Chemical Society.

For the flavor formation of the black tea, in particular, the enzyme action during the manufacturing process is significantly important (*1-4*). As the characteristic process of the black tea production, it definitely utilizes the enzyme reaction during the withering and fermentation processes. On the other hand, the enzymes in green tea leaves are inactivated by steaming or parching, and there is only slight enzymatic activity. In order to clarify the relationship of the manufacturing method of black tea and the formation of the 4,5-epoxy-(*E*)-2-decenal isomers, a comparison of the contents of **1** and **2** in black and green teas was done. It appeared that the amounts of these isomers in black tea were much greater in comparison to that in green tea (Table II). Therefore, **1** and **2** seem to be characteristic compounds of black tea, and it can be presumed that the process of black tea production was important for the formation of **1** and **2**. The model reactions that focused on the enzyme reaction during the withering and fermentation processes of black tea production were carried out using linoleic acid and its hydroperoxide. As a result, it was shown that **1** and **2** were generated from linoleic acid and its hydroperoxide by heating. However, the generated amounts of these isomers from the linoleic acid hydroperoxide were much greater than that from linoleic acid (Table III). This finding explained the different amounts of **1** and **2** in the black and green teas, and strongly suggested that the enzyme reaction plays an important role in forming these isomers during the manufacturing process of the black tea leaves.

On the basis of these results, it is suggested that **1** and **2** were generated from the linoleic acid contained in the tea leaf during the manufacturing process of the black tea, and it can be assumed that the formation mechanism is as follows. First, the withering and fermentation steps, which are characteristic processes in black tea production, convert linoleic acid to its hydroperoxide in which the oxygen adds to the 13 carbon due to lipoxygenase activity. It is well known that tea lipoxygenase has a high specificity to form the 13-hydroperoxide of linoleic acid (*18, 19*). In addition, by heating during the drying process of black tea production, the 13-hydroperoxide of linoleic acid produced **1** and **2** via the *cis-* and *trans*-epoxyallylic radicals, respectively. Thus, the formation of **1** and **2** have a close relation to the manufacturing process, especially, the enzyme reaction in black tea seems to be one of the most important factors for the formation of these isomers.

Contribution of 4,5-Epoxy-2-alkenals in Ceylon Black Tea Flavor

The so-called Ceylon black teas, which are produced in Sri Lanka, have a typical floral and juicy-sweet note, and this note in Dimbula is particularly remarkable. In the volatile concentrate of the Ceylon black tea (Dimbula), four kinds of 4,5-epoxy-2-alkenals (**1, 2, 3,** and **4**) were found, and three compounds, except for **2** are reported here for the first time as components of black tea. The
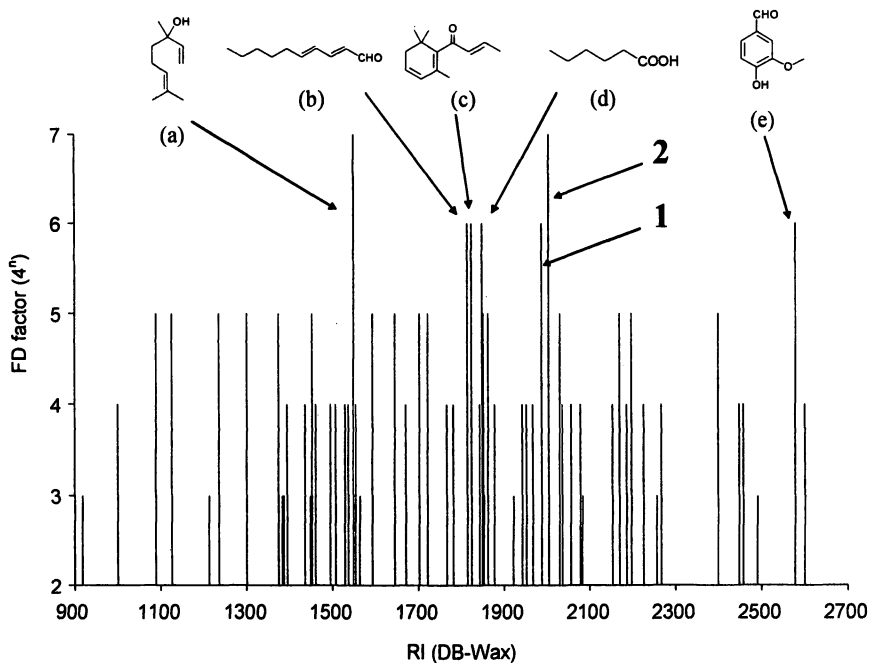
*Figure 4. Flavor dilution chromatograms of the black tea (Dimubla) infusions.
(1: cis-4,5-epoxy-(E)-2-decenal, 2: trans-4,5-epoxy-(E)-2-decenal, a: linalool,
b: (E,E)-2,4-decadienal, c: β-damascenone, d: hexanoic acid, e: vanillin).
(Reproduced from reference 14. Copyright 2006 American Chemical Society.)*

first identification of **1** was from the aroma of fresh field tomatoes (*20, 21*), however, **1** has not yet been identified in other kinds of natural sources. AEDA applied to the volatile fraction, which had been prepared from a freshly filtered Ceylon black tea (Dimbula) infusion, observed **1** and **2** with extremely high FD factors ($\geq 4^6$) (Figure 4). Among the perceived odorants, **1** and **2** have been proved to be most important components in the Ceylon black tea flavor. However, the odor-active peaks corresponding to the 4,5-epoxy-2-heptenals were not able to be detected. This finding can be explained by the difference in the odor threshold of the 4,5-epoxy-2-alkenals. Namely, it was reported that the odor thresholds of the series of the 4,5-epoxy-(*E*)-2-alkenals (C-7 to C-12) dramatically changed with the chain length, and the 4,5-epoxy-(*E*)-2-decenal (C-10 homologue) had the lowest odor threshold (*22*).

Each odorant (**1, 2**) has a common juicy and sweet note based on a metallic note. In addition, the contents of **1** and **2** differ in every black tea cultivar, and the amount of these odorants in Dimbula was greater than in the other kinds
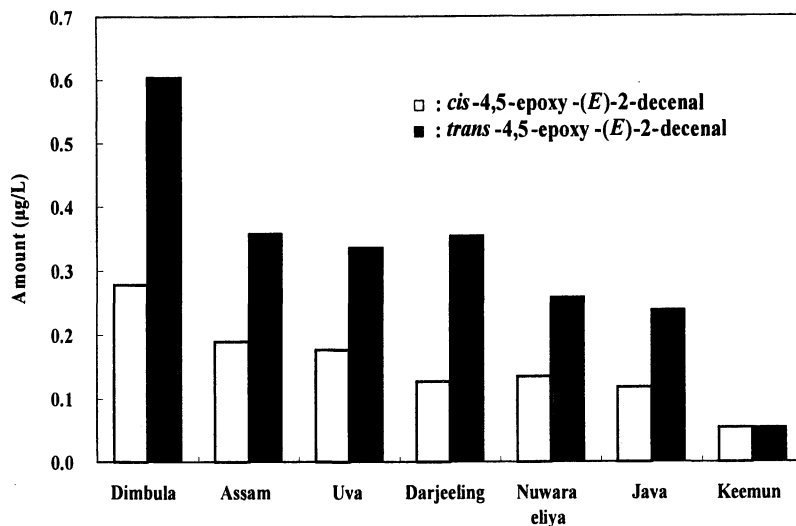
Figure 5. Amounts of 4,5-epoxy-(E)-2-decenal isomers in the different black tea cultivars.

of black tea cultivars (Figure 5). Therefore, the epoxydecenal isomers (**1**, **2**) seem to be responsible for the characteristic flavor of Ceylon black tea, especially, the juicy-sweet note.

Acknowledgment

References

1. Wang, D.; Kurasawa, E.; Yamaguchi, Y.; Kubota, K.; Kobayashi, A. *J. Agric. Food Chem.* **2001**, *49*, 1900-1903.
2. Saijo, R.; Takeo, T. *Agric. Biol. Chem.* **1970**, *34*, 227-233.
3. Sanderson, G. W.; Graham H. N. *J. Agric. Food Chem.* **1973**, *21*, 576-585.
4. Hatanaka, A.; Kajiwara, J.; Sekiya, M.; Imoto, M.; Inouye, S. *Plant & Cell Physiol.* **1982**, *23*, 91-99.
5. Guth, H.; Grosch, W. *Flavour and Fragrance J.* **1993**, *8*, 173-178.

6. Schuh, C.; Schieberle, P. Characterization of the key aroma compounds in the beverage prepared from Darjeeling black tea: Quantitative differences between tea leaves and infusion. *J. Agric. Food Chem.* **2006**, 54, 916-924.
7. Gardner, H. W.; Selke, E. *Lipids* **1984**, *19*, 375-380.
8. Gssenmeier, K.; Schieberle, P. *J. Am. Oil Chem. Soc.* **1994**, *71*, 1315-1319.
9. Anan, T.; Takayanagi, H.; Ikegaya, K.; Nakagawa, M. *Nippon Shokuhin Kogyo Gakkaishi* **1982**, *29*, 706-711.
10. Barrett, A. G. M.; Head, J.; Smith, M. L.; Stock, N. S.; White, A. J. P.; Williams, D. J. *J. Org. Chem.* **1999**, *64*, 6005-6018.
11. Engel, W.; Bahr, W.; Schieberle, P. *Eur. Food Res. Technol.* **1999**, *209*, 237-241.
12. Schieberle, P. In *Characterization of Food: Emerging Methods*; Goankar, A., Ed.; Elsevier: Amsterdam, 1995; pp 403-431.
13. Kumazawa, K.; Masuda, H. *J. Agric. Food Chem.* **2003**, *51*, 3079-3082.
14. Kumazawa, K.; Wada, Y.; Masuda, H. *J. Agric. Food Chem.* **2006**, *54*, 4795-4801.
15. Buettner, A.; Schieberle, P. *J. Agric. Food Chem.* **2001**, *49*, 3881-3884.
16. Gardener, H. W.; Kleiman, R. *Biochimica et Biophysica Acta* **1981**, *665*, 113-125.
17. Schieberle, P.; Trebert, Y.; Firl, J.; Grosch, W. *Chemistry and Physics of Lipids* **1985**, *37*, 99-114.
18. Hatanaka, A.; Kajiwara, T.; Sekiya, J.; Fujimura, K. *Agric. Biol. Chem.* **1979**, *43*, 175-176.
19. Kajiwara, T.; Nagata, N.; Hatanaka, A.; Naoshima, Y. *Agric. Biol. Chem.* **1980**, *44*, 437-438.
20. Mayer, F.; Takeoka, G.; Buttery, R.; Nam, Y.; Naim, M.; Bezman, Y.; Rabinowitch, H. In *Freshness and Shelf Life of Foods*, Cadwallader, K.R.; Weenen, H., Eds.; American Chemical Society, Washington, DC, 2002; ACS Symposium Series **836**, pp 144-161.
21. Mayer, F.; Takeoka, G.; Buttery, R.; Whitehand, L.; Bezman, Y.; Naim, M.; Rabinowitch, H. In *Food Science and Technology 131 (Handbook of Flavor Characterization)*; Deibler, K. D.; Delwiche, J., Eds.; Marcel Dekker: New York, 2004; pp 189-205.
22. Schieberle, P.; Buettner, A. In *Aroma Active Compounds in Foods: Chemistry and Sensory Properties*; Takeoka, G. R.; Güntert, M.; Engel, K. H., Eds.; American Chemical Society, Washington, DC, 2001; ACS Symposium Series **794**, pp 109-118.

Chapter 13

Maillard Volatile Generation from Reaction of Glucose with Dipeptides, Gly-Ser, and Ser-Gly

Chih-Ying Lu[1], Richard Payne[2], Zhigang Hao[2], and Chi-Tang Ho[1]

[1]Department of Food Science, Rutgers, The State University of New Jersey, 65 Dudley Road, New Brunswick, NJ 08901
[2]Colgate-Palmolive Company, 909 River Road, Piscataway, NJ 08855

Peptides abundant in food and protein hydrolysates are known to be important to both unprocessed and processed flavors. We studied the effect of peptide bond hydrolysis on the formation of Maillard volatile compounds. The Gly-Ser dipeptide bond was found to be the most labile among all the Gly-X dipeptides (X= Ala, Cys, Gln, Glu, Gly, His, Leu, Lys, Phe, Pro, Ser, Thr, Tyr and Val). However, Ser-Gly was found to be two to three times more stable than Gly-Ser. Volatiles formation was investigated using Gly-Ser and Ser-Gly as precursors in the reaction with glucose. Gly-Ser generated more volatiles than Ser-Gly which confirmed the positive correlation between peptide bond susceptibility and volatiles generation.

The thermal generation of aromas has long been a topic of interest in flavor research. An insight into the chemistry and mechanisms underlying the generation of these aromas in food systems has become a necessity for the development of high quality products for the food industry. Maillard reaction has traditionally been responsible for the generation of roasted, toasted, or caramel like aromas, as well as the development of brown colors in foods (1). The vast majority of the mechanistic chemistry of the Maillard reaction was determined by investigating the interactions of reducing sugars and free amino acids in simple systems. However, the chemical characteristics and reactivity of peptides have not been studied to an appreciable extent.

147

Peptide-carbonyl Reaction

Some works investigated various peptides in reaction with carbonyls to determine the reactivity of peptides or to understand the flavor profile. Mori et al. (*2*) investigated the reactivity of peptides reaction with glyceraldehydes by determining the disappearance of the peptides. They reported that Ala-His and Val-His had shown the same reactivity in the study; however, the reactivity of His-Ala (basic amino acid with the second neutral amino acid residue) was decreased by about 50% compared to that of Val-His in that study. The authors pointed out that the acidic/basic level and the position of the amino acid plays important roles in the reaction rate of the peptides. They also observed that the reduced reaction rate of two neutral amino acids, Val-Gly, are of similar extent to His-Ala. Where there is a presence of an acidic amino acid in the second residue, as in Ala-Asp, it is found to have very low reaction rate with glyceraldehyde. The pH range of 6.5-8.0 was found to be optimum for the dipeptide reactions in this study. The study further found that tripeptide, Gly-His-Gly or Gly-Ser-Ala, was 3-5 times more reactive than related dipeptides, when reacted with glyceraldehydes. They concluded that the positively charged amino acid at the second position of dipeptides, and especially tripeptides, increases the reaction rate, and the increased rate is not believed to correlate with the pKa of NH_2-terminus.

Rizzi (*3*) conducted the reaction of Val-Gly, Gly-Val, Leu-Gly and Gly-Leu, separately with fructose, at 120 °C for 30 min. He reported that the Gly-Val produced more alkylpyrazines than Val-Gly, and the Gly-Leu produced more alkylpyrazines than Leu-Gly. Where comparing reaction of fructose with Ala-Leu-Gly and Gly-Leu-Ala, results showed that Ala-Leu-Gly produced about 2 fold more alkylpyrazines than the other tripeptides.

Oh et al. (*4*) compared volatile formation from glycine, diglycine, triglycine and tetraglycine reactions with glucose in aqueous solution, at 180 °C for 2 h. They found that glycine and triglycine generated similar amounts of volatiles while diglycine was similar to tetraglycine. Larger amounts of pyrazines were generated by glycine and triglycine than by diglycine and tetraglycine. The study suggested that triglycine could be degraded into glycine through DKP, whereas tetraglycine was primarily cleaved into diglycine and it required extra energy to further break it down into glycine.

Oh et al. (*5*) also reported that Gly-Pro generated a larger amount of proline-specific Maillard volatile compounds, 5-acetyl-2,3-dihydro-1*H*-pyrrolizine and 5-formyl-2,3-dihydro-1*H*-pyrrolizine, than the Pro-Gly peptide at 130 °C, for 2 h, at pH 5.3-5.5. This study suggests that the primary amino group of Gly-Pro is more reactive in catalyzing glucose transformation and fragmentation than Pro-Gly. The formation of Schiff base of Gly-Pro with glucose, or its degradation, is faster than Pro-Gly with glucose. It was explained by these authors that the Schiff base form of Gly-Pro may promote the hydrolysis of dipeptide bonds due to the neutral charge at the N-terminal amino group; whereas the positive charge of the N-terminal amino group of the Schiff base of Pro-Gly retards peptide bond hydrolysis (*6*). The study stated that Schiff base

formation may precede and catalyze peptide bond hydrolysis. Larger amounts of leucine Strecker aldehydes were observed in Gly-Leu than Leu-Gly; the shift equilibrium towards Gly-Leu and susceptible hydrolysis of Gly-Leu were suggested to play important roles in this phenomenon (6).

Materials and Methods

Peptide Hydrolysis of Glycine Dipeptides

The hydrolysis susceptibility of fourteen Gly-X dipeptides was investigated; X= Ala, Cys, Gln, Glu, Gly, His, Leu, Lys, Phe, Pro, Ser, Thr, Tyr and Val. The hydrolysis of dipeptide Cys-Gly was also included in this experiment. Each dipeptide was dissolved in water and adjusted to pH 7.5 with NaOH. The final concentration of the solution was 0.006 M. The solution was then heated, without glucose, at 160 °C for 1 h. The susceptibility of dipeptide bonds was determined by the degree of glycine peptide hydrolysis, which was calculated as (number mol of glycine/number of dipeptide) x 100%. The amount of glycine (number mol of glycine) was determined by HPLC-Tandem-MS method by using external standards.

Degree of hydrolysis of Gly-Ser and Ser-Gly was determined by the amount of glycine in heated dipeptide solution (0.04 M), without glucose, at pH 7.5, with NaOH at 160 °C for 1 h at 10% water in glycerol medium and 100% water.

Instrumental Analysis of Heated Peptide Solutions

An aliquot (1 mL) of reaction product was dissolved into 200 mL of methanol/water (1:1, v/v) solution containing 0.5% formic acid (v/v) for HPLC-ESI-MSMS (high-performance liquid chromatography-electrospray ionization-tandem mass spectrometry) analysis. Briefly, a TSQ Quantum tandem mass spectrometer (Thermo-Finnigan, San Jose, CA) was equipped with an ESI interface and Agilent 1100 HPLC system (Agilent Technologies, Palo Alto, CA). HPLC separation was performed using a ThermoHypersil-Keystone Silica column (Agilent Technologies), 2.1 mm i.d. x 210 mm with a particle size of 5 μm, at room temperature. The reaction components were eluted using a mobile phase of 25% acetonitrile-water containing 0.5% formic acid (v/v/v). The flow rate was 0.75 mL/min. The TSQ Quantum was operated in the positive ion mode under the following conditions: (i) nitrogen (>99.7%) was used for the sheath gas and auxiliary gas at a pressure of 30 psi and 5 units, respectively; (ii) the temperature of the heated capillary was maintained at 350 °C; (iii) the spray voltage of ESI was set at 4.5 kV; (iv) a collision-induced dissociation was achieved using argon as the collision gas at a pressure adjusted to 0.8 mTorr above the normal; and (v) the applied collision offset energy was set to -45 eV. Identification of reaction component was accomplished by comparing the HPLC retention time and selected reactant monitoring (SRM) analysis of the sample peak

area with that of the authorized pure commercial compounds (external standards). The quantitative m/z from 76.1 (molecular ion) to 30.4 (responding major fragment ion) was set for glycine quantitation. Data were acquired with an Xcalibur software system (Thermo-Finnigan).

Maillard Reaction of Gly-Ser, Ser-Gly, and Gly+Ser Mixture with Glucose, Individually

Equimolar (0.0002 mol) amounts of dipeptides, Gly-Ser and Ser-Gly, and amino acids Gly + Ser (Sigma Chemical Co., St. Louis, MO) were heated, individually, with glucose in oil bath at temperature 160 °C, for 1 h, at 10% water content in glycerol medium (99.5% +, spectrophotometric grade, Sigma-Aldrich, Milwaukee, WI) and 100% aqueous solution. The total volume of solution in the reaction vial (Fisher Scientific, Pittsburgh, PA) was 5 mL. The concentration of the solution was, therefore, 0.04 M. 4-methylpyrimidine (50 µL) (Sigma Chemical Co.) was used as surrogate internal standard for semi-quantitation.

Instrumental Analysis of Volatile Reaction Products

Stir Bar Sorptive Extraction (SBSE)

An aliquot of the reaction product (1 mL) was transferred to the extraction vial. It was then diluted with 9 mL of phosphate buffer (pH 8 with 27% NaCl). In the dilution, the amount of glycerol, water, and buffer solution was kept constant at all extractions to eliminate a possible matrix effect on the extraction. The diluted samples were then extracted with a conditioned Gerstel stir bar [10 mm length x 0.5 mm of polydimethylsiloxane (PDMS) film thickness, Twister, Gerstel GmbH, Mulheim and der Ruhr, Germany] at room temperature, at 1100 rpm, for 1 h.

Thermal Desorption-Gas Chromatography (GC)-Mass Spectrometry (MS) Analysis

After extraction, the PDMS stir bar was removed from the sample solution using a nonmagnetic forcep, rinsed with Milli-Q purified water, dried with a kimwipe, and then placed in a glass thermal desorption tube. The analytes were thermally desorbed in the splitless mode using a Gerstel TDU system (Twister Desorption Unit) by programming from 40 to 280 °C at 40 °C /min and holding the final temperature for 7 min. The desorbed compounds were cryofocused in the CIS-3s PTV injector (cooled injection system, programmed temperature vaporization, Gerstel, Inc., Baltimore, MD) at -100 °C and programmed from -100 to 280 °C and held for 5 min at 12 °C /s to vaporize the trapped compounds in the injector. A Varian model 3800 gas chromatograph with a 30 m x 0.25 mm x 0.25 µm ZB-5ms column (Phenomenex, Torrance, CA) was used to separate

the compounds in the reaction products. Chromatographic grade helium (99.9999%) (BOC Gases, Murray Hill, NJ) was used as the carrier gas and was maintained at constant flow of 1 mL/min. Chromatographic separation was achieved using a temperature program with the following conditions: the initial temperature of 50 °C was held for 1 min and then ramped at 3 °C/min to a temperature of 209 °C. A final temperature of 280 °C was reached by ramping at 20 °C/min. A Saturn 2000 Ion Trap Detector (Varian Instruments, Walnut Creek, CA) was interfaced to the GC for detection of eluting compounds. Detector conditions applied were as follows: ion trap, manifold, and transfer lines were held at 120, 40, and 175 °C, respectively. The Detector scan range (in EI mode) was set from 40 to 450 Da and scan rate was five times per second.

Results and Discussion

Peptide Hydrolysis of Gly-X Dipeptide

The hydrolysis susceptibility of fourteen Gly-X dipeptides was investigated; X= Ala, Cys, Gln, Glu, Gly, His, Leu, Lys, Phe, Pro, Ser, Thr, Tyr and Val. The susceptibility of dipeptide bonds was determined by amount of glycine in the heated mixtures. The degree of hydrolysis was calculated as (number mol of glycine/ number mol of dipeptide) x 100%. Results are shown in Figure 1. The susceptibility of peptide bonds was similar among dipeptides investigated, except for Gly-Ser and Gly-Thr which shows 60% and 25% hydrolysis, respectively. Several studies reviewed by Hill (7) investigated the hydrolysis of peptide bond under extreme acidic solution, such as $10 N$ HCl at 30 °C. Studies showed that dipeptides containing serine or threonine were more labile than other dipeptides. The lability of the seryl and threonyl bond was proposed to be caused by the self-catalysis from the internal hydroxyl group through N-O acyl rearrangement (Figure 2) (7).
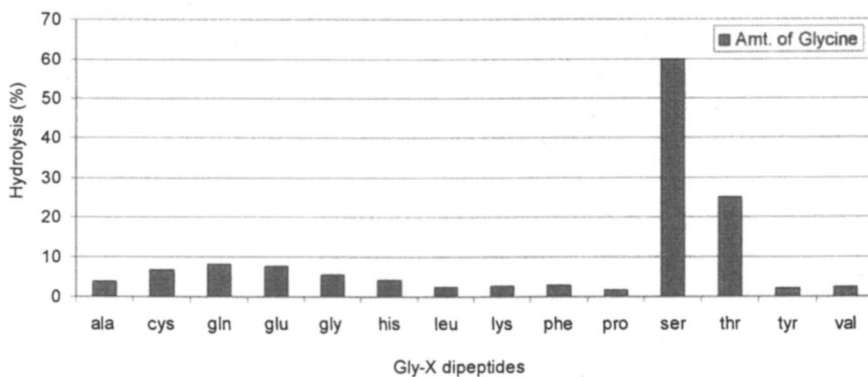
Figure 1. Degree of peptide hydrolysis of Gly-X dipeptides.
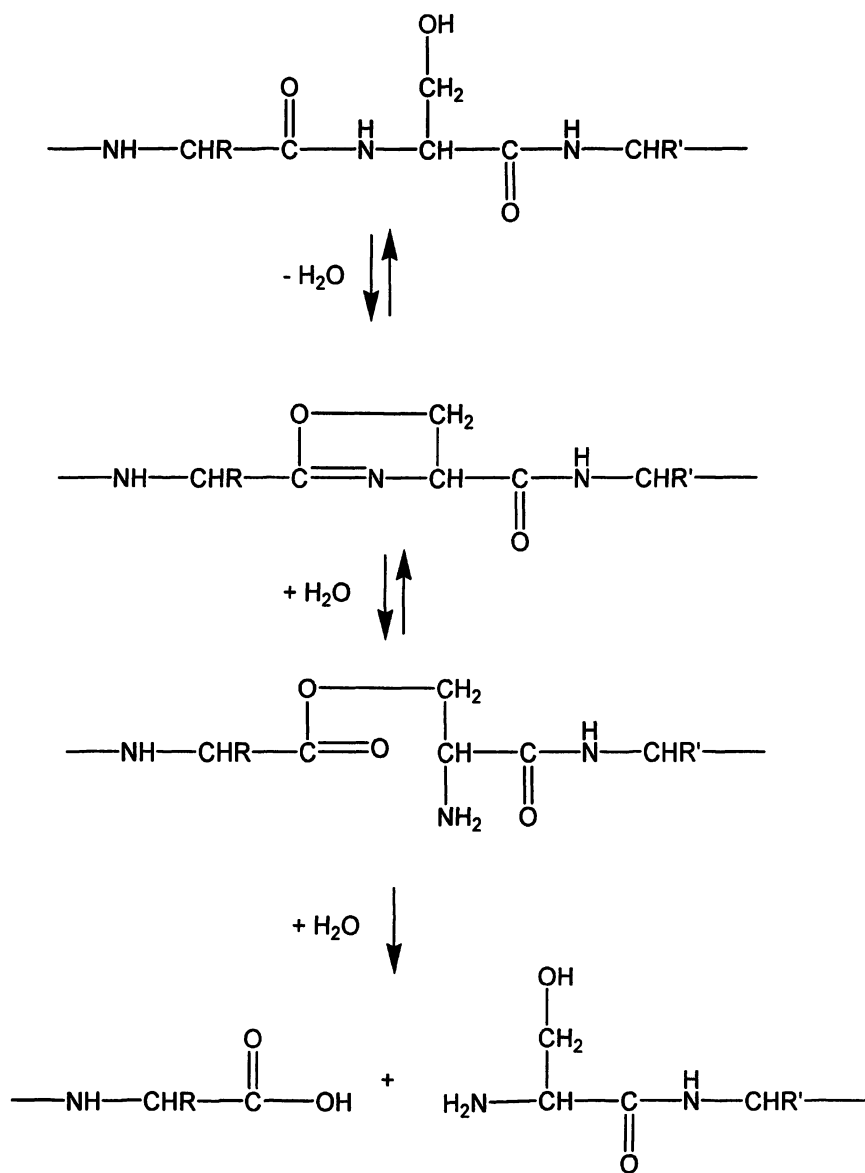
Figure 2. Proposed mechanism of seryl and threonyl peptide bond hydrolysis through N-O acyl migration (Modified from reference 7).

Peptide Hydrolysis of Gly-Ser and Ser-Gly Dipeptides and Their Volatile Formation

Because of the unusual hydrolysis behavior of serine-containing peptides, Gly-Ser and Ser-Gly were selected to study their peptide bond hydrolysis, as well as their relationship to the volatile formation in Maillard reactions.

Equimolar (0.0002 mol) amounts of dipeptides, Gly-Ser and Ser-Gly, and amino acids Gly + Ser were heated, individually, with glucose, in an oil bath at temperature 160 °C for 1 h at 10% water content in glycerol medium and 100% aqueous solution. The final concentration of the solution was 0.04 M. Degree of hydrolysis of Gly-Ser and Ser-Gly was determined by the amount of glycine formed in heated dipeptide solution (0.04 M), without glucose at 160 °C for 1 h at 10% and 100% water content.

Figure 3 shows the amount of glycine formed from heated Gly-Ser and Ser-Gly dipeptides, without glucose, at 10% and 100% water content. Gly-Ser evidently was two to three times more susceptible to cleavage than Ser-Gly under the same water content. This phenomenon was also reported in Yashiro et al. (8) in which they investigated the hydrolysis of Gly-Ser and Ser-Gly dipeptides with metal in buffer solution at pH 7, 70 °C, 24 h. The degree of hydrolysis of dipeptides was determined by the formation of their corresponding amino acids. They found a marked difference in hydrolysis of Gly-Ser and Ser-Gly and suggested that the hydroxyl group of Ser can intramolecularly attack the amide carbonyl carbon in Gly-Ser then undergo N-O acyl rearrangement but not in Ser-Gly due to the unfavorable four-membered ring transition state (Figure 4) (8). The hydrolysis degree of Gly-Ser and Ser-Gly with metal was 83% and 4%, respectively; without metal, 6% and 0%, respectively (8). The heating condition, e.g., 160 °C, for 1 h used in our study led to a significant increase in the degree of hydrolysis of these two dipeptides.

Results of volatile formation from Gly-Ser, Ser-Gly, and Gly + Ser reaction with glucose are reported in Table I. Results showed that the reaction of amino acids Gly and Ser with glucose generated the most volatiles in our model system when compared with dipeptides. Gly-Ser generated more pyrazines than Ser-Gly, particularly trimethylpyrazine. Ser-Gly generated more furans, which were formed from sugar degradation, than Gly-Ser and Gly+ Ser. This study indicated again that the susceptibility of a dipeptide bond correlates to the formation of sugar-amino reaction volatiles; in other words, the easiness of the peptide bond cleavage facilitates volatile generation.

References

1. Nursten, H. *The Maillard Reaction: Chemistry, Biochemistry and Implications*. The Royal Society of Chemistry, Cambridge, UK, 2005.
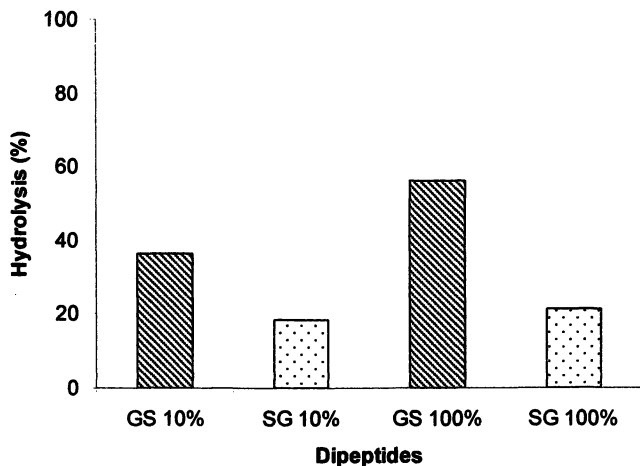
Figure 3. The hydrolysis degree of gly-ser (GS) and ser-gly (SG) by determination of glycine formation at 160 °C for 1 h, 10% and 100% water content at pH 7.5 without glucose. (Reproduced with permission from J. Sep. Sci. **2002**, 25, Figure 3, 153. Copyright 2002 Wiley VCH-STM.)
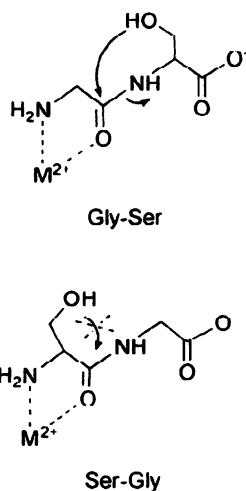
Gly-Ser

Ser-Gly

Figure 4. A comparison of hydroxyl group attack in Gly-Ser and Ser-Gly (8).

Table I. Volatile Compounds Formed from Gly-Ser, Ser-Gly, Gly+Ser Reaction with Glucose under 10% and 100% Water at 160 °C for 1 hr Heating

Compound	Amount, mg/mol					
	Gly-Ser 10%	Ser-Gly 10%	Gly+Ser 10%	Gly-Ser 100%	Ser-Gly 100%	Gly+Ser 100%
Pyrazine	811	471	885	125	12	284
1-methyl-1H-pyrrole	142	70	155	0	1	37
Pyridine	21	36	29	11	7	20
4,5-dimethyloxazole	32	16	41	1	0	2
3,5-dimethylisooxazole	11	0	10	0	0	11
Cyclopentanone	0	3	8	0	0	0
Dihydro-2-methyl-3(2H)furanone	0	0	0	0	0	4
Methylpyrazine	1555	1127	2051	103	11	172
Furfural	52	148	38	79	112	87
2,5-dimethyl-1H-pyrrole	254	128	251	0	167	0
2-Furanmethanol	22	18	24	8	8	13
2,6-dimethylpyridine	47	46	73	63	42	67
2-ethylpyridine	13	5	24	1	0	1
2,5-dimethylpyrazine	1561	817	3635	369	45	511
2-ethylpyrazine	1801	1100	1961	21	3	47
2,3-dimethylpyrazine	646	389	1402	23	1	62
2,4-dimethylpyridine	328	34	529	3	3	8
2,3-dimethylpyridine	0	1	25	0	0	1
5-methylfurfural	59	153	36	27	34	26
2-ethyl-5-methylpyrazine	632	377	1159	132	17	253

Continued on next page.

Table I. Continued.

Compound	Amount, mg/mol					
	Gly-Ser 10%	Ser-Gly 10%	Gly+Ser 10%	Gly-Ser 100%	Ser-Gly 100%	Gly+Ser 100%
Trimethylpyrazine	899	350	3853	298	14	692
2-ethyl-3-methylpyrazine	341	209	717	132	17	240
2-propylpyrazine	44	19	63	0	0	0
2-vinyl-6-methylpyrazine	244	103	264	24	2	45
Isopropenylpyrazine	111	46	181	13	1	20
2-acetylpyridine	10	0	36	2	0	4
1-ethyl-1H-pyrrole-2-carboxaldehyde	6	3	5	0	0	0
2,3,6-trimethylpyridine	46	2	87	0	0	0
2-acetylpyrrole	71	25	65	8	2	14
1-methyl-2-acetylpyrrole	127	53	396	1	0	4
2,6-diethylpyrazine	371	141	1292	14	1	36
2-ethyl-2,5-dimethylpyrazine	207	96	725	21	1	81
2,3-dimethyl-5-ethylpyrazine	374	178	1398	42	2	150
2,5-diethylpyrazine	328	161	1309	36	1	132
2-methyl-5-(1-propenyl)pyrazine	274	62	433	109	6	162
2,3-diethyl-5-methylpyrazine	11	2	52	0	0	0
3,5-diethyl-2-methylpyrazine	53	16	364	4	0	18
2,3-dimethyl-5-(1-propenyl)pyrazine	56	11	104	12	0	31
1-(2-furanylmethyl)-1H-pyrrole	24	17	11	2	0	1

2. Mori, N.; Bai, Y.; Ueno, H.; Manning, J. *Carbohydr. Res.* **1989**, *189*, 49-63.

3. Rizzi, G. P. In *Thermal Generation of Aromas*; Parliment, T. H.; McGorrin, R. J.; Ho, C.-T., Eds.; ACS Symp. Ser. 409; American Chemical Society: Washington, DC, **1989**, pp 285-301.

4. Oh, Y. C.; Shu, C. K.; Ho, C.-T. *J. Agric. Food Chem.* **1991**, *39*, 1553-1554.

5. Oh, Y. C.; Hartman, T. G.; Ho, C.-T. *J. Agric. Food Chem.* **1992**, *40*, 1878-1880.

6. Oh, Y .C.; Shu, C. K.; Ho, C.-T. *J. Agric. Food Chem.* **1992**, *40*, 118-121.

7. Hill, R. L. *Adv. Protein Chem.* **1965**, *20*, 37-107.

8. Yashiro, M.; Yoko, S.; Yamamura, A.; Takarada, T.; Komiyama, M.; Fujii, Y. *Org. Biomol. Chem.* **2003**, *1*, 629-632.

Chapter 14

The role of (5*E*)-2,6-Dimethyl-5,7-octadiene-2,3-diol as Aroma Precursor in Badea (*Passiflora quadrangularis* L.) Fruit

Coralia Osorio and Carmenza Duque

Departamento de Química, Universidad Nacional de Colombia,
AA 14490 Bogotá, Colombia

Model reactions at pH 3.2 were used to study the acid-catalyzed transformation of the monoterpenediol (5*E*)-2,6-dimethyl-5,7-octadiene-2,3-diol (one of the major constituents of *Passiflora quadrangularis* fruit flavour) into the isomeric *cis*- and *trans*-4-hydroxylinalool 3,6-oxides. The chemical structure of these new monoterpenoid oxides was elucidated by using GC-MS and ^{1}H- and ^{13}C-NMR. Total conversion of the diol was obtained after 40 days, in yields of 28.5 and 71.5%, respectively. Additionally, it was confirmed that the amount of the monoterpenoid oxides is increased when *P. quadrangularis* fruit is heated.

Tropical fruit and their products have entered the worldwide market because they are considered healthy products exhibiting novel sensory properties, high nutritional value, and antioxidant properties. Colombia is one of the five major tropical fruit-producing countries, with a high production which is consumed internally and also exported. The exports of fresh fruit during 2004 was 62% higher than 2000, the major products being cape gooseberry (*Physalis peruviana*), baby banana (*Musa paradisiaca)*, passion fruit (*Passiflora edulis*),

© 2008 American Chemical Society

and other Passifloraceaes. The Passifloraceaes are considered as promising fruits due to their exotic aroma.

Passiflora quadrangularis, commonly named as *badea*, *corvejo*, *parcha granadilla*, or giant granadilla, is a vigorous tropical vine with large bright-green oval leaves and flowers typical of Passifloraceae family. Fruits are oblong, reach a length of up to 12 inches and turn yellow when mature. The colorless and slightly acid pulp around the numerous seeds is used to make ice cream and different kinds of soft drinks. The fully ripe flesh is eaten alone or in combination with such fruits as papaya and pineapple; however it is also used to prepare candies, jellies, and pastries. The green fruit is boiled and eaten as a vegetable.

The aroma of *Passiflora quadrangularis* fruit was previously studied by us finding the monoterpenediol (5*E*)-2,6-dimethyl-5,7-octadiene-2,3-diol [1] as the major constituent (*1, 2*). However, qualitative and quantitative differences in the composition of volatiles, when using liquid-liquid extraction and SDE were observed; most significant was the disappearance of diol **1** after thermal treatment under acidic conditions. Thus, the purpose of this work was to study the transformation of diol **1** and to confirm its role as aroma precursor in this fruit.

Experimental Procedures

Plant Material

Passiflora quadrangularis L. (Passifloraceae) fruits, grown in Carimagua (Meta, Colombia) were purchased from a local market. Fully ripe fruits were selected according to the pulp pH value (3.2), 13.2 °Brix, and fruit peeling color (yellowish green).

Sample preparation

As preliminary assay, the volatile compounds of *P. quadrangularis* fruit pulp (500 g) were isolated by two different procedures. These were continuous liquid-liquid extraction with pentane-dichloromethane (1:1, *v/v*) and Simultaneous Steam Distillation-Extraction (SDE) at atmospheric pressure in a modified Likens-Nikerson apparatus using pentane-ether (1:1, *v/v*, 2h) (*3*). Each aroma extract was dried over Na_2SO_4, concentrated by using a Vigreux column, and analyzed by GC and GC-MS.

In order to obtain a high amount of diol **1**, 6 kg of fruit pulp (46 kg of fruit) was blended and the homogenate was centrifuged (10000 *g*, 8 °C) for 45 min to obtain a clear juice which was extracted with pentane-dichloromethane (1:1, *v/v*)

in a continuous liquid-liquid extractor (105 x 45 cm) for 36 h. The organic phase was dried over anhydrous sodium sulphate and concentrated using a Vigreux column (40°C) to 0.2 mL. The volatile-enriched extract was fractionated over silica gel using a discontinuous gradient of pentane-ethyl ether (9:1 → 1:2). The more polar fraction was further fractionated by chromatography over silica gel using hexane-EtOAc (7:1 → 4:1) as eluent to yield 6 mg of diol **1**, whose purity and identity were assessed by GC-MS analyses.

A solution of 3 mg of the diol **1** was kept at pH 3.2 and 18 °C until total conversion of diol **1** into compounds **2** and **3**. The mixture of compounds **2** and **3** was extracted with EtOAc, purified by preparative TLC over silica (hexane-EtOAc, 3:1), and submitted to spectroscopic analyses (GC-MS and ¹H- and ¹³C-NMR) in order to determine their chemical structures.

Instrumental Analysis

Nuclear Magnetic Resonance (NMR) spectra were taken on a Bruker Avance DRX500 spectrometer in $CDCl_3$ with tetramethyl silane as internal standard.

Each volatile extract was analyzed by using a HP 5890 series II gas chromatograph, operated in split mode (1:10, injected volume, 1 μL), and equipped with a flame ionization detector. A DB-Wax fused silica column (30 m x 0.25 mm i.d., 0.25 μm film thickness) was used. The column oven was programmed from 50 (4 min isothermal) to 220 °C at 4 °C/min and the final temperature was held for 20 min. The injector temperature was maintained at 250 °C. Helium carrier gas was used at a flow rate of 1.0 mL/min. Nitrogen make up gas was used at 30 mL/min. GC-EIMS analyses were carried out on a Hewlett Packard 5970 mass selective detector directly coupled to a HP 5890 gas chromatograph. The same types of column and temperature conditions as mentioned above for GC analysis were used. MS-data were recorded in a 30—350 u mass range, with electron energy of 70 eV and processed by HP5970 MS-Chemstation software.

Spectroscopic Data

IE-MS and ¹³C NMR data of compounds **1**, **2** and **3** were published elsewhere (*1, 2*). ¹H-NMR data of **1, 2,** and **3** are presented in Table I.

Model Reactions

To study the role of diol **1** as precursor of compounds **2** and **3** under acidic conditions, a solution of 3 mg of the diol in 1 mL of citrate-phosphate buffer

(100 mM, pH 3.2) was prepared and divided into three portions. One of these was heated at 100 °C, another was placed under an air stream, and the third was kept at room temperature (18 °C) during 24 hours. The volatile compounds generated in each experiment were extracted with ethyl acetate and analyzed by GC and GC-MS. In all cases the percentage conversion of diol **1** into *cis*-4-hydroxylinalool 3,6-oxide [**2**] and *trans*-4-hydroxylinalool 3,6-oxide [**3**] was determined from their relative areas in the GC profile.

Results and Discussion

The strong aroma of *P. quadrangularis* fruit was described as aqueous, fruity and very sweet. In our earlier work, GC and GC-MS analyses of the volatile extract obtained by continuous liquid-liquid extraction showed that this fruit possesses high contents of organic acids, oxygenated monoterpenoids, and aliphatic alcohols (*2*). However, when the volatile compounds were obtained by SDE of the fruit at native pH (3.2), significant differences in comparison with liquid-liquid extraction were detected (Figure 1). Thus, by liquid-liquid extraction (*5E*)-2,6-dimethyl-5,7-octadiene-2,3-diol [**1**], (*2E*)-2,6-dimethyl-2,5-heptadienoic acid [**7**], benzoic acid [**8**], furaneol [**6**], benzyl alcohol [**5**], and 2,6-dimethyl-5-hepten-1-ol [**4**] were identified as major components. In contrast, by effect of heating during SDE, (*5E*)-2,6-dimethyl-5,7-octadiene-2,3-diol [**1**], benzyl alcohol [**5**], benzoic acid [**8**], and furaneol [**6**] were not detected, and the amount of compounds **2** and **3**, as well as, β-ocimene [**9**] and ethylene glycol [**10**] was increased.

Based on the above results, the not so easy work of purifiying the volatile and acid-sensitive diol **1** was performed by column chromatography. This compound was kept at pH 3.2 whereby two isomeric compounds [**2** and **3**] were obtained as transformation products.

EI-MS spectra of compound **2** and **3** resemble each other, thus indicating their isomeric nature. A mixture of these compounds were analyzed by ^{1}H- and ^{13}C-NMR. In the ^{1}H-NMR spectra of compound **3** (the major degradation product of diol **1**) the presence of a 2-hydroxypropyl group, one methylene with diasterotopic protons, two oxymethines, and one vinyl group was evident (Table I). Minor signals belonging to compound **2** could also be identified in this spectrum, showing a similar multiplet pattern and slighlty different chemical shifts to those exhibited by compound **3**.

The ^{1}H- and ^{13}C-NMR spectral data provided evidence that the chemical structure of compounds **2** and **3** is related to that of diol **1**. However, the comparison between NMR data of these two compounds indicated absence of one olefinic system and presence of one additional hydroxyl group in the structure of **3**. With the aid of HMQC and HMBC experiments, the structure of
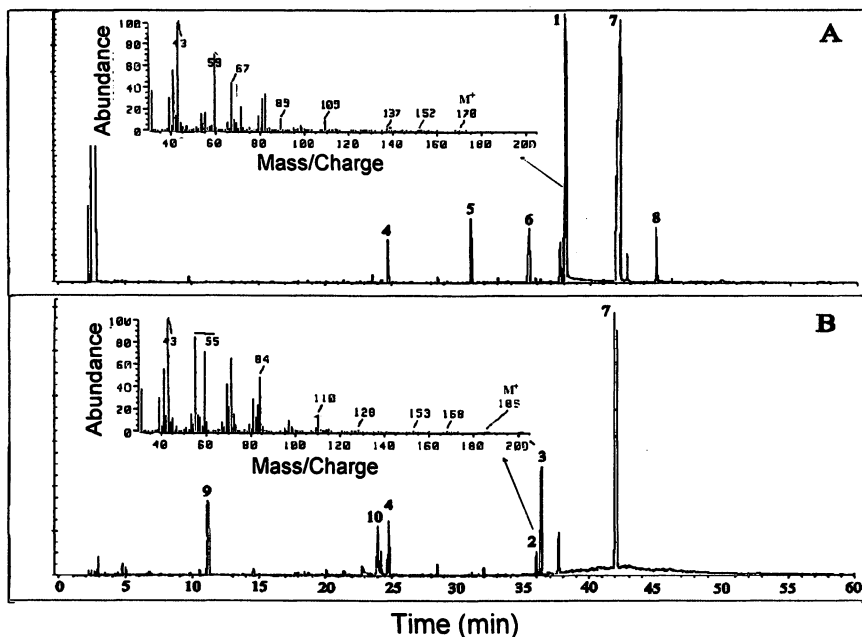
Figure 1. GC chromatograms of volatiles obtained from badea fruit by liquid-liquid extraction (A) and SDE (B) at pH 3.2.

compound **3** was concluded to be *trans*-4-hydroxylinalool 3,6-oxide, and all of its NMR signals were assigned, as was published elsewhere (*2*). The *trans*-configuration was confirmed by NOESY experiment where non-correlation between methyl group at 1.33 ppm and oxymethine proton at 3.87 was observed. Furthermore, H-2 and H-6 proton signals of compound **2** appear at lower field than those showed in the ¹H-NMR spectrum of *trans*-isomer **3**, thus confirming *cis*-geometry of compound **2** (*4*). To the best of our knowledge, this is the first time that *trans*-4-hydroxylinalool 3,6-oxide and *cis*-4-hydroxylinalool 3,6-oxide are reported from natural sources.

To investigate the role of (*5E*)-2,6-dimethyl-5,7-octadiene-2,3-diol [**1**] as precursor of compounds **2** and **3**, three model reactions catalyzed by acid were carried out: one at 18 °C, another at 100 °C, and the third in the presence of oxygen from air. Figure 2 shows the contribution of diol **1** and the isomeric 4-hydroxylinalool 3,6-oxides [**2** and **3**] to the overall mixture of volatiles formed during these model experiments after 2 and 24 hours. In all cases, volatile compounds were extracted and analyzed by GC-MS.

Table I. ¹H-NMR Data of Oxygenated Monoterpenoids 1, 2, and 3

H	1^a	2^b	3^b
1	1.21 (s)	5.16 (dd, 10.9, 1.3)	5.06 (dd,10.7, 1.5)
		5.34 (dd, 17.3, 1.3)	5.26 (dd, 17.2, 1.5)
2	-	*	5.82 (dd, 17.2, 10.2)
3	3.47 (dd, 9.5, 3.4)	-	-
4	2.29-2.35 (m)	*	3.85 (m)
5	5.59 (t, 7.3)	1.80 (m)	1.90 (dd, 14.5, 3.0)
		2.37 (m)	2.29 (m)
6	-	3.92 (dd, 9.7, 3.5)	3.87 (dd, 9.7, 3.2)
7	6.41 (dd, 17.3, 10.7)	-	-
8	4.99 (d, 10.7)	*	1.39 (s)
	5.14 (d, 17.3)		
9	1.25 (s)	1.14 (s)	1.17 (s)
10	1.78 (s)	1.32 (s)	1.33 (s)

[a] CDCl₃, 400 MHz, data from reference 1; [b] CDCl₃, 500 MHz, data from reference 2;
* obscured signals by overlapping.
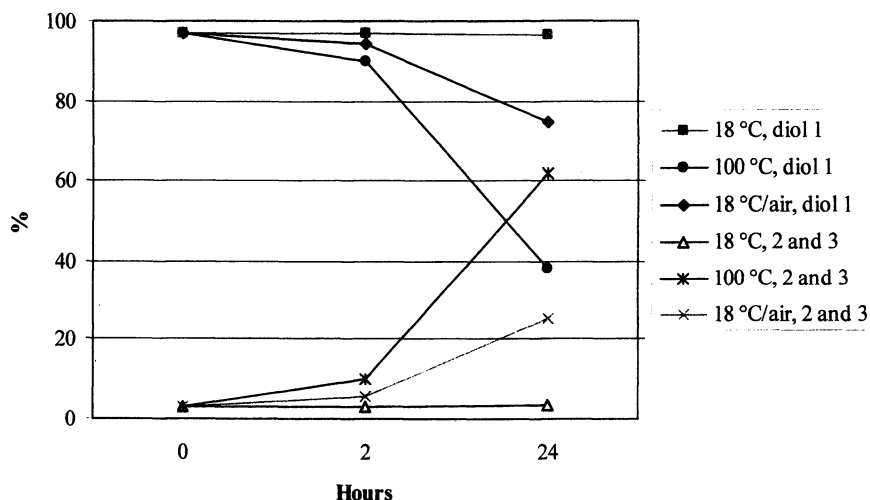
Figure 2. Acid-catalyzed (pH 3.2) model reactions of diol 1.

When diol **1** is submitted to acidic conditions (pH 3.2), its transformation into compounds **2** and **3** is activated, obtaining a total conversion after 40 days at a ratio of 28.5/71.5, respectively. However, if this reaction is performed at 100 °C the conversion percentage after one day (61.8%) is higher in comparison to that obtained at room temperature (3.5%), thus indicating that temperature accelerates the course of the reaction. It is important to point out that the thermal acid-catalyzed treatment increases the amount of the *cis*-4-hydroxylinalool-3,6-oxide isomer in comparison with the reaction placed at room temperature (compounds **2** and **3** ratio: 15.9/45.9 -vs- 0.2/3.3, respectively). Additionally, the presence of oxygen also catalyzes the transformation of diol **1** into isomers **2** and **3** (conversion percentage after one day: 25.5%).

Based on these results it is possible to assure that the (5*E*)-2,6-dimethyl-5,7-octadiene-2,3-diol **[1]** isolated from badea fruit is the precursor of *cis*- **[2]** and *trans*-4-hydroxylinalool 3,6-oxides **[3]** by the influence of acid pH. The proposed pathway for this reaction is shown in Figure 3. Double bond of diol **1** is oxidized to produce 2,6-dimethyl-oct-7-ene-2,3,5,6-tetraol (this compound has not yet been detected in *P. quadrangularis*) which is subsequently dehydrated by a nucleophilic substitution mechanism to produce the isomeric 4-hydroxylinalool 3,6-oxides **[2 and 3]**, involving a five-membered ring formation.
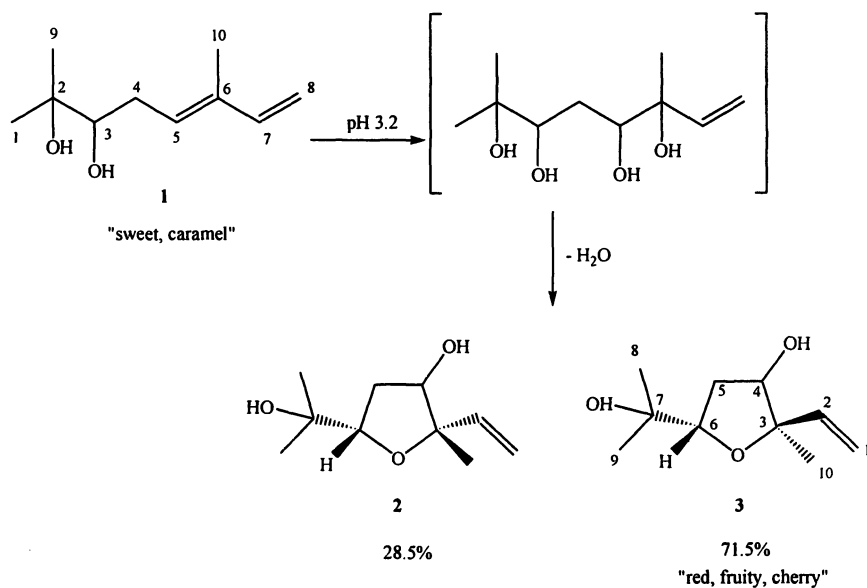
Figure 3. Chemical transformation of (5E)-2,6-dimethyl-5,7-octadiene-2,3-diol 1 into cis- 2 and trans-4-hydroxylinalool 3,6-oxides 3. (Reproduced from reference 2. Copyright 2002 Wiley-VCH.)

With this information in hand, our preliminary results were checked and it was found that the new monoterpenoids **2** and **3** had been detected as minor constituents of badea fruit aroma contributing with a fruity, red, cherry-like, pleasant odor note.

The role of terpene polyols in the generation of volatile monoterpenes was studied during the 80's in grape, papaya and passion fruit, confirming the fact that not only glycosides but also polyols must be considered in any analysis of hydrolytically generated flavor (*5*). Williams *et. al.* (*6*) examined the thermal induction of monoterpenes in Muscat grape (*Vitis vinifera*) juice finding that 3,7-dimethyloct-1-ene-3,6,7-triol was rearranged rapidly at pH 3.2 to give exclusively the furan linalool oxides, with a higher amount of *trans* isomer. This result is in agreement with those obtained in passion fruit (*Passifloraceae*) at pH 3.0 (*7*) and also with this work, thus supporting the proposed pathway presented in Figure 3. In contrast, Winterhalter *et al.* (*8*) did not detect the formation of pyranoid or furanoid linalool oxides from 3,7-dimethyloct-1-ene-3,6,7-triol in model experiments carried out at natural pH of papaya fruit (pH 5.6). This is evidence that generation of linalool oxides from polyols is strongly influenced by the native pH of fruits.

Conclusion

This work illustrates the role of (*5E*)-2,6-dimethyl-5,7-octadiene-2,3-diol as aroma precursor of *cis*- and *trans*-4-hydroxylinalool 3,6-oxides in *Passiflora quadrangularis* fruit. This reaction is spontaneously activated by cell disruption at natural pH of the fruit and is also favored by heating and oxygen. It is expected that this transformation takes place during the processing (pasteurization, concentration, storage) of badea fruit to obtain food products, and could have influence on the total aroma. The odor note of *trans*-4-hydroxylinalool oxide is quite different from that showed by (*5E*)-2,6-dimethyl-5,7-octadiene-2,3-diol. However, to predict their contribution to the total aroma of the fruit, further analyses such as the determination of odor activity values and sensory experiments need to be done.

Acknowledgements

References

1. Osorio, C.; Duque, C.; Fujimoto, Y. *Phytochemistry* **2000**, *53*, 97-101.
2. Osorio, C.; Duque, C.; Suárez, M.; Salamanca, L. E.; Urueña, F. *J. Sep. Sci.* **2002**, *25*, 147-154.
3. Schultz, T. H.; Flath, R. A.; Mon, T. R.; Eggling, S. B.; Teranishi, R. *J. Agric. Food Chem.* **1977**, *25*, 446-449.
4. Moon, J-H.; Watanabe, N.; Sakata, K.; Yagi, A.; Ina, K.; Luo, S. *Biosci. Biotech. Biochem.*, **1994**, *58*, 1742-1744.
5. Williams, P. J. In: *Flavor Science, Sensible Principles and Techniques*; Acree, T. E.; Teranishi, R., Eds.; American Chemical Society: Washington, DC, 1993; p. 289.
6. Williams, P. J.; Strauss, C. R.; Wilson, B. *J. Agric. Food Chem.* **1980**, *28*, 766-771.
7. Engel, K-H.; Tressl, R. *J. Agric. Food Chem.*, **1983**, *31*, 998-1002.
8. Winterhalter, P.; Katzenberger, D.; Schreier, P. *Phytochemistry* **1986**, *25*, 1347-1350.

Chapter 15

Genes and Enzymes Involved in Strawberry Flavor Formation

W. Schwab[1], S. Lunkenbein[1], D. Klein[1], E. M. J. Salentijn[2], T. Raab[3], and J. Muñoz-Blanco[4]

[1]Biomolecular Food Technology, Technical University Muenchen, 85354 Freising, Germany
[2]Plant Research International, Business Unit Genetics and Breeding, 6700 AA, Wageningen, Netherlands
[3]Chair of Food Chemistry, University Würzburg, 97074 Würzburg, Germany
[4]Departamento de Bioquímica y Biología, Campus Universitario de Rabanales, Universidad de Córdoba, 14071 Cordoba, Spain

Strawberry (*Fragaria x ananassa*) aroma consists of a blend of hundreds of components but only a handful are considered as key flavor compounds. The most important is 4-hydroxy-2,5-dimethyl-3(2*H*)-furanone (HDMF) but during the ripening process it is metabolized further by FaOMT (*Fragaria x ananassa* O-methyltransferase) to 2,5-dimethyl-4-methoxy-3(2*H*)-furanone (DMMF). We have discovered the first enzyme involved in the biosynthesis of HDMF in strawberries. The protein was partially purified and peptide sequence analyses of the digested protein showed total identity with the corresponding sequences of a strongly ripening induced, auxin-dependent putative quinone oxidoreductase (FaQR). The recombinant FaQR protein, expressed in *E. coli* catalyzed the formation of HDMF from a novel metabolite. In addition, we showed that *Agrobacterium*-mediated transformation of strawberry with the *Fragaria x ananassa* O-methyltransferase (*FaOMT*) gene in sense and antisense orientation, under the

© 2008 American Chemical Society 167

control of a constitutive promoter resulted in a nearly complete loss of DMMF. The levels of the other volatiles remained unchanged. For the first time strawberry flavor has been successfully modified by genetic engineering.

Strawberry (*Fragaria ananassa* Duch) is cultivated almost worldwide and constitutes a highly appreciated food crop due to its nutritional value and attractive flavor (*1*). Strawberry flavor is extremely popular as part of the fruit or as an added flavoring in many manufactured foodstuffs (*1*). The volatile components of strawberry fruits formed during ripening have been intensively studied, and more than 360 volatiles have been identified (*2, 3*). By application of the aroma value concept 4-hydroxy-2,5-dimethyl-3(2H)-furanone (HDMF, Furaneol®) was identified as the most important volatile because of its high concentration (up to 55 mg kg^{-1} strawberry fruit fresh weight) (*4*) and low odor threshold (10 ppb) (*5*). Already in 1963, HDMF was characterized as a product of the Maillard reaction (*6*), and it was then isolated from a number of different fruits like pineapples, strawberries, and mangoes (*5*). HDMF is frequently accompanied by its methyl ester 2,5-dimethyl-4-methoxy-3(2H)-furanone (DMMF, methoxyfuraneol). DMMF was first detected in pineapples but meanwhile it was also identified in a multitude of fruits such as overripe strawberries, mango fruits and arctic bramble (*5, 7*). Although the composition of the strawberry volatiles has been intensively studied, few detailed biochemical and genetic studies have been performed in relation to their biosynthesis. Only recently it was shown that the *FaOMT* (*Fragaria x ananassa* O-methyltransferase) gene encodes for an O-methyltransferase responsible for DMMF biosynthesis (*8, 9*). Studies demonstrating the correlation of strawberry fruit ripening stage and HDMF concentration provided the first evidence for the biochemical formation of HDMF in fruits (*10*). Radiotracer experiments pointed to D-fructose-1,6-diphosphate as a significant precursor of HDMF because after the application of 15 different water-soluble, radioactively labeled substances, D-[U-^{14}C]-fructose–1,6-diphosphate showed the highest incorporation rate into the furanone structures (*11*). Additional experiments performed to identify intermediates in the biogenetic pathway from D-fructose-1,6-diphosphate to HDMF remained unsuccessful but all studies indicate that HDMF is derived from carbohydrate metabolism.

Here, we describe the isolation and characterization of a protein involved in the biosynthesis of HDMF, one of the key aroma compounds in strawberry fruits. Sequence information of the isolated enzyme led to the cloning and characterization of the fruit ripening induced FaQR gene. The corresponding protein was expressed in *E. coli* and on the basis of the observed reaction catalyzed by the FaQR protein, an unknown intermediate of the HDMF biosynthetic pathway was identified in strawberry as the natural substrate for the

novel enzyme. In addition, we show that transformation of strawberry with the *FaOMT* gene in antisense orientation, under the control of the CaMV 35S promoter resulted in a near total loss of DMMF, proving the significance of FaOMT in the biosynthesis of DMMF. This paper reviews previously published work (*14, 19*)

Fragaria x ananassa Quinone Oxidoreductase (FaQR)

Polyvinylpolypyrrolidone was added to strawberry fruits to adsorb polyphenols. Crude protein extracts were prepared by homogenizing the fruits and adsorbant with water followed by pH adjustment to 7.0. HDMF already formed by the fruits was removed by dialysis against a phosphate buffer solution (pH 7.0). Mixtures consisting of the dialyzed crude strawberry protein extract, D-fructose-1,6-diphosphate as HDMF precursor and the reducing agent NADH were used for enzyme activity tests. After 24 hours of incubation, a single compound was detected by LC-UV and LC-DAD-MS/MS. The product showed the same retention time, UV-spectrum and mass and product ion spectrum as commercially available HDMF (Aldrich, USA) (Fig. 1). HDMF was only formed in incubation experiments after addition of NADH. Small amounts of HDMF formed when D-fructose-1,6-diphosphate was incubated with NADH in a buffer solution, indicating a chemical side reaction (*12*). Formation of enantiomerically enriched HDMF provided clear evidence for an enzymatically catalyzed reaction (*13*). Experimental details are provided in (*14*).

Enzyme Characterization and Purification

The HDMF-forming enzymatic activity showed a temperature optimum of 37°C and a broad pH optimum peaking at pH 7.0. The kinetics were dependent on the concentrations of D-fructose-1,6-diphosphate as well as NADH. The apparent Michaelis-Menten constant, K_m, was determined graphically from double reciprocal plots. Values of 3.5 mM for D-fructose-1,6-diphosphate and 30 µM for NADH were obtained. The K_m value for NADH is in the expected order of magnitude but the value for D-fructose-1,6-diphosphate is high for an enzymatically catalyzed reaction. Therefore, due to the long incubation periods and high K_m value we assumed that D-fructose-1,6-diphosphate is not the primary substrate of the isolated enzyme. D-fructose-1,6-diphosphate probably first forms an intermediate in a rate limiting process that is then enzymatically transformed by an oxidoreductase.

The protein was purified by employing ultrafiltration membranes (Millipore, USA) with defined exclusion limits of 10, 30, 50 and 100 kDa. The majority of the activity (79% of total) was recovered in the molecular weight fraction

between 30 and 50 kDa. Further purification steps were accomplished using gel permeation chromatography on Sephacryl S300 (GE Healthcare, USA) as well as ion exchange chromatography on Q-Sepharose FF. SDS-PAGE analyses showed that the presence of a single protein band with a molecular weight of approximately 37 kDa correlated with the observed distribution of activity. The 37 kDa protein band was excised, digested and sequenced by automated Edman degradation. Details have been published in (*14*).
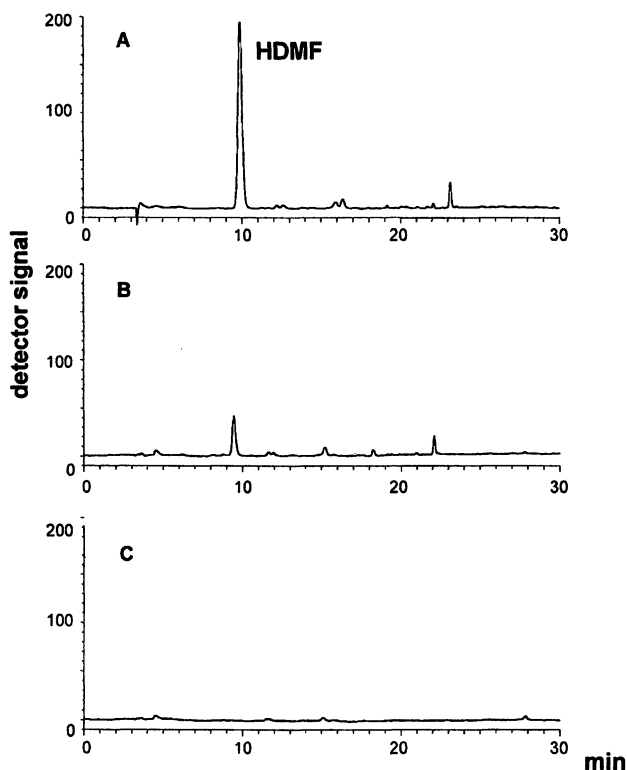
Figure 1. LC-UV analysis of products formed by incubation of strawberry protein extract with D-fructose-1,6-diphosphate and NADH (A), by incubation of D-fructose-1,6-diphosphate with NADH (B) and by incubation of strawberry protein extract with D-fructose-1,6-diphosphate (C).

The sequences of two peptides showed total identity with the corresponding protein sequence (Fig. 2) of a strongly ripening induced putative *Fragaria x ananassa* quinone oxidoreductase (*FaQR*) gene. The corresponding cDNA had been recently isolated from ripe strawberry fruits (GenBank[TM] accession number: AY048861).

```
                    Fragment 2
                    ──────────►
1       MAA APSES IP   SVNKAWVYSE   YGKTSDVLKF   DPSVAVPEIK   EDQVLIKVVA

51      ASLNPVDFKR   ALGYFKDTDS   PLPTIPGYDV   AGVVVKVGSQ   VTKFKVGDEV

101     YGDLNETALV   NPTRFGSLAE   YTAAYERVLA   HKPKNLSFIE   AASLPLAIET

151     AHEGLERAEL   SAGKSVLVLG   GAGGVGTHII   QLAKHVFGAS   KVAATASTKK

201     LDLLRTLGAA   DLAIDYTKEN   FEDLPEKFDV   VYDAVGETDK   AVKAVKEGGK

251     VVTIVGPATP   PAILFVLTSK   GSVLEKLKPY   LESGKVKPVL   DPTSPYPETK

301     VVEAFGYLES   SRATGKVVVY   PIP                      Fragment 1
        ─►
```

*Figure 2. Corresponding protein sequence of the ripening induced Fragaria x
ananassa oxidoreductase (FaQR) gene. Peptide sequences (fragment 1 and 2)
obtained by automated Edman degradation of the protein isolated from
strawberry fruit showed total identity with the FaQR sequence.*

Recombinant FaQR Protein

The strawberry *FaQR* cDNA is a full-length cDNA because the cDNA is
1187 bp long and agrees with the size of the mRNA detected in northern
hybridization experiments (data not shown). The insert consists of a 969-bp
open reading frame and encodes a 322 amino acid-long protein with a calculated
molecular mass of 34.3 kDa and a pI of 6.2. Recombinant FaQR His-tagged
fusion protein was obtained by heterologous expression in *E. coli.* Because the
His-tagged fusion protein was not sufficiently purified by His tag affinity
chromatography, ultrafiltration was applied as an additional purification step to
isolate proteins of the molecular weight range from 30 – 50 kD (Fig. 3).

QR activity of the recombinant protein was first determined
spectrophotometrically following the addition of 1,2- or 1,4-quinones and
NADH. However, HDMF forming activity was confirmed with the addition of
D-fructose-1,6-diphosphate and NADH by LC-MS/MS (*14*). Recombinant
FaQR reduced only the artificial substrate 9,10-phenanthrene quinone (K_m= 35
µM) out of a number of 1,2- and 1,4-quinones tested, but produced HDMF from
the phosphorylated hexose. The fact that a non-natural quinone represents a
substrate for FaQR and the observation that HDMF formation from D-fructose-
1,6-diphosphate proceeds very slowly led us to conclude that D-fructose-1,6-
diphosphate is not the actual substrate for FaQR. A dual mode of reaction,
reduction of quinones and alkenals has also been shown for an enzyme isolated
from *Arabidopsis thaliana* (*15, 16*). Further details are provided in (*14*).
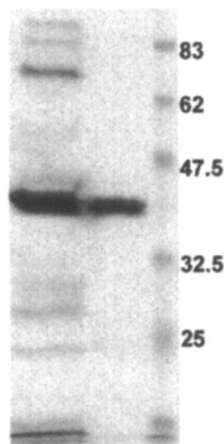
Figure 3. SDS-PAGE of the His-tagged purified recombinantFaQR protein (first lane) and following ultrafiltration (30 – 50 kD fraction (second lane). Protein markers (in kDa) are shown in the third lane (adapted from 14).
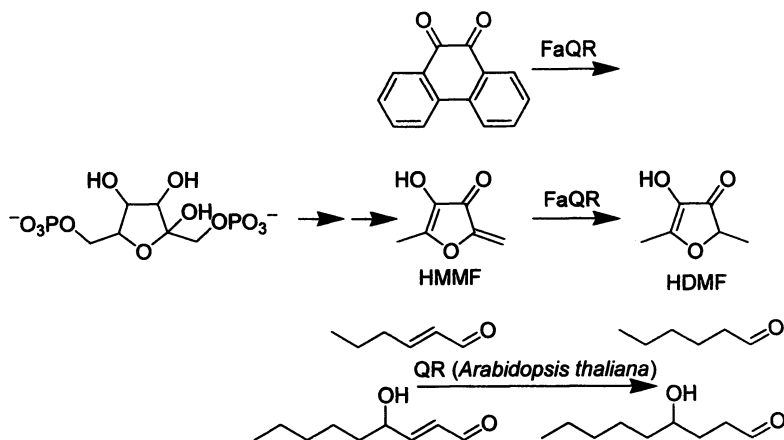
Figure 4. Reactions catalyzed by FaQR and a quinone oxidoreductase isolated from Arabidopsis thaliana.

Because 1,2-quinones and alkenals show some structural similarities we proposed 4-hydroxy-2-methylen-5-methyl-3(2H)-furanone (HMMF) as the putative natural precursor of HDMF which is converted by the enzyme *in vivo* (Figure 4). We synthesized this unstable, α,β-unsaturated compound from norfuraneol and formaldehyde and confirmed its structure by spectroscopic

means. The *in vitro* enzymatic transformation of HMMF to HDMF by FaQR was observed using LC-MS/MS. Additionally, HMMF was also found by LC-MS/MS in solutions containing D-fructose-1,6-diphoshate and in strawberry fruits after derivatization with 3-mercaptobenzoic acid to a stable thioether product as described in (*14*). Although proper V_{max} and K_m values could not be obtained with HMMF because of the instability of HMMF in aqueous solution, (3E)-2-ethylidene-4-hydroxy-5-methyl-3(2H)-furanone (EDHMF), a substrate analogue, was stable enough, and a K_m of 2.1 ± 0.1 mM and a V_{max} of 56 ± 4 nkat/mg could be determined The values for substrates of other oxidoreductases lie in the same order of magnitude (*15, 16*). Thus, it appears that FaQR is actually an enone oxidoreductase (*14*).

Fragaria x ananassa O-Methyltransferase (FaOMT)

In vitro experiments demonstrated that the FaOMT protein catalyzes the transfer of the methyl group from SAM not only to HDMF but also to caffeic acid, thereby forming the corresponding O-methyl ethers (*8*). Although heterologously expressed FaOMT shows a preference (~100:1) for caffeic acid over HDMF, only DMMF can be found in appreciable amounts in strawberries.

Because we could not exclude the presence of further OMTs involved in the methylation of HDMF, we decided to assess the function of the FaOMT enzyme *in planta* by up- and downregulating FaOMT using the CaMV 35S promoter. Strawberries from transgenic plants with a lower or higher content of *FaOMT* transcripts determined by using the quantitative real time PCR (QRT-PCR) approach were selected and their ratios of HDMF to DMMF and caffeoyl ß-D-glucose to feruloyl ß-D-glucose were compared with those of control strawberries. Significantly lower levels of the methylated product DMMF as compared to the substrate HDMF were produced by strawberries from four of the seven transgenic lines (FaOMT AS2, FaOMT AS4, FaOMT AS11 and FaOMT S9), resulting in a higher proportion of HDMF relative to the total amount of furanones (Fig. 5). *FaOMT* transcript levels in fruit correlated fairly well with HDMF-DMMF ratios. The FaOMT S9 line showed a lower expression level (24% of the control level) although it contained a sense construct. We assume that the reduced levels of *FaOMT* transcripts result from the known phenomenon called co-suppression (*17, 18*). The transgenic lines with strongly reduced levels of FaOMT mRNA (FaOMT AS4, FaOMT AS11, and FaOMT S9) also contained significantly lower levels of the FaOMT product (ferulic acid) compared to the substrate of FaOMT (caffeic acid), quantified as glucose esters (*19*). However, in contrast to the results obtained for the production of DMMF, in none of the transgenic plants did the reduction of the transcripts result in a near total loss of feruloyl ß-D-glucose. Experimental details are provided in (*19*).

FaOMT transcripts relative to cv. Calypso control (CC):

1.00   5.78   4.66   0.74   0.03   0.08   0.04   0.24
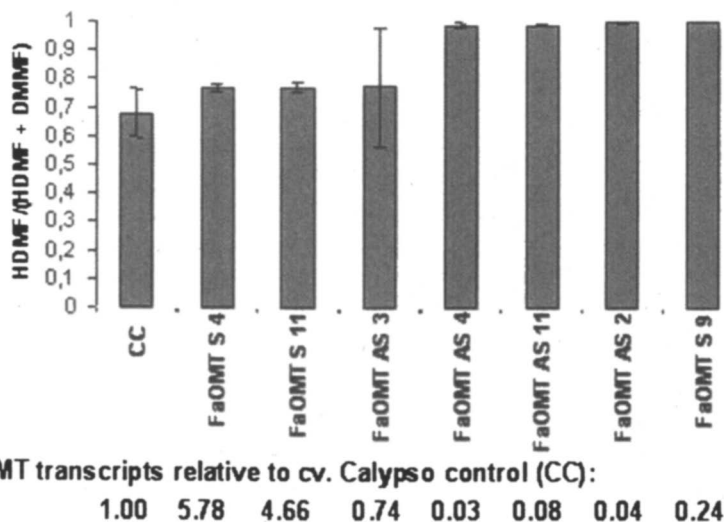
Figure 5. Normalized concentration of HDMF and DMMF in control fruit (CC) and fruit of plants transformed with the sense (FaOMT S) and antisense (FaOMT AS) constructs (adapted from 19).

Consequently, transgenic lines with strikingly reduced amounts of *FaOMT* transcripts contain the lowest proportion of the methylated products DMMF and feruloyl ß-D-glucose. Thus, FaOMT is involved in both pathways despite a much higher preference of the recombinant enzyme for caffeic acid as seen in *in vitro* studies (*8, 9*).

References

1. *Strawberries*; Hancock, J.F., Ed.; CABI Publishing: Wallingford, UK, 1999.
2. Honkanen, E.; Hirvi, T. The flavour of berries. In *Food Flavours*, Morton, I.D.; MacLeod, A.,J., Eds.; Elsevier Scientific Publications: Amsterdam, 1990; pp. 125-193.
3. Latrasse, A. Fruits III. In *Volatile Compounds in Foods and Beverages*, Maarse, H., Ed.; Dekker: New York, 1991; pp 329-387.
4. Larsen, M.; Poll, L.; Olsen, C.E. *Z. Lebensm. Unters. Forsch.* **1992**, *195*, 536-539.
5. Schwab, W.; Roscher, R. *Recent Res. Devel. Phytochemistry* **1997**, *1*, 643-673.
6. Hodge, J.E.; Fisher, B.E.; Nelson, H.A. *Am. Soc. Brew. Chem. Proc.* **1963**, *83*, 84-92.

7. Roscher, R.; Schreier, P.; Schwab, W. *J. Agr. Food Chem.* **1997**, *45*, 3202-3205.

8. Wein, M.; Lavid, N.; Lunkenbein, S.; Lewinsohn, E.; Schwab, W.; Kaldenhoff, R. *Plant J.* **2002**, *6*, 755-765.

9. Lavid, N.; Schwab, W.; Kafkas, E.; Koch-Dean, M.; Bar, E.; Larkov, O.; Ravid, U.; Lewinsohn, E. *J. Agric. Food Chem.* **2002**, *50*, 4025-4030.

10. Sanz, C.; Richardson, D.G.; Pérez, A.G. 2,5-Dimethyl-4-hydroxy-3(2H)-furanone and derivatives in strawberries during ripening. In *Fruit Flavors, Biogenesis, Characterization, and Authentication*, Rouseff, R.L.; Leahy, M.M., Eds.; American Chemical Society: Washington, DC, 1995; pp 268-275.

11. Roscher, R.; Bringmann, G.; Schreier, P.; Schwab, W. *J. Agr. Food Chem.* **1998**, *46*, 1488-1493.

12. Hauck, T.; Landmann, C.; Raab, T.; Bruhlmann, F.; Schwab, W. *Carbohydr. Res.* **2002**, *337*, 1185-1191.

13. Raab, T.; Hauck, T.; Knecht, A.; Schmitt, U.; Holzgrabe, U.; Schwab, W. *Enantiomer* **2003**, *15*, 573-578.

14. Raab, T.; López-Ráez, J.A.; Klein, D.; Caballero, J.L.; Moyano, E.; Schwab, W.; Muñoz-Blanco, J. *Plant Cell* **2006**, *18*, 1023-1037.

15. Mano, J.I.; Babiychuk, E.; Belles-Boix, E.; Hiratake, J.; Kimura, A.; Inze, D.; Kushnir, S.; Asada, K. *Eur. J. Biochem.* **2000**, *267*, 3661-3671.

16. Mano, J.; Torii, Y.; Hayashi, S.; Takimoto, K.; Matsui, K.; Nakamura, K.; Inzé, D.; Babiychuk, E.; Kuhnir, S.; Asada, K. *Plant Cell Physiol.* **2002**, *43*, 1445-1455.

17. Van der Krol, A.R.; Mur, L.A.; Beld, M.; Mol, J.N.; Stuitje, A.R. *Plant Cell*, **1990**, *2*, 291-299.

18. Hamilton, A.J.; Baulcombe, D.C. *Science* **1999**, *286*, 950-952.

19. Lunkenbein, S.; Salentijn, E.M.J.; Coiner, H.A.; Boone, M.J.; Krens, F.A.; Schwab, W. *J. Exp. Bot.* **2006**, *57*, 2445-2453.

Chapter 16

Volatiles from the Thermal Interaction of *E*-2-Pentenal with Methionine or Cysteine under Non-Aqueous Conditions

Dimitrios Zabaras[1] and Peter Varelis[1,2]

[1]Food Quality Stream, CSIRO/Food Science Australia, P.O. Box, North Ryde, NSW 2113, Australia
[2]Current address: Department of Biological, Chemical and Physical Sciences, Ilinois Institute of Technology, Chicago IL 60501–1957

A large number of volatiles were detected in the headspace above model systems containing *E*-2-pentenal and methionine or cysteine following thermal treatment (140 °C for 40 min). Alkylpyridines were the major nitrogen-containing group of compounds detected in both systems. Experiments with glutamine-*amino*-^{15}N confirmed that the majority of alkylpyridines in these systems were formed by reactions between amino acid-derived volatiles and *E*-2-pentenal or its thermal-degradation products, in the presence of free ammonia. The formation and odour-quality attributes of 3-methylthiopentanal and 3-(methylthiomethyl)pyridine, two interesting sulfur-containing compounds detected in the headspace above the *E*-2-pentenal/methionine system, are also described.

The Maillard reaction (or non-enzymatic browning) and the degradation of lipids are two flavour-impact processes that occur in a majority of foods. Both reactions have been extensively studied and a great deal of information is available in the literature (*1, 2*). However, the interaction between volatile

176 © 2008 American Chemical Society

compounds generated from these two reactions has not received much attention especially when the interaction occurs under conditions similar to those encountered during roasting or extrusion (3). Examples of reports describing reactions between amino acids (or other amine sources) and aldehydes (or their sources) are shown in Table I. As can be seen, in most of the previous works cysteine was reacted under aqueous conditions with a lipid or lipid-degradation volatile (e.g., an aldehyde).

Table I. Examples of reports describing 'Maillard-lipid' product interactions

Reactants	Conditions	Reference
fatty aldehydes/NH$_3$, H$_2$S, thiols	various	4
2-butenal/H$_2$S	aqueous	5
propanal,crotonal/glycine	aqueous	6
2,4-decadienal/cysteine, glutathione	aqueous	7
corn oil/cysteine	non-aqueous	8
ribose & phospholipid/cysteine	non-aqueous	9
ribose & phospholipid/cysteine	low-moisture	10
fish oil & trimethylamine oxide/cysteine	non-aqueous	11

The following text will give an overview of the volatile products generated from the thermal interaction of a sulfur-containing amino acid (methionine or cysteine) with E-2-pentenal under non-aqueous conditions. Methionine and cysteine, upon thermal treatment, are known to be precursors of potent odour-active sulfur-containing flavour components (12,13). A product of the breakdown of linolenic acid, E-2-pentenal is found to be present in many lipid-rich foods such as meat, cheese and seafood (14-16).

Distribution of Volatiles Produced by the Two Model Systems

The GC/MS analysis of the SPME headspace extracts from the reaction of either cysteine or methionine with E-2-pentenal under non-aqueous conditions (heated at 140 °C for 40 min.) resulted in the detection of a large number of volatiles in both systems (152 and 133, respectively). The distribution of volatiles in the headspace above these mixtures is shown in Figure 1.

As can be seen from Figure 1, the methionine/E-2-pentenal (MP) system produced a higher relative amount of sulfur-containing compounds than the cysteine/E-2-pentenal (CP) system. However, when the sulfur-nitrogen-
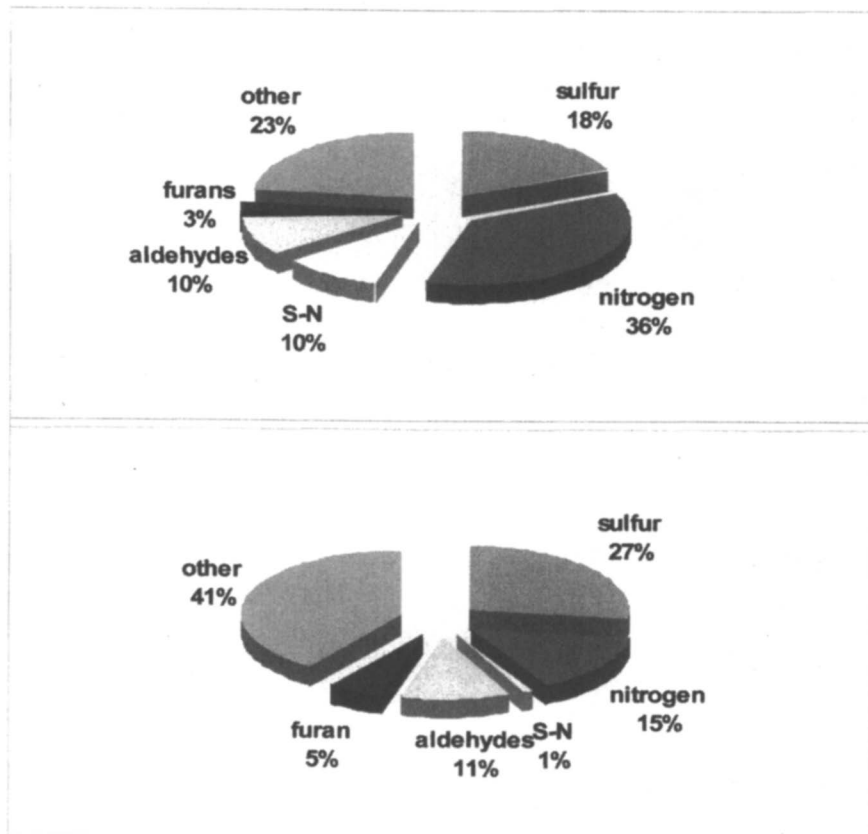
Figure 1. Distribution of volatiles in the headspace extracts above the cysteine/E-2-pentenal (a) and methionine/E-2-pentenal (b) model systems as determined by SPME-GC/MS.

containing volatiles are considered, the amount of sulfur released from both amino acids appears to be approximately the same. The clear difference between the headspace profiles from the two systems is in the nitrogen-containing volatiles. In this category, the CP system generated more than twice the relative amount of volatiles compared to the MP system (15% vs. 36%). The CP system also produced a much higher proportion of sulfur-nitrogen-containing volatiles (Figure 1). As expected from previous studies (*17,18*) characteristic amino acid-derived compounds such as thiophenes, thiazoles (CP) and methanethiol, sulfides (MP) were found to be abundant in the headspace of each system. Alkylpyridines were the major contributors to the nitrogen-containing category in both systems. Several volatiles, derived from the thermal degradation of *E*-2-pentenal (and subsequent reactions of these products), such as simpler aldehydes and
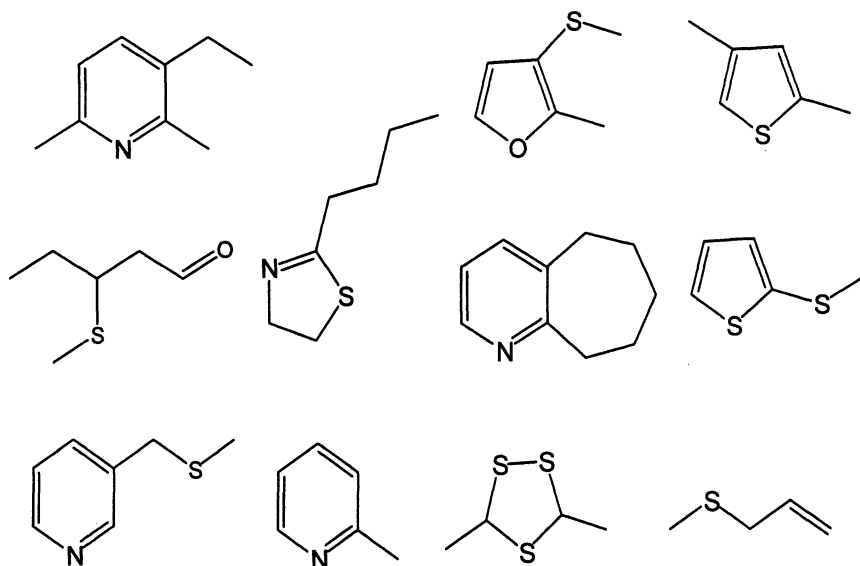
Figure 2. Structures of some of the volatiles detected in the headspace extracts above the cysteine/E-2-pentenal and methionine/E-2-pentenal model systems.

furans (*19,20*) were also abundant in both systems. Some examples of volatiles detected in these systems are shown in Figure 2.

The formation of compounds such as thiazoles, thiophenes and sulfides in food has been extensively investigated (*18,21*). The following text will present information related to the formation of a few flavour-impact compounds that have not received much attention: the alkylpyridines and selected methylthio-containing compounds.

Formation of alkylpyridines

Although the presence of alkyl-substituted pyridines has been reported in many foods (*22-25*), they have not attracted the same attention as some other nitrogen-containing compounds (e.g., pyrazines). This perhaps can be attributed to their undesirable, grassy odour-qualities (*6,26*).

Table II below shows a selection of some major pyridines that were detected in the CP and MP model systems. The first observation that can be made is that the CP system produced approximately 3.5 times more pyridines than the MP system. This is likely to be directly linked to the higher generation of ammonia from cysteine compared to methionine, as shown by previous work (*27*). The correlation between the levels of alkylpyridines detected in these systems and the

ability of sulfur-containing amino acids to generate free ammonia indicated that the alkylpyridines were formed through the 'conventional' pathway and not via the 'pyridinium betaine' pathway. According to the 'pyridinium betaine' pathway, aldehydes (or other carbonyls) can react with amino acids, under neutral conditions at room temperature. This reaction is known to produce quaternary pyridinium salts which upon heat treatment are known to easily decompose leading to pyridines (*6,28*) (Figure 3).

Table II. Selected pyridines (major components) detected in the methionine/*E*-2-pentenal (MP) and cysteine/*E*-2-pentenal (CP) model systems (heated at 140 °C for 40 min.) as determined by SPME-GC/MS

Alkyl substituent	MP	CP
	(mg mol^{-1} of amino acid)	
-	8.2	18.3
2-methyl	0.7	79.3
2-ethyl	5.2	110.6
3-methyl	33.4	39.4
2,3-dimethyl	8.5	84.3
2-ethyl-6-methyl	63.4	59.8
3-propyl	24.5	16.4
2,6-diethyl	2.3	32.1
3-ethyl-4-methyl	-	11.6
3-ethyl-2,6-dimethyl	4.7	75.3
2-methyl-6-propyl	6.2	5.7
Total	163.1	526.8

Glutamine-*amino*-^{15}N was used in order to investigate further the formation pathway of alkylpyridines in these systems. Glutamine-*amino*-^{15}N was an ideal candidate for this work as it contained two nitrogen atoms, one of which, the *amino* nitrogen atom in this case, was labeled. The level of incorporation of ^{15}N in the resulting products would indicate the alkylpyridine formation pathway in these systems. Experiments using glutamine-*amino*-^{15}N and *E*-2-pentenal showed that the vast majority of 2-ethyl-6-methylpyridine (one of the few alkylpyridines detected in this system) was formed by the ammonia released through the deamidation of glutamine (Figure 4). This result confirmed the theory that alkylpyridines in these systems were formed through the 'free ammonia' or 'conventional' pathway and also suggested that, to a large extent, the amino acids in these model systems did not interact with *E*-2-pentenal through the formation of Schiff-like bases. The generation of only a few minor alkyl-

a

$$3(RCH_2CHO) \quad + \quad NH_3 \longrightarrow$$

b

$$3(R_1CH_2CHO) + R_2\overset{NH_2}{\underset{|}{CH}}COOH \longrightarrow$$

Pyrolysis $\longrightarrow$ Pyridines
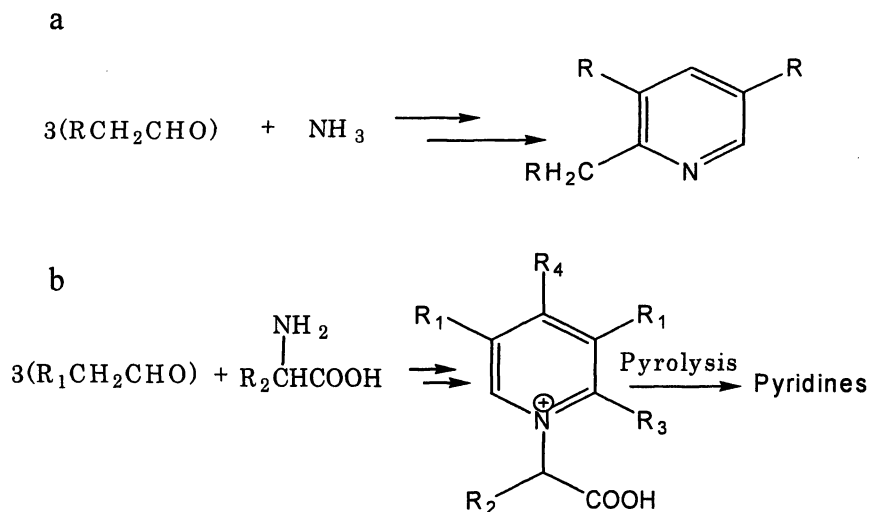
Figure 3. Possible reaction pathways to the formation of pyridines in food: a) from reaction of aldolisation products with free ammonia ('conventional' pathway) and b) from condensation of aldolisation products with α-amino acids followed by pyrolysis of the pyridinium betaines (adapted from 6).

pyridines from the glutamine-*amino*-^{15}N/*E*-2-pentenal system may reflect the limited amount of water (possibly originating from the atmosphere or generated from Strecker-like reactions) available for the hydrolytically-favoured deamidation reaction (*29*).

E-2-pentenal

(15%)   (85%)
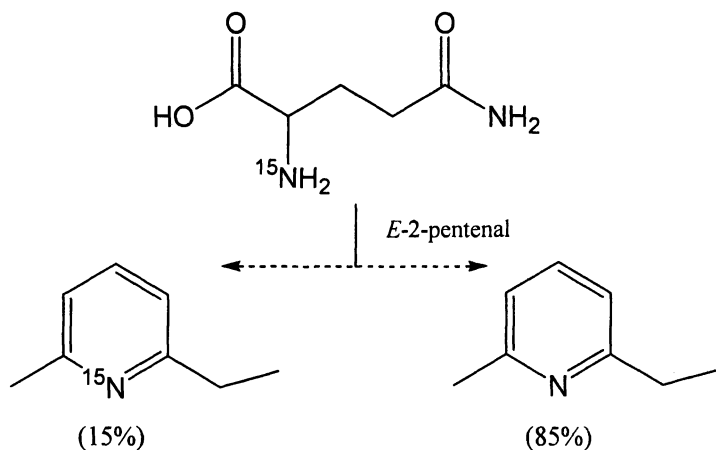
Figure 4. Incorporation of ^{15}N into 2-ethyl-6-methylpyridine from the reaction of glutamine-amino-^{15}N and E-2-pentenal.

A closer look at the nature of alkylpyridines generated from the MP and CP systems highlights the presence of amino acid-specific pyridines in each system. For example, the MP system generated mostly 3-substituted pyridines (e.g 3-methylpyridine) whilst the CP system produced high amounts of 2-alkylpyridines (e.g.. 2-ethylpyridine) (Table II). This suggested that sulfur-containing amino acids played a role, in addition to generating free ammonia, in the formation of alkylpyridines. The generation, upon thermal degradation, of large amounts of highly reactive volatiles such as acetaldehyde (cysteine) and 2-propenal (methionine) has been well established (30,31). Experiments, carried out in our laboratory, showed that reactions between these amino acid-derived volatiles and E-2-pentenal or its thermal-degradation products (e.g., propanal), in the presence of free ammonia, can generate the alkylpyridines detected in the CP and MP systems (Figure 5).

Methylthio-containing volatiles

It is well known that the thermal or Strecker degradation of methionine results in the generation of 3-methylthiopropanal (or methional) which can further degrade into methanethiol and 2-propenal (32). Both methional and methanethiol are very reactive and, under appropriate conditions, can readily contribute to the formation of methylthio-containing volatiles (32).
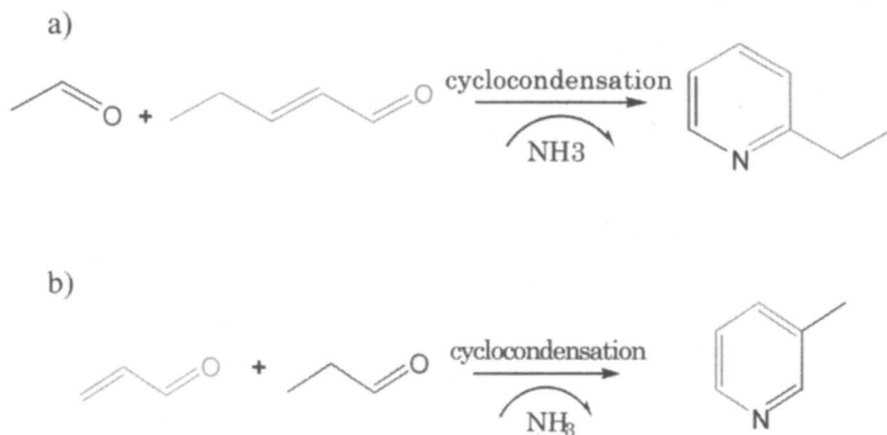
Figure 5. Proposed formation pathways to some of the major alkylpyridines detected in the model systems: a) formation of 2-ethylpyridine from acetaldehyde and E-2-pentenal (CP system) and b) formation of 3-methylpyridine from 2-propenal and propanal (MP system).

3-Methylthiopentanal and 3-(methylthiomethyl)pyridine were the most abundant methylthio-containing compounds detected in the MP system. However, each compound peaked at different time-points over the course of the reaction (Figure 6).

3-Methylthiopentanal (3-MTP) is most likely formed via the conjugate addition of methanethiol onto E-2-pentenal. The presence of this compound in foods or model systems has not been reported in the literature although a number of other methylthioalkanal homologues have been detected in various foods (Table III).

3-(Methylthiomethyl)pyridine (3-MTMP) was first reported by de Rijke *et al.* (*33*) as an 'unusual minor product' of the reaction between methionine and several sugars. Since then 3-MTMP has been detected in cysteine/methionine/furfural (*34*) and methionine/glucose (*18*) model systems. de Rijke *et al.* (*33*) suggested that methional and sugar-derived carbonyls such as glyceraldehyde were involved in the formation of 3-MTMP. However, our results obtained from various model systems demonstrated that 3-MTMP formation could be effected from the pyrolysis of methionine alone, possibly via the condensation of methional with 2-propenal (Figure 7).
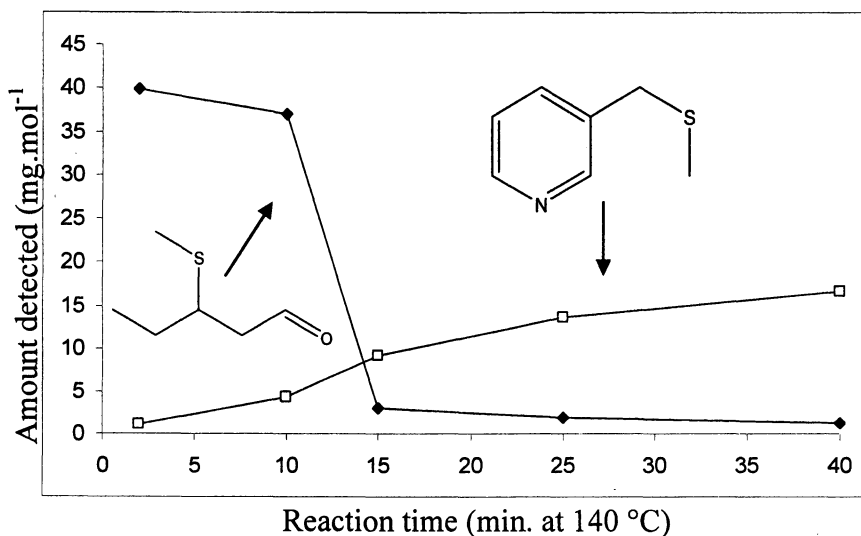
Figure 6. Formation of 3-methylthiopentanal and 3-(methylthiomethyl)pyridine over time in the MP model systems.

Table III. Methylthioalkanals reported in various foods

Alkanal	Food	Reference
3-(methylthio)butanal	Antarctic krill	35
	Fried potatoes	36
	Cooked beef liver	37
3-(methylthio)hexanal	Tomato paste	38
	Dried squid	39
	Cooked beef liver	37
3-(methylthio)heptanal	Fried potatoes	36
	Cooked beef liver	37
3-(methylthio)nonanal	Cooked beef liver	37
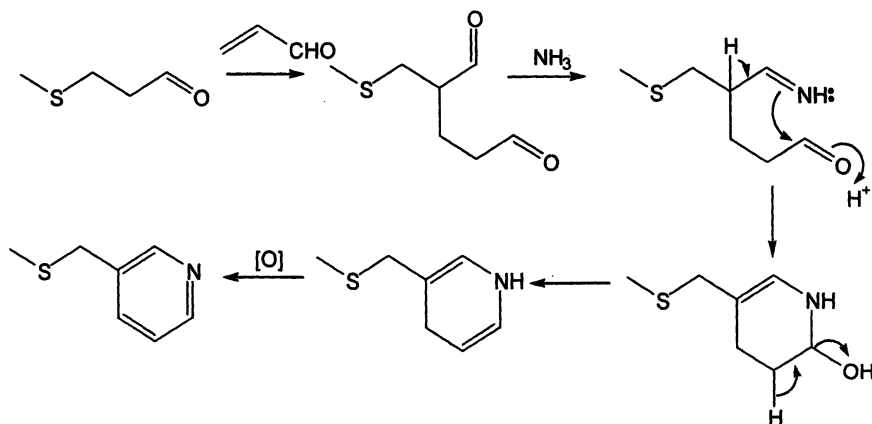
Figure 7. Proposed formation mechanism for 3-(methylthiomethyl)pyridine from methional and 2-propenal.

GC/MS-O assessment of the volatiles generated by the MP and CP systems

The headspace extracts from both systems were found to be very complex when assessed by gas chromatography/mass spectrometry-olfactometry (GC/MS-O) using the *Osme[1]* approach. The consensus aromagrams constructed from headspace extracts of both MP and CP systems contained more than one hundred different odour-active volatiles. Table IV summarises the main odour-groups detected in the two systems together with the compounds (or groups of compounds) identified in the regions of the odours. Both 3-MTMP and 3-MTP were found to be odour-active exhibiting fresh, minty, pleasant (3-MTMP) and green, fatty, metallic (3-MTP) properties.

A more detailed account of the volatiles generated from both systems will be published elsewere.

Table IV. Grouping of main odour-active volatiles detected in the CP and MP systems

Odour-group qualities	CP system Volatiles detected in the region of the odour
raw, green, sweet	pyridines, aldehydes
cooked, savoury	thiazoles
sulfur, rotten	H_2S, thiols
garlic	thiazoles
burnt rubber	thiophenes
fermented, cheesy	acetaldehyde, acids
Odour-group qualities	MP system Volatiles detected in the region of the odour
raw, green, sweet	pyridines, aldehydes
boiled, green	not detected
onion, sulfur, garlic	sulfides
plastic, chemical	not detected
green, fatty metallic	3-methylthiopentanal
cheesy	not detected

---

[1] In the *Osme* (Greek word meaning smell) approach the non-diluted extracts are investigated by gas chromatography-olfactometry using several assessors. The averaged perceived intensities of odour-active volatiles are then used to generate an aromagram (*40*).

Conclusions

The thermal interaction between *E*-2-pentenal and methionine or cysteine generated a large number of flavour-impact volatiles. Alkylpyridines were found to be the dominant nitrogen-containing compounds in the headspace of both systems, formed by reactions between amino acid-derived volatiles and *E*-2-pentenal or its thermal-degradation products, in the presence of free ammonia.

Interesting odour-active compounds such as 3-methythiopentanal (3-MTP) and 3-(methylthiomethyl)pyridine (3-MTMP) were detected in the headspace above the *E*-2-pentenal/methionine system. Methional, directly (3-MTMP) or indirectly through its oxidation product methanethiol (3-MTP), is the precursor of both these volatiles.

GC-O assessment revealed that the headspace extracts from both systems contained many potent odour-active components enclosing a wide range of odour-qualities.

Acknowledgements

References

1. Grosch, W. In *Food Flavours, Part A*; Morton, A. D.; MacLeod, A. J., Eds; Elsevier: Amsterdam, 1982; pp 325-334.
2. Rizzi, G. P. In *Maillard Reactions in Chemistry, Food and Health*; Labuza, T. P.; Reineccius, G. A.; Monnier, V. M.; O'Brien, J.; Baynes, J. W., Eds; Royal Society of Chemistry: Cambridge, 1994; pp 11-19.
3. Whitfield, F. B. *Crit. Rev. Food Sci. Nutr.* **1992**, *31*, 1-58.
4. Boelens, M.; van der Linde, L. M.; de Valois, P. J.; van Dort, H. M.; Takken H. J. *J. Agric. Food Chem.* **1974**, *22*, 1071-1076.
5. Badings, H. T.; Maarse, H.; Kleipool, R. J. C.; Tas, A. C.; Neeter, R.; ten Noever de Brauw, M. C. *Z. Lebensm. Unters.-Forsch.* **1976**, *161*, 53-59.
6. Suyama, K.; Adachi, S. *J. Agric. Food Chem.* **1980**, *28*, 546-549.
7. Zhang, Y.; Ho, C.-T. *J. Agric. Food Chem.* **1989**, *37*, 1016-1020.
8. Macku, C.; Shibamoto, T. *J. Agric. Food Chem.* **1991**, *39*, 1987-1989.
9. Mottram, D. S.; Whitfield, F. B. *J. Agric. Food Chem.* **1995**, *43*, 1302-1306.
10. Mottram, D. S.; Whitfield, F. B. *J. Agric. Food Chem.* **1995**, *43*, 984-988.

11. Horiuchi, M.; Umano, K.; Shibamoto, T. *J. Agric. Food Chem.* **1998**, *46*, 5232-5237.
12. Yaylayan, V. A.; Keyhani, A. *J. Agric Food Chem.* **2001**, *49*, 800-803.
13. Hofmann, T.; Schieberle, P. *J. Agric. Food Chem.* **1998**, *46*, 235-241.
14. Umano, K.; Shibamoto, T. *J. Agric. Food Chem.* **1987**, *35*, 14-18.
15. Barbieri, G.; Bolzoni, L.; Careri, M.; Mangia, A.; Parolari, G.; Spagnoli, S.; Virgili, R. *J. Agric. Food Chem.* **1994**, *42*, 1170-1176.
16. Josephson, D. B. ; Lindsay, R. C. ; Stuiber, D. A. *J. Agric. Food Chem.* **1984**, *32*, 1347-1352.
17. Whitfield, F. B; Mottram, D. S. In *The Contribution of Low- and Nonvolatile Materials to the Flavour of Foods*; Pickenhagen, W.; Ho, C.-T.; Spanier, A. M., Eds; Allured Publishing: Carol Stream Illinois, 1996; pp 149-181.
18. Yu, T-H.; Ho, C.-T. *J. Agric. Food Chem.* **1995**, *43*, 1641-1646.
19. Josephson, D. B.; Glinka, J. In *Thermal Generation of Aromas*; Parliment, T. H.; McGorrin, R. J.; Ho, C.-T., Eds; American Chemical Society: Washington DC, 1989; pp 242-246.
20. Locas, P. C.; Yaylayan, V. A. *J. Agric. Food Chem.* **2004**, *52*, 6830-6836.
21. Mottram, D. S.; Mottram, H. R. In *Heteroatomic Aroma Compounds*; Reineccius, G. A.; Reineccius, T. A., Eds; American Chemical Society: Washington DC, 2002; pp 73-92.
22. Watanabe, K.; Sato, Y. *J. Agric. Food Chem.* **1971**, *19*, 245-247.
23. Buttery, R. G.; Ling, L. C.; Teranishi, R.; Mon, T. R. *J. Agric. Food Chem.* **1977**, *25*, 1227-1229.
24. Yajima, I.; Yanai, T.; Nakamura, M.; Sakakibara, H.; Habu, T. *Agric. Biol. Chem.* **1978**, *42*, 1229-1232.
25. Peppard, T. L; Halsey, S.A. *J. Chromatogr.* **1980**, *202*, 271-278.
26. Shibamoto, T. In *Thermal Generation of Aromas*; Parliment, T. H.; McGorrin, R. J.; Ho, C.-T., Eds; American Chemical Society: Washington DC, 1989; pp 134-142.
27. Sohn, M.; Ho, C.-T. *J. Agric. Food Chem.* **1995**, *43*, 3001-3003.
28. Suyama, K.; Adachi, S. *J. Org. Chem.* **1979**, *44*, 1417-1420.
29. Wright, T. H. *CRC Crit. Rev. Biochem. Mol. Biol.* **1991**, *26*, 1-52.
30. Fujimaki, M.; Kato, S.; Kurata, T. *Agric. Biol. Chem.* **1969**, *33*, 1144-1151.
31. Ballance, P. E. *J. Sci. Food Agric.* **1961**, *12*, 532-533.
32. Tressl, R.; Helak, N.; Martin, N.; Kersten, E. In *Thermal Generation of Aromas*; Parliment, T. H.; McGorrin, R. J.; Ho, C.-T., Eds; American Chemical Society: Washington DC, 1989; pp 156-171.
33. de Rijke, D.; van Dort, J. M.; Boelens, H. In *Flavour '81*; Schreier, P., Ed; Walter de Gruyter: Berlin, 1981; pp 417-431.
34. Silwar, R.; Tressl, R. *Z. Lebensm. Unters.-Forsch.* **1989**, *189*, 205-211.
35. Kubota, K.; Kobayashi, A.; Yamanishi, T. *Agric. Biol. Chem.* **1982**, *46*, 2835-2839.

36. Carlin, J. T.; Ho, C.-T.; Chang, S. S.; Velluz, A.; Pickenhagen, W. *Lebensm.-Wiss. u.-Technol.* **1990**, *23*, 276.
37. Werkhoff, P.; Brüning, J.; Güntert, M.; Kaulen, J.; Krammer, G.; Sommer, H. *Adv. Food Sci.* **1996**, *18*, 19-27.
38. Buttery, R. G.; Teranishi, R.; Flath, R. A.; Ling, L. C. *J. Agric. Food Chem.* **1990**, *38*, 792-795.
39. Kawai, T.; Yazaburo, I.; Hirofumi, K.; Nobuo, I.; Toshihisa, H.; Nakamura, S. *J. Agric. Food Chem.* **1991**, *39*, 770-777.
40. Grosch, W. *Chem. Senses* **2001**, *26*, 533-545.

Chapter 17

Mixture Suppression of Perceived Intensities in an Odor Mixture

Masahiro Chida and Hirotoshi Tamura

Department of Biochemistry and Food Science, Kagawa University, 2393 Miki-Cho, Kita-Gun, Kagawa 761–0795, Japan

Four components (geranylacetone, 2-pentylfuran, 2-ethyl-1-hexanol and n-valeraldehyde) were selected as representative model chemicals for evaluation of perceived odor intensities. Initially, odor intensity adjustment of these four components was performed at the 'moderate' level on a labeled magnitude scale. The contribution of individual components around the moderate concentration was evaluated as follows: (I) measurement of the odor intensity change of single components, (II) measurement of the odor intensity change in a mixture when one component in the 4 chemical mixture was increased in concentration, (III) comparison between the intensity change of single component (I) and the intensity change in the mixed solution (II). In the case of 2-ethyl-1-hexanol and 2-pentylfuran, both intensities were strongly suppressed in the mixture. Conversely, the intensity change of n-valeraldehyde in the mixture was almost the same as that of the single component. Four compounds had different contributions to the odor intensities in the mixture. Therefore, mixture suppression has to be re-evaluated on the basis of individual chemical characters.

191

An important objective in food aroma research is to minimize the number of components in a model oil by selecting those volatile components that contribute significantly to the original aroma (*1-4*). Those minimal characteristic aroma compounds selected would ideally produce a closely related aroma to the corresponding foods without compounding all volatile chemicals identified by modern instrumental techniques. A superior method for selecting character impact components from complex constituents in foods would be a sensory-driven chemical analysis. Gas chromatography-Olfactometry (GC-O) (*5-9*) is one of the most developed techniques that is comprised of the discrimination of chemical odors and the recognition of their odor detection limits with human senses. This method does not involve the psychophysical quantification of odor intensities. However, reliable relationships between the stimulus concentration and the number of coincident respondents have been reported (*10*). Bult *et al.* (*1*) took up partial mutual masking of aroma components in an apple mixed model. They pointed out the positive effect of sub-threshold aroma compounds on the overall perception even though GC-O had overlooked these very small contributions. These effects were also found in an Arabica coffee model (*11*) and a white wine model (*12*). In order to generalize the rules, Berglund *et al.* (*13*) proposed that the intensity of odor mixtures would be estimated by the principle of vector summation on the basis of empirical approximation. Laing et al. (*14, 15*) and Derby *et al.* (*16*) reported that the total intensity of a binary mixture is less than the sum of the intensities of the two components, and also showed that the total intensity is never less than the intensity of the weaker component. Apparently the two-component system easily illustrates itself as an angle between the vectors. However, the vector model is difficult to apply with complicated multicomponent food flavors. No one has yet established universal and comprehensive rules for the estimation of odor intensity of specific individual components in multicomponent odor mixtures. Rather, many of these kinds of studies focus on the discrimination and identification of odorants in multicomponent odor mixtures (*17,18*).

The aim of the current study was to expand the binary mixture suppression concept to tertiary or higher order mixtures of aroma compounds such as occur with natural oils. Using a quaternary odor mixture as a case-study, we tried to understand the causal relationship between odor suppression and odor quality of complex mixtures.

Materials and Methods

Subjects

All subjects were volunteers who provided signed informed-consent forms. We instructed them not to eat, drink, chew gum, or smoke for at least 1-hour prior to testing. Twenty-seven panelists (12 females, 15 males, and average age

of 32±8 years) participated in odor intensity matching test and odor quality cross-matching test. For measurement of odor intensity around the 'moderate' concentration on labeled magnitude scale (LMS, *19, 20*), seven panelists (2 females, 5 males, and average age 35±4 years) participated in measurement of odor intensity changes and odor matching tests. Panels consisted of subjects who had previous experience with odor matching tests.

Odor Chemicals

The stimuli were four single chemicals and their mixtures. They are common and useful aroma characters in the flavor industry. Those four chemicals were 2-pentylfuran (PH, fruity and green earthy, CAS: 3777-69-3, FEMA: 3317, Tokyo Kasei, Tokyo, Japan), geranylacetone (GA, 6,10-dimethyl-5,9-undecadien-2-one, fresh-floral and sweet-rosy, CAS: 3796-70-1, FEMA: 3542, Sigma-Aldrich, St. Louis, MO, USA), *n*-valeraldehyde (VA, woody, vanilla, fruity, or nutty on dilution, CAS: 110-62-3, FEMA: 3098, Sigma-Aldrich), and 2-ethylhexanol (EH, slightly floral-rosy, CAS: 104-76-7, FEMA: 3151, Sigma-Aldrich). The odor dilution was carried out with polyethylene glycol 200 (Wako Pure Chem. Industry Co., Tokyo, Japan).

Olfactometer

A hand-made olfactometer (Figure 1) was designed for generating various odor concentrations (manufactured by Seiwa Kikai Kogyo, Ltd., Kanagawa, Japan). This instrument not only provided a single component under the various concentrations but also generated various mixed gases by controlling individual concentrations of five chemicals with five isolated nozzles. The gas line system consisted of sample bottles (d), mass flow controllers (c) and an odor-mixer (e). Five electric mass-flow controllers (c) (CMQ0002C, Yamatake Co., Kanagawa, Japan) controlled air current into sample bottles (d) and the gas mixer (e) for odor dilution. To avoid condensation of odor gases in the 1/4-inch electropolished stainless steel tubings, heater bands were rolled on all stainless tubings and maintained at 45°C. To provide sufficient concentration of a single odor gas or a mixed gas, a programmable controller (g) (FX2N-32MT, Mitsubishi Electric Co., Tokyo, Japan) combined with an EST555Z monitor (Yamatake Co.) was used to manipulate the mass flow controllers. Pure odor chemicals were diluted with PEG 200 in the sample bottles (d). After blowing pure air into the sample bottles, odor stimulants in the headspace were immediately swept to the subjects by the controlled air.

The total flow rate was arbitrarily set at various values by the programmable controller (g). The compositions of the total gases were determined on the basis of the flow rate ratio of individual odorants under the constant flow rate of the

total current (1000 mL/min). The ventilation of odor stimuli was done with a vacuum pump (h) near the sniffing ports (f) for every inter-stimulus interval. The programmable controller (g) emitted beep sounds and then odorants were supplied to the subject's nose at the 'moderate' concentrations. All odor stimuli were presented to subjects randomly with a double blind method (subjects and examiners did not know the real concentrations during the operation because concentrations were randomly changed by the pre-programmed controller).
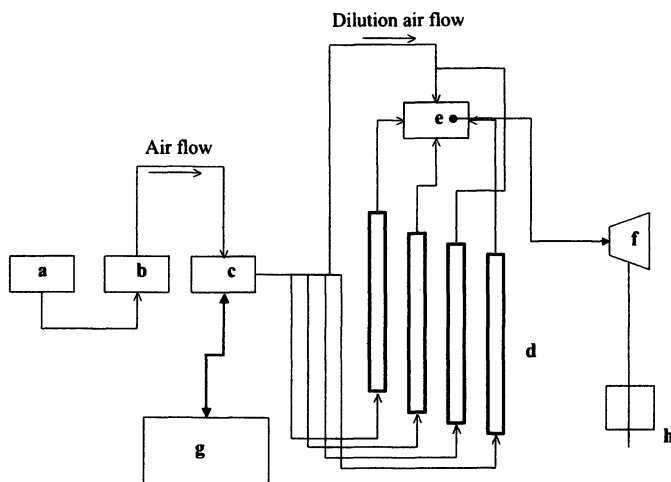
Figure 1. Olfactometer. a: air compressor; b: gas purifier; c: mass flow controllers; d: sample bottles; e: gas mixer; f: sniffing port; g: programmable controller; h: vacuum pump

Odor 'Moderate' Intensity Adjustment

Odor intensity adjustment was performed with the LMS method (*19, 20*). An automated scaling system (vertical scale 20 cm in length on a 17 inch computer screen display) was incorporated in a computer program. Odor stimuli were supplied to subjects in the range of 4.9 ppb-2.43 ppm for GA (7 steps), 11.60 ppb-11.60 ppm for PF (7 steps), 21.50 ppb-10.76 ppm for EH (7 steps) and 1.95 ppb-1.95 ppm for VA (7 steps). The actual concentrations were determined by collecting the eluate gas at the sniffing port, adding an internal standard and analyzing by GC-MS as described below. The order for presenting each stimulus was determined with a balanced randomized design. On sniffing an odor stimulus, subjects initially recognized and evaluated an annoyance concentration of each stimulus on the LMS in order to avoid psychological errors (expectation effects), and then an accurate perceived intensity was evaluated immediately by clicking the mouse leaving checkmarks on the scale on

the computer display. The inter-stimulus interval was sixty seconds for reducing nasal fatigue. Each stimulus was evaluated in triplicate over a one week period. The perceived intensity data was expressed as an average concentration for 'moderate' intensity on LMS (27 subjects x 3 replications for each odor).

Measurement of Odor Intensity Changes from 'Moderate' Intensity

Table I shows an experimental design for this study. A concentration of 'moderate' intensity and a seven times higher concentration of the 'moderate' intensity were presented to subjects randomly. The odor intensity change could also be calculated by subtraction of 'moderate' concentration from seven times concentration of 'moderate' as follows. Each odor intensity was expressed as a logarithmic value according to the Weber-Fechner law.

$$IC_{Asingle} = \log \{ I [7X] \} - \log \{ I [X] \} \text{ -----------------------(1)}$$

where: X: 4 odors, GA, PF, EH, VA
$IC_{Xsingle}$: intensity change of X single stimulus
I[7X]: intensity of seven times higher X 'moderate' concentration
I [X]: intensity of X at the 'moderate' concentration

$$IC_{Xmixture} = \log \{ I [MIX\_7X] \} - \log \{ I [MIX] \} \text{----------(2)}$$

where: X: 4 odors, GA, PF, EH, VA
$IC_{Xmixture}$: intensity change of A in mixture
I [MIX_7X]: intensity of seven times higher X concentration in a four odor mixture (GA-PF-EH-VA)
I [MIX]: intensity of 'moderate' mixture (GA-PF-EH-VA)

Odor Quality Cross-matching

An odor quality cross-matching test was done as previously described (*21*). For binary mixtures, the concentrations of two components were each set at 'moderate' intensity (the ratio of each intensity was 1:1) and for a quaternary mixture, the concentration of each of the four components was also set to the 'moderate' intensity.

Subjects consisted of twenty-seven panelists (12 females, 15 males), the same number of participants as the measurement of odor intensity changes. Subjects sniffed the headspace gas from a 5 mL sample solution (four single compounds, six binary mixtures or a quaternary mixture) in a 45 mL brown glass bottle. The subjects initially sniffed the aromas of the 4 single compounds, and

Table I. Experimental Design and Stimulus Concentrations

Presentation Type	Sample Code	Resource Flow Rate[a]				Dilution Air Flow Rate[a]	Total Flow Rate[a]	Final Concentration (ppm)			
		GA	PF	EH	VA			GA	PF	EH	VA
Mix	MIX	100	100	100	100	600	1000	0.52	0.42	0.74	0.34
	MIX_7GA	700	100	100	100	-	1000	3.64	0.42	0.74	0.34
	MIX_7PF	100	700	100	100	-	1000	0.52	2.94	0.74	0.34
	MIX_7EH	100	100	700	100	-	1000	0.52	0.42	5.18	0.34
	MIX_7VA	100	100	100	700	-	1000	0.52	0.42	0.74	2.38
Single	GA	100	-	-	-	900	1000	0.52	-	-	-
	PF	-	100	-	-	900	1000	-	0.42	-	-
	EH	-	-	100	-	900	1000	-	-	0.74	-
	VA	-	-	-	100	900	1000	-	-	-	0.34
	7GA	700	-	-	-	300	1000	3.64	-	-	-
	7PF	-	700	-	-	300	1000	-	2.94	-	-
	7EH	-	-	700	-	300	1000	-	-	5.18	-
	7VA	-	-	-	700	300	1000	-	-	-	2.38

[a] Flow rate: mL/min

Abbreviations of chemicals are described in the text.

memorized their odor characters. Finally, subjects matched the odors of six binary mixtures and a quaternary mixture to those four single compounds by means of odor character impression using the forced choice method. The matching frequencies of each mixture into the odor qualities of 4 single compounds were summed up in quadruplicate. The original data in the cross-matching frequency table were assigned to cells according to two criteria: items and categories. The contingency data were handled by the reciprocal averaging algorithm of the correspondence analysis (CA) done by the SAS-JMP™ software (SAS Institute Inc., San Francisco, CA).

Quantitative Analysis for Odor Stimuli

A Hewlett Packard (HP) 5890 gas chromatograph equipped with an HP 5971 mass spectrometer and a vapor sampler (*22*) was used for quantifying the amount of odorants in the gas phase. An HP-wax capillary column (60 m length, 0.25 mm i.d. and 0.5 μm film thickness, Agilent Technologies, Palo Alto, CA) was used for gas chromatography. Each chemical concentration in a mixture was determined by using extracted ion chromatography (EIC), (*23, 24*). In fragment ion peaks, a proper target ion and a qualifier ion in a mass range from 27 to 300 amu were selected for calculation of peak areas. The temperatures of the transfer line and injection port were maintained at 120°C and 150°C, respectively. The temperature of the column oven was programmed from 40°C (held for 5 min) to 240°C (held for 10 min) at 4°C/min. The MS ion source and the quadrupole were heated at 230°C and 160°C, respectively. Their collision energy at 70eV in the laboratory frame was used. Each odorant was re-checked for chemical purity by comparison of the peak area ratio of the target ion to that of the internal standard. Five replicates for each sample were performed.

Results and Discussion

Odor 'Moderate' Intensity Adjustment

For 'moderate' intensity adjustments, the relations between the stimulus concentrations and the perceived intensities on LMS were plotted and then linear regression equations for each component were mathematically fit to the data as shown in Figure 2. The 'moderate' concentrations were determined after transformation of 'moderate' intensities as follows: GA 0.52 ppm, PF 0.42 ppm, VA 0.34 ppm, EH 0.74 ppm. EH had a relatively large inclination (the psychophysical slope: 0.36). The slopes of GA, VA and PF were 0.30, 0.29 and 0.22, respectively. The calculated 'moderate' concentrations of each chemical were used in all following experiments.

Figure 3 shows the perceived intensity changes of each single chemical as the concentration increased from 'moderate' to '7-times the moderate' concentration. The odor intensities as logarithmic means were 1.38 ± 0.15 for EH, 1.44 ± 0.16 for GA, 1.35 ± 0.10 for VA and 1.28 ± 0.25 for PF, respectively. By equation (1), the odor intensity changes for EH, GA, VA and PF were 0.52, 0.32, 0.23 and 0.30, respectively when each 'moderate' concentration was compared with seven times the 'moderate' concentration.

On the other hand, Figure 4 shows odor intensities of 4 chemicals in a mixture (sample code "MIX" in Table I). The odor intensity of MIX was initially 1.17 ± 0.31. When the concentration of one of 4 chemicals was increased up to 7-fold in the mixture (MIX_7GA, MIX_7PF, MIX_7EH and MIX_7VA), the logarithmic values of the individual odor intensities were 1.41 ± 0.22 for MIX_7EH, 1.42 ± 0.17 for MIX_7GA, 1.38 ± 0.20 for MIX_7VA and 1.30 ± 0.22 for MIX_7PF, respectively. The perceived intensity changes of EH, GA, VA and PF calculated by equation (2) were 0.4, 0.25, 0.22 and 0.15 in the mixture, respectively. Every component increased their intensities. However, each increment in value was not as high as that observed with single chemicals. In addition, when PF and EH were added at a 7-times higher concentration to the mixture, the increment in perceived intensity was not significantly different from the intensity in the original mixture, suggesting that odor intensities of PF and EH were significantly suppressed in the quaternary mixture.

Odor Quality Cross-matching Test

Table II summarizes the cross-matching data of the seven mixtures and four single chemicals. Comparing observed counts with theoretically expected ones, the odor quality of GA-PF-EH-VA was similar to that of PF (matched frequency 10/29, Chi-square (χ^2)=2.815.

The frequency data of Table II was applied to correspondence analysis (CA) (21) in order to see the relationship between single odor characters and the mixed odorants. CA provides information which is similar in nature to those produced by factor analysis techniques. However, CA is a descriptive technique designed to analyze two-way and multi-way tables containing some measure of correspondence between the rows and columns. Table III summarizes the result of CA. The first dimension (C1) had a singular value of 0.528 and inertia of 0.279. This dimension explained 71.6% of all data. The second dimension (C2) had a singular value of 0.297 and inertia of 0.088. This dimension explained 22.7% of all data. Thus, the ground plan by C1 and C2 explained 94.3% of the data. Table III and Table IV show the category scores and the item scores, respectively. The synchronous scatter plots (CA biplot) of the four single odors (categories) and their binary and quaternary mixtures (items) are shown in Figure 5. The score of EH was plotted at the point of C1 = 0.268 and C2 = 0.327. The score of GA was plotted at -0.715 for C1 and -0.179 for C2. PF was plotted at
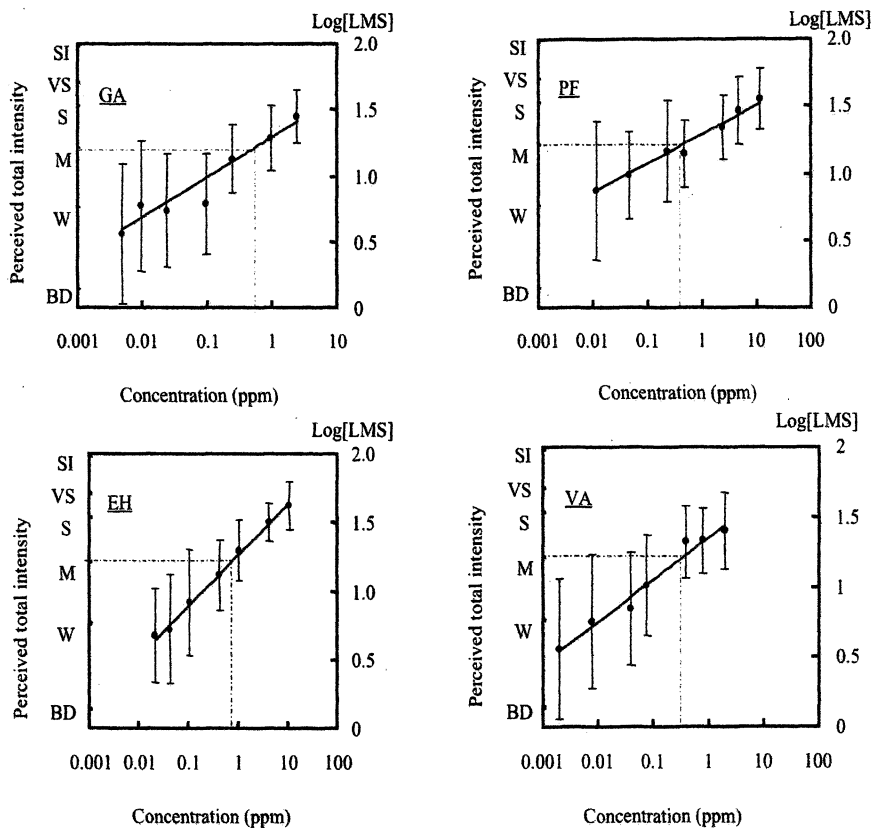
Figure 2. 'Moderate' intensities of four chemicals. Abbreviations of chemicals are described in the text. SI: strongest imaginable; VS: very strong; S: strong; M: moderate; W: weak, BD: barely detectable.
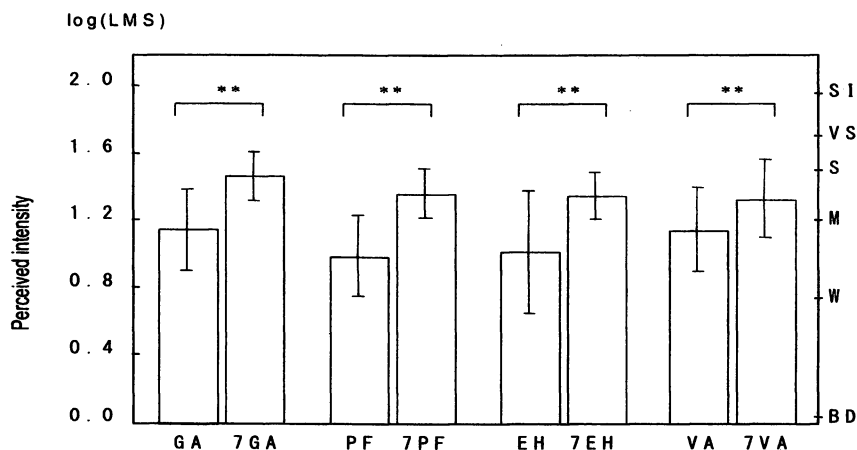
Figure 3. Odor intensity changes of single chemicals. Abbreviations of chemicals are described in the text. Mean ± s.d are shown. **p < 0.01, two-tailed paired t-test.
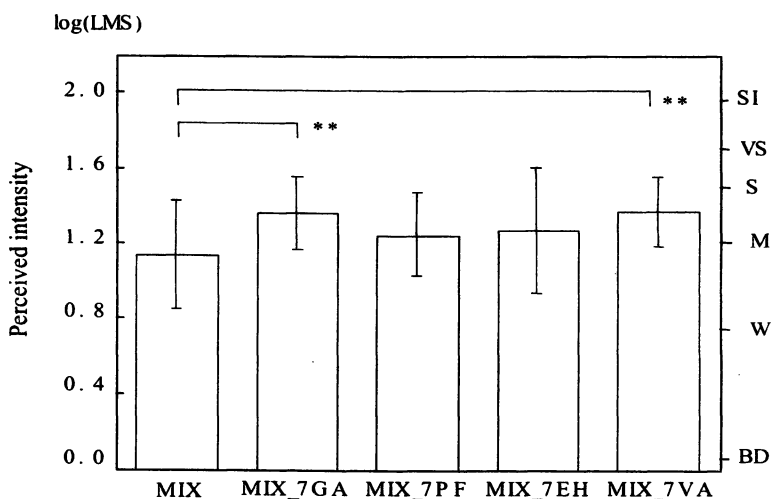
Figure 4. Odor intensity changes of chemicals in mixture. Abbreviations of chemicals are described in the text. Mean ± s.d. are shown **p< 0.01, two-tailed paired t-test.

-0.035 for C1 and 0.314 for C2. VA was plotted at 0.656 for C1 and -0.364 for C2. On the other hand, the score of quaternary mixture was plotted at -0.076 for C1 and 0.214 for C2. The score of the quaternary mixture was not near the centroid of all of the data. However, the quaternary mixture was located near the points of PF and EH. EH did not have a significant matching frequency with the quaternary mixture. Therefore, odor quality of the quaternary mixture seemed to be similar to PF odor quality. Additionally, the plot of VA was located very far away from those of other single compounds in Figure 5.

Figure 6 shows the differences of the increments between the single odor and mixed odor. GA, PF and EH have changed the increments significantly ($p < 0.05$, two-tailed pair wise t-test), meaning that odor intensities of PF, EH and GA were significantly suppressed in the mixture. In contrast, the intensity difference between single VA and VA in the mixture was not significant ($p = 0.36$, two-tailed pair wise t-test). VA intensity was not suppressed by the quaternary mixture. Greater odor intensity suppression between two odors may correspond to higher similarity of both odor qualities (*25, 26*). Therefore, the quaternary mixture has a quite similar odor quality to single PF and EH. This result does not contradict the odor similarity shown in Figure 5. Furthermore, as the odor change of VA single in Figure 6 was not different from that in the quaternary mixture, the VA odor did not interfere with the odor of the mixture because of the dissimilarity in odor quality.

The mixture suppression reported by Berglund *et al.* (*13*) indicates that intensity of odor mixtures can be expressed by the summation of each of the two individual odor intensity vectors. The resultant summation vector may also provide an indication of the degree of the similarity of both odor qualities. Olsson *et al.* (*25*) and Laing *et al.* (*14*) reported that mixture suppression was related to the individual constituent's odor qualities in binary mixtures. This idea was also derived from mathematical summation of odor intensity. Livermore and Laing further pointed out that odor type will influence the discrimination and identification of odorants in multicomponent odor mixtures (*17*). Our data, shown in Figure 5 and Figure 6, supported Olsson's refined model and indicate this model may be applicable for quaternary mixtures as well as binary mixtures. Thus, odor character in the quaternary mixture can be realized by summation of odor intensities of the individual components in the mixture but odor intensities themselves can be influenced by the odor quality of each odor component in the quaternary mixture. This conclusion can be deduced from the odor similarity difference of 4 chemicals by cross-matching tests and by odor intensity changes. In other words, it is implied that dissimilar odor chemicals maintain their odor intensity in mixtures relative to their odor intensity when perceived alone and the characteristic odor quality may also be maintained in the mixture. Therefore, some selected characterisitic aroma chemicals in a natural aroma oil (*27*) may maintain their odor intensity without any interference from the entire odor of the mixture because of the dissimilarity in odor qualities (*21*).

Table II. Observed and Expected Frequency of Cross-Matching Test

	EH			GA			PF			VA			Row total
	Observed Counts	Expected Frequency	χ^2	Observed Counts	Expected Frequency	χ^2	Observed Counts	Expected Frequency	χ^2	Observed Counts	Expected Frequency	χ^2	
GA-PF-EH-VA	6	7.10	0.171	8	8.88	0.087	10	5.92	2.815	5	7.10	0.622	29
EH-PH	13	6.86	5.503	5	8.57	1.488	8	5.71	0.914	2	6.86	3.441	28
GA-EH	3	6.86	2.170	20	8.57	15.238	3	5.71	1.289	2	6.86	3.441	28
GA-PF	5	6.86	0.503	15	8.57	4.821	6	5.71	0.014	2	6.86	3.441	28
GA-VA	5	6.61	0.393	8	8.27	0.009	5	5.51	0.047	9	6.61	0.862	27
VA-EH	10	6.86	1.441	0	8.57	8.571	3	5.71	1.289	15	6.86	9.670	28
VA-PF	6	6.86	0.107	4	8.57	2.438	5	5.71	0.089	13	6.86	5.503	28
Column Total	48			60			40			48			196

Abbreviations of chemicals are described in the text.

Table III. Summary of Correspondence Analysis

Dimension	Singular value	Inertia	Portion	Category Score			
				EH	GA	PF	VA
C1	0.53	0.28	0.72	0.268	-0.174	-0.035	0.655
C2	0.30	0.09	0.23	0.327	-0.179	0.314	-0.364
C3	0.15	0.02	0.06	-0.190	-0.041	0.025	0.033

Abbreviations of chemicals are described in the text.

Table IV. Summary of Item Score

Odor	Item Score		
	C1	C2	C3
GA-PF-EH-VA	-0.08	0.21	0.28
EH-PH	0.06	0.62	-0.15
GA-EH	-0.83	-0.29	-0.14
GA-PF	-0.56	0.01	0.00
GA-VA	0.09	-0.19	0.07
VA-EH	0.84	-0.15	-0.16
VA-PF	0.48	-0.23	0.09

Abbreviations of chemicals are described in the text.
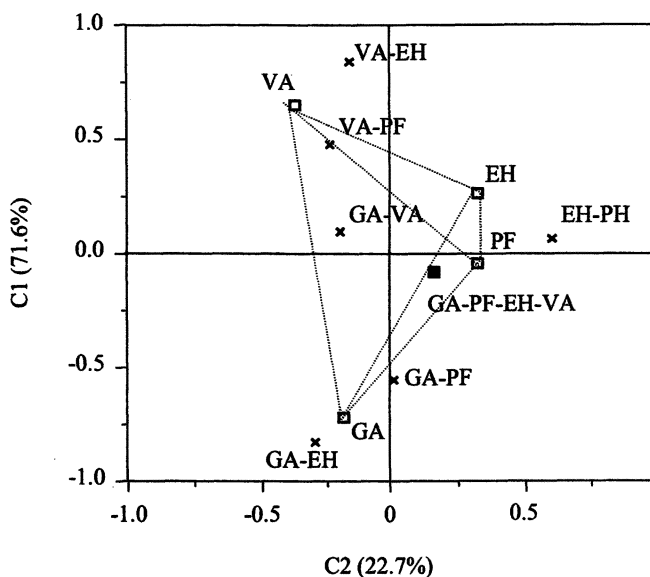
Figure 5. Correspondence analysis biplot. Abbreviations of chemicals are described in the text.
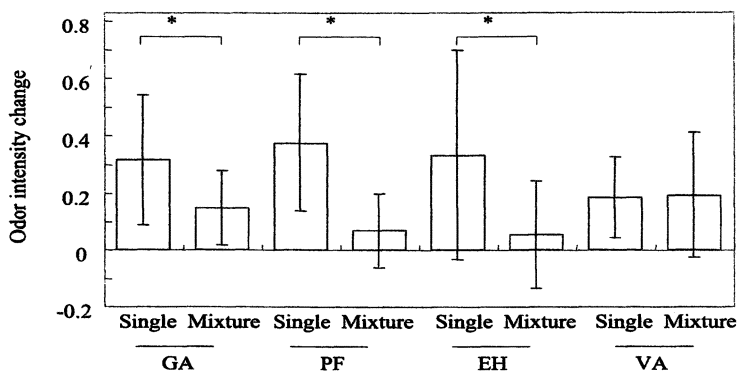
Figure 6. Change of odor intensity. Abbreviations of chemicals are described in the text. Mean ± s.d. are shown   *: p<0.05, two tailed paired t-test.

References

1. Bult, J. H. F.; Schifferstein, H. J. N.; Roozen, J. P.; Boronat, E. D.; Voragen, G. J.; Kroeze, H. E. *Chem. Senses* **2002**, *27*, 485-494.
2. Blank, I; Grosch, W. *J. Food Sci.* **1992**, *56*, 63-67.
3. Reiners, J.; Grosch, W. *J. Agric. Food Chem.* **1998**, *46*, 1754-2763.
4. Boonbumrung, S.; Tamura, H.; Mookdasanit, J.; Nakamoto, H.; Ishihara, M.; Yoshizawa, T; Varanyanond, W. *Food Sci. Technol. Res.* **2001**, *7*, 200-206.
5. Dravnieks, A.; O'Donnell, A. *J. Agric. Food Chem.* **1971**, *19*, 1049-1056.
6. Acree, T. E.; Barnard, J.; Cunningham, D. G. *Food Chem.* **1984**, *14*, 273-286.
7. Ullrich, F.; Grosch, W. *Z. Lebensm. Unters. Forsch.* **1987**, *184*, 277-282.
8. Pollien, P.; Ott, A.; Montigon, F.; Baumgartner, M.; Muñoz-Box, R.; Chaintreau, A. *J. Agric. Food Chem.* **1997**, *45*, 2630-2637.
9. van Ruth, S.M.; Roozen, J.P. *Food Chem.* **1994**, *51*, 165-170.
10. Pollien, P.; Fay, L.B.; Baumgartner, M.; Chaintreau, A. *Anal. Chem.* **1999**, *71*, 5391-5397.
11. Czerny, M.; Mayer, F.; Grosch, W. *J. Agric. Food Chem.* **1999**, *47*, 695-699.
12. Grosch, W. In: *Frontiers of Flavour Science, Proceedings of the 9th Weurman Flavor Research Symposium*, Schieberle, P. and Engel, K. H. Eds.; Deutsche Forschungsanstalt für Lebensmittelchemie: Garching, Germany, **2000**, pp. 213-219.
13. Berglund, B.; Berglund, U.; Lindvall, T.; Svensson, L. T. *Neurosci. Letter* **1973**, *328*, 309-313.
14. Laing, D. G.; Panhuber, H.; Willcox, M. E.; Pittman, E. A. *Physiol. Behav.* **1984**, *33*, 309-319.
15. Laing, D. G.; Willcox, M. E. *Chem. Senses* **1983**, *7*, 249-264.
16. Derby, C.D.: Ache, B. W.: Kennel, E. *Chem. Senses* **1985**, *10*, 301-316.
17. Livermore, A.; Laing, D.G. *Physiol. Behav.* **1998**, *65*, 311-320.
18. Livermore, A.; Laing, D.G. *J. Exp. Psychol. Hum. Percept. Perform.* **1996**, *22*, 267-277.
19. Green, B. G.; Shaffer, G. S.; Gilmore, M. M. *Chem. Senses* **1993**, *18*, 683-702.
20. Green, B. G.; Dalton, P.; Cowart, B.; Shaffer, G.; Rankin, K. R.; Higgins, *J. Chem. Senses* **1996**, *21*, 323-324.
21. Chida, M., Yamashita, K.; Izumiya, U.; Watanabe, K; Tamura, H. *J. Food Sci.* **2006**, *71*, S54-58.
22. Omori, F.; Higashi, H.; Chida, M.; Sone, Y.; Suhara, S. *Beitr Tabakforsch* **1999**, *18*, 131-146.
23. Takanami, Y.; Chida, M.; Hasebe, H.; Sone, Y.; Suhara, S. *J. Chromatogr. Sci.* **2003**, *41*, 317-322.

24. Chida, M.; Sone, Y.; Tamura H. *J. Agric. Food Chem.* **2004**, *52*, 7918-7924.
25. Olsson, M. J.; Cain, W. S. *Chem. Senses* **2000**, *25*, 493-499.
26. Lawless, H.T. *Sensory Processes* **1977**, *1*, 227-237.
27. Tamura, H.; Hata, Y.; Chida, M.; Yamashita, K. In: *Food Flavor: Chemistry, Sensory Evaluation and Biological Activity*; Tamura, H.; Ebeler S.; Kubota, K.; Takeoka, G., Eds.; ACS Symposium Series 988; American Chemical Society: Washington, D.C., **2008**, Chapter 20 pp 229-242.

Chapter 18

Some Mutual Interactions between Lactones and Other Aroma Constituents of Food Present in Concentrations below Their Odor Threshold

Yoko Hashimoto, Yuriko Ito, and Kikue Kubota

Department of Food and Nutritional Sciences, Graduate School of Humanities and Sciences, Ochanomizu University, Tokyo 112–8610, Japan

To investigate the contribution of subthreshold aroma constituents to the flavor of food, mutual interaction between saturated gamma- and delta lactones (C_6- C_{12}) and some minor odorants found in various food materials was investigated by sensory evaluation. By the triangle test, the detection odor threshold value of the mixture of (E)-2-hexenyl hexanoate and each of 4-octanolide, 5-hexanolide, 5-nonanolide and 5-decanolide at the ratio of 90:10 decreased significantly from 1 ppm to 0.1 ppm. The (Z)-3-hexenol and the mixture of (Z)-3-hexenol and saturated gamma and delta lactones (C_6- C_{12}) were evaluated by the same method. The odor intensity of the mixture of (Z)-3-hexenol and each of the following eight lactones such as 4- and 5-hexanolide, 4-octanolide, 4- and 5-nonanolides, 5-decanolide, and 4- and 5-undecanolides present in each concentration below their odor threshold was enhanced significantly. In addition, the odor intensity was enhanced significantly in the mixture of d-limonene + 4-hexanolide, vanillin + 5-hexanolide, and citronellol + both 4-, and 5-hexanolides. The effect of addition of 4-hexanolide on self-adaptation in concentration below its odor threshold to the

© 2008 American Chemical Society

207

model solution of some supra-threshold odorants was also studied. The presence of 4-hexanolide in the (E)-2-hexenyl hexanoate and (Z)-3-hexenol suppressed self-adaptation and the prolongation of the odor sensation by mutural interaction between two odorants was indicated.

To date, a large number of compounds have been identified as volatile constituents in foods. Recently, odor active compounds have been noted and GC-olfactometry is usually used to determine the potent odorants in the volatiles. It is often found in GC-olfactometry, that even a very small peak could be the most important compound to characterize the odor of the sample. However, there has been only a little work focused on subthreshold odor compounds and the mutual interaction among food flavor constituents. Hirvi and Honkanen (1) have pointed out that most of the blueberry flavor compounds were present below their odor threshold values and it seemed that synergism played an important role in the overall impression of the odor of blueberry. Our group has reported that the mixtures of 4-hexanolide and (E)-2-hexenyl hexanoate, and of 4-nonanolide and 4-hydroxy-2,5-dimethyl-3(2H)-furanone were the most odor-active compounds in the Chinese jasmine tea, even though these compounds were present in the infusion at concentrations below their odor threshold levels (2). We also described that the odor intensity of (E)-2-hexenyl hexanoate, (Z)-3-hexenol and indole were strengthened from subthreshold to supra-threshold level when 5% of each compound was replaced by 4-hexanolide (3). From these results we took interest in the mutual interaction among these subthreshold aroma compounds in food, and since lactones are found in various food materials, we examined the interaction of some lactones with some minor odorants found in foods.

This paper investigated whether or not other lactones besides 4-hexanolide exhibit synergistic interaction with (E)-2-hexenyl hexanoate or (Z)-3-hexenol. Moreover, other kinds of odorants which have the same interaction effect with 4-hexanolide or other lactones were examined. Additionally, the effect on self adaptation by adding 4-hexanolide in concentration below its odor threshold to the model solution of some supra-threshold odorants was also studied to investigate the diversity of mutual interaction among odorants.

Experimental

Sample Preparation

Authentic chemicals of saturated 4-heptanolide (99.4%), 4-octanolide (98.6%), 4-nonanolide (99.8%), 4-decanolide (98.1%), (E)-2-hexenyl hexanoate

(97.0%), (Z)-3-hexenol (99.2%), linalool (98.7%), alpha-terpineol (99.9%), geraniol (97.5%), 2-phenylethanol (96.9%), d-limonene (97.3%), vanillin (99.9%) and citronellol (97.0%) were purchased from Tokyo Kasei Kogyo (Tokyo, Japan) and 4-hexanolide (99.8%), 4-undecanolide (99.1%), 4-dodecanolide (98.6%), 5-hexanolide (99.9%), 5-octanolide (98.5%), 5-nonanolide (98.7%), 5-decanolide (98.5%), 5-undecanolide (98.9%), and 5-dodecanolide (98.4%) were purchased from Wako Pure Chemical Industries (Osaka, Japan). The individual chemicals dissolved in a small amount of propylene glycol were each diluted to the desired concentration with deodorized water with activated charcoal. A 20 mL of each sample solution was put in a 50 mL screw-capped glass bottle that was labeled randomly with a three-digit code and allowed to equilibrate for about 1 h at room temperature.

Selection of Panelists, Environmental Conditions and Experimental Design

To select panelists who had an accurate sense of smell, a screening test was conducted by having them evaluate the T & T olfactometer (Daiich Yakuhin Sangyo, Tokyo, Japan). The sensory analysis was conducted in a testing room that was quiet and provided with an air conditioner and ventilation fan. The randomized complete block design was adopted for the sensory analysis tests, except for the session during which the recognition odor threshold was measured.

Measurement of the Recognition Odor Threshold

Recognition odor threshold of lactones and other odorants used in this study was carried out to investigate the mutual interaction between lactones present in concentration below their threshold and other odorants. It was done by asking whether the panelist could identify the quality of the odor of the sample solution by the staircase procedure (3, 4). The most appropriate term to express the odor quality of each odorant was decided through several consultations with all the panelists. Three samples at different concentrations were presented for panelist consultation, e.g., 10 ppm, 100 ppm, and 1000 ppm for 4-hexanolide. The odor quality common in all concentrations of each solution was discussed and the term that best explained the odor quality of the odorant was decided. Each sample was presented twice to the panelists starting from the maximum concentration at intervals of 30 s. The minimum concentration at which the odor quality of a sample solution could be recognized with both trials exactly was considered as the recognition odor threshold.

Measurement of the Detection Odor Threshold

To investigate the synergistic interaction of lactones with (E)-2-hexenyl hexanoate, effect of lactones on the detection odor threshold of the mixture was examined. Triangle test was performed to measure the detection threshold. Each mixture was tested at six different concentrations ranging from 1×10^{-4} ppm to 10 ppm. Ten panelists underwent two sessions with an interval of at least 24 h between sessions. The results of the triangle tests were statistically analyzed (5). The minimum concentration at which a sample solution could be significantly distinguished from the blank sample (water) was considered as the detection odor threshold.

Measurement of the Odor Intensity

The labeled magnitude scale (LMS) (6,7) was used to measure the strength of the stimulus of each sample. The scale used in this study is shown in Figure 1. The magnitude of the sensation, which was determined by the position indicated on the scale by the panelists, was calculated as the percentage of the maximum strength. These were categorized as follows: barely detectable, 1.4; weak, 6.1; moderate, 17.2; strong, 35.4; very strong, 53.3; strongest imaginable, 100 (%). After at least a 24 h interval, the same panelists tested the same odorant, with 5% of the odorant having been replaced by a lactone, at the same concentration The raw data were normalized by converting to the logarithmic value (0.15-2.0) before statistical analyses using repeated-measure ANOVA.

B.D.	Weak	Moderate	Strong	Very Strong	Strongest Imaginable
(0.15)	(0.79)	(1.24)	(1.55)	(1.75)	(2.00)
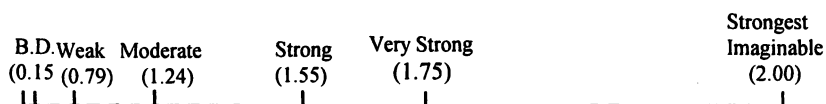
Figure 1. LMS that was used for the evaluation. It was devised by Green et al. (6). B.D. represents "barely detectable".

Self Adaptation

Three samples, 10 ppm (E)-2-hexenyl hexanoate, 10 ppm (E)-2-hexenyl hexanoate + 0.5 ppm 4-hexanolide, and 10 ppm (Z)-3-hexenol + 0.5 ppm 4-hexanolide, were prepared as adapting stimuli. The same sample with adapting stimulus and another sample with different stimulus in which 4-hexanolide was added or removed were prepared as test stimuli. The odor intensity was evaluated for the odor attribute of each odorant by using LMS. Before the test was started, it was made sure that the odor intensity of the two kinds of stimuli was almost equal. First, the panelist sniffed the adapting stimulus (control)

several times within 30 s and remembered the smell and then evaluated the odor intensity of the other test stimuli which was different from the adapting stimulus. Again the panelist sniffed the control for 30 s and evaluated the intensity of another test stimulus which was the same odorant with the adapting stimulus. This procedure was repeated several times for 10 minutes.

Results and Discussion

Mutual Interactions of Lactones with Other Odorants

Recognition Threshold Values of gamma- and delta-Lactones

Recognition threshold values of gamma- and delta-lactones in aqueous medium with carbon numbers six to twelve except 5-heptanolide, which was not available, were measured. Testing sample was prepared as a ten-fold dilution series in a decreasing order. A triangle test was applied. The distribution of odor threshold values by the panelists used here are shown in Figure 2. It is noted that the odor thresholds of both 4-hexanolide (80-10 ppm) and 5-hexanolides (1280-160 ppm) were much higher than the other lactones tested here.

Effect of Lactones on the Detection Odor Threshold Values of (E)-2-Hexenyl hexanoate

We reported in the previous paper (3) that the detection odor threshold level of the binary mixtures of (E)-2-hexenyl hexanoate and 4-hexanolide in the content ratios in % (weight/weight) of 95:5 and 90:10 fell to a lower value (0.1 ppm) compared to those of the single (E)-2-hexenyl hexanoate (1.0 ppm). In this study, we also examined the change of the threshold value in the same way by replacing the (E)-2-hexenyl hexanoate solution with 1.0 to 10% gamma- or delta-lactones described in Table I in concentrations below their odor threshold. In the concentration of 0.1 ppm which is below the odor threshold of (E)-2- hexenyl hexanoate, 0.01 ppm corresponded to 10% concentration of the original solution of the odorants and the concentration was much lower than the threshold of gamma-C_6, C_7, and C_8 lactones and delta-C_6, C_8, C_{10} and C_{12} lactones, so none of the panelists could perceive the odor of lactones. On the other hand 0.01 ppm is over threshold for gamma-C_9, C_{10}, C_{11}, and C_{12}, and delta-C_9 and C_{11} lactones. Then in the case of these lactones, the threshold of (E)-2-hexenyl hexanoate was measured at the replaced ratio of 99:1 to 95:5 (%). Ten panelists had two sessions of the triangle tests with an interval of at least 24 h between sessions. The numbers in Table I show the panelists who correctly selected the mixtures.

Concentration (ppm)	gamma-Lactones and Odor Attribute of Each Lactone						
	C_6 Sweet, Coconut-like	C_7 Sweet, Coconut-like	C_8 Fruity, Coconut-like	C_9 Fruity, Peach-like	C_{10} Peach-like Fatty, Pungent	C_{11} Peach-candy	C_{12} Green, Fruity, Peack-like
80.000	•						
40.000	•••••						
20.000	•••						
10.000	••						
5.000							
2.500							
1.250		••					
0.625		•••••					
0.313		•	•				
0.156		•••	•••	••••			
0.078			•••••	•••	•		
0.039				••	••		
0.020			••		••	•••	•••••
0.010					•	••••	
0.005					•••	•	•••••

Concentration (ppm)	delta-Lactones and Odor Attribute of Each Lactone					
	C_6 Caramel-like	C_8 Coconut-like	C_9 Sweet, Peach-like	C_{10} Sweet, Peach-like	C_{11} Fatty, Peach-like	C_{12} Sweet, Peach-like
1280.000	••••					
640.000	•					
320.000	••					
160.000	••••					
80.000						
″						
2.500						
1.250		••				
0.625		•••		•		••
0.313		•••		••		•
0.156		•		••	••••	•
0.078		••	•••	•••		•••••
0.039				•	••••	
0.020			••••		••	
0.010			•••			

Figure 2. Distribution of recognition odor threshold in water plotted for each panelist.

For (*E*)-2-hexenyl hexanoate alone, the detection level was 1.0 ppm. On the other hand, the threshold values of the binary solutions of (*E*)-2-hexenyl hexanoate and a lactone such as 4-hexanolide, 4-octanolide, 5-hexanolide, or 5-decanolide at the content ratio of 90:10, or 5-nonanolide at the content ratio of 97.5:2.5 also fell to a lower level (0.1 ppm) compared to that of (*E*)-2-hexenyl hexanoate alone. However, no effect was observed in the replacing ratio lower than 5% lactones (gamma-C_9, C_{10} and C_{12}, gamma- and delta-C_{11}) except 5-nonanolide. From these results, it was clarified that in addition to 4-hexanolide (*3*), three more lactones have the synergistic effect on the odor threshold value of (*E*)-2-hexenyl hexanoate.

Table I. Number of Panelists who Gave Correct Answers during the Triangle Tests

Concentration of Odorant (ppm)	Control[a]	Mixture of (E)-2-Hexenyl hexanoate and gamma-Lactone Content Ratio in Water (90:10)						
		C_6	C_7	C_8	C_9	C_{10}	C_{11}	C_{12}
10	20[**]	20[**]	20[**,e]	20[**,e]	20[**,e]	20[**,e]	20[**,e]	20[**,e]
1	20[**]	20[**]	20[**,b]	20[**,e]	20[**,e]	20[**,e]	20[**,e]	20[**,e]
1×10^{-1}	8	16[**]	11	15[**]	11[c]	8[e]	10[e]	11[e]
1×10^{-2}	3	9	7	1	4	2	4	4
1×10^{-3}	3	6	8	3	1	2	2	5
1×10^{-4}	1	5	3	3	2·	2	2	2
Concentration of Odorant (ppm)	Control[a]	Mixture of (E)-2-Hexenyl hexanoate and delta-Lactone Content Ratio in Water (90:10)						
		C_6	C_7	C_8	C_9	C_{10}	C_{11}	C_{12}
10	20[**]	20[**]	–	20[**,e]	20[**,e]	20[**,e]	20[**,e]	20[**,e]
1	20[**]	20[**]	–	20[**,c]	20[**,e]	20[**,e]	20[**,e]	20[**,e]
1×10^{-1}	8	16[**]	–	8	16[**,d]	14[**]	7[c]	9[e]
1×10^{-2}	3	10	–	3	3	2	2	2
1×10^{-3}	3	4	–	4	3	2	2	5
1×10^{-4}	1	0	–	0	0	1	3	5

Panelist number N=10 x 2. Asterisks represent the significance: **p<0.01.
[a] Control: (E)-2-hexenyl hexanoate.
[b, c, d, and e] The concentration of each lactone in the mixture was b: 8.0%, c: 5.0%, d: 2.5% and e: ≦1.0%,.

Effect of Lactones on the Green Odor Intensity of (Z)-3-Hexenol

The effect of lactones on the odor intensity of (Z)-3-hexenol using a labeled magnitude scale (LMS) from barely detectable to strongest imaginable was examined, and the raw data were normalized by converting to logarithmic values. In the previous paper (*3*), the aqueous solutions of (Z)-3-hexenol (green odor) at three concentration levels, was each replaced with 5% 4-hexanolide, and the intensity of each characteristic odor was sensorially evaluated. The odor intensity of (Z)-3-hexenol was enhanced significantly from 0.44 to 0.81 in the below concentration level (0.1 ppm). A similar phenomenon was also observed in the case of (E)-2-hexenyl hexanoate (*3*). Due to these facts, the change in the
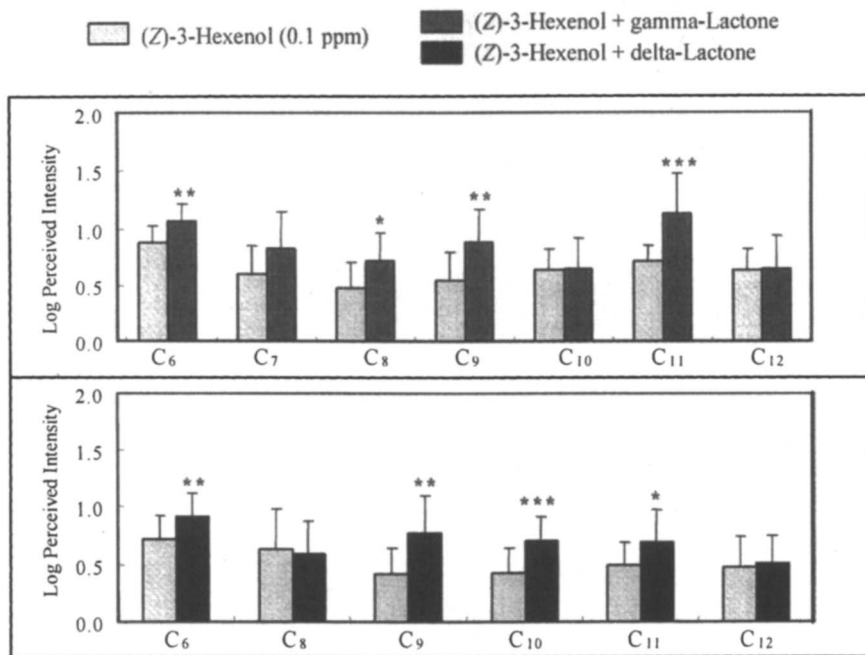
Figure 3. Intensity of (Z)-3-hexenol and the mixture of (Z)-3-hexenol and lactones at 0.1 ppm. The intensity was enhanced by mixing some lactones at the concentrations below their threshold (shown in Table I). Asterisks represent the significance by One-way ANOVA (***p<0.01, **p<0.05, *p<0.1).

intensity of green odor of (Z)-3-hexenol at 0.1 ppm which is the concentration below its threshold was investigated by replacing 5.0%-1.0% of the odorant with gamma- and delta-lactones (C_6-C_{12}). The odor intensity of the mixture of (Z)-3-hexenol and each of the following eight lactones such as 4- and 5-hexanolide, 4-octanolide, 4- and 5-nonanolides, 5-decanolide, and 4- and 5-undecanolides present in each concentration below their odor threshold was enhanced significantly as shown in Figure 3 by replacement in the same manner in Table I.

Other Odorants Affected by 4- or 5-Hexanolides

The effect of 4- or 5-hexanolide on the odor intensity of several odorants, such as linalool, alpha-terpineol, geraniol, 2-phenylethanol, 2-phenylethanal, *d*-limonene, vanillin, and citronellol, which were often found in concentrations

below their odor threshold in some foods, like blueberry (*8*), apricot (*9*), butter (*10*), and tea (*11*), was also examined in the same way with (*Z*)-3-hexenol. No positive change was found when linalool, α-terpineol, geraniol, 2-phenylethanol, and 2-phenylethanal were replaced with 4- or 5-hexanolide in the same manner as in Figure 3. However, consequently, the odor intensity was enhanced significantly in the mixture of *d*-limonene + 4-hexanolide, vanillin + 5-hexanolide, and citronellol + both 4-, and 5-hexanolides as shown in Figure 4. Interestingly, clear synergism was observed only in the subthreshold concentration.

From the results obtained here, although the relationship between chemical structure of odorant and effect of mutual interaction have not been clarified, it was suggested that the odor of some odorants that existed in concentrations below their odor threshold was perceived because of the synergistic effect with some lactones.

Effect of 4-Hexanolide on Self-adaptation

The effect of addition of 4-hexanolide on self-adaptation (*12*) in concentration below its odor threshold to the model solution of supra-threshold (*E*)-2-hexenyl hexanoate or (*Z*)-3-hexenol was studied to investigate the additional mutual interaction among odorants (*13*).

Three odorant samples were prepared as adapting stimuli (control) as shown in the caption of Figure 5. Two kinds of testing stimuli, 1) the same sample with adapting stimulus and 2) different stimulus in which 4-hexanolide was added or omitted were used for the individual odorant. In the case of (*E*)-2-hexenyl hexanoate as adapting stimulus (session A), the intensity of the test solution including 4-hexanolide did not change significantly as shown in Figure 5. On the other hand, the odor intensity of test stimulus of (*E*)-2-hexenyl hexanoate was reduced clearly 5 min after the test started by repeating the sniffing. This means that the self-adaptation of (*E*)-2-hexenyl hexanoate was suppressed by addition of 4-hexanolide. When the mixture of (*E*)-2-hexenyl hexanoate and 4-hexanolide was used as adapting sample (session B), the intensity of the test solution including 4-hexanolide did not change significantly, but that of (*E*)-2-hexenyl hexanoate solution was reduced in the same way with session A. Additionally, the same effect was found for (*Z*)-3-hexenol.

From these results it was suggested that the presence of 4-hexanolide suppressed self-adaptation and prolonged the odor sensation which could be explained as another mutual interaction between two odorants.

In conclusion, it was clarified partially in this study that in food materials, in addition to quantitatively main compounds, minor compounds such as lactones play an important role in characterizing odors because of mutual interactions.
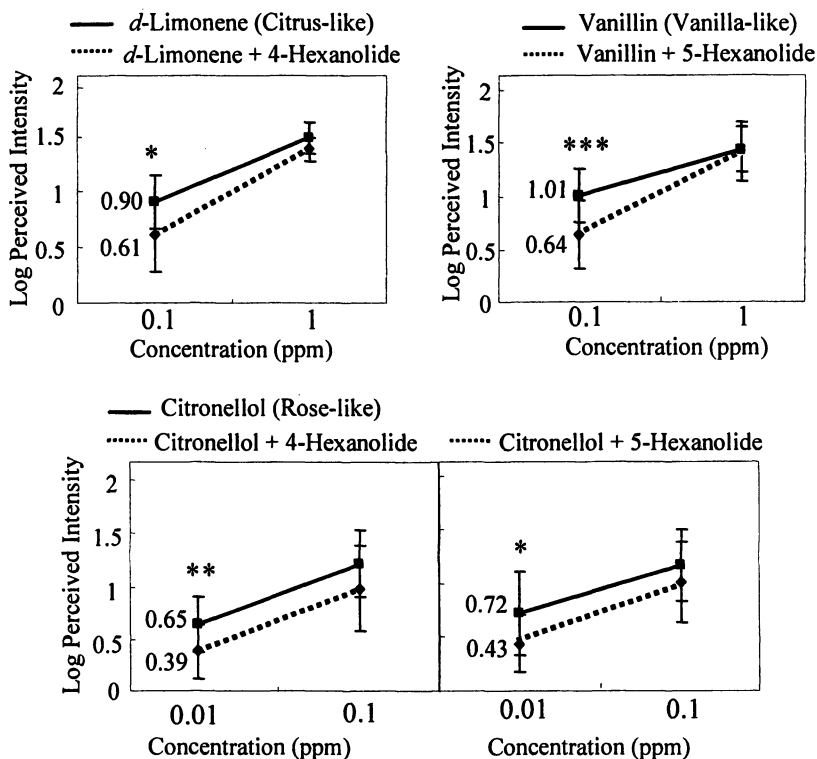
Figure 4. Results of LMS are shown for d-limonene, vanillin and citronellol by dotted line and the mixture with 4- or 5-hexanolide by full line (5% of each concentration). The tested odorants are shown with odor attributes. Asterisks represent the signicance by One-way ANOVA (***p<0.01, **p<0.5, *p<0.1).
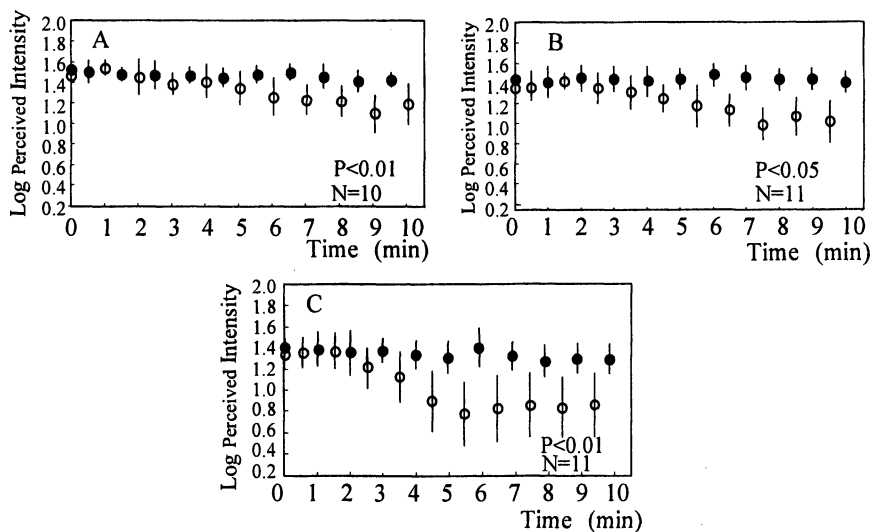
Figure 5. Results of self-adaptaton with LMS are shown by black circle for the mixture with 4-hexanolide and white circle for the odorant only. Significance was analysed by One-way ANOVA. A: adapting stimulus (AS), (E)-2-hexenyl hexanoate, testing stimuli (TS), (E)-2-hexenyl hexanoate and (E)-2-hexenyl hexanoate + 4-hexanolide; B: AS, (E)-2-hexenyl hexanoate + 4-hexanolide, TS, (E)-2-hexenyl hexanoate + 4-hexanolide and (E)-2-hexenyl hexanoate; C: AS, (Z)-3-hexenol + 4-hexanolide, TS, (Z)-3-hexenol + 4-hexanolide and (Z)-3-hexenol.

References

1. Hirvi, T.; Honkanen, E. *Z. Lebensm. Unters. Forsch.* **1983**, *176*, 346-349.
2. Ito, Y.; Sugimoto, A.; Kakuda, T.; Kubota, K. *J. Agric. Food Chem.* **2002**, *50*, 4878-4884.
3. Ito, Y.; Kubota, K. *Mol. Nutr. Food Res.* **2005**, *49*, 61-68.
4. Cornsweet, T. N. *Am. Jour. Psychol.* **1962**, *75*, 485-491.
5. Aishima, T. *Nippon Shokuhin Kagaku Kogaku Kaishi* **2001**, *48*, 378-392.
6. Green, B. G.; Shaffer, G. S.; Gilmore, M. M. *Chem. Senses* **1993**, *18*, 683-702.
7. Green, B. G.; Dalton, P.; Cowart, B.; Shaffer, G. S.; Rankin, K. R.; Higgins, J. *Chem. Senses* **1996**, *21*, 323-324.
8. Hirvi, T.; Honkanen, E. *J. Sci. Food Agric.* **1983**, *34*, 992-998.
9. Guichard, E.; Souty, M. *Z. Lebensm. Unters. Forsch.* **1988**, *186*, 301-307.
10. Peterson, D. G.; Reineccius, G. A. *Flavour Fragr. J.* **2003**, *18*, 215-220.
11. Kumazawa, K.; Masuda, H. *J. Agric. Food Chem.* **1999**, *47*, 5169-5172.
12. Cain, W. S.; Polak, E. H. *Chem. Senses* **1992**, *17*, 481-491.
13. Ito, Y.; Kubota, K. *Jpn. J. Taste Smell Res.* **2003**, *10*, 273-278.

Chapter 19

Why Naturally Healthy Berries May Be Seen as Unpleasant and Non-Appetitive?

M. A. Sandell[1,2,*], K. M. Tiitinen[2,3], T. A. Pohjanheimo[3],
H. P. Kallio[2], and P. A. S. Breslin[1]

[1]Monell Chemical Senses Center, 3500 Market Street,
Philadelphia, PA 19104
[2]Department of Biochemistry and Food Chemistry and [3]Functional Foods
Forum, University of Turku, FI–20014 Turku, Finland
[*]Corresponding author: mari.sandell@utu.fi

Given the variety of essential nutrients, berries such as strawberry, sea buckthorn and black currant are a good choice for a healthy food. However, they may be tasted as unpleasant for many reasons. Strawberry flavor depends on a ratio of sugars and acids and is sensitive to numerous pre- and post-harvesting factors. Both the sea buckthorn and black currant are naturally sour, bitter tasting and highly astringent. This chapter focuses on a relationship between chemical composition and flavor of selected berries. Taste is a strong component of berry flavor. In addition, quality of berry taste might also depend on which form of taste gene we possess. Consumers live in their own personal sensory worlds.

219

A high nutritional value has become one of the main factors in food and diet selection. In addition to the health promotion, the sensory qualities of food products are important to consumers. The sensory properties such as taste, aroma and appearance have a large impact on food choice. Strawberry (*Fragaria x ananassa* Duch.), sea buckthorn (*Hippophaë rhamnoides* L.) and black currant (*Ribes nigrum* L.) are regarded in their entities as high value food products and good sources of many nutritional components such as vitamin C, mineral elements and essential fatty acids (Table I). In general, they are full of water and their energy level is low. They are free of lactose, cholesterol and gluten. Compared to orange these berries would be also a good choice for daily diet and healthy lifestyle. Despite their positive nutritional value, consumers find them often unpleasant because of their strong sensory properties, especially taste.

Berries are rich in healthful phytonutrients and sensitive to quality changes in different ways. The chemical composition of strawberry and sea buckthorn depend on many factors such as genotype and origin of berry (*1,2*). In general, the correlation between food healthiness and flavorfulness might be weak. Many of the plant phytonutrients such as polyphenols, terpenes and carotenoids are thought to be bitter tasting (*3*). Consumers live in their own personal sensory worlds, which may result in their expressing very personal food preferences. This chapter focuses on the relationships of 1) healthfulness and unpleasant flavor and 2) chemical composition and flavor by using different berries as model food samples. The aim of this study was to better understand the physico-chemical factors of berry composition contributing the taste properties and furthermore on the pleasantness.

Table I. Average amounts (g) of selected nutritional components in 100 g of the edible portion of selected berries compared to orange.

	Strawberry	Sea buckthorn	Black currant	Orange
Energy (8000 kJ)	180	329	200	180
Fat	0.2	5	0.4	0.3
Organic acids	1.6	2	2.7	0.6
Sugars	8.4	6.3	7.8	8.9
Fibre (25)	1.9	6	5.8	2.1
Linolenic acid	0.064	0.250	0.045	0.032
Linoleic acid	0.064	0.090	0.027	0.028
Vitamin C (0.075)	0.060	0.165	0.120	0.051
Ca (0.080)	0.021	0.042	0.072	0.054
Na (0.001)	0.0007	0.0035	0.005	0.0016

NOTE: The recommended daily intakes are inside the parentheses.

SOURCE: National Public Health Institute of Finland (2005).

Materials and Methods

Strawberry

Varieties 'Senga Sengana', 'Jonsok', 'Korona', 'Polka', 'Honeoye', and 'Bounty' were cultivated by professional farmers in Finland (4). Following the industrial mode of action, class I –type of berries were frozen immediately after harvest, pooled and stored for analyses. Four flavor attributes (sweetness, sourness, strawberry, fruity) and six odor attributes (total odor, sweet, green, fruity, strawberry, off-odor) of strawberries were evaluated with a trained panel (n=14) applying quantitative sensory profiling (QSP). A structured line scale of 0-10 was used. The evaluation was performed at the sensory laboratory in accordance with the ISO 8589-1988 standard. In addition, tristimulus color (L*, a*, b*, Hue, chroma) was determined using a Minolta CR 200 color meter. For the determination of sugars (fructose, glucose and sucrose) and acids (citric and malic acid) in juice the gas chromatographic analysis of TMS-derivatives were applied and soluble solids (°Brix), pH and titratable acidity were also measured as well (4). Total sugars were calculated as a sum of sucrose, fructose and glucose, and total acids as a sum of citric and malic acid. Volatile aroma compounds were extracted from the berry headspace by purge and trap isolation and analysed by gas chromatography coupled to mass spectrometry (5). Mineral elements (Ca, Mg, K, Fe, Zn, Cu, Mn, Cd, Pb) were analyzed with atomic absorption spectrometer and vitamin C with HPLC (6). The standard statistical methods for parametric and non-parametric data matrices were applied in order to determine the differences between strawberry varieties. The characterization of samples were achieved by applying a principal component analysis (PCA) and multivariate regression analysis (PLS) to the data matrix using Unscrambler (Camo ASA, Oslo Norway).

Sea buckthorn

The varieties 'Avgustinka', 'Oranzhevaya', 'Botanicheskaya' 'Trofimovskaya', 'Prozcharachnaya', 'Prevoshodnaya' and 'Raisa' were grown in Finland (7). The berries were handpicked fully ripe, pooled after freezing, and stored for analyses. Sensory profile attributes (fruity, sweetness, sourness, astringency, fermented flavor, strength of odor) of sea buckthorn were evaluated with a trained panel (n=11) by applying quantitative sensory profiling (7). In addition to the sensory profiling, the influence of chemical treatments on astringency was studied with the trained sensory panel (8). Treatments were: 1) added sweetness with sucrose-fructose or aspartame-acesulfame K solutions, 2) modified pH with HCl or NaOH, 3) increased acidity with malic acid, 4) modified viscosity with

egg white, 5) combination of sweetness and pH. Sugars and acids were measured from juice of thawed berries (*7,9*). The tristimulus color was determined using the color meter (*7*). Statistics were performed as described in strawberry.

Black currant

Variety 'Mortti' grown in Finland was studied. Black currant berries were handpicked fully ripe and frozen for study. Sensory quality was evaluated with a trained panel (n = 35). Consumer panel (n = 42) was asked to rank different 'Mortti' samples based on their pleasantness. In addition, sugar and acid composition of black currant juice were studied as trimethylsilyl derivatives using gas chromatography (*4*). Vitamin C was determined from the diluted juices using a slight modification of a published HPLC method (*6*). Volatile aroma compounds were studied by SPME-GC-sniffing (*10*). Statistics were performed as described in strawberry. Preference mapping was used to explain the berry pleasantness by measured chemical composition.

Results and Discussion

Strawberry

In general strawberry is very pleasant. However, its fruit is very perishable and susceptible to injuries. The quality of the strawberry fruit is determined by the chemical composition, the nutritional quality and properties perceived by our chemical senses. Many kinds of natural preharvest (genotype, climate, cultivation, maturity) and postharvest (harvest, post-harvest handling, packing, pre-processing treatment) factors have an effect on flavor (*1*). Also the method of processing affects the quality.

Figure 1 shows the scatter plot of X-loading weights and Y-loadings with two dimensions from partial least square analysis. It shows the importance of the different variables for PC1 and PC2 components and can be used to understand the relationships between sensory properties (Y) and chemical composition (X). Our model includes 6 different strawberry varieties and all the measured variables, but only the most significant variables are included into the plot. Sweetness and strawberry flavor were located at the opposite side relative to sourness and strawberry odor. This indicates that taste is more important flavor component of frozen strawberries than odor. In general, the regression revealed that 66 % of all the chemical properties explained 80 % of the variance in

sensory properties when two components were used. The strongest predictors for sweetness within varieties were the ratio of total Sugars/Acid, sucrose, sum of fructose, glucose and sucrose (Sugars), methyl pentanoate, methyl butanoate, and pH.
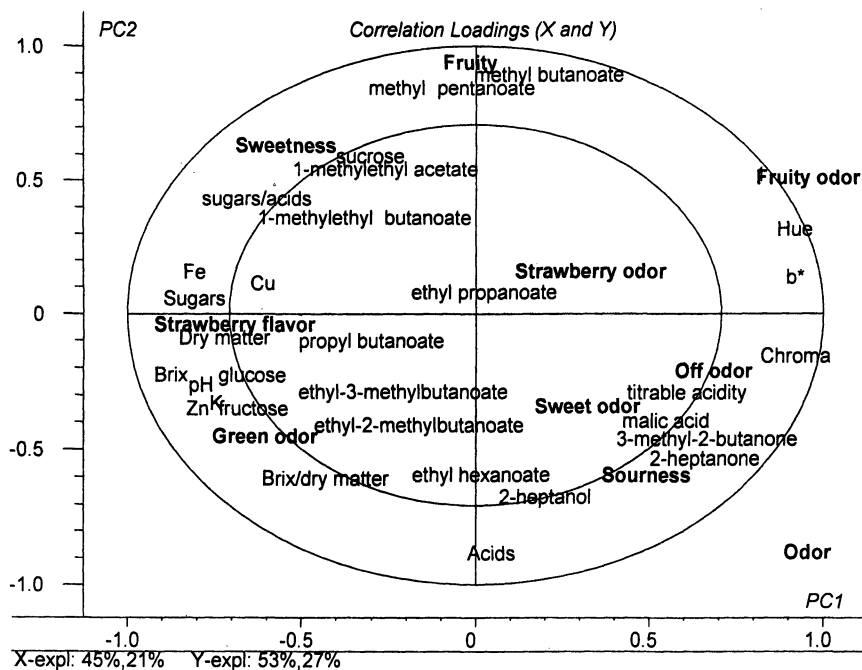
Figure 1. Strawberry PLS plot regarding the relations between sensory properties (bold) and instrumentally measured volatile compounds, sugars, acids, minerals and color variables. 'Sugars' is the sum of fructose, glucose and sucrose.' Acids' is the sum of malic and citric acid.

Practically, all the steps in the life cycle of a strawberry fruit from anthesis to processing have been studied and many details are known. However, data related to the influence of factors on the overall flavor of strawberry fruit are somewhat limited (*5,11,12*). The taste is mainly perceived through the composition of sugars and acids. Volatile compounds of strawberry are responsible for the ortho- and retronasal part of the strawberry flavor. Although especially volatile aroma compounds of strawberry are important and well studied (*13,14,15*), for consumers one of the main quality factors measuring the good flavor of strawberry may be simply the ratio of sugar and acid components.

Sea buckthorn

In general the aroma of sea buckthorn is mild. However, the sourness and astringency of sea buckthorn are easily perceived as strong sensations. Because of these properties sea buckthorn berries are usually not liked by consumers. The berry is rich in malic acid. Of sugars, sea buckthorn contains only fructose and glucose and no sucrose (7,9,16). From a nutritional point of view sea buckthorn berry and seed oil are rich in flavonoids, vitamin C and many oil-soluble bioactive phytonutrients such as tocopherols, tocotrienols, carotenoids and plant sterols that act like antioxidants (2,17,18,19,20, 21).
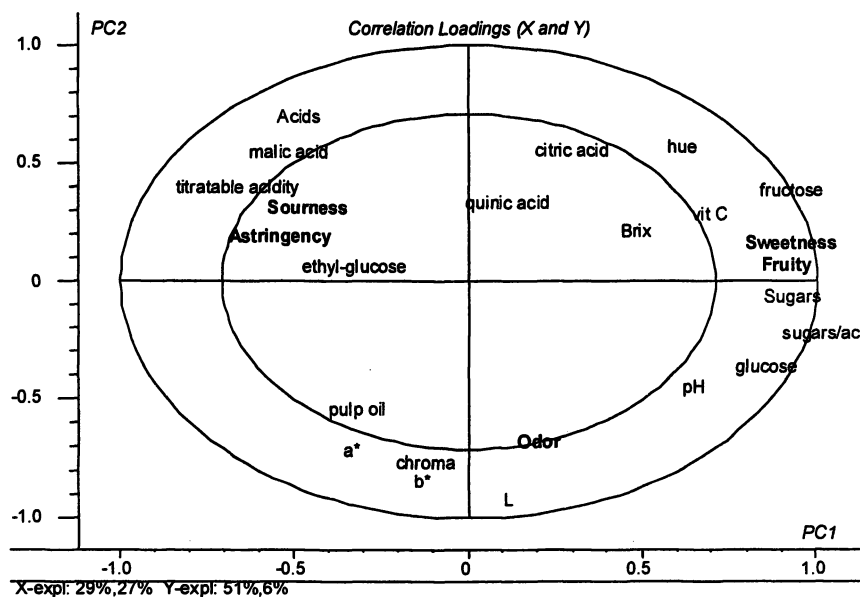
Figure 2. Sea buckthorn PLS plot regarding the relations between sensory properties (bold) and instrumentally measured sugars, acids and color parameters. Reproduced with permission from reference 22. Copyright 2006.

Figure 2 is formed from the sensory profile, the sugar and acid composition and different color properties. The regression revealed that 65 % of all the chemical properties explained 56 % of the variance in sensory properties when two components were used. Total sugar and sugar/acid ratio correlated positively with sweetness, and negatively with sourness and astringency. Total acid and titratable acidity correlated positively with sourness and negatively with sweetness. Fruity flavor had a positive correlation both with total sugar and sugar/acid ratio.

Astringency in wines is an important sensory property and is caused by the presence of acids and phenolic compounds (*22*). However, in sea buckthorn the astingency is not a pleasant sensory dimension (*23*). When our trained panel ranked the treated juice samples by their astringency, the sensation decreased when the juice was sweetened with fructose and glucose. This was also found with sweeteners of equal sweetness. There was no difference whether the sweetening was performed with sugars or sweeteners. An increase in malic acid concentration also increased the astringency. The influence on astringency was not significant when the pH of untreated juice was lowered with HCl to an equivalent level of juice with malic acid addition. An increase in the juice's original pH of 2.9 to 3.1 either with NaOH or egg white decreased astringency. Neither proteins nor increased viscosity in juice with egg white affected the perception. This study suggest that astringency in sea buckthorn is mainly caused by malic acid and the effect of protein precipating phenolic compounds is not so evident.

Black currant

Black currant is a good source of vitamins, phenolic compounds, fiber and essential amino acids (*24,25,26*). Its aroma is very unique and mainly caused by terpenes and esters (*10*). PCA-biplot (Figure 3) shows the relationship between measured non-volatiles and volatile compounds of black currant berries. In general, consumers find the berry as sour and bitter tasting. Based on preference mapping results black currant pleasantness had a positive correlation with sucrose, fructose and malic acid.

Quality of berry taste and taste genes

Each human carries their own distinctive set of the taste receptors, which gives them a unique perception of taste compounds and foods (*27,28*). For example, the perception of bitterness is known to be very complex and involves twenty-five putative TAS2R receptors. Humans' ability to detect bitter compounds that contain a thiourea (-N-C=S) moiety, such as phenylthiocarbamide (PTC) and its chemical relative propylthiouracil (PROP), show a bimodal distribution that distinguishes two main phenotypes, sensitive and insensitive (*29*). This difference has been linked to variability in a single gene, *hTAS2R38* gene, a member of the TAS2R family of bitter taste receptors.

The sweet fruit Bignay (*Antidesma bunius*) is used as raw material in jam and wine manufacturing. Human's sensitivity to bitterness from Bignay is known to correlate inversely with their ability to taste bitterness of PTC (*30*) and moreover with the *hTAS2R38* gene (*31*). While PTC-sensitive subjects rated

PC2   **Bi-plot**

pH

ethyl butanoate

ethyl 3-methylbutanoate

methyl butanoate

camphene   *cis*-ocimene

Malic acid
          alpha-terpinene   **Brix**   *trans*-ocimene
Fructose
          Sucrose   beta-myrcene
toluene
          alpha-phellandrene   sabinene

Glucose

hexanal   **Citric acid**

                                   limonene
          alpha-pinene   methyl hexanoate

beta-pinene   terpinolene

                       d-3-carene   **PC1**

X-expl: 65%,20%
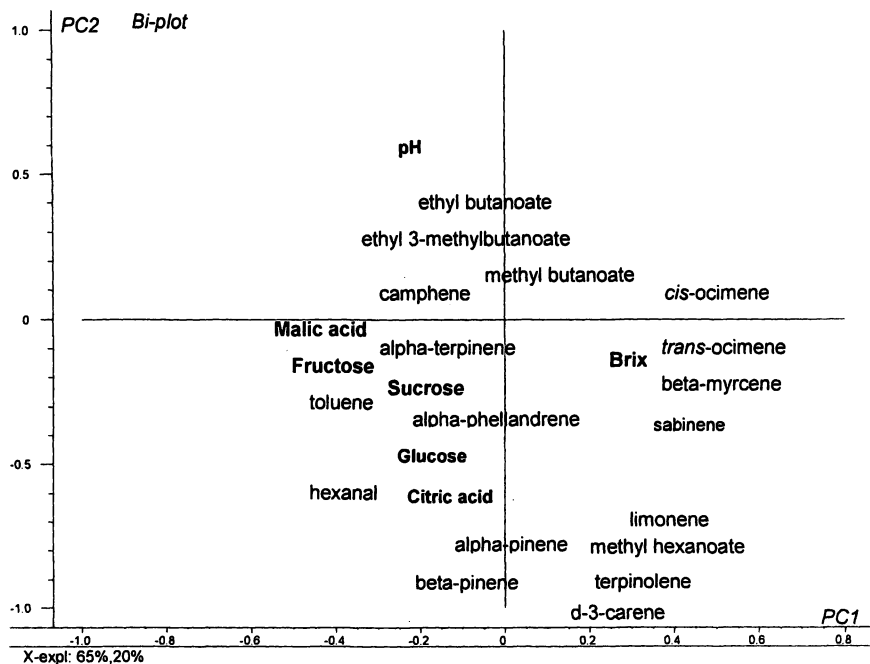
Figure 3. Black currant PCA plot of non-volatile sugars and acids (bold) and volatile compounds.

bignay berry as sweet, PTC-insensitive subjects rated and described the same berry as bitter. PTC-sensitivity of every subject was tested with PTC following good sensory evaluation protocol and practise. The relationships among genotypes and perceived berry bitterness emphasize the role that taste genetics play in individual differences in berry perception.

Conclusions

Strawberry, sea buckthorn and black currant are sources of many essential nutritive compounds. However, their flavor may be very unpleasant for consumers. Although aroma of these berries is an important sensory dimension, the effect of their taste on overall flavor and pleasantness is even more important. Different pre-and post-harvest factors are known to change the quality of berries for human consumers. Chemosensory psychogenomic studies have recently shown common genetic variations in human taste genes that cause individual difference in taste perception also with berries as well.

References

1. Hakala, M. Factors affecting the internal quality of strawberry (*Fragaria* x *ananassa* Duch.) fruit. Ph.D. thesis, University of Turku, Finland, 2002, p 89.
2. Yang, B. Lipophilic components of sea buckthorn (*Hippophae rhamnoides*) seeds and berries and physiological effects of sea buckthorn oils. Ph.D. thesis, University of Turku, Finland, 2001, p 110.
3. Drewnowski, A.; Gomez-Carneros, C. *Am. J. Clin. Nutr.* **2000**, *72*, 1424-1435.
4. Kallio, H.; Hakala, M.; Pelkkikangas, A. M.; Lapveteläinen, A. *Eur. Food Res. Technol.* **2000**, *212*, 81-85.
5. Hakala, M.; Lapveteläinen, A.; Kallio, H. *J. Agric. Food Chem.* **2002**, *50*, 1133-1142.
6. Hakala, M.; Lapveteläinen, A.; Huopalahti, R.; Kallio, H.; Tahvonen, R. *J. Food Comp. Anal.* **2003**, *16* (1), 67-80.
7. Tiitinen, K.; Hakala, M.; Kallio, H. *J. Agric. Food Chem.* **2005**, *53*, 1692-1699.
8. Tiitinen, K.; Järvinen, A.; Hakala, M.; Kallio, H. In abstract book of 6th Pangborn Sensory Science Symposium, Yorkshire, UK, **2005**, p 37.
9. Tiitinen, K.; Yang, B.; Haraldsson, G.; Jonsdottir, S.; Kallio, H. *J. Agric. Food Chem.* **2006**, *54*, 2508-2513.
10. Tiitinen, K.; Hakala, M.; Pohjanheimo, T.; Tahvonen, R; Kallio, H. In *State-of-the-Art in Flavour Chemistry and Biology*; Hofmann, T.; Rothe, M.; Schieberle, P., Eds.; Deutsche Forschungsanstalt für Lebensmittelchemie: Garching; 2005, pp 518-522.
11. Forney, C.; Kalt, W.; Jordan, M. *HortScience*, **2000**, *35*(6), 1022-1026.
12. Honkanen, E.; Hirvi, T. In *Food Flavours. Part C: The Flavour of Fruits*; Morton, I. D.; MacLeod, A. J., Eds.; *Elsevier*, **1990**, pp 125-193.
13. Zabetakis, I.; Holden, M. *J. Sci. Food Agric.* **1997**, *74*, 421-434.
14. Dirinck, P.; De Pooter, H.; Willaert, G.; Schamp, N. *J. Agric. Food Chem.* **1981**, *29*, 316-321.
15. Larsen, M.; Poll, L. Z. *Lebensm. Unters. Forsch.* **1992**, *195*, 120-123.
16. Ma, Z.; Cui, Y.; Feng, G. Studies on the fruit character and biochemical compositions of some forms within Chinese sea buckthorn (*Hippophae rhamnoides* ssp. *sinensis*) in Shanxi, China. In *Proceedings of the International Symposium on Sea Buckthorn (H. rhamnoides L.)*; Feng et al. (eds). The Secretariat of the International Symposium on Sea Buckthorn, Xian, China; **1989**, pp 106-112.
17. Kallio, H.; Yang, B.; Peippo, P.; Tahvonen, R.; Pan, R. *J. Agric. Food Chem.*, **2002**, *50*, 3004-3009.
18. Rösch, D.; Bergman, M.; Knorr, D.; Kroh, L. *J. Agric. Food Chem.* **2003**, *51*, 4233-4239.

19. Yang, B.; Kallio, H. *J. Food Compos. Anal.* **2002**, *15*, 143-157.
20. Yang, B.; Kallio, H. *J. Agric. Food Chem.* **2001**, *49*, 1939-1947.
21. Yang, B.; Karlsson, R.; Oksman, P.; Kallio, H. *J. Agric. Food Chem.* **2001**, *49*, 5620-5629.
22. Tiitinen, K. Factors contributing to sea buckthorn (*Hippophae rhamnoides* L.). Ph.D. thesis, University of Turku, Finland, 2006, p 67.
23. Tang, X.; Kälviäinen, N.; Tuorila, H. *Lebensm. Wiss. u. Technol.* **2001**, *34*, 102-110.
24. Johansson, A.; Laakso, P.; Kallio, H. *Lebensm. Untersuch. u. Forsch.* **1997**, *204*, 300-307.
25. Tahvonen, R.; Schwab, U.; Yli-Jokipii, K; Mykkänen, H.; Kallio, H. *J. Nutr. Biochem.* **2005**, *16*, 353-359.
26. Kallio, H.; Nieminen, R.; Tuomasjukka, S.; Hakala, M. *J. Agric. Food Chem.* **2006**, *54*, 457-462.
27. Kim, U.; Breslin, P. A. S.; Reed, D.; Drayna, D. *J. Dent. Res.* **2004**, *83*, 448-453.
28. Mueller, K.; Hoon, M.; Erlenbach, I.; Chandrashekar, J.; Zuker, C.; Ryba, N. *Nature* **2005**, *434*, 225-229.
29. Bufe, B.; Breslin, P. A. S.; Kuhn, C.; Reed, D.; Tharp, C.; Slack, J.; Kim, U; Drayna, D.; Meyerhof, W. *Current Biology* **2005**, *15*, 322-327.
30. Henkin, R.; Gillis, W. *Nature* **1977**, *265*, 536-537.
31. Tharp, C.; Tharp, A; Alarcon, S.; Reed, D.; Breslin, P. A. S. In *Proceeding Book of AChemS XXVII*, **2005**, Sarasota, FL.

Chapter 20

Picking Aroma Character Compounds in *Citrus limon* Oils by Using Odor Thresholds in Aroma Mixtures

Hirotoshi Tamura, Yuko Hata, Masahiro Chida, and Keiko Yamashita

Department of Biochemistry and Food Science, Kagawa University, 2393 Miki-Cho, Kagawa 761–0795, Japan

Seven aroma chemicals identified in *Citrus limon* oils were selected as potent character-impact compounds on the basis of their limited odor unit values (Lod). Those seven compounds selected have high aroma intensities. The recognition threshold of a target lemon oil against a reference lime oil was 32.9 ppm. A model oil (Oil_{model7}) prepared by mixing the natural abundance of the 7 impact chemicals from *Citrus limon*, gave a recognition threshold against the target lemon oil at 55.1 ppm, indicating a high similarity of the model to the target oil in aroma quality. Thus, the selected 7 compounds having high aroma intensities contributed to the high similarity of aroma quality to the target oil. Odor detection thresholds of 10 chemicals that have high Lod values were comparably determined in water and in model oils at 329 ppm by using an omission test and a cumulative test. Consequently, the odor detection threshold of geranial in the 329 ppm $Oil_{model10}$ was 2.86 ppm and the change of the value was 30 fold higher than

© 2008 American Chemical Society

229

that in water and the smallest change among other nine compounds. So, the greatest contast in aroma quality of geranial against the aroma of the model oil was proved. The important contribution of geranial to lemon aroma was attributed to the relative immutableness of the odor threshold between water and model oil mixture.

The characterization of food aroma plays an important role in the production of high-quality processed foods and in the quality control of foods. Without sensory tests, the evaluation of aroma quality based solely on instrumental analysis and statistical analysis is impossible and makes no realistic sense; meanwhile sensory testing is time-consuming and may not be reproducible and quantitative without significant training of panelists. Sensory testing coupled with chemical instrumental analysis has been intensively applied in order to find characteristic aroma components that contribute to the highest sensory impact, such as 'character-impact compounds' or 'contributory flavor compounds' (1). GC-Olfactometry (GC-O) (2, 3) and the odor unit (Uo) method (4-6) have been typical and suitable tools for the elucidation of potent aroma chemicals, leading to further steps for the reconstruction of nature identical model oils from the viewpoint of aroma quality. These analytical-oriented sensory judgments have been adopted to identify odor detection limits of individual compounds and then the high impact aroma chemicals are further evaluated in mixtures to determine their effects on aroma intensity and aroma quality.

For the quality assessment, we have felt that more sensory-oriented judgments of the aroma impacts of chemicals in an oil mixture is practically lacking. Thus, aroma impact chemicals are always smelled with other volatile compounds present at supra-threshold in our daily life. In order to bridge the gap on sensory assessment of isolated single chemicals and chemicals in a complicated oil mixture, omission tests (7) and aroma recognition tests (8) have been introduced. The objective of the present study is to introduce further trials toward picking character-impact compounds in supra-threshold volatile mixtures by using odor unit techniques.

Materials and Methods

Essential Oils

Citrus limon fruits (18 kg) imported from Sunkist Growers, Inc. (Sherman Oaks, California, U.S.A.) were purchased from a local market and then immediately peeled (6.6 kg yield). Finally, the essential oil (51.2 g) was isolated

by the modified solvent extraction method reported in a previous paper (9). The lemon oils did not contain any solvents.

Reagents

Thirty-three authentic chemicals were purchased from Fluka Chemika-BioChemika (Tokyo, Japan), Wako Pure Chemical Industries, Ltd. (Osaka, Japan) and the Aldrich Chemical Co., Inc. (Milwaukee, Wisconsin, U.S.A.). Geranial was synthesized from geraniol by the oxidation with manganese dioxide at -10°C for 3 h. The purity of geranial was more than 86%.

GC and GC-MS analysis

GC analysis was carried out on a Hewlett Packard 6890 (Agilent Technologies, Inc., CA), equipped with a flame ionization detector (FID) with a Shimadzu C-R6A Chromatopack integrator. The GC separation was carried out by using a DB-Wax fused silica column, (60 m X 0.25 mm i.d.; J&W Scientific, Folsom, CA). GC-MS was conducted on a JEOL JMS-SX102A. Analytical conditions of GC and GC-MS were as follows: detector and injector temperatures were kept at 230 °C; oven temperature was programmed from 50°C to 210°C at 2°C/min and held at the final temperature for 60 min; split ratio was 1:50; carrier gas was He (1.0 mL/min). Identification of volatile constituents was achieved by comparison of their GC retention indices and mass spectra with those of standard compounds and published data (10). The quantities of compounds identified were calculated based on the gas chromatographic area percentage, the oil weight and relative response factor for FID, and then expressed as ppm.

Odor Unit Values

The individual concentrations in the oil were calculated on the basis of the oil weight and peak area % of each component, determined by GC-FID. Thus, the concentration of individual volatile compounds was determined by the ratio of the oil weight of each volatile component to the total oil weight and then expressed as parts per million. To obtain precise data for each chemical concentration, GC-FID responses of individual compounds were taken into account by determining their FID response factors relative to that of limonene. The odor unit values of 34 chemicals were calculated according to the concept of the odor unit proposed by Rothe and Thomas (11) and Guadagni et al. (4) as follows,

$$Uo= \frac{\text{Concentration of the volatile in food (ppm)}}{\text{Detection threshold (ppm)}} \qquad (1)$$

Odor Recognition Threshold

The recognition threshold is the concentration at which panelists can recognize the differences of the concentration and the quality in two kinds of oils presented. One series of the sensory test was composed of 8 samples, including 4 aqueous solutions of a target oil (lemon oil) at four different concentrations (300 ppm, 30 ppm, 3 ppm and 0.3 ppm), 3 aqueous solutions of a reference oil (lime oil) at three different concentrations (100 ppm, 10 ppm and 1 ppm) and one of odorless water. The panel members were asked to distinguish which 4 cups contain the target oil, and which 3 cups contain the reference oil and then to rearrange the four cups of the target oil in the order from the highest to the lowest concentration. In another series of the sensory test, 100 ppm, 10 ppm, 1 ppm and 0.1 ppm of the target oil were tested. The minimum concentration at which the panel members correctly distinguished the target oil was defined as the recognition threshold (12). The average of the recognition threshold values obtained by 16 panel members (6 males and 10 females) was determined by the means of the logarithmic values of the individual recognition threshold values.

Lemon oil was dissolved in a small amount of methanol. The solution was diluted with distilled water until the final concentration of methanol was less than 200 ppm at which concentration the panel members judged the methanol odor was no longer detected.

Limited Odor Unit Values

The potent character-impact components of lemon were selected according to their limited odor unit (Lod, this abbreviation is derived from the use of "detection" threshold as the denominator for the limited odor unit as shown below) values in the manner reported previously (12). The Lod equation is as follows:

$$\text{Limited odor unit (Lod)} = \frac{Cr}{Td} \qquad (2)$$

where: Cr is the concentration of the individual components at the recognition threshold of lemon oil (ppm) against lime oil, and Td is the detection threshold of the individual volatile components (ppm).

Sensory Tests

With a line scale, the panel members rated the intensity of a lemon aroma by making a mark on a horizontal line. The marked point corresponds to the impact of the perceived stimulus. The length of the line was 14 cm with anchors at both ends. The left end of the scale corresponded to "none" while the right end was standardized by the natural aroma of lemon peel. The panel consisted of more than 9 males and 8 females. Their ages ranged from 20 to 48 years with a mean of 22 years. Model samples were prepared according to the natural abundance of each volatile compound in the original oil and then the oils were dissolved in a minimum required methanol and then diluted with water to adjust the concentration to 10,000 ppm, 1,000 ppm and 100 ppm, respectively. Lemon oil was also diluted to the same concentration as described above. Two-way analysis of variance (F-test, $P = 0.05$) was performed as a statistical tool. The statistical significance was judged by studentized range quantiles ($P = 0.05$).

Results and Discussion

Similarity of Aroma Quality Between the Model Oils and Natural Lemon

GC-MS analysis of volatile oils from *Citrus limon* allowed us to identify 11 hydrocarbon compounds and 25 oxygenated compounds. For the validity check of key aroma compounds, recognition thresholds of two model oils mixed either with 3 compounds (limonene, geraniol, 1,8-cineole) or with 7 compounds (limonene, geraniol, 1,8-cineole, γ-terpinene, linalool, geranial and terpinolene) that have the highest Uo values (Table I) were determined against the original, target lemon oil. Recognition thresholds of the two lemon model oils, Oil_{model3} and Oil_{model7} against the target lemon oil were 20.1 ppm and 55.1 ppm, respectively (Figure 1).

Furthermore, the recognition threshold of the target lemon oil against a lime oil was determined as 32.5 ppm whereas recognition thresholds of orange against Iyo-orange and *Citrus sudachi* against lemon were 4.62 and 0.18, respectively (*13*). Therefore, the mean recognition threshold of lemon against lime at 32.5 ppm seems to be a relatively high value indicating that the lemon and lime show a high similarity in aroma quality. Thefore in our study, the differences in the recognition threshold values between the target lemon oil and the model oils can be used as an indication of the similarity of their aroma quality. The similarity among lemon, lime and sudachi aromas are reported by cluster analysis based on sensory evaluation (*6*). Since the odor threshold of Oil_{model7} at 55.1 ppm is greater than the recognition threshold between lemon oil and lime oil, the lemon aroma showed a greater similarity to the model oil than lime oil. Therefore, 7

Table I. Representative Volatile Compounds in *Citrus limon* Oil

No.	Compound	RI^1	Conc (%)	Th (ppm)	Lod^2
1	(+)-limonene	1218	64.68	0.506	42.1
2	geraniol	1823	0.56	0.009	21.7
3	1,8-cineole	1198	0.49	0.009	18.3
4	γ-terpinene	1239	9.82	0.264	12.2
5	linalool	1517	0.33	0.010	10.4
6	geranial	1720	2.61	0.083	10.3
7	terpinolene	1277	0.48	0.041	3.9
8	β-pinene	1122	11.26	1.304	2.8
9	geranyl acetate	1744	1.26	0.155	2.7
10	hexyl acetate	1274	1.00	0.133	2.5
11	myrcene	1169	1.57	0.307	1.7
12	α-pinene	1035	1.07	0.206	1.7
13	decanal	1471	0.09	0.032	0.9
14	neryl acetate	1702	2.02	1.205	0.6
15	heptyl acetate	1380	0.16	0.220	0.2

[1]DB-WAX, 60 X 0.25mm I.D.

[2]Lod of lemon oil was determined by the recognition threshold (32.9 ppm) against lime oil
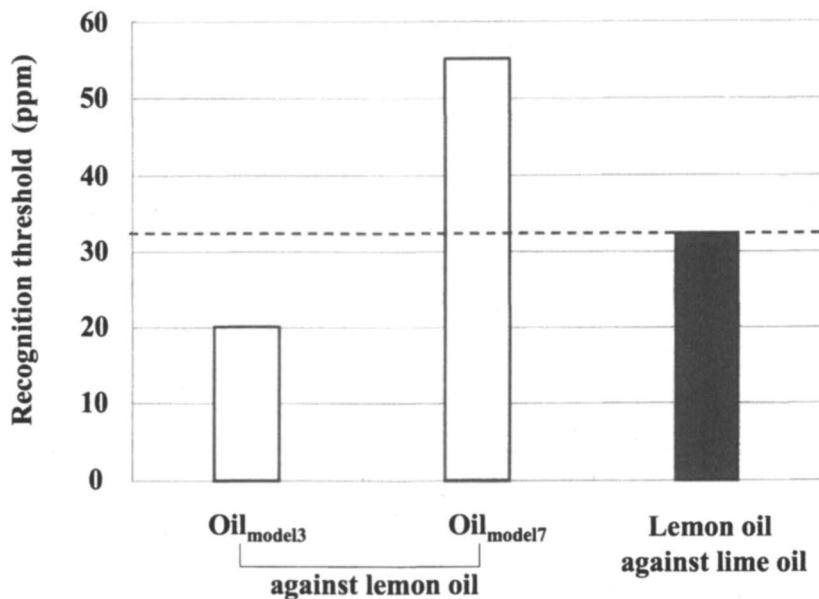
Figure 1. Odor recognition thresholds of Oil_{model3} and Oil_{model7} against lemon oil.

compounds (limonene, geraniol, 1,8-cineole, γ-terpinene, linalool, geranial and terpinolene) that were selected on the basis of greater Lod values were chosen to be one of the representative model oils of natural lemon oil.

Sensory Assessment of Lemon Oils and the Model Oil Mixtures at the Supra-thresholds

Sensory researchers have tried to measure human perception as precisely as possible (*14, 15*). To be able to quantify the impressions of test subjects as effectively as possible, different kinds of sensory scales have been developed. In our experiments, a line scale was used to rate the similarity of model lemon oil mixtures to reference samples and was adopted to obtain more information about aroma quality and similarity. Two model oils (Oil_{model3} and Oil_{model7}) prepared from three chemicals (limonene, geraniol and 1,8-cineole) and seven chemicals (limonene, geraniol, 1,8-cineole, γ-terpinene, linalool, geranial and terpinolene) were prepared according to the relative natural abundance of the compounds in the original lemon oil. The model mixtures were then diluted to 10,000 ppm, 1,000 ppm and 100 ppm. The similarity of model mixtures to lemon peel were rated (Figure 2). There was no significant difference in the ratings among 17

panel members, therefore, it is said that the panel members were quite homogeneous in their responses. One hundred ppm solution of the target lemon oil was weak in intensity and the quality was least similar to the lemon peel aroma. At 10,000 ppm and 1,000 ppm, Oil_{model3} and Oil_{model7} aromas were the closest to natural lemon peel aroma, respectively.
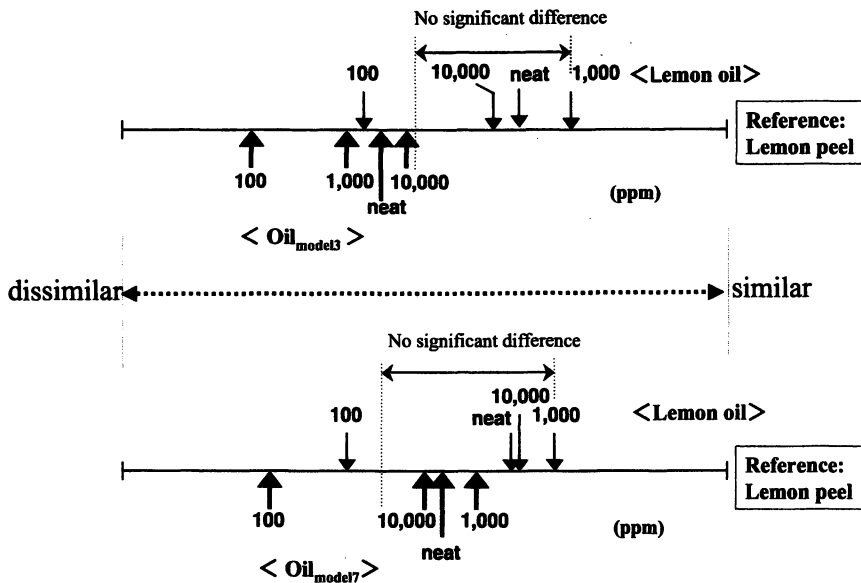
Figure 2. Sensory test by line scales for the similarity of lemony note.

However, aroma of Oil_{model3} at 10,000 ppm was significantly different from 1000 ppm of lemon oil while Oil_{model7} at 10,000 ppm, 1,000 ppm and the neat oil did not show any significant difference with 1,000 ppm of natural lemon peel aroma. Therefore, higher aroma similarity of Oil_{model7} at 1000 ppm as well as 10,000 ppm and the neat oil was clarified. Furthermore, one hundred ppm of the two model solutions showed significant differences with other concentrations of model solutions statistically and was least similar to the reference lemon peel. A critical border between the 100 ppm solution and the 1000 ppm solution of Oil_{model7} was statistically observed: concentrations of 1000 ppm or greater were most similar to the reference lemon peel and were not different from each other, while the 100 ppm solution was least similar to the reference and was perceived to be significantly different from the higher concentrations.

Selection of Potent Character-impact Compounds from Aroma Quality Assessment

In the past two decades, flavor chemists have developed methods for evaluation of sensory impact using odor detection limits such as AEDA, Charm analysis, Uo and Lod instead of hedonic scales. However, these methods obtain sensory data from the values associated with individual compound detection limits. Aroma impacts have to be finally extrapolated to supra-threshold levels. This requires an inductive leap between data obtained at threshold levels and that at supra-threshold levels unless further testing is done. Therefore, omission tests using mixtures at supra-theshold concentrations are frequently used to evaluate the impact of odorants. As an alternative to ordinary omission tests (16-19) we have described a new methodology, the cumulative test, for the assessments of odor activity at a supra-threshold.

Omission test

Ten compounds that have the highest Lod values (Table I) were mixed together at their relative concentrations in the original lemon oil and were diluted to a final total concentration of 329 ppm (Figure 3). Three hundred and twenty nine ppm of the solution is 10 times higher than the previously determined recognition thresholds of lemon against lime oil.

Selected 10 compounds
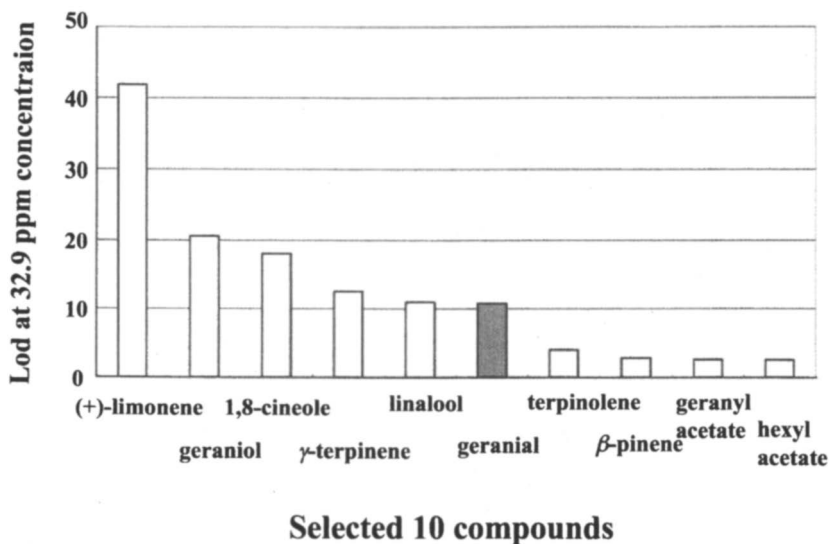
Figure 3. Lod of Oil$_{model10}$ against lime oil at 32.9 ppm.

Moreover, as described in a previous part of this chapter, panel members rated 1000 ppm of lemon oil as the most similar to the natural peel aroma while the 100 ppm solution was the least similar to lemon peel aroma. Three hundred and twenty nine ppm of the model oil solution falls within this range and therefore may be an appropriate model solution, with an aroma similar to the lemon peel (although similarity to lemon peel was not specifically tested for this solution). From ten compounds contributing to the lemon aroma at 329 ppm, one chemical was omitted and then the odor threshold of the omitted compound was determined against the mixture of the remaining 9 chemicals (Figure 4). Thus, if the omitted compound is important to the aroma, the panel members should recognize the difference in aroma between the omitted compound and that of the other 9 chemicals. The odor detection thresholds of each of the 10 chemicals were compared to those thresholds measured in water (Table II). The thresholds of geraniol, 1,8-cineole and terpinolene were greatly increased but limonene, geranial and hexyl acetate did not change their thresholds as much. These results may lead to the generalization that those compounds which changed their odor thresholds contribute to reinforcing the overall aroma intensity whereas those compounds that did not change their thresholds so much in the mixture can be attributed to characterization of aroma quality. In particular, (+)-limonene,

Table II. Variation of Odor Threshold in Omission Test

No.	Compound	Odor Threshold (ppm)	
		in Water	in $Oil_{model10}$[1]
1	(+)-limonene	0.51	7.93
2	geraniol	0.01	17.42
3	1,8-cineole	0.01	7.26
4	γ-terpinene	0.26	22.96
5	linalool	0.01	3.08
6	geranial	0.08	2.86
7	terpinolene	0.04	20.13
8	β-pinene	1.3	140.02
9	geranyl acetate	0.16	5.87
10	hexyl acetate	0.13	4.4

[1] $Oil_{model10}$ excludes one chemical as a testing compound

geranial and γ-terpinene, which have the greatest Lod values at 329 ppm ((+)-limonene: 27.1, geranial: 3.0, γ-terpinene: 1.3), may significantly contribute to the overall aroma quality (Figure 4).

Omission test shown here does not include ordinal hedonic judgements such as scoring, category scaling and magnitude estimation. Therefore, some of the psychological bias for the sensory evaluation may be avoided.
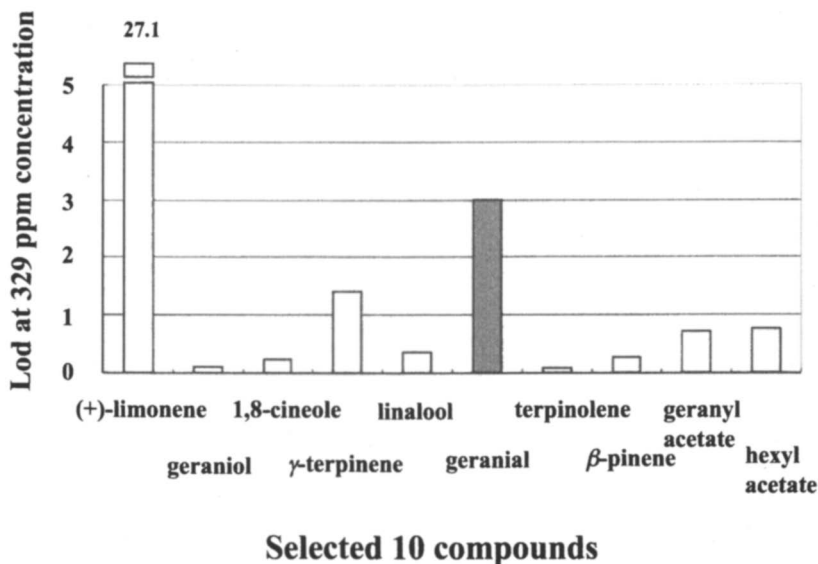
Figure 4. Lod values of 10 chemicals by using odor thresholds and omission test at the expected 329 ppm of the Oil$_{model10}$.

Cumulative test

Omission tests have often been used in flavor studies (*7, 16-19*). There is a disadvantage in omission test because of the large number of compounds and test mixtures that must be analyzed in order to obtain the composition of the important odorants in the final model solution. For example, when we determine aroma activity of the 11th chemical against the remaining 10 chemicals, we have to perform another set of omission tests to clarify the changes of individual odor thresholds in water and solutions as mentioned above. Therefore, we invented another strategy to establish more practical methodology to determine their thresholds in certain solutions. Thus, the odor threshold of a given chemical

should be determined in an oil mixture prepared from those compounds having greater Lod values than the given chemical being tested. For example, the odor threshold of geraniol having the 2nd greater Lod value was determined against limonene that had the greatest Lod value. The expected concentration was set at 329 ppm of lemon oil. The expected concentration is a cumulative value of each concentration of all 10 volatile components. Limonene concentration was set at 212.8 ppm because it comprises 64.68% of the total oil. The odor detection threshold of 1,8-cineole was determined in a mixture of limonene and geraniol at 214.6 ppm (64.68% limonene and 0.56% geraniol in the original oil, Table I). Geraniol, linalool and β-pinene showed greater variations of odor thresholds (Table III) followed by 1,8-cineole and terpinolene as shown in Figure 5. Using odor thresholds obtained from cumulative aroma chemicals, odor units at expected 329 ppm solution of the model oil clarified that geranial had the greatest value, indicating a higher contribution of this chemical to lemon aroma as a characteristic compound. Additionally, as we expected, variations of odor detection thresholds of these 9 compounds showed almost the same tendency with those of omission test.

Table III. Variation of Odor Threshold in Cumulative Test

No.	Compound	Odor Threshold (ppm)	
		in Water	in Oil$_{model10}$[1]
2	geraniol	0.01	11.25
3	1,8-cineole	0.01	2.7
4	γ-terpinene	0.26	30.64
5	linalool	0.01	5.62
6	geranial	0.08	5.5
7	terpinolene	0.04	7.83
8	β-pinene	1.3	582.24
9	geranyl acetate	0.16	6.62
10	hexyl acetate	0.13	3.49

[1] Determined in model solutions prepared by sequential additions of the test compound to model solutions containing limonene plus all other test compounds with Lod values greater than the compound being tested.
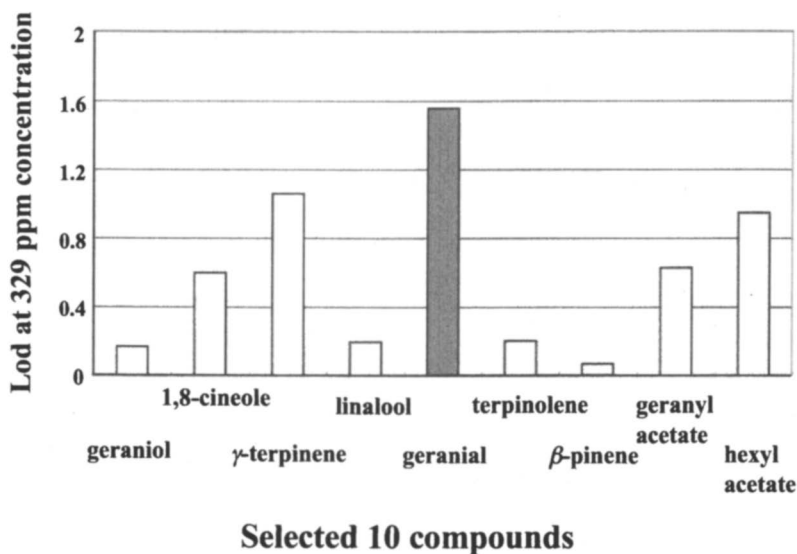
Figure 5. Lod value of 9 chemicals by using odor thresholds and cumulative test at the expected 329 ppm of $Oil_{model10}$.

In conclusion, omission tests and cumulative tests both showed that geranial has the highest Lod value at 329 ppm whereas geraniol has a higher Lod value in water but in mixtures showed a smaller value. Aroma character of geraniol may be suppressed and overlap with that of limonene even though geraniol in water has been shown to have a large contribution to lemon aroma. In our experiment, it was found that geranial would be apparently detectable in the oil mixture at supra-threshold concentrations. Furthermore, we can interpret that in sensory tests, since Oil_{model7} contained geranial as a component, panel members could detect the existence and gave higher scores on the line scale. These omission tests and cumulative tests provide us unique methods for picking aroma character compounds in *Citrus limon* oil. Especially the cumulative test may be more valuable for sequential sensory experiments because of the reduced number of mixtures that must be evaluated compared to traditional omission tests.

References

1. Belitz, H.D.; Grosch, W. *Food Chemistry*; Springer Verlag: Berlin Heidelberg, 1986, p 258.
2. Schieberle, P.; Grosch, W. *J. Food Sci.* **1990**, *55*, 193-195.
3. Roberts, D. D.; Acree, T. E. *J. Food Sci.* **1996**, *44*, 3919-3925.

4. Guadagni, D. G.; Okano, S.; Buttery, R. G.; Burr, H. K. *Food Technol.* **1966**, *20*, 166-169.
5. Buttery, R. G.; Teranishi, R.; Ling, L. C.; Turnbaugh, J. G. *J. Agric. Food Chem.* **1990**, *38*, 336-340.
6. Tamura, H.; Yang, R. H.; Sugisawa, H. In *Bioactive Volatile Compounds from Plants*; Teranishi, R.; Buttery, R. G.; Sugisawa, H., Eds. ACS Symposium Series 525; American Chemical Society: Washington, DC, 1993; pp 121-136.
7. Grosch, W. *Chem. Senses* **2001**, *26*, 533-545.
8. Boonbumrung, S.; Tamura, H.; Mookdasanit, J.; Nakamoto, H.; Ishihara, M.; Yoshizawa, T.; Varanyanond, W. *Food Sci. Technol. Res.* **2001**, *7*, 200-206.
9. Mookdasanit, J.; Tamura, H.; Yoshizawa, T.; Tokunaga, K. *Food Sci. Technol. Res.* **2003**, *9*, 54-61.
10. Jennings, W.; Shibamoto, T. In *Qualitative Analysis of Flavor and Fragrance Volatiles by Gas Chromathgraphy*, Academic Press: New York, 1980.
11. Rothe, M.; Thomas, B. *Z. Lebensm. Unters. Forsch.* **1963**, *119*, 302-310.
12. Tamura, H.; Fukuda, Y.; Padrayuttawat, A. In *Biotechnology for Improved Foods and Flavors*; Takeoka, G. R.; Teranishi, R.; Williams, P. J.; Kobayashi, A. Eds.; ACS Symposium Series 637; American Chemical Society: Washington, DC, 1996; pp 282-294.
13. Chida, M.; Yamashita, K.; Izumiya, U.; Watanabe, K.; Tamura, H. *J. Food Sci.* **2006**, *71*, S54-58.
14. Green, B. G.; Dalton, P.; Cowart, B.; Shaffer, G.; Rankin, K. R.; Higgins, J. *Chem. Senses* **1996**, *21*, 323-324.
15. Olsson, M. J.; Cain, W. S. *Chem. Senses* **2000**, 25, 493-499.
16. Mayer, F.; Czerny, M.; Grosch, W. *Eur. Food Res. Technol.* **2000**, *211*, 272-276.
17. Engel, E.; Nicklaus, S.; Septier, C.; Salles, C.; Le Quere, J. L. *J. Agric. Food Chem.* **2000**, *48*, 4260-4267.
18. Reiners, J.; Grosch, W. *J. Agric. Food Chem.* **1998**, *46*, 2754-2763.
19. Escudero, A.; Gogorza, B.; Melus, M. A.; Ortin, N.; Cacho, J.; Ferreira, V. *J. Agric. Food Chem.* **2004**, *52*, 3516-3524.

<center>

Chapter 21

Flavor Release and Perception of Custard Desserts: Influence of Food Composition and Oral Parameters

</center>

<center>

Saskia M. van Ruth[1,2], Amaya Rey Uriarte[2,3], Eugenio Aprea[2,4], and Elizabeth Sheehan[2,5]

[1]RIKILT – Institute of Food Safety, P.O. Box 230, 6700 AE Wageningen, The Netherlands
[2]University College Cork, Western Road, Cork, Ireland
[3]Departamento de Teconologia de Alimentos, Universidad Politecnica de Valencia, Apdo. Correos 22012, 46071 Valencia, Spain
[4]Istituto Agrario di S. Michele a/A, S. Michele, Via E. Mach 2, 38010 Italy
[5]Independent Sensory Services Ltd., Glanmire Estate, Glanmire, County Cork, Ireland

</center>

The influence of oral processing on *in vivo* flavor release and perception was evaluated for a firm and a soft custard which varied in carboxymethyl cellulose concentrations. The group of sensory assessors could be divided in two, one group rating higher odor/flavor scores for the firmer custard and the other group for the softer custard. In-nose analysis also revealed two groups with one group showing higher in-nose flavor concentrations for the firmer custard, and the other group for the softer custard. The maximum in-nose flavor concentrations were related to the time to swallowing. Both model mouth and static headspace analysis showed higher flavor release from the softer custard. The study showed the importance of time for oral processing on flavor release and perception.

The formulation of foods with controlled sensory properties remains a challenge. The composition and structure of a food system, as well as oral processing, determine a food's sensory flavor and texture properties. Texturing agents are added to food products to modify a product's viscosity. Their addition sometimes results in a significant decrease in perceived flavor (*1*). Increased viscosity may hinder mass transfer of flavor compounds to the surface of the food product (*2*). However, different texturing agents resulting in solutions of similar viscosity do not induce the same flavor perception. Furthermore, sometimes texturing agents affect flavor perception but do not exhibit a change in in-nose measured flavor concentrations (*3,4*).

Descriptive sensory analysis is a valuable technique to evaluate the sensory perception of the flavor of food products. Volatile flavor compounds can only contribute to flavor perception when present at sufficiently high nasal concentrations. Intranasal flavor concentrations can be measured by *in vivo* direct mass spectrometry (MS) techniques, such as Proton Transfer Reaction-Mass Spectrometry (PTR-MS) (*5*). These in-nose concentrations are determined by the rates of release of the compounds in the mouth during consumption of the food product. Flavor release is determined by a thermodynamic and a kinetic component (*6*), the former of which can be assessed by static headspace analysis. The influence of oral physiological parameters on volatile flavor release, such as mastication, can be further evaluated by *in vitro* measurements using mouth analogues (*7*).

In the present study, two strawberry flavored custard desserts varying in texturing agent concentration were evaluated for their sensory characteristics. The sensory properties of the samples were compared to in-nose flavor concentrations, which were measured by PTR-MS. The contribution of the thermodynamic factor to the measured in-nose flavor concentrations was examined by means of static headspace gas chromatography analysis (SHGC). The study is a follow-up to previous studies with the aim of further examination of the impact of oral processing on flavor perception in vivo (*8*).

Materials and Methods

Materials

A commercial strawberry flavor mixture was obtained from Givaudan (Duebendorf, Switzerland). Its composition was published previously (*8*). Ethyl butyrate was present at 90 mg/g. High viscosity carboxymethyl cellulose (CMC; C-5013; Sigma-Aldrich Chemie, Steinheim, Germany) was used for custard preparation.

Custard Preparation

Two different custards were prepared. They were composed of 0.1% and 1.0% CMC, respectively. For custard preparation, 936 g (0.1% CMC custard) or 927 g (1.0% CMC custard) homogenized full-fat milk (4% fat) was heated to 60°C in a water bath. Sucrose (63 g; Siucra; Irish Sugar Ltd, Carlow, Ireland) was added and the mixture stirred for 3 min using a kitchen appliance. The CMC was added in small increments to ensure that the CMC was fully dispersed. To obtain the custard texture, the mixture was stirred again for 5 min. The temperature of the water bath was increased to 95°C, while stirring continued. When the custard reached a temperature of 90°C, heating continued for another 10 min. The custard was subsequently cooled down at room temperature for 15 minutes and further down to 30°C by placing the bottle in cold water (room temperature). Forty g of the custard was placed in a 100 mL glass bottle, 14 μL of the flavor mixture was injected in the custard and the bottle sealed. The mixture was stirred for 5 min and stored at 6°C for 24 h prior to analysis. Final total flavor concentration was 56 mg/kg custard (not including the solvent triacetin). For each type of custard duplicate batches were prepared.

Sensory Analysis

Descriptive sensory analysis using a panel of 7 assessors was carried out on the two custards, which was part of a larger experiment. Methodology and experimental design have been described elsewhere (8). The examination of the two custards was composed of two replicate sessions.

In-nose PTR-MS Analysis

For in-nose analysis, a fork-shaped glass nosepiece was placed with its two inlets in the nostrils of a subject. The air was drawn in at a rate of 100 mL min^{-1}, 15 mL of which was led into the PTR-MS. The background was measured for at least 60 s. During that time seven g of custard (20°C) was placed on a spoon. The subject transferred the custard to his/her mouth. Subjects were allowed to chew and swallow freely. Subjects raised their hands to indicate time of swallowing (tswallow). Preliminary scans (mass range m/z 30-220) of the flavored custards as well as the individual flavor compounds revealed that the mass m/z 117 could be exclusively assigned to ethyl butyrate. Twenty-one subjects participated in the in-nose analyses: nine males and 12 females (aged 20-40). Two batches of the individual custards were analysed (2 replicates per type of custard per person). The samples were analysed according to the method described by Lindinger and co-workers (5). The spectra were background and

transmission corrected. From the individual curves, maximum intensities (Imax) were determined.

Model Mouth PTR-MS Analysis

For model mouth analysis, 7 g of custard was placed in the flask of the model mouth (7). Two mL of artificial saliva (9) were added and a mastication rate of 52 rpm was applied. Two replicates of each batch were analysed (=four samples of each custard). The headspace of the samples was analysed by PTR-MS according to the method described by Lindinger (5). The headspace was drawn from the model mouth at 100 mL/min by a vacuum pump, 15 mL/min of which was led through a heated transfer line into the PTR-MS for on-line analysis for three minutes. Data were collected for a number of ions, based on preliminary scans (m/z 30-220). Similar scans were carried out on the individual strawberry flavor compounds. Combination of the results resulted in the selection of the ion m/z 117 for ethyl butyrate, which was specific for this compound.

Static Headspace Gas Chromatography (SHGC) Analysis

For SHGC analysis 2 g of each custard were placed in a 10 mL glass vial. Two replicate vials were prepared for each batch (=four samples for each type of custard). Samples were incubated at 37°C and agitated at 750 rpm for 10 min in the automated headspace unit (Combipal-CTC Analytics System, JVA Analytical Ltd., Dublin, Ireland) of the gas chromatograph (GC; Varian CP-3800; JVA Analytical Ltd.). The GC was equipped with an injector at 225°C, a BPX5 capillary column (60 m length, 0.32 mm i.d., 1.0 µm film thickness, helium carrier gas 1.9 mL/min; SGE, Kiln Farm Milton Keynes, UK) and a flame ionisation detector (FID) at 275°C. One mL of headspace was injected on the GC by the automated headspace unit. An initial oven temperature of -30°C was used for 1 min, followed by a rate of 100°C/min to 40°C. The oven temperature was maintained at 40°C for 4 min, and programmed to 250°C at 8°C/min. Individual compounds were used to identify the compounds detected (Aldrich, Steinheim, Germany). Peak areas of ethyl butyrate and ethyl hexanoate were determined.

Statistical Analysis

The sensory and instrumental data were subjected to Principal Component Analysis (PCA) with Varimax rotation, which was followed by Hierarchial Cluster Analysis. A significance level of $P<0.05$ was used throughout the study. Model mouth and SHGC data were compared using Student's t-tests.

Results and Discussion

Sensory Analysis

The sensory characteristics of the two custards were evaluated by descriptive sensory analysis. Differences between the two custards have been described elsewhere (8). To examine differences between subjects PCA was carried out over the data of the seven assessors. Loadings of assessors on F1 and F2 are presented in Table I. Hierarchical cluster analysis revealed two clusters. Cluster A was characterized by relatively high loadings on F2 and low loadings on F1, which corresponded to Assessor 4, 5 and 6. These assessors correlated with high ratings for milky, grassy, and overripe fruit odors and flavors (Table II). Cluster B was characterized by relatively high loadings on F1 and low loadings on F2, which corresponded to Assessor 1, 3 and 7. High ratings for sweet flavor and thickness correlated with these assessors. Strawberry odor and flavor did not correlate specifically with any group, as it had a relatively high score on both F1 and F2. The panel was experienced and well-trained. Therefore, it is remarkable that the cluster A assessors provided generally higher ratings for the taste/texture attributes compared to their fellow assessors, whereas cluster B assessors provided higher ratings for the odor/flavor attributes. This is an interesting aspect related to inter-assessor differences on the flavor/texture interactions level. For some assessors the texture aspect was predominant, for others the flavor. The latter may be related to differences at the perceptual level. However, it may also be due to differences in flavor concentrations available for perception. This was later evaluated by in-nose analysis. The average strawberry, grassy, milky, and overripe fruit flavor rating for the 0.1% CMC custard was for cluster A assessors 44.4 and for cluster B assessors 48.0. For the 1.0 % CMC custard the ratings were closer for the two clusters: the average rating for the specified attributes was for cluster A 46.5 and for cluster B 46.1. However, these results indicate that the average flavor rating (excl sweet flavor) for cluster A was higher for the 1% CMC custard, and for the cluster B for the 0.1% CMC custard.

In-nose Analysis

In-nose analysis was carried out on the two types of custard using 21 subjects and two batches of each type of custard. The Imax data were subjected to PCA, the results of which are presented in Fig. 1. The group of subjects was divided in two, with one group showing highest Imax values for the softer custard (0.1% CMC) and another group for the firmer custard (1.0% CMC). Subject 1, 3, 4, 9, 11, 12, 14, 15, and 19 had higher Imax values for the 1.0% CMC custard; the others for the 0.1% CMC custard. These differences in

Table I. Results of Principal Component Analysis and Hierarchical Cluster Analysis Carried Out on the Custard Sensory Data: Factor Loadings of Assessors

	F1	F2
Assessor 1	0.51	0.23
Assessor 2	0.22	0.11
Assessor 3	0.64	0.07
Assessor 4	0.00	0.81
Assessor 5	0.21	0.57
Assessor 6	0.09	0.49
Assessor 7	0.65	0.00
Cluster A	0.04	0.84
Cluster B	0.77	0.20

Table II. Results of Principal Component Analysis Carried Out on the Custard Sensory Data: Scores of the Seven Assessors

	F1	F2
Strawberry odor	1.29	1.63
Milky odor	0.61	7.08
Grassy odor	0.46	1.79
Overripe fruit odor	0.83	6.43
Strawberry odor	1.16	1.29
Milky flavor	0.33	1.93
Grassy flavor	0.06	0.86
Sweet flavor	3.52	1.07
Overripe fruit flavor	0.41	2.81
Thickness	16.0	0.12

physical volatile flavor concentrations at the nostrils in groups of subjects may result in a difference in flavor perception. The sensory study also indicated two groups of subjects, with one group rating flavor attributes higher for the 0.1% CMC custard, and another group for the 1.0% CMC custard. Direct comparison of individuals is not possible, since the sensory assessors were not included in the group of in-nose subjects.

In order to examine underlying causes for the differences in in-nose flavor concentrations in the two groups, the time to swallowing was evaluated by PCA (Fig. 2). Subjects 4, 7, 11, 14, 16, 17, 18, 19, and 21 showed fairly similar tswallow values for both custards. Another group of subjects, including subjects 1, 3, 5, 6, 8, 9, 10, 12, 15, and 21 showed higher tswallow values for the 1.0% CMC custard. The group could also be divided based on their tswallow: those with an average tswallow<4s (eight subjects), those with an average tswallow>6s (five subjects), as well as an intermediate group (8 subjects). Generally, subjects with a tswallow<4s showed higher Imax concentrations for the 1.0% custard. Ethyl butyrate Imax for the 0.1% CMC custard was for this group 150 ppb and for the 1.0% CMC custard 211 ppb. Subjects with a tswallow>6s had higher Imax concentrations for the 0.1% CMC custard. Ethyl butyrate Imax for the 0.1% CMC custard was for this group 430 ppb and for the 1.0% CMC custard 280 ppb. Volatile flavor release is determined by both release rates and time available for release. The balance of these two factors determines individual differences in volatile flavor release.

Model Mouth Analysis

Real-time model mouth analysis was carried out on the two types of custard. The results are presented in Table III. The 0.1% CMC custard showed higher Imax concentrations than the 1.0% CMC custard. The 1.0% Imax ethyl butyrate concentration was 26% lower (Student's t-test, $P<0.001$). The tmax values were higher for the 1.0% CMC custard. Therefore, under model mouth conditions flavor release rates are higher for the softer custard. In the model mouth sample size, mouth temperature, mouth volume, salivation, and mouth movements are taken into account.

Table III. Results of Real Time Model Mouth Analysis on the Two Custard Desserts: Maximum Intensities of Ethyl Butyrate (Imax) and Time to Maximum Intensities (Tmax) (mean±SD, n=4)

	0.1% CMC CUSTARD	1.0% CMC CUSTARD
Imax (ppbv)	20759±799	15417±733
Tmax (s)	87±27	122±43

Biplot after Varimax rotation
(axes F1 and F2: 81.89 %)
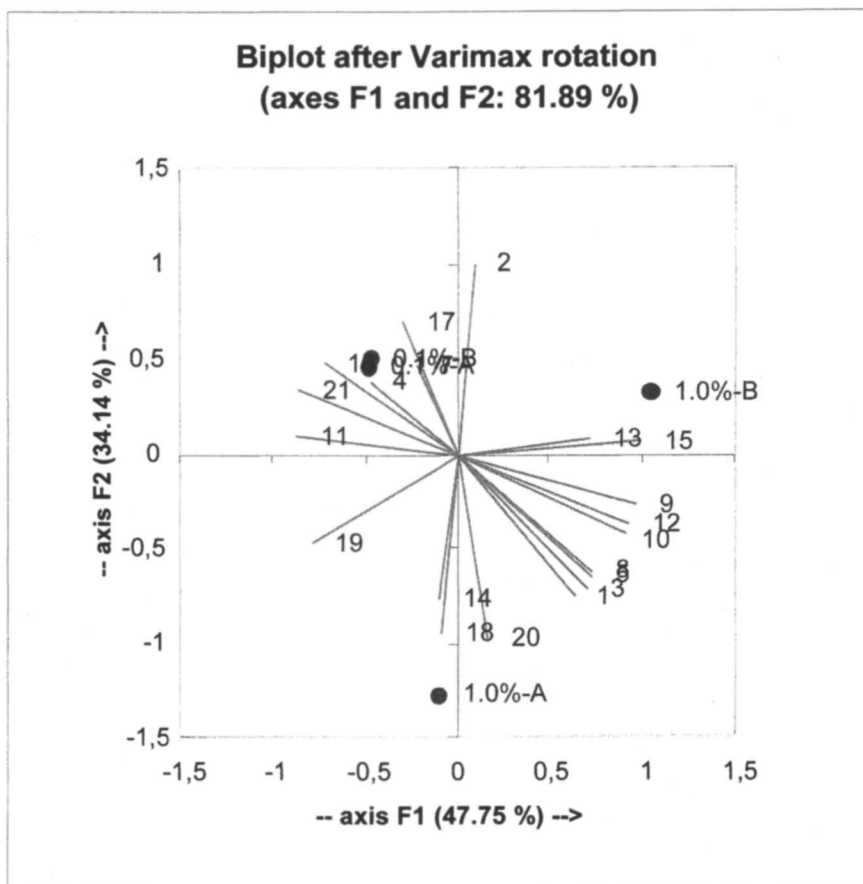
Figure 1. First two dimensions of Principal Component Analysis on maximum intensities of ethyl butyrate measured in in-nose analysis for 21 subjects (nr 1-21) and 2 custards (0.1% and 1.0%) and 2 batches (A and B).
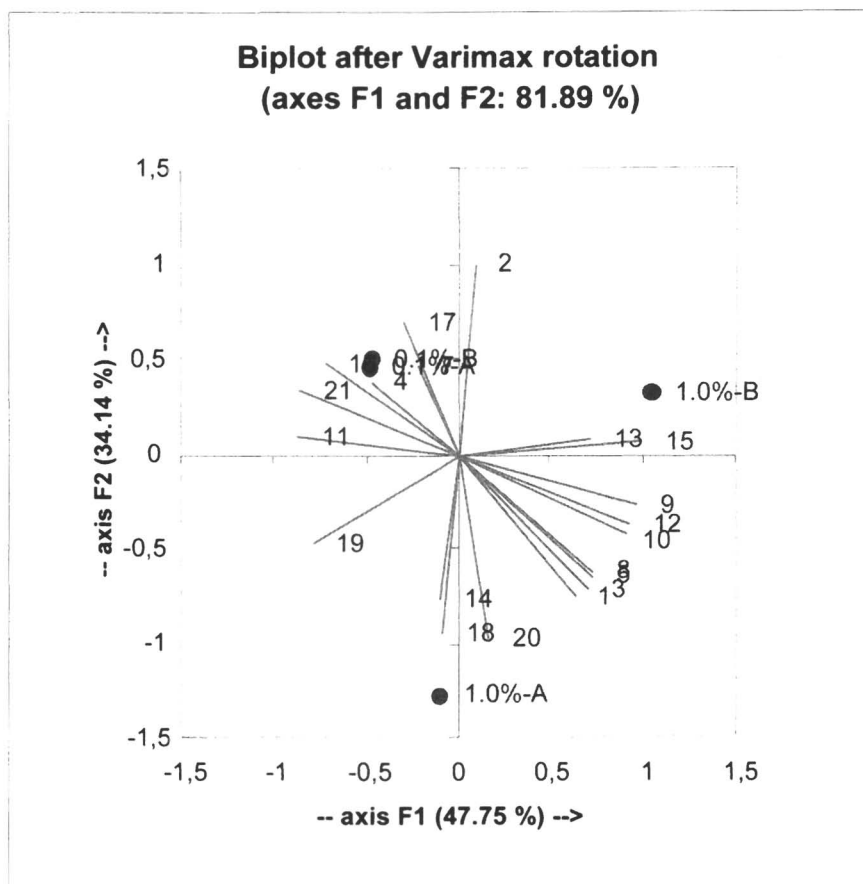
*Figure 2. First two dimensions of Principal Component Analysis on time
to swallowing measured during in-nose analysis for 21 subjects (nr 1-21)
and 2 custards (0.1% and 1.0%) and 2 batches (A and B).*

Table IV. Results of Static Headspace Analysis on the Two Custard Desserts: Peak Areas (mean±SD, n=4)[*]

	0.1% CMC CUSTARD	1.0% CMC CUSTARD
Ethyl butyrate	386131±7847	340138±9850
Ethyl hexanoate	13461±261	9359±1252

[*] Table adapted from (8)

Static Headspace Analysis

Static analysis was carried out on the two types of custard. The results are presented in Table IV. This type of analysis showed similar differences between the two custards as the model mouth analysis. Higher headspace concentrations were determined for the 0.1% CMC custard compared to the 1.0% CMC custard (Student's t-test, $P<0.001$). The ethyl butyrate peak areas of the 1.0% CMC custard was 12% lower than those of the 0.1% CMC custard. These results show that the CMC had an effect on the thermodynamics of flavor release from the custards. Differences between the custards in terms of ethyl butyrate release were similar for static headspace analysis and model mouth analysis. As kinetics do not play a role under static conditions, differences in phase partitioning rather than differences in resistance to mass transfer are likely to contribute to the differences between the custards observed in model mouth analysis.

Conclusions

This study showed that two groups of sensory assessors rating odor/flavor attributes were discriminated. One group rated the softer custard generally higher for the odor/flavor attributes, and the other group the firmer custard. Similarly for one group of subjects in-nose concentrations were higher when the softer custard was consumed, and for the other group the higher in-nose concentrations were recorded for the firmer custard. Intensity of in-nose concentrations was related to the time to swallowing. Therefore, oral physiology was considered an important parameter for individual flavor release. The basic differences between the softer and firmer custard in flavor release under model mouth conditions were shown to have a thermodynamic origin.

Acknowledgements

References

1. *Frontiers in Carbohydrate Research*; Chandrasekaran, R., Ed.; Elsevier: New York, USA, 1992; p 85.
2. Stephen, A. M. *Food Polysaccharides and their Application*; Marcel Dekker: New York, USA, 1995; p 517.
3. Hollowood, T. A;. Linforth, R. S. T.; Taylor., A. J. *Chem. Senses* **2002**, *27*, 583-591.
4. Weel, K. G. C.; Boelrijk, A. E. M.; Alting, A. C.; van Mil, P. J. J. M.; Burger, J. J.; Gruppen, H; Voragen, A. G. J.; Smit, C. *J Agric. Food Chem.* **2002**, *50*, 5149-5155.
5. Lindinger, W.; Hansel, A.; Jordan, A. *J. Mass Spectrom. Ion Proc.* **1998**, *173*, 191-241.
6. de Roos, K. B. In *Flavor Release*; Roberts, D. D.; Taylor, A. J., Eds; ACS Symposium Series 763; American Chemical Society: Washington, DC, 2000, pp 126-141.
7. van Ruth, S. M.; Roozen, J. P.; Cozijnsen, J. L. In *Trends in Flavour Research;* Maarse, H.; van der Heij, D. G., Eds; Elsevier: Amsterdam, 1994, pp 59-64.
8. van Ruth, S. M.; de Witte, L.; Rey, A. *J. Agric. Food Chem.* **2004**, *52*, 8105-8110.
9. van Ruth, S. M.; Grossmann, I.; Geary, M.; Delahunty, C. M. *J. Agric. Food Chem.* **2001**, *49*, 2409-2413.

Chapter 22

Evaluation of the Antioxidant Potential of Various Plant Essential Oils

Alfreda Wei and Takayuki Shibamoto[*]

Department of Environmental Toxicology, University of California, Davis, CA 95616

The antioxidant activities of extracts from medicinal plant essential oils were evaluated using an aldehyde/carboxylic acid assay. The extracts from basil and thyme inhibited the oxidation of hexanal by 100% at a level of 500 µg/mL over 40 days. Rosemary (58%) and chamomile (44%) extracts exhibited moderate antioxidant activities, whereas cinnamon and lavender extracts did not show any appreciable activity. Clove bud extract inhibited hexanal oxidation by 100% at the levels of 200 and 500 µg/mL. Among three different species, *E. polyanthemon* showed the strongest antioxidant activity of 100% at the level of 500 µg/mL. Among the essential oils tested, rose essential oil exhibited the highest activity (90%) at the level of 500 µg/mL, followed by ylang (87%), and jasmine (86%). Eugenol, which is one of the major constituents of eucalyptus oil, exhibited potent antioxidative activity. Antioxidants such as eugenol and thymol may play an important role in the pharmaceutical activities of natural plant extracts used for aromatherapy.

© 2008 American Chemical Society

257

Since ancient times, people in all cultures have known that many natural plants contained aroma chemicals and have used them in baths for medicinal purposes. Combinations of resins, oils, and fragrant plants were used in ceremonies and medicine in most ancient civilizations. The Chinese may have been one of the first cultures to use aromatic plants for well-being. The Romans are also well-known for their elaborate baths. Later, the Egyptians invented a rudimentary distillation machine that allowed for the crude extraction of cedar wood oil. In many places, the steam bath has been enjoyed for the benefits of total relaxation of mind and body: to ease stress; relieve muscle tension and stiff joints; sweat out body toxins; stimulate circulation; increase body metabolism; keep skin glowing and youthful; and to alleviate sinus congestion due to colds, asthma, or allergies. Lavender oil and chamomile oil were used for the treatment of insomnia. Digestive problems were treated with coriander oil. Chamomile, celery, juniper, and coriander oils were used as anti-inflammatory medicines. Eucalyptus oil was known to relieve muscle pain.

Until recently, aroma chemicals have been investigated from the viewpoint of flavor and fragrance chemistry. However, some medicinal activities of aroma chemicals, such as antioxidative activity, have been discovered through using essential oils in aromatherapy. Recently, we reported that aroma chemicals found in brewed coffee possess antioxidative activity (1–3). Also, antioxidant activities of natural plant essences including beans (4), clove bud (5), Eucalyptus (6), herbs and spices (7), and teas (8) have been reported.

In the present study, essential oils obtained from various natural plants were examined for antioxidant activities.

Materials and Methods

Materials

Essential oils of cinnamon, lavender, chamomile, rosemary, basil, thyme, ylang, rose, jasmine, and peppermint were gifts from International Flavor and Fragrance Co., Ltd. (Keyport, New Jersey). Hexanal, hexanoic acid, and undecane were purchased from Aldrich Chemical Co. (Milwaukee, WI). Authentic aroma chemicals were obtained from reliable commercial sources or as gifts from Takata Koryo Co., Ltd. (Osaka, Japan).

Isolation of Essential Oils from Medicinal Plants

Clove buds (200 g) and eucalyptus leaves (200 g) were placed in a round-bottom flask with 1 L deionized water and then steam distilled at 55 °C for 3 h

under reduced pressure (95 mmHg). The distillate (200 mL) was extracted with 50 mL dichloromethane using a liquid-liquid continuous extractor for 6 h. After the extract was dried over anhydrous sodium sulfate, the solvent was removed by distillation with a Vigreux column. The distillation was stopped when the volume of extract was reduced to approximately 1 mL, and then the solvent was further removed under a purified nitrogen stream. The sample was stored at 5 °C until the antioxidative tests and analyses.

Antioxidative Tests of Samples Using the Aldehyde/Carboxylic Acid Assay

Various concentrations of testing samples were added to a 2 mL dichloromethane solution of hexanal containing undecane as a gas chromatographic internal standard. Oxidation of the sample solution was initiated by heating at 60 °C for 10 min in a sealed vial; it was then stored at room temperature. The headspace of each vial was purged with pure air every 24 h for the first 10 days. Hexanal concentrations were monitored at 5-day time intervals. BHT and α-tocopherol were used as controls to compare the antioxidative activity of the plant extracts. All sample vials were wrapped with aluminum foil to avoid UV oxidation. The quantitative analysis of hexanal was conducted according to a previously reported internal standard method (*9*). A gas chromatograph equipped with a 30 m × 0.25 mm i.d. (d$_f$ = 0.1 μm) DB-1 bonded-phase fused-silica capillary column and a flame ionization detector (FID) was used.

Results and Discussion

The most common method used to determine the antioxidative activity of a chemical or a group of chemicals is the thiobarbituric acid assay (TBA). The TBA assay involves measurement of so-called thiobarbituric acid reactive substances (TBARS), including malonaldehyde (MA), formed from a lipid upon oxidation. A capillary gas chromatographic method for specific determination of MA has been also used (*10–13*). Methods involved in lipid/MA assay are useful for a rapid analysis of samples, but occur under artificially strong oxidative conditions. Therefore, these assays may not accurately represent oxidative processes, which are often associated with food systems. Generally, in food systems, oxidation processes occur slowly over a period of 40 days. Because the lipid/MA assays measure short-term oxidation, the aldehyde/carboxylic acid assay was developed for determining the long-term antioxidant potential of a chemical or a group of chemicals (*14*). This method is based on the auto-oxidation of aldehydes to carboxylic acids with active oxygen species such as a

hydroxyl radical (15). Fatty aldehydes are readily converted to the corresponding fatty acid in an oxygen-rich dichloromethane solution through a radical-type reaction as shown in Figure 1 (16). Although the aldehyde/carboxylic acid assay requires prolonged time periods, it offers a better measure of the oxidation process that occurs in foods and beverages.

Figure 2 shows the antioxidative activities of extracts from herbs and spices, and the standards (BHT and α-tocopherol) obtained using a hexanal/hexanoic acid assay throughout a storage period of 40 days at the level of 500 μg/mL. The antioxidant activity of samples was directly related to the remaining amount (%) of hexanal. The extracts from basil and thyme inhibited the oxidation of hexanal by 100% at a level of 500 μg/mL over 40 days. Their activities were comparable to those of standard antioxidants BHT and α-tocopherol. Rosemary (58%) and chamomile (44%) extracts exhibited moderate antioxidant activities, whereas cinnamon and lavender extracts did not show any appreciable activity. Thyme, basil, rosemary, and chamomile extracts showed the dose response activity. All extracts exhibited dose-related activity and Figure 3 show a typical example of dose-related activity (basil extract). This extract inhibited hexanal oxidation over 40 days at levels of 200 and 400 μg/mL. On the other hand, it inhibited only 10% and 35% over 40 days at the levels of 10 μg/mL and 20 μg/mL, respectively.

Figure 4 shows antioxidant activities of various essential oils over 40 days. Rose oil exhibited the highest activity (90%) among the oils tested, at the level of 500 μg/mL, followed by ylang (87%), and jasmine (86%). Rose and jasmine essential oils inhibited hexanal oxidation by over 80% at the level of 100 mg/mL, whereas ylang oil did not exhibit appreciable activity at the same level. Lavender oil exhibited slight antioxidant activity at the level of 500 mg/mL. However, chamomile and peppermint oils did not show appreciable activity at any level tested.

Figure 5 shows the antioxidant activities of medicinal plant extracts examined over 40 days at various levels. Clove bud extract exhibited the highest antioxidant activity with dose-response. It inhibited hexanal oxidation 100% at the levels of 200 and 500 μg/mL. Its activity was consistent with that of α-tocopherol at the level of 50 μg/mL. Among three different species of eucalyptus oils, the oil from *E. polyanthemos* showed the strongest antioxidant activity. It inhibited hexanal oxidation by 100% at the level of 500 μg/mL. The oil from *E. globulous* exhibited moderate dose-response activity. The oil of *E. perriniana* inhibited hexanal oxidation by 30% at the level of 100 mg/mL, but it showed less activity at the higher levels. It is interesting that the well-known medicinal plant, aloe vera, did not exhibit appreciable antioxidant activity at any of the levels tested.
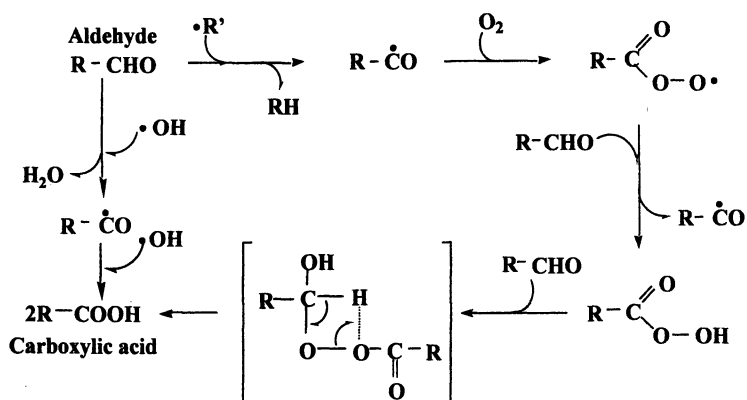
Figure 1. Oxidative conversion mechanisms of aldehyde to carboxylic acid.
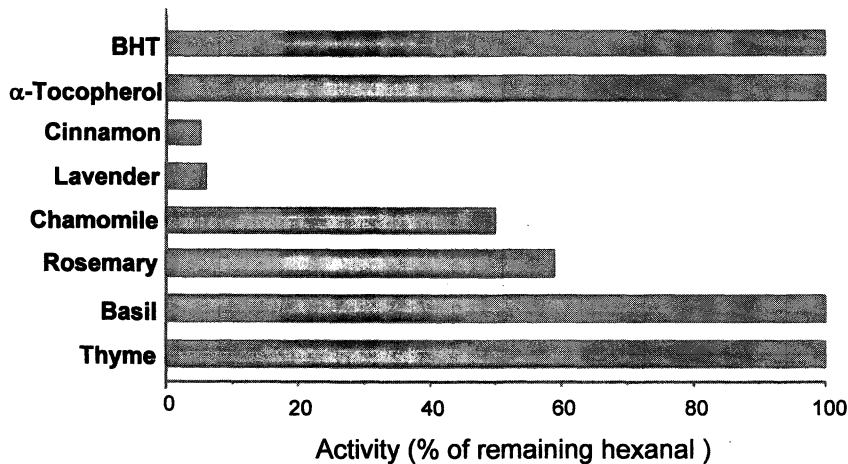
Figure 2. Antioxidative activities of extracts from herbs and spices.
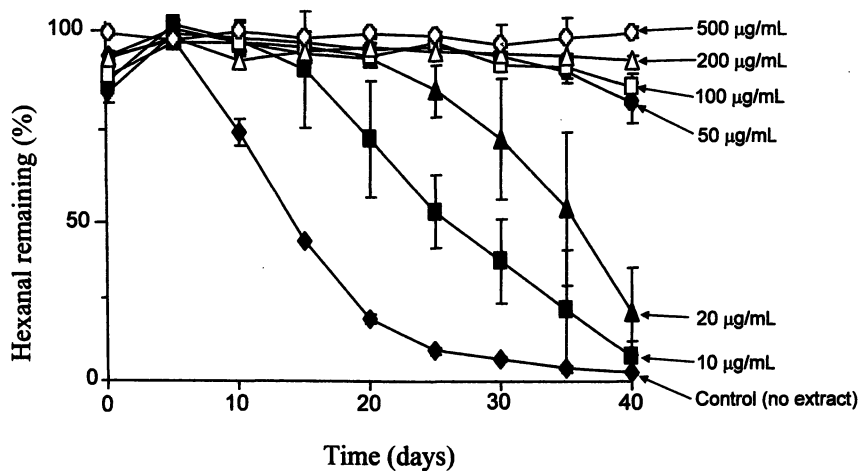
Figure 3. Typical example of dose-related activity obtained from basil extract.
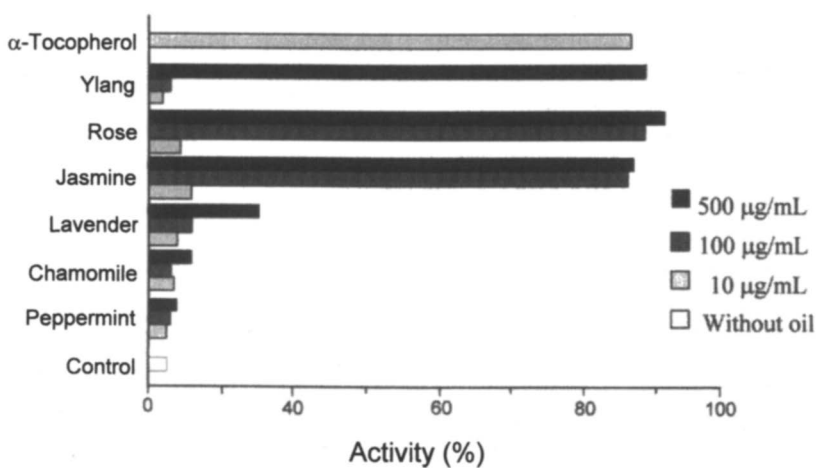
Figure 4. Antioxidant activities of various essential oils over 40 days.
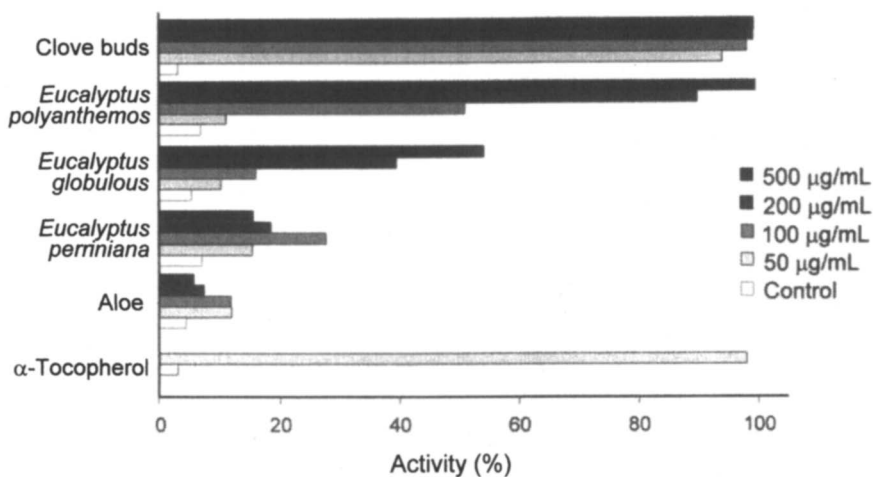
Figure 5. Antioxidant activities of medicinal plant extracts over 40 days.
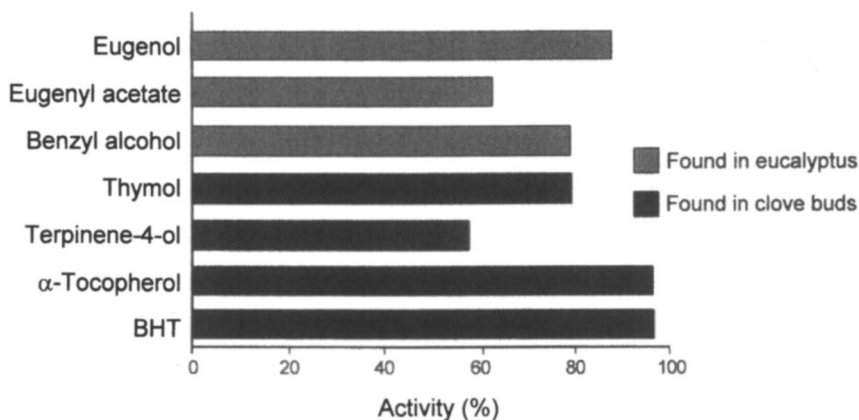
*Figure 6. Antioxidant activities of chemicals found in clove buds and eucalyptus
leaves over 40 days at the level of 160 ug/mL.*

Figure 6 shows the antioxidant activities of chemicals found in clove buds and eucalyptus leaves over 40 days at the level of 160 µg/mL. Eugenol exhibited the highest activity (90%), followed by benzyl alcohol (80%), thymol (80%), eugenyl acetate (62%), and terpinene-4-ol (57%). The results indicate that eugenol, eugenyl acetate, and benzyl alcohol contribute significantly to the antioxidant activity of eucalyptus oils. Also, the strong antioxidant activity of clove buds is due to the presence of thymol and terpinene-4-ol.

Our preliminary experiments indicate that the antioxidative activities of aroma constituents—including maltol, eugenol, 1-octen-3-ol, and benzaldehyde—are not as potent as those of known antioxidants, BHT and α-tocopherol. However, large amounts of these aroma chemicals are present in natural plants. Therefore, their total activity may be comparable to those of known antioxidants. Investigation of the antioxidative activity of each aroma chemical found in natural plants is currently underway.

References

1. Singhara, A.; Macku, C.; Shibamoto, T. In *Functional Foods for Disease Prevention II: Medicinal Plants and Other Foods;* T. Shibamoto, J. Terao and T. Osawa, eds, ACS Symposium Series 701, ACS, Washington, DC, 1998, pp. 101-109.
2. Fuster, M. D.; Mitchell, A. E.; Ochi, H.; Shibamoto, T. *J. Agric. Food Chem.* **2000**, *48*, 5600-5603.
3. Yanagimoto, K.; Ochi, H.; Lee, K.-G.; Shibamoto, T. *J. Agric. Food Chem.* **2004**, *52*, 592-596.
4. Lee, K. -G.; Mitchell, A. E; Shibamoto, T. *J. Agric. Food Chem.* **2000**, *48*, 4817-4820.
5. Lee, K.-G.; Shibamoto, T. *J. Sci. Food Agric.* **2001**, *81*, 1573-1579.
6. Lee, K.-G.; Shibamoto, T. *J. Sci. Food Agric.* **2001**, *81*, 1573-1579.
7. Lee, K.-G.; Shibamoto, T. *J. Agric. Food Chem.* **2002**, *50*, 4947-4952.
8. Yanagimoto, K.; Ochi, H.; Lee, K.-G.; Shibamoto, T. *J. Agric. Food Chem.* **2003**, *51*, 7396-7401.
9. Ettre, L. S. In *The Practice of Gas Chromatography,* L. S. Ettre and A. Zlatikis, eds, Interscience Publishers: New York, NY, 1967, pp. 402-440.
10. Umano, K.; Dennis K. J.; Shibamoto, T. *Lipids* **1988**, *23*, 811-814.
11. Osawa, T.; Katsuzaki, H.; Hagiwara, Y; Hagiwara, H.; Shibamoto, T. *J. Agric. Food Chem.* **1992**, *40*, 1135-1138.
12. Nishiyama, T.; Hagiwara, Y; Hagiwara, H.; Shibamoto, T. *J. Agric. Food Chem.* **1994**, *42*, 1728-1731.
13. Ogata, J.; Hagiwara, Y; Hagiwara, H.; Shibamoto, T. *J. Am. Oil Chem. Soc.* **1996**, *73*, 653-656.

14. Macku, C.; Shibamoto, T. *J. Agric. Food Chem.* **1991**, *39*, 1990-1993.
15. Horner, L. In *Auto-oxidation and Antioxidants,* W. O. Lundberg, ed, John Wiley & Sons: New York, NY, 1961, pp. 197-202.
16. Nonhebel, D. C.; Tedder, J. M.; Walton, J. C. In *Radicals,* Cambridge University Press, London, 1979, pp. 155-157.

Chapter 23

Some Biological Effects of Raspberry Ketone and Its Precursor

Takeshi Ikemoto, Tomohiro Yokota, and Shintaro Inoue

Basic Research Laboratory, Kanebo Cosmetics Inc., 3–28, 5-Chome, Kotobuki-Cho, Odawara, Kanagawa 250–0002 Japan

Natural fragrant chemicals have been screened for their potential uses as alternatives such as antimicrobials and antioxidants. Recently, glycosidically bound volatiles have been studied as fragrant precursors in essential oil plants and have also been the subject of interest in various industries. Raspberry ketone (RK; 4-(p-hydroxyphenyl)-2-butanone) is well known as a typical aroma chemical of red raspberry *(Rubus idaeus)*, and its β-D-glucoside (RaG) has been isolated as its precursor. RK has a similar structure to capsaicin, a compound known to exert an anti-obesity action. We confirmed that RK accelerated lipolysis *in vitro* more potently than capsaicin and prevented high-fat diet (HFD)-induced elevations in body and liver weights. We found that RaG inhibited melanin synthesis more than hydroquinone β-D-glucoside (arbutin), a compound that is already used as a melanin inhibitor in cosmetics.

© 2008 American Chemical Society

Essential oils have provoked interest as sources of natural fragrant chemicals and some of them such as eugenol from clove buds and *iso*-eugenol from nutmeg have been screened for potential uses as antimicrobials and antioxidants (*1*). Capsaicin (*N*-[(4-hydroxy-3-methoxyphenyl)-methyl]-8-methyl-6-nonamide), a pungent principle of hot red pepper, is known to exert an anti-obesity action. Fragrant chemicals and spice ingredients have been subjects of interest not only in food industries but also in pharmaceutical and cosmetics companies.

Raspberry ketone (RK; 4-(*p*-hydroxyphenyl)-2-butanone), a typical aroma chemical of red raspberry, is mainly used by flavorists (Figure 1). RK has GRAS (Generally Recognized As Safe) status and was also on the list of artificial flavoring substances given by the Council of Europe. Its world consumption for all uses is estimated at over 10,000 kg per year (*2*). We expected that RK might influence lipid metabolism in ways similar to capsaicin due to its structural similarity. In this study, the effects of RK on obesity and lipid metabolism are discussed.

Numerous glycosidically bound volatiles (GBVs) have been isolated from flowers, fruits and tea leaves (*3*). GBVs have been known to be flavoring and fragrance precursors, and have been the subject of interest in the food, tobacco and wine industries. Arbutin (hydroquinone β-D-glucoside), isolated from the leaves of *Arctostaphylos uva-ursi*, is widely used in skin care cosmetics as a tyrosinase inhibitor (*4*). However, there is little discussion about the effects of other glycoside derivatives. The depigmentation activity of several GBVs, especially raspberry ketone β-D-glucoside, in cultured B16 melanoma cells are discussed.

Raspberry ketone (RK)

Raspberry ketone β-D-glucoside (RaG)

Capsaicin

Arbutin
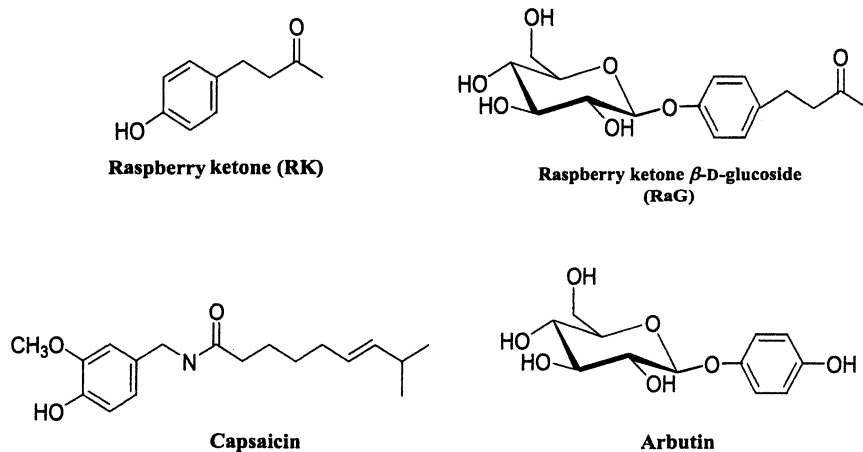
Figure 1. Structures of Raspberry ketone and its β-D-glucoside.

Anti-obesity Action of Raspberry Ketone

Effect of RK on Norepinephrine-Induced Lipolysis and Localization of HSL in White Adipocytes

To compare the effects of RK and capsaicin on norepinephrine-induced lipolysis, the following *in vitro* examination was performed. Young male Crj: Wistar rats were sacrificed by cervical dislocation to minimize endogenous catecholamine secretion, and their epididymal adipose tissues were quickly removed. Isolated fat cells were obtained from the removed epididymal adipose tissue by the method of Rodbell (*5*). The fat cells were incubated at 37°C for 1h in Hanks' buffer (pH 7.4) supplemented with 2.5% (w/v) bovine serum albumin and the indicated concentrations of each sample and norepinephrine. After incubation, the reaction mixture was centrifuged to separate the medium and fat cells. The free fatty acids (FFAs) contents of the medium was estimated by the method of Warnick (*6*). It was observed that 10^{-3} M of capsaicin and RK increased norepinephrine-induced lipolysis though the effect was only significant with RK (Figure 2). RK enhanced FFAs release by fat cells in a dose-dependent manner (Figure 3). RK significantly increased the amount of hormone-sensitive lipase protein (HSL, 84kDa) in the fat layer and concominantly reduced the amount in the supernatant. We also confirmed that RK didn't enhance HSL activity at the same concentration (data not shown). Morimoto et al. (*7*) reported that the conversion of HSL translocation to its substrate on the surfaces of lipid droplets is a crucial step for triacylglycerol hydrolysis. The results suggest that RK enhances norepinephrine-induced lipolysis but not via HSL activation.
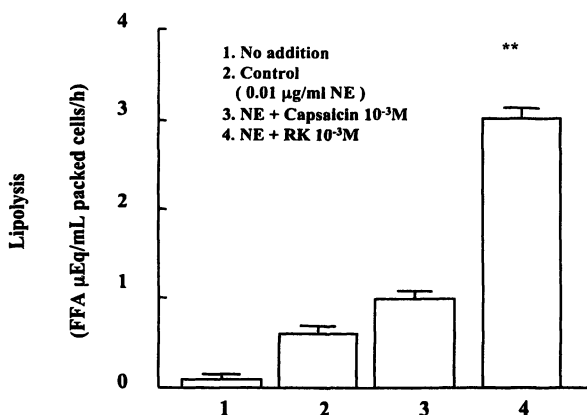
Figure 2. Effect of raspberry ketone and capsaicin on lipolysis. Lipolysis was expressed as free fatty acids mEq/mL packed fat cells per h. * * p<0.01 vs. values of norepinephrine-treated cells. NE, norepinephrine; RK, raspberry ketone.
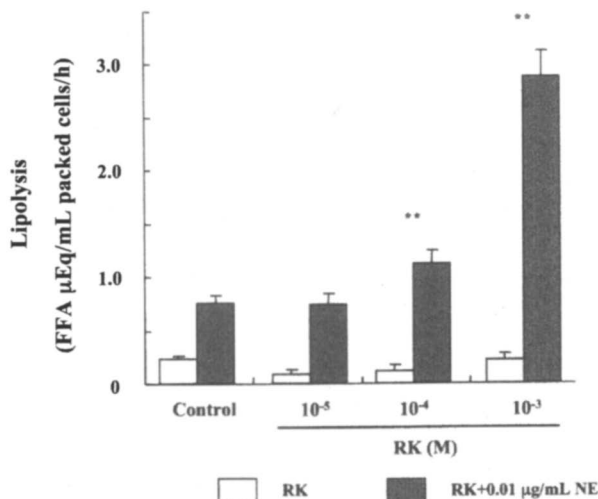
*Figure 3. Effect of raspberry ketone on lipolysis in rat epidermal fat cells.
Lipolysis was expressed as free fatty acids μEq/mL packed fat cells per h.
* * p<0.01 vs. values of norepinephrine-treated cells. RK, raspberry ketone;
NE, norepinephrine.*

Effect of Dietary Supplementation of RK on Obesity

Male ICR mice (4-weeks old) were obtained from CLEA Japan (Osaka, Japan) and housed in a light/dark cycle controlled room. After the animals were given a standard laboratory diet (Oriental Yeast Co., Ltd., Tokyo, Japan) and water for 1 week, they were divided into five groups matched for body weight. The normal diet group (ND) was fed a standard laboratory diet and the three experimental groups were fed one of two experimental diets, the high-fat diet (HFD) and the high-fat diet plus RK (HFD-RK). The experimental diets shared the following basic composition: beef tallow 40%, casein 34-36%, corn starch 10%, sugar 9%, vitamin mixture (AIN-93G) 1% and mineral mixture (AIN-93G) 4% (w/w per 100g diet). The compositions for the respective experimental groups were as follows (each n=6): high-fat diet group, casein 36% and basic components; HFD-RK group, different amounts of casein (34%, 35% and 35.5%) and RK (0.5%, 1% and 2%). The total amount of food intake of each mouse was recorded at least three times and the body weight of each mouse was recorded weekly. The mice fed on the HFD for 10 weeks had a significantly higher body weight than mice fed on the ND. In the mice fed the HFD-RK (2% and 1%), the body weight elevation that took place over the initial 6 weeks on

the HFD was significantly reduced (Figure 4). The mean energy intake per week per mouse (kJ/week/mouse) during the whole experimental period differed significantly between the ND group (500.3 ± 9.1 kJ/week/mouse) and the HFD group (760.7 ± 38.4 kJ/week/mouse), but was not different between the HFD group and the HFD-RK group (1% RK diet; 805.0 ± 14.6 kJ/week/mouse, 2% RK diet; 799.4 ± 14.5 kJ/week/mouse).

The final visceral adipose tissues and liver weights of the groups are shown in Table I. The HFD led to significant increases in the weights of liver and visceral adipose tissues (e.g., epididymal, retroperitoneal and mesenteric adipose tissues) compared to the ND group, but the HFD-RK (especially 2%) groups tended to have reduced final liver weights and weights of retroperitoneal and mesenteric adipose tissues compared to the HFD group. These results indicate that orally fed RK prevents obesity and the fatty liver induced by feeding a high-fat diet.
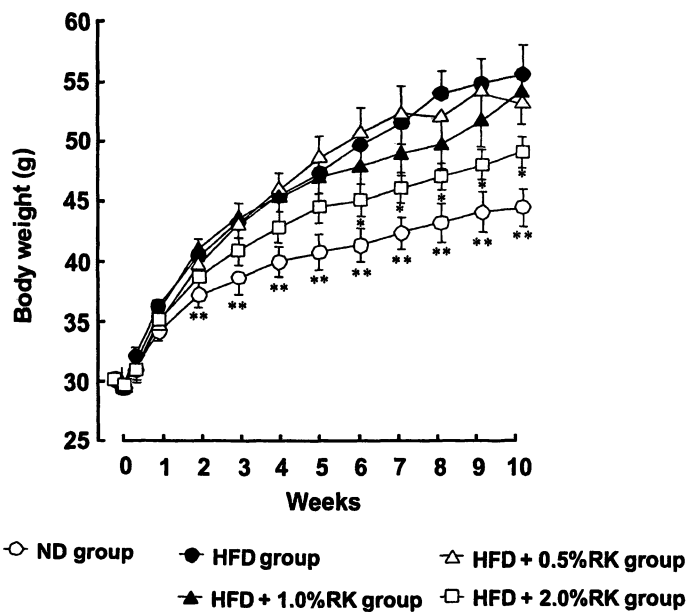
Figure 4. Effect of raspberry ketone on body weight in mice fed a high-fat diet for 10 weeks. Each value represents the mean ± SE of 6 mice; * p<0.05 and ** p<0.01 vs. values in high fat diet group. ND, normal diet; HFD, high fat diet; RK, raspberry ketone. (Reproduced from reference 8. Copyright 2005 Elsevier Inc.)

Table I. Effect of Raspberry Ketone on the Weights of Liver and Visceral Adipose Tissues in Mice Fed a High-Fat Diet for 10 Weeks.

Group	Adipose Tissue Weight (g)			Liver Weight (g)
	Epididymal	Retroperitoneal	Mesenteric	
ND	0.86 ± 0.24^b	0.38 ± 0.03^b	0.29 ± 0.07^b	2.67 ± 0.07^b
HFD	3.19 ± 0.30	1.01 ± 0.18	1.02 ± 0.10	3.37 ± 0.25
HFD+0.5%RK	2.35 ± 0.24^b	0.58 ± 0.10^a	0.92 ± 0.15	3.35 ± 0.13
HFD+1.0%RK	2.76 ± 0.16	0.72 ± 0.13	1.06 ± 0.16	2.88 ± 0.14^a
HFD+2.0%RK	2.21 ± 0.11^b	0.55 ± 0.05^b	0.83 ± 0.08^b	2.63 ± 0.09^a

NOTE: Each value represents the mean ± SE of 6 mice; [a] $p<0.05$ and [b] $p<0.01$ vs. values in high fat diet group. ND, normal diet; HFD, high fat diet. RK, raspberry ketone

Effect of Topical Applications of RK on Subcutaneous Fat

The effect of topical applications of RK on subcutaneous fat was also examined. Thirty-one female 10-week-old Sprague-Dawley rats that had been ovariectomized one week in advance were divided into four groups (each n=3) matched for body weight. The control group was fed the normal diet and three experimental groups were changed to high fat diets that contained 20% beef tallow. The experimental groups were treated topically on the interscapular skin (0.1 mL solution applied to 2 cm x 2 cm square) once a day for 4 weeks with the 50% ethanol solutions containing 0%, 1% and 2% RK. On the final day of the experiment, rats of all groups were sacrificed. Interscapular, inguinal, and mesenteric white adipose tissues (WATs) were removed and weighed. In addition, the RK content in the WATs were measured by gas chromatography. The topically applied RK selectively reduced the weight of the interscapular WATs under the site of application but no reductions were observed in the other sites such as inguinal and mesenteric WATs (data not shown). RK was only detected from within the reduced subcutaneous fat samples. The average amount of RK (nmol/g fat) increased with its topical amount up to 2% RK (the vehicle group, not detected; 1% RK, 2.3 nmol/g fat; 2% RK, 3.5 nmol/g fat). It was found that topically applied RK selectively reduced the weight of subcutaneous fat directly beneath the sites of application (Figure 5).

This investigation demonstrated that RK has an anti-obesity function that might exert its effect via an increase of norepinephrine-induced lipolysis. Although more detailed studies in the future should help clarify the mechanisms of the anti-obesity function of RK, RK given both orally and topically was concluded to reduce body fat and subcutaneous fat without any stimulation like capsaicin.
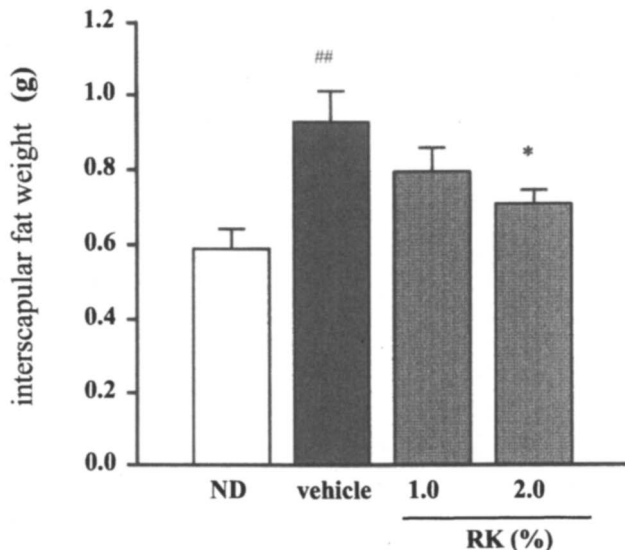
*Figure 5. Effect of topically applied raspberry ketone on interscapular fat weight under the site of application. Each value represents the mean ± SE of 7-8 mice; ## p<0.01 vs. ND and * p<0.05 vs. vehicle in high fat diet group. ND, normal diet; RK, raspberry ketone.*

Depigmentation Action of Raspberry Ketone β-D-Glucoside

A number of patents have dealt with melanogenesis inhibitors to answer the demand for skin lighteners in Asia Pacific region countries. Among them, arbutin (hydroquinone β-D-glucoside), isolated from the plant, is very popular to use in skin care cosmetics as a tyrosinase inhibitor (*4*). On the other hand, it has been previously reported that glycosidically bound volatiles might be metabolized by skin microflora to release fragrance materials (*9*). In this study, the effect of raspberry ketone β-D-glycoside on inhibition of melanin synthesis in B16 melanoma cells was examined.

Effect of RaG on Inhibition of Melanin Synthesis in Cultured B16 Melanoma Cells

B16 F0 melanoma cells (ICN Biomedicals, Costa Mesa, CA, USA) were grown in 75cm² plastic tissue flasks in Eagle's minimal essential supplemented with 10% fetal bovine serum and 2 mM *L*-glutamine at 37°C in a humidified

atmosphere. The melanin content in the cultured cells was measured according to the modified method of Oikawa *et al.* (*10*). B16 melanoma cells were cultured at an initial density of 3×10^5 cells/ϕ 90mm culture dishes and added to each sample. After culturing for three days, the cells were collected after trypsinization and centrifugation. The collected cells were treated with as follows, 5% trichloroacetic acid, ethanol-diethyl ether (3:1) and diethyl ether. The treated cells were dissolved in Soluene 350 and the melanin content was measured with a spectrophotometer at 400 nm.

The effect of five kinds of β-D-glucosides, i.e., vanillin, eugenol, raspberry ketone, citronellol and menthol on melanin synthesis in cultured B16 melanoma cells is shown in Figure 6. Raspberry ketone β-D-glucoside (RaG) was the most effective glucoside in reducing melanin synthesis with higher activity than arbutin. Three kinds of raspberry ketone β-D-glycosides, glucoside, galactoside and xyloside, were also examined. RaG was the only glycoside to have significant inhibitory activity against melanin synthesis. RK had a stronger inhibitory effect than RaG (Figure 7). These results are probably due to the respective levels of enzymatic activity as the activity of β-glucosidase is reported
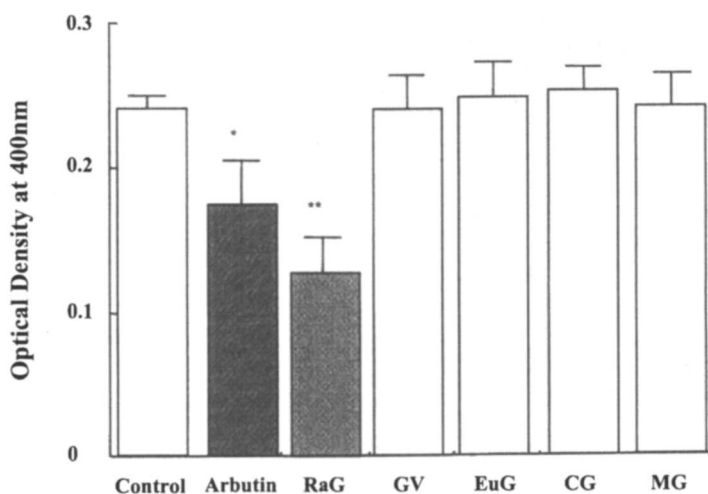
Figure 6. Inhibitory effect of glucosides derived from plants on melanin synthesis in B16 melanoma cells. The glucoside concentrations were $3 \times 10^{-5} M$. Each value represents the mean ± SE of 3 experiments; * p<0.05 and ** p<0.01 vs. values of control group. RaG: raspberry ketone β-D-glucoside, GV: glucovanillin, EuG: eugenyl β-D-glucoside, CG: citronellyl β-D-glucoside, MG: Menthyl β-D-glucoside.
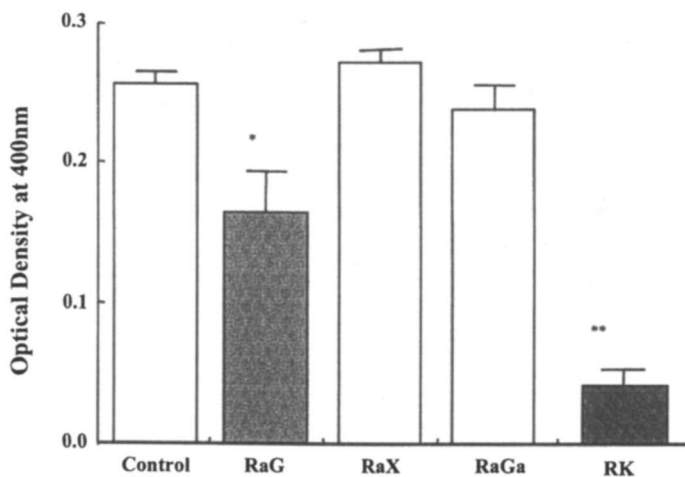
*Figure 7. Inhibitory effect of raspberry ketone and its glycosides on melanin synthesis in B16 melanoma cells. The concentration of RK and its glycosides was $3 \times 10^{-5}M$. Each value represents the mean ± SE of 3 experiments; * p<0.05 and ** p<0.01 vs. values of control group. RaG: raspberry ketone β-D-glucoside, RaX: raspberry ketone β-D-xyloside, RaGa: raspberry ketone β-D-galactoside, RK: raspberry ketone.*

to be higher than the other glycosidase activities in human skin (*11*) and RK generated from RaG showed a potent inhibitory effect on melanin synthesis in cultured cells. We had reported that the release of RK from the glucoside on human skin increased just after application, and was maintained for more than 6 hours (*9*). This indicated that RaG would be a good candidate for novel melanogenesis inhibition. Our future studies will include the confirmation of the efficacy of RaG (especially compared to arbutin) through *in vivo* examinations.

Summary

The anti-obesity effect of RK and the depigmentation effect of RaG as biological activities of fragrant chemicals has been demonstrated though their potentials have not yet been elucidated. The biological activities of other fragrant chemicals and their precursors will be the subject of further study.

References

1. Laekeman, G. M.; Hoof, L. V.; Haemers, A.; Vanden Berghe, S. A.; Herman, A. G.; Vlietinck, A. J. *Phytother. Res.* **1990**, *4*, 90-96.
2. Clark, G. S. *Perfum. Flav.* **1992**, *17*, 21-26.
3. Stahl-Biskup, E.; Intert, F.; Holthuijzen, J.; Stengele, M.; Schulz, G. *Flavour Fragr. J.* **1993**, *8*, 61-80.
4. Akiho, A.; Suzuki, Y.; Yuasa, T.; Fujinuma, Y.; Fukuda, M. *Jpn. J. Dermatol.* **1991**, *101*, 609-613.
5. Rodbell, M. *J. Bio. Chem.* **1964**, *239*, 375-380.
6. Warnick, G. R. In *Methods in Enzymology*; Albers, J. J.; Segrest, J. P., Eds.; Plasma Lipoproteins, Part B: Characterization, Cell Biology, and Metabolism; Academic Press, Inc.: Orlando, FL, 1986, Vol. 129, pp 101-123.
7. Morimoto, C.; Kameda, K.; Tsujita, T.; Okuda, H. *J. Biochem.* **2001**, *42*, 120-127.
8. Morimoto, C.; Satoh, Y.; Hara, M.; Inoue, S.; Tsujita, T.; Okuda, H. *Life Sci.* **2005**, *77*, 194-204.
9. Ikemoto, T.; Okabe, B.; Mimura, K.; Kitahara, T. *Flavour Fragr. J.* **2002**, *17*, 452-455.
10. Oikawa, A.; Nakayasu, M. *J. Biol. Med.* **1973**, *46*, 500-507.
11. Chang, F.; Wertz, P. W.; Squier, C. A. *Comp. Biochem. Phisiol.* **1991**, *100*, 137-139.

Author Index

Subject Index

O

Obesity. *See* Anti-obesity
Octakis(2,3-di-*O*-methoxymethyl-6-
O-tert-butyldimethylsilyl)-γ-
cyclodextrin, 26–27, 28
Octalactones in mesquite pods, 101–
102, 103*t*–106*t*
See also Lactones
Odor dilution analysis, headspace
volatiles, 60, 61, 64–65*f*
Odor intensity and changes,
measurement, 195–196*t*, 210
Odor mixture, perceived intensities,
mixture suppression, 191–
206
Odor moderate intensity adjustment,
194–195, 197–200*f*
Odor quality cross-matching, 197,
200–204*f*
Odor recognition thresholds in *Citrus
limon* and model oils, 232, 233–
235*f*
Odor unit values, measurements in
Citrus limon oils, 231–232
Odorants in headspace aroma,
Philippine pineapple, 64, 66*t*
See also Aroma entries; *Volatile
entries*
Olfactometer for generation, various
odor concentrations, 193–
194*f*
Olfactometry. *See* GC^{x}GC-
olfactometry
Omission test, lemon oils, character-
impact compound selection, aroma
quality assessment, 237–239*f*
Oral processing influence on *in vivo*
flavor release and perception, 243–
253
Oriental Beauty, oolong tea, aroma
component identification during
processing, 87–97
Osme approach, 185

P

Packaging materials and sorbate
addition, influence on flavor quality,
irradiated apple cider, 128–130
Palatability effects by celery odor
constituents in chicken broth, 84–
86
Parcha granadilla. *See* Badea fruit
Passiflora quadrangularis L. *See*
Badea fruit
Pasteurization, apple cider, effect on
flavor and appearance, 122
E-2-Pentenal with methionine or
cysteine, volatile formation under
non-aqueous conditions, 176–188
2-Pentylfuran in four component
system for evaluation, perceived
odor intensities, 191–206
Peptide-carbonyl reaction, 148–
149
Peptide hydrolysis, effect on Maillard
volatile compound formation,
147–157
glycine-serine and serine-glycine
dipeptides, volatile formation,
153–156*t*
glycine-X dipeptides, 151–152*f*
Perceived odor intensities, mixture
suppression, 191–206
Philippine pineapple, volatile
components and odorants in
headspace aroma, 57–67
Phthalides in celery, 79–82*f*, 84–86
Pineapple. *See* Philippine pineapple
Plant essential oils, antioxidant
potential, 257–265
Pom-Fong tea. *See* Oriental Beauty,
oolong tea
Prosopis spp. See Mesquite
Proton Transfer Reaction-Mass
Spectrometry (PTR-MS) analysis.
See In-nose Proton Transfer
Reaction-Mass Spectrometry;